

---

# **TRANS-SCALE MODELLING OF RIVER MORPHODYNAMICS**

Jacobus Marthinus Andreas Grobler

A thesis submitted to the Faculty of Engineering and the Built Environment, University of the Witwatersrand, in fulfilment of the requirements for the degree of Doctor of Philosophy.

Johannesburg 2009

---

## Contents

<b>Chapter 1 – Introduction – The need for trans-organisational modelling</b> .....	1
1.1 Introduction.....	1
1.1.1 River management .....	1
1.1.2 Geomorphological prediction.....	2
1.2 Aim .....	3
1.2.1 Motivation for study.....	3
1.2.2 Objectives.....	5
1.2.3 Approach.....	6
<b>Chapter 2 – River complexity</b> .....	8
2.1 Complexity and modelling .....	8
2.2 Reasons for river complexity.....	10
2.3 Hierarchical description.....	12
2.4 Non-linearity of river processes.....	15
2.4.1 Up-scaling .....	15
2.4.2 Self-organisation .....	16
2.4.3 Emergence and emergent structures.....	17
2.5 Conclusion.....	19
<b>Chapter 3 - Processes affecting river geomorphology</b> .....	21
3.1 Vegetation dynamics .....	21
3.1.1 Riparian vegetation.....	21
3.1.2 Vegetation establishment and succession.....	22

3.1.3 Flow resistance of vegetation .....	24
3.1.4 Large Woody debris .....	25
3.2 Sediment dynamics .....	25
3.2.1 Sediment movement.....	25
3.2.2 Erosion and deposition .....	27
3.2.3 River bank-stability .....	28
3.2.4 Vegetation-sediment interaction.....	29
3.3 River form.....	31
3.3.1 Effect of flooding on river form .....	31
3.3.2 Vegetation-river form interaction.....	31
3.3.3 Effect of geology on river form.....	33
3.3.4 Bar formation .....	35
3.4 Conclusion.....	38
<b>Chapter 4 – Geomorphological modelling .....</b>	<b>40</b>
4.1 Modelling methods.....	40
4.1.1 Physical modelling .....	40
4.1.2 Numerical modelling.....	42
4.1.3 Computational fluid dynamics .....	43
4.1.4 Rule-based modelling.....	45
4.1.5 Cellular Automata modelling .....	47
4.2 River process modelling.....	49
4.2.1 Sediment transport and bed evolution .....	49
4.2.2 Channel sedimentology and planform.....	53
4.2.3 Modelling stable channel morphology .....	59

4.2.4	Equilibrium approaches.....	62
4.2.5	Modelling spatial vegetation interaction.....	64
4.3	Geomorphic modelling codes.....	70
4.3.1	One-dimensional codes .....	70
4.3.2	Multi-dimensional codes .....	73
4.4	Conclusion.....	75
<b>Chapter 5 – Hierarchical modelling.....</b>		<b>76</b>
5.1	Reach scale water flow.....	78
5.1.1	One-dimensional Saint-Venant equations .....	78
5.1.2	Flow resistance .....	79
5.1.3	The MacCormack method for solving 1-D flow .....	79
5.1.4	Stability Condition.....	80
5.2	Reach scale sediment flow and bed elevation .....	80
5.2.1	Model overview .....	80
5.2.2	Intermittency .....	80
5.2.4	Numerical solution scheme for the Exner equation.....	82
5.2.5	Sediment feed.....	83
5.2.6	Sediment transport.....	83
5.2.7	Grain size calculation .....	84
5.2.8	The surface-based relation of Wilcock and Crowe (2003).....	85
5.2.9	Computation of the shear stress.....	86
5.3	Reach scale reed population dynamics.....	86
5.3.1	Model overview .....	86
5.3.2	Inference procedure.....	89

5.3.3 Reed biomass-elevation data .....	92
5.3.4 Rule-base .....	93
5.3.5 Model Output .....	97
5.4 Channel-type scale water flow .....	100
5.4.1 2-D Saint-Venant equations .....	100
5.4.2 Bed friction modelling.....	100
5.4.3 Turbulent shear stress modelling .....	101
5.4.5 The MacCormack Method for solving 2-D flow .....	102
5.5 Channel-type scale bar evolution .....	106
5.5.1 Sediment routing .....	106
5.5.2 Sediment allocation according to local slope.....	108
5.5.3 Sediment storage .....	109
5.5.4 Bagnold's empirical bed-load formula .....	111
5.5.5 Angle of repose .....	111
5.6 Channel-type scale reed expansion.....	112
5.6.1 Model overview .....	112
5.6.2 Model outputs.....	113
5.7 Geomorphological-unit scale water flow .....	117
5.7.1 Model overview .....	117
5.7.2 The residual method.....	118
5.8 Geomorphological-unit scale bed-form development .....	119
5.9 Geomorphological-unit scale reed growth .....	121
5.9.1 Model overview .....	121
5.9.2 Model closures .....	123
5.9.3 Model Output .....	126

5.10 Conclusion.....	127
<b>Chapter 6 – Organisational modelling integration.....</b>	<b>129</b>
6.1 Process coupling.....	129
6.2 Trans-scale linkage.....	132
6.3 Modelling integration.....	135
6.3.1 Scale dependent variability of roughness .....	135
6.3.2 Flow resistance formulations.....	137
6.3.3 Boundary conditions.....	140
6.3.4 Linkage procedure.....	141
6.4 Conclusion.....	148
<b>Chapter 7 – Modelling results .....</b>	<b>149</b>
7.1 Modelling Scenarios.....	150
7.2 Results and discussion.....	155
7.3 Conclusion.....	182
<b>Chapter 8 – Conclusion .....</b>	<b>185</b>
Appendix A - One-dimensional water flow model code.....	220
Appendix B – Reach scale sediment flow and self-organisation model code .....	221
Appendix C - Reach scale reed community model code.....	222
Appendix D - Two-dimensional water flow model code .....	223
Appendix E – Channel-type scale bar evolution model code.....	224
Appendix F – Channel-type scale reed expansion model code .....	225

Appendix G – Geomorphological-unit scale water flow code .....	226
Appendix H – Geomorphological-unit scale bed-form development model code .....	227
Appendix I – Reed growth at geomorphological-unit scale model code.....	228

**Declaration**

I declare that this dissertation is my own, unaided work. It is being submitted for the Degree of Doctor of Philosophy to the University of the Witwatersrand, Johannesburg. It has not been submitted before for any degree or examination in any other University.

---

\_\_\_\_ day of \_\_\_\_\_ year \_\_\_\_\_



## **Abstract**

In a river, the local hydraulics, channel form and in-stream vegetation are interdependent. Although water, sediment and vegetation processes interact, they respond individually to flow characteristics at different spatial and temporal scales. This study employs a modelling approach that is based on the tendency of river systems to self-organise and produce emergence (emergent structures) in scale hierarchies. A hierarchical modelling strategy is proposed that arranges separate models describing vegetation and sediment dynamics at their appropriate scales, with their interaction described through feedback between the models.

Prediction of the river state at time scales of decades, over a range of spatial scales, is required for ecological river management to be more effective. However, river systems are complex, with complexity rooted deep in the river processes of water, sediment and vegetation holding implications for their modelling. Dealing with complexity in river geomorphological modelling is vital for achieving reliable predictions over decades, especially when considering that small-scale processes must be described to achieve this. Description of small-scale river form is not only required for river habitat management, but also affects the rates at which river form at larger scales changes. Hierarchy and non-linear theory provide a way to deal with the complexity of rivers by separating the river system into parts, and enabling these parts to interact.

Appropriate models and modelling methodologies were chosen or developed to represent the effect of interacting river processes of water, sediment and reeds at the progressively nested (largest) reach scale, the channel-type scale and (smallest) geomorphological-unit scale.

Existing water flow models at the reach scale and the next largest channel-type scale are used. The reach scale water flow model solves one-dimensional (1-D) Saint-Venant equations whereas the channel-type scale water flow model is governed by two-dimensional (2-D) Saint-Venant equations.

The water flow model at the smallest organisational level chosen for modelling is the geomorphological-unit scale. Water flow at the geomorphological-unit scale is not based on the actual physics of water flow, but it does account for the smaller scale variability of the water distribution.

The sediment model at the reach scale employs the Exner equation of sediment continuity in combination with gravel-bed-load transport equations to determine changes in bed elevation. At the channel-type scale, a Cellular Automaton (CA) model describes sediment transport through a river. The CA represents the river as a lattice of cells and predicts the volume of sediment stored in the cells. The sediment distribution obtained from the CA model describes the habitat for reeds. At the geomorphological-unit scale, a combination of existing formulations is used to predict the dimensions and growth of bed-forms representing sediment dynamics.

The vegetation models at the reach scale and the channel-type scale were developed specifically to describe dynamics of common reeds or *Phragmites Australis*. Reeds were chosen for modelling because of the large role they play as geomorphological modifiers. The reach scale model predicts the distribution of reed populations along the lateral river bank gradient whereas the channel-type scale reed model is a CA model that predicts the expansion of reed patches. The vegetation model at the geomorphological-unit scale is an existing model describing the growth of reeds by integrating finite differential equations of reed biomass growth.

River process interactions affect river geomorphology across these organisational levels. The models are integrated to provide feedback within a hierarchical modelling structure. Process models simulating sediment, water and vegetation dynamics within a specific organisational level are coupled through sharing the same spatial scale. Models of the same process producing patterns at various organisational levels are linked to share model information across organisational levels. Trans-organisational modelling linkage allows models to share outputs which provide boundary conditions and values for model parameters at specific locations within the modelling domain. A hierarchical framework allows prediction of small-scale geomorphology and accounts for its variability at the large scale.

The modelling strategy is demonstrated by simulations based on hypothetical scenarios of a gravel-bed river. The effect of sediment size and frequency of the flood event moving sediment, together with typical channel geometry, is shown for these. The modelling was computationally very intensive.

Results show that models focusing on only one organisational level can have very different outputs from those produced by trans-organisational modelling. The difference is due to emergence produced by dynamic small-scale processes that manifest at large scales.

Emergence was found in changing flow resistance coefficients obtained from smaller scale modelling. The flow resistance affected the river bed elevation at the reach scale. Emergence was indicated by the channel aggrading more for modelling with the inclusion of the effect of smaller scale river process interactions than without it.

These small-scale process interactions include water flow affected by bed-forms and reeds. Bed-forms and reeds affected energy loss significantly and provided a strong coupling between the flow and the river bed elevation. Hierarchical modelling therefore allows for reliable river geomorphology modelling over a decadal time scale by describing river complexity more realistically.

## **Acknowledgements**

I would firstly like to thank my parents for their unwavering support and encouragement who have helped me so much over the years. Professor Chris James, my supervisor, whose advice, guidance and example were both invaluable and greatly appreciated. Above all I am grateful to God the Father for all he has given me.

## List of figures

Figure 1.1 Representation of fluvial and ecological processes at different organisational levels of rivers (Richards, 2001) .....	4
Figure 1.2 Representation of the hierarchical modelling strategy used to incorporate feedback between models across organisational levels .....	7
Figure 2.1 A diagram showing the effective complexity varying as the system moves towards a state between order and disorder.....	10
Figure 2.2 Schematic showing sediment-hydraulics-vegetation interaction (James <i>et al.</i> , 2001a) .....	11
Figure 2.3 Ripples observed at a particular scale .....	11
Figure 2.4 Hierarchical descriptions of levels of organisation that characterise the geomorphological, hydrological and ecological subsystems of a river (Dollar <i>et al.</i> , 2007).....	13
Figure 2.5 Representation of river form linked through a hierarchical framework (adapted from Sear <i>et al.</i> 1995) .....	14
Figure 2.6 Process models linked to produce self-organisation and emergence (an emergent structure) at a particular organisational level (Adapted from Baas and Emmeche, 1997).....	19
Figure 3.7 Mid-channel bar formation (Hooke, 1997).....	37
Figure 3.8 Different types of alluvial bar. Increasing stability from mid-channel bar to scroll bar (Hooke, 1997).....	38
Figure 4.9 Fuzzy expert system (Passino and Yurkovich, 1998).....	46
Figure 4.10 Flow configuration (Wang and Weiming, 2004).....	51
Figure 4.11 Water and sediment routing in the Murray and Paola (1994) braid model. A given cell receives and distributes water from its neighbouring cells. Water flux is shown by blue arrows, direct sediment flux by yellow arrows and lateral sediment transport by brown arrows .....	57
Figure 4.12 No year-to year change in seedling recruitment due to germination falling in a zone where flooding occurs (Auble and Scott, 1998) .....	66

Figure 4.13 Seedling establishment in a zone where germination is unaffected by flooding and drought (Auble and Scott, 1998) .....	67
Figure 4.14 Inclusion of geomorphological change affecting seedling germination (Auble and Scott, 1998).....	67
Figure 5.1 Hierarchical models of sediment, water and vegetation processes across the reach scale, channel-type scale and geomorphological-unit scale. Downward arrows represent feedback through boundary conditions and upward arrows represent feedback through model parameters. Horizontal arrows represent feedback between water, sediment and reed processes .....	77
Figure 5.2 Idealised hydrograph associated with intermittency .....	81
Figure 5.3 Numerical solution scheme for the Exner equation of sediment continuity ...	82
Figure 5.4 Reed growth according to seasonal variation of water level in relation to ground level. Shoots are not drawn to scale (Karunaratne <i>et al</i> , 2003) .....	87
Figure 5.5 Asymmetrical triangle, which peaks at 1 and has a width of $w$ .....	90
Figure 5.6 Diagram indicating the distances to the centre of gravity .....	91
Figure 5.7 Final biomass (gDWT) of reeds after being subjected to four amplitudes of water level fluctuation (static, 15, 30 and 45 cm) at three elevations (20, 40 and 60 cm) (Deegan <i>et al</i> , 2007) .....	92
Figure 5.8 Membership functions for Average Yearly Water Flow Depth .....	96
Figure 5.9 Membership function for flow variability ( $COV_H$ ) for $H_{ave}$ = “Very High” ...	96
Figure 5.10 Membership function for flow variability ( $COV_H$ ) for $H_{ave}$ = “Very Low” .....	96
Figure 5.11 Membership function for Average yearly water flow depth. The DOTs for $H_{ave}$ = 0.58 m are indicated by the dashed line .....	98
Figure 5.12 Membership function for Flow variability associated with $H_{ave}$ = 0.58 m. The DOTs for $COV_H$ of 33 % are indicated by the dashed line .....	98
Figure 5.13 Membership function for % Maximum reed biomass associated with $H_{ave}$ = 0.58 m and $COV_H$ = 33 % .....	99

Figure 5.14 Typical model output providing the vertical distribution of percentage of the maximum <i>Phragmites</i> biomass density along the river bank. In the example above, a value of 66.7 % of the maximum possible biomass obtained at elevation above river bed $z = 1$ m .....	99
Figure 5.15 Staggered "MAC" mesh definition for 2-D shallow-water flow modelling .....	103
Figure 5.16 Flow chart of the procedure for the sediment model at the channel-type scale .....	107
Figure 5.17 Movement of sediment through a cell in a rectangular gridded computational domain .....	108
Figure 5.18 Sediment outflow determined from the Storage State $S_s$ and the sediment inflow for a given cell .....	110
Figure 5.19 Sediment distribution provided by a simulation of the sediment model at the channel-type scale .....	114
Figure 5.20 Maximum potential biomass for given cell elevations .....	115
Figure 5.21 Typical reed expansion at the channel-type scale. Rapid growth of reeds during summer months increases biomass density quickly, allowing expansion, which slows down during winter months when reed growth decreases. Expansion occurs after a biomass density of $2.6 \text{ kg/m}^2$ dry weight is reached .....	116
Figure 5.22 Volume element of a general interior cell $i,j$ for two-dimensional flow in rectangular coordinates .....	118
Figure 5.23 Growth events and average air temperature used as inputs to the reed growth model .....	122
Figure 5.24 Typical model output showing seasonal variation of <i>Phragmites</i> biomass (ash free dry weight) of shoots, inflorescence, roots, old rhizomes and new rhizomes .....	126
Figure 5.25 Geomorphological-unit scale reed model output with a change in initial rhizome biomass .....	127

Figure 6.1 A flow chain model, representing the integration of models providing output associated with a particular organisational level. The models are linked to provide feedback between sediment, water flow and vegetation processes (after Dollar <i>et al</i> , 2007) .....	130
Figure 6.2 Representation of trans-scale linkage where information produced by models representing the same physical processes (sediment, water and vegetation) at various organisational levels is shared. The grain of the higher-level model forms the extent of the lower-level model.....	134
Figure 6.3 Hierarchical modelling integration of sediment, water and vegetation processes across the reach scale, channel-type scale and geomorphological-unit scale. Arrows represent feedback through provision of model inputs, boundary conditions and parameters .....	142
Figure 6.4 Sub-procedure for water flow modelling at the reach scale.....	144
Figure 6.5 Sub-procedures for reed and sediment modelling at the reach scale .....	145
Figure 6.6 Sub-procedures for reed and water flow modelling at the channel-type scale .....	146
Figure 6.7 Sub-procedures for sediment modelling at the channel-type scale and reed modelling at the geomorphological-unit scale.....	147
Figure 6.8 Sub-procedures for water flow and sediment modelling at the geomorphological-unit scale.....	148
Figure 7.1 Schematic showing variables describing the channel dimensions. A trapezoidal channel was assumed .....	151
Figure 7.2 Flow regime specified for the particular modelling scenarios .....	151
Figure 7.3 Grain size distribution for feed and substrate typical for the stream type modelled (Rosgen, 1996). The initial $D_{50}$ of 0.011 m is indicated .....	153
Figure 7.4 Bedrock outcrops specified for scenario 3 .....	154
Figure 7.5 Self-organisation of bed elevations for scenario 1 at the reach scale. Self-organisation at the channel-type scale is shown for the hatched section in Figure 7.8.....	155



Figure 7.6 Self-organisation of bed elevations for scenario 2 at the reach scale. Self-organisation at the channel-type scale is shown for the hatched section in Figure 7.9 .....	156
Figure 7.7 The available reed habitat on the river bank lying on the entire area above the green line determined by the reach scale reed model for scenario 1 and 2 .....	157
Figure 7.8 Self-organisation of bed elevation for scenario 1 at the channel-type scale. The river between 900 m and 1000 m is shown for a 30 minute flood event beginning at 4 years and 6 months. The blue lines indicate the velocity vectors of the water flow and are placed at the water surface.....	158
Figure 7.9 Self-organisation of bed elevation for scenario 2 between 900 m and 1000 m beginning at 4 years and 6 months .....	159
Figure 7.10 Initial and 10 year reach scale bed elevations for scenario 1 with and without integrated smaller scale models. Details of the modelling results at the channel-type scale are shown for the hatched section in Figure 7.12 .....	159
Figure 7.11 Reach scale Manning's $n$ values along the river after every year for scenario 1 obtained from integrated smaller scale models. Details of the modelling results at the channel-type scale are shown for the hatched section in Figure 7.12.....	160
Figure 7.12 The yearly modelled river between distance 900 m and 1000 m for scenario 1 .....	161
Figure 7.13 Initial and 10 year bed elevations for scenario 2 with, and without integrated smaller scale models. Details of the modelling results at the channel-type scale are shown for the hatched section in Figure 7.15.....	162
Figure 7.14 Reach scale Manning's $n$ values for scenario 2 obtained from integrated smaller scale models. Details of the modelling results at the channel-type scale are shown for the hatched section in Figure 7.15 .....	162
Figure 7.15 The yearly modelled river between distance 500 m and 600 m for scenario 2 .....	163

Figure 7.16 Illustration of bedrock influencing 2-D water flow at the channel-type scale. The modelled river between distance 500 m and 600 m for scenario 3 is shown.....	164
Figure 7.17 Initial and 10 year bed elevations for scenario 3 with, and without integrated smaller scale models. Details of the modelling results at the channel-type scale are shown for the hatched section in Figure 7.19.....	165
Figure 7.18 Reach scale Manning's $n$ values for scenario 3 obtained from integrated smaller scale models. Details of the modelling results at the channel-type scale are shown for the hatched section in Figure 7.19 .....	165
Figure 7.19 The yearly modelled river between distance 500 m and 600 m for Scenario 3 .....	166
Figure 7.20 Reach scale Manning's $n$ values for all the modelling scenarios after year 2 and year 10. The scenarios gave significantly different Manning's $n$ values. Details of the modelling results at the channel-type scale are shown for the hatched section in Figure 7.22, Figure 7.23 and Figure 7.24.....	167
Figure 7.21 Downstream variation of $D_{50}$ for modelling scenarios initially and for year 10. Details of the modelling results at the channel-type scale are shown for the hatched section in Figure 7.22, Figure 7.23 and Figure 7.24 .....	168
Figure 7.22 The modelled river for scenario 1 between 400 m and 1000 m showing the template provided by the reach scale sediment model and flow depth provided by the reach scale water flow model.....	169
Figure 7.23 Modelled river scenario 2 between 400 m and 1000 m.....	170
Figure 7.24 Modelled river scenario 3 between 400 m and 1000 m.....	171
Figure 7.25 Reed height (m) and bed elevation (m) distribution for the flood flow modelling of scenario 1 in year 4. The river between 900 m and 1000 m is shown. ....	172
Figure 7.26 Velocity (m/s) and effective flow resistance height $k_e$ (m) distribution for the flood flow modelling of scenario 1 in year 4. The river between 900 m and 1000 m is shown. ....	173

Figure 7.27 Reed height (m) and bed elevation (m) distribution for the flood flow modelling of scenario 2 in year 4. The river between 900 m and 1000 m is shown. ....	174
Figure 7.28 Velocity (m/s) and effective flow resistance height $k_e$ (m) distribution for the flood flow modelling of scenario 2 in year 4. The river between 900 m and 1000 m is shown. ....	175
Figure 7.29 Reed height (m) and bed elevation (m) distribution for the flood flow modelling of scenario 3 in year 4. The river between 500 m and 600 m is shown. ....	176
Figure 7.30 Velocity (m/s) and effective flow resistance height $k_e$ (m) distribution for the flood flow modelling of scenario 3 in year 4. The river between 500 m and 600 m is shown. ....	177
Figure 7.31 Reach scale sediment transport rates along the river after every year for scenario 1 .....	181
Figure 7.32 Reach scale sediment transport rates along the river after every year for scenario 2 .....	181
Figure 7.33 Reach scale sediment transport rates along the river after every year for scenario 3 .....	181

## List of tables

Table 3.1 Factors affecting sediment transport (Heritage and van Niekerk, 1995).....	26
Table 5.1 Typical time steps used in the modelling at the various organisational levels for the vegetation, water and sediment hierarchies .....	78
Table 5.2 Data set used to determine the rule base for finding the percentage of total biomass density given average flow depth and flow variability.....	93
Table 5.3 Rule base for finding the percentage of total biomass density given average flow depth and flow variability .....	95
Table 5.4 Monthly flow depths at a point within the reach and associated Yearly Average and Covariance.....	97
Table 5.5 Angle of repose for various sediment sizes (van Rijn, 1993).....	112
Table 5.6 Monthly average daily temperature.....	114
Table 5.7 Parameters used in the reed growth model at geomorphological-unit scale (Asaeda and Karunaratne, 2000) .....	123
Table 5.8 Monthly global radiation and sun angle inputs to the reed growth model .....	125
Table 6.1 Range of variables for which the resistance equation (6.12) is applicable (Jordanova <i>et al</i> , 2006) .....	139
Table 6.2 Values of <i>a</i> and <i>b</i> coefficients for estimation of the drag coefficient as a function of the stem Reynolds number (Jordanova <i>et al</i> , 2006).....	140
Table 7.1 Monthly discharges input data into the 1-D water flow model to predict the monthly flow depths used by reach scale reed model to predict the maximum biomass density growing at a given elevation.....	152
Table 7.2 Average values for water flow and channel sediment attributes that impact on Manning's <i>n</i> values for scenario 1 between 900 m and 1000 m at various points in time.....	179
Table 7.3 Average values for water flow and channel sediment attributes that impact on Manning's <i>n</i> values for scenario 2 between 900 m and 1000 m at various points in time.....	180

Table 7.4 Average values for water flow and channel sediment attributes that impact  
on Manning's  $n$  values for scenario between 500 m and 600 m at  
various points in time..... 180

## List of symbols

$a$	Stem spacing
$A$	Flow area
$Age_{rt}$	Age of roots
$b$	Channel width
$B$	Biomass
$B_{leaf}$	Leaf biomass
$c_a$	Cohesion
$c_{bk}$	Equilibrium concentration
$C_D$	Drag coefficient
$c_k$	Local concentration
$C_n$	Courant Number
$COV_H$	Coefficient of variance for yearly flow depth
$c_s$	Non-dimensional Chezy coefficient
$C_{tk}$	Depth-averaged sediment concentration
$d$	Water depth
$D$	Representative grain-size
$D_{50}$	Median grain size
$D_{bk}$	Downward sediment flux
$D_H$	Hydraulic diameter
$D_{stem}$	Stem diameter
$E_{bk}$	Upward sediment flux
$F$	Reed resistance coefficient
$f$	Coriolis coefficient

$f$	.....	Dimensionless Darcy–Weisbach friction coefficient
$g$	.....	Gravitational acceleration
$g_m$	.....	Maximum specific growth rate
$G_{rt}$	.....	Photosynthesized material for root growth
$G_t$	.....	Annual sediment yield
$G_{tf}$	.....	Sediment feed rate
$H$	.....	Height of the water surface
$H_{ave}$	.....	Mean yearly flow depth
$H_b$	.....	Bed-form height
$H_{be}$	.....	Equilibrium bed-form height
$i$	.....	Computational node
$i_b$	.....	Specific bedload transport rate
$I_f$	.....	Intermittency
$I_{PAR}$	.....	Photosynthetically active radiation
$k$	.....	Erodibility coefficient
$k$	.....	Turbulent kinetic energy
$k_e$	.....	Effective hydraulic roughness height
$k_{frac}$	.....	Photosynthesis fraction
$k_{li}$	.....	Light extinction coefficient
$L$	.....	Reach length
$LAI$	.....	Leaf area index
$L_b$	.....	Bed-form length
$L_{be}$	.....	Equilibrium bed-form length
$l_d$	.....	Turbulence length-scale

$L_s$	Nonequilibrium adaptation length
$m$	Cell weight
$n$	Manning's hydraulic roughness coefficient
$p$	Pressure
$p_{frac}$	Panicles fraction
$Ph_{sht}$	Photosynthesis of shoots
$P_m$	Maximum specific net daily photosynthesis rate of the plant
$Q$	Discharge
$q$	Shoot elongation fraction
$q_b$	Bed-load sediment transport
$Q_o$	Water flow
$Q_s$	Sediment transport flux
$r$	Ratio of lift to drag
$R$	Hydraulic radius
<b>Re</b>	Reynolds number
$Rhif$	Biomass mobilization
<b>s</b>	Submerged specific gravity
$S$	Bed slope
$S_e$	Energy gradient
$S_f$	Friction slope
$S_i$	Topographic gradients
$S_l$	Lateral slopes
$SO$	Sediment outflow
$S_r$	Earth shear stress at failure



$T$	.....	Daily average temperature
$t$	.....	Time
$t_e$	.....	Equilibrium time
$t_f$	.....	Flood duration
$Th$	.....	Sediment transport threshold
$U^*$	.....	Shear velocity
$U$	.....	Depth-average flow velocity
$V$	.....	Depth-average flow velocity
$W$	.....	Vertical flow velocity
$x$	.....	Length
$y$	.....	Length
$y$	.....	Water surface elevation
$y_{frac}$	.....	Shoot assimilates fraction
$z$	.....	Length
$\alpha_{rhi}$	.....	Specific rhizome biomass transfer rate
$\delta_b$	.....	Bed-load layer with a thickness
$\delta_j$	.....	Kronecker delta
$\varepsilon$	.....	Erosion rate
$h$	.....	Bed elevation
$\theta$	.....	Sun elevation
$I_p$	.....	Porosity
$\mu$	.....	Dynamic Coulomb coefficient of friction
$\mu_a$	.....	Air pressure
$\mu_w$	.....	Pore water pressure

$v_t$	.....	Eddy viscosity
$\rho$	.....	Fluid density
$\rho_s$	.....	Sediment density
$t$	.....	Shear stress
$t^*$	.....	Shields' shear stress
$(\tau)_c^*$	.....	Shields' entrainment number
$t_b$	.....	Boundary shear stress
$t_c$	.....	Critical shear stress
$\tau_o$	.....	Average shear stress
$\psi$	.....	Matric-suction
$\omega$	.....	Stream power
$\omega_o$	.....	Critical specific stream power
$\omega_{sk}$	.....	Settling velocity

# **Chapter 1 – Introduction – The need for trans-organisational modelling**

---

## **1.1 Introduction**

### **1.1.1 River management**

River management is multi-objective, inherently interdisciplinary and is concerned with a range of spatial and temporal scales. There is a range of ways in which river managers can effect change in rivers. The introduction of environmental values has led to a shift from reactive river engineering to proactive sustainable management of rivers over decadal time scales. However, in order to manage rivers, decision-makers need to know how their actions will affect other components of the complex, interconnected systems involving water, sediment and biota. Managers need to consider effects of vegetation biomass change and changing land use on sediment deposition rates and channel plan form change. Managers need to understand what effect changes in timing and magnitude of water flows have on ecosystem productivity and biodiversity. To reduce uncertainty, river managers require prediction of the behaviour of the river patterns arising at various scales.

The complexity of rivers is well illustrated by the problems experienced by the Kruger National Park (KNP) in managing the Sabie River. Development in the Sabie River catchment changes flow and sediment regimes of the river (Birkhead and James, 2000), making it more difficult for management to keep to its vision: “To maintain biodiversity in all its natural facets and fluxes to provide human benefits, in a manner that detracts as little as possible from the wilderness qualities of the KNP”. The changes in sediment and flow regimes lead to adjustments to river geomorphology with associated changes in aquatic and riparian fauna and flora (Birkhead and James, 2000). There is intense pressure on KNP management to understand and conserve the natural role of aquatic systems in the Park (Rogers and Bestbier, 1997).

Management of the Sabie River is further complicated by a highly diverse and mixed bedrock alluvial geomorphological structure (van Niekerk *et al*, 1995). The high degree of patchiness of different geomorphic units plays an important interactive role in influencing species distribution patterns (Hupp and Osterkamp, 1985). The general sequence of succession in KNP rivers progresses by open water and rock areas being occupied by sediment which is colonised by reeds, followed by bushes and finally by trees (Rogers, 2002).

*Phragmites* reeds play a large role as a geomorphological modifier within rivers in the KNP. In the Sabie River, for example, there is a high diversity of geomorphological features due to a mixture of alluvial sediment and bedrock characteristics and a variable flood regime. Among these geomorphic features are sediment bars which are often colonised by reeds (Nicolson, 1999). When floods pass through bars covered with *Phragmites* reeds the shear stresses on the bars will not be as high as with unvegetated bars and they will therefore not erode (James *et al*, 2001a). Reeds and other herbaceous vegetation are pioneer species and provide a suitable habitat for the establishment of tree species (van Niekerk and Heritage, 1993). As a consequence, reeds are modelled in this study.

### **1.1.2 Geomorphological prediction**

River geomorphology is founded on the shapes or forms observed in rivers. The prediction of the state of river geomorphology caused by modified land and water use is becoming increasingly important in environmental management of rivers. Modified amounts of sediment flowing into rivers, the flow regime and riparian vegetation cover can greatly affect the river form on a decadal scale. River geomorphology affects the river ecology through changes in riverine habitat (Nicolson, 1999). Habitat and biota are affected and, in turn, affect river processes over a range of scales (Nestler *et al*, 2005; Dollar *et al*, 2007). Biological response may be directly related to habitat at various scales (Heritage *et al*, 1997) in which discharge is manifest as flow depth, velocity and boundary shear stress (James *et al*, 2001a). Prediction of river state at timescales of decades is required for ecological river management to be effective (Hooke *et al*, 2005).

The prediction period, however, is limited firstly through uncertainty about the water and land use and secondly through the feedback that smaller scale changes have on larger scale events, which becomes increasingly unknown over longer prediction periods. The size of evolving bed-forms or whether there will, in fact, be vegetation growing in a reach in future years, for example, can greatly affect river geomorphology. Knowledge about such geomorphic modifiers decreases for prediction further into the future. Currently, predictive capability regarding habitat is satisfactory at small spatial scales (metres) but insufficient at large time scales (decadal) because of river complexity. The complexity of river processes prevents current prediction at a large scale from including the effect of smaller scale variability. In that sense, river complexity also hinders the possibility of deriving smaller scale habitat from large-scale river form and therefore makes habitat difficult to predict over larger time scales. This study employs a 10 year period over which simulations were made to show that the hierarchical modelling strategy can improve modelling at these large temporal scales.

## **1.2 Aim**

### **1.2.1 Motivation for study**

Patterns forming at slow and large scales are constructed and organised by the interaction of many small and fast processes (Zhang *et al*, 2004). For example, the movement of sediment particles, which are observed at a resolution of milliseconds and millimetres, determines bed-form dynamics on the bed observed at a resolution of minutes and centimetres. At even larger scales, sediment movement determines where sandbars are formed. These are observed at a resolution of hours and metres. At still larger scales, sediment movement determines the channel plan form observed at a resolution of days and tens of metres.

Although the individual components of rivers can in themselves be complex, it is easier to describe them individually. A river in its whole however, is more than the sum of the parts and new or hidden properties may emerge that cannot be readily predicted from its basic components (Haschenburger and Souch, 2004). For example, the movement of sediment

grains under the action of water sets up distinct bed-forms. The bed-forms affect water flow to result ultimately in a particular channel pattern or arrangement, which in turn affects how the grains within a river move. It is these emerging patterns that cannot be discerned from the movement of sediment grains only. In order to simulate the behaviour of rivers, it is necessary to understand not only how the individual parts behave in isolation, but also how they interact, to determine the behaviour of the whole river (Malanson, 1999; Michaelides and Wainwright, 2004).

To determine the behaviour of a river as a whole it is necessary to account for feedback between organisational levels (Spedding, 1997; Harrison, 2001; Richards, 2001). Figure 1.1 identifies a range of organisational levels and their related processes. The diagram implies feedback between successive scales (Richards, 2001) and concerns smaller scale heterogeneity affecting larger-scale modelling (Albert, 2000).

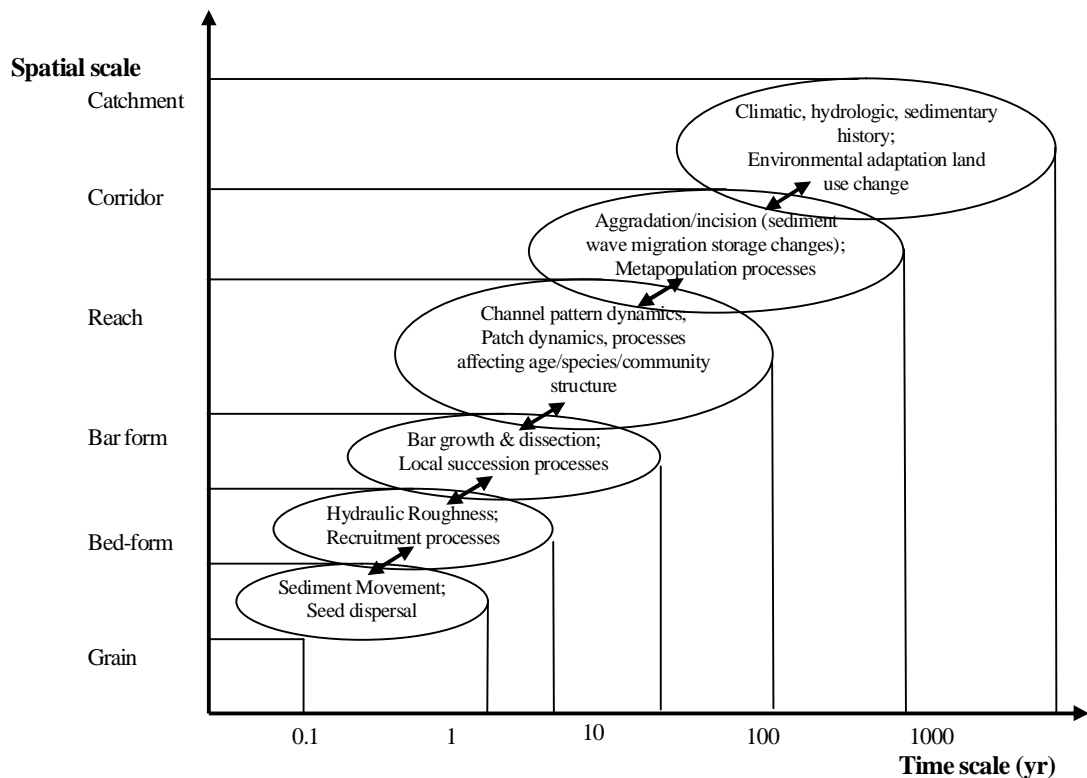


**Figure 1.1 Representation of fluvial and ecological processes at different organisational levels of rivers (Richards, 2001)**

Better geomorphological prediction depends not only on how well modelling describes the patterns at a particular organisational level but also on how well feedback from higher or lower organisational levels can be incorporated (Dollar *et al.*, 2007). Processes can be unified across scales via so-called nested models, which link models of similar river processes but describe patterns at different scales, to share model output (Paola, 2001; Lenaerts *et al.*, 2002). This can be achieved by the dynamical hierarchies concept, where higher-order structures are a product of the interactions and properties of the lower-level components (Lenaerts *et al.*, 2002; Dollar *et al.*, 2007). Organisational models may produce spatial patterns which affect the way regularities at higher levels emerge (Harrison, 2001) and can be linked through models describing emergent structures, as described in section 2.4 (Lane and Richards, 1997). This concept is reinforced by Harrison (2001), who states that rivers, as dissipative geomorphological systems, adjust form over various scales through emergent structures affecting one another.

### **1.2.2 Objectives**

The aim of this study is to show that models providing feedback in a hierarchical modelling framework deal better with the complexity of river morphodynamics than disconnected scale-specific models. A hierarchical modelling framework allows process interactions over various scales to be integrated by links that are able to transmit feedback between models logically. It allows effective use of models representing small-scale process to explain events at the larger spatio-temporal scales where much geomorphological prediction for environmental management is required. Hence, modelling frameworks set up a coherent way to allow non-linear processes of water sediment and vegetation to interact over a range of scales. The objective of this study is to link models within a hierarchical modelling framework to simulate river form for a period of 10 years.

River morphodynamics are simulated to include *Phragmites* reeds interacting with water and sediment processes, modelled using a hierarchical strategy. Patterns produced by these process interactions at a range of scales are described by process models which are progressively nested to account for smaller scale variability while still allowing interacting processes at similar scales to provide feedback. The complexity of rivers necessitates

separate models for sediment water flow and vegetation processes at various scales to allow “real time” up-scaling, which is achieved by allowing models representing large-scale processes (kilometres and years) to affect smaller scale process models (metres and seconds) continuously, through boundary conditions. Small-scale models influence material flows of larger scale models by adjusting model parameters.

In order to achieve these aims, the specific objectives are:

- 1) To determine appropriate models and modelling methodologies to represent the effect of interacting river processes of water, sediment and vegetation at various organisational levels;
- 2) To further the predictive capability of river geomorphological modelling by developing an approach that incorporates the feedback amongst processes across organisational levels.

### **1.2.3 Approach**

The hierarchical modelling strategy that allows trans-scale linkage of water sediment and vegetation processes is shown in Figure 1.2 and proceeds as follows:

- 1) At the reach scale, a water flow model drives a sediment model predicting bed elevation. The bed elevation is fed back to the water flow model to determine the resulting water flow distribution. The new bed elevations from the sediment model together with the monthly flow depths from the water flow model are used. A reed model at the same scale is used to determine the reed population distribution after every year.
- 2) At the channel-type scale, a detailed flow model drives the sediment model, which predicts new bed elevations, updated in the water flow model to result in a new flow distribution. The reed patch dynamics, determined at the same scale, affects the resistance to water flow.
- 3) At the geomorphological-unit scale, an interpolated flow distribution allows bed sedimentary characteristics to be estimated by a sediment model. At the same scale a reed model determines reed growth according to the weather.
- 4) The water flow model at the reach scale provides the boundary conditions for the water flow model to determine the intermediate flow distribution at the channel-type scale.



Similarly, the sediment model at the reach scale provides the initial template for predicting bed elevations at the channel-type scale. The reed model at the same scale predicts the manner in which patches of reeds expand, based on the available habitat provided by the reach scale reed model.

- 5) The water flow model at the channel-type scale provides boundary conditions to determine the intermediate flow distribution at the geomorphological-unit scale. The grain size is also transferred to lower organisational levels to determine sedimentary characteristics.
- 6) The reed model at the channel-type scale predicts the expansion of reed patches according to biomass growth determined at the geomorphological-unit scale. The modelled sedimentary characteristics at the geomorphological-unit scale affect shear stresses which are averaged to determine flow resistance for water flow modelling at the channel-type scale.
- 7) The shear stresses due to flow resistance at the channel-type scale are further averaged to determine flow resistance values for water flow modelling at the reach scale.

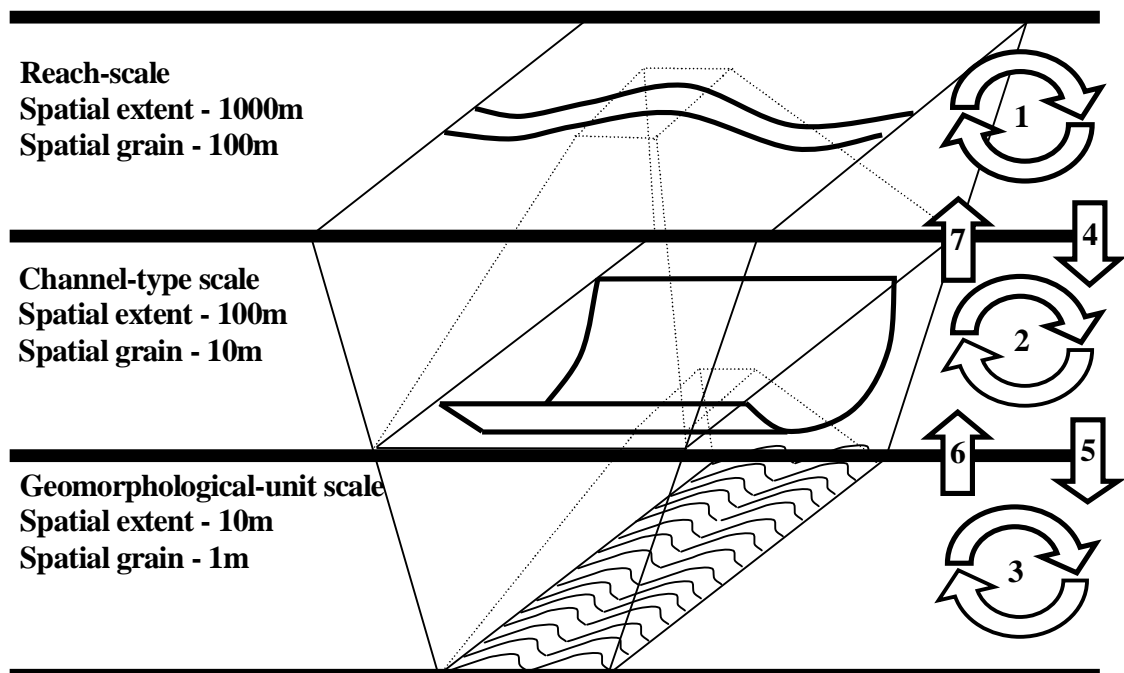


**Figure 1.2 Representation of the hierarchical modelling strategy used to incorporate feedback between models across organisational levels**

## Chapter 2 – River complexity

---

Rivers are complex systems existing in states somewhere between order and disorder. Order refers to the patterns arising from a multitude of processes. Ripples on the river bed arising from sediment processes constitute such patterns, for example. It is by virtue of the development of such patterns that rivers are not completely chaotic, and a measure of predictability does exist. Patterns arise as the river approaches stability, which is a function of the availability, movement and organisation of water, sediment and vegetation through time. The effect of these patterns is non-linear.

Non-linearity implies that it is difficult to create a model that would describe patterns observed over a wide range of scales. It is easier to break the river system up into different parts and have a model for each part, but ignoring their interactions would result in incomplete description of the whole-system behaviour. Hierarchy and non-linear theory provide a way to deal with the complexity of rivers by breaking up the river system into parts and allowing these parts to interact.

This chapter reviews what is thought of as complexity and exactly why rivers are considered to be complex systems. It discusses how models of rivers unravel river complexity and how complexity theory can help to achieve reliable river modelling.

### 2.1 Complexity and modelling

The root meaning of the word complexity is “interfolded” or “braided together”, implying that a complex system is not easy to understand. Gell-Mann (1994) studied complexity and set out to find out what constitutes a complex system. He defined the term “crude complexity” as simply the length of description. If a complex system, for example, were described using words, it would take a great number of words to describe that system and all its attributes. The greater the number of words, the higher the crude complexity of the

system. When a part of the system is well understood, the length of description of that part can be shortened into a single concept or even a single word.

“Effective complexity” is the length of description using the separate parts already shortened. Effective complexity is a good way to determine how complex the system models really are and is discussed in more detail below (Gell-Mann, 1994).

Models demonstrate a scientific understanding. While a complex system is an open system, models usually describe only a part of the system (Cilliers, 2001). Often mathematical equations are used to explain the part of a system using dependent variables given independent variables. Gell-Mann (1994) gives the example of an ecologist counting trees of a species used as independent variables. The ecologist may realise that for much less effort, groups of these trees could be counted and would still provide the data necessary to verify the model. Even large patches of tree species can be counted and still verify the model. It is, therefore, necessary to specify a level of detail up to which the system is described, whilst ignoring the finer details. This is known as coarse-graining. Coarse-graining adapts the dependent variables, enabling the model to be more easily described mathematically. Such a model is still able to explain how the system is understood.

The way the model is coarse-grained will therefore result in some information being lost but it would add to the understanding of the system since the effective complexity is reduced. Effective complexity involves two aspects of a model. The first is how difficult it is to formulate the model for the part of the system it is coarse-grained to describe. The second is how difficult it is to apply the model practically. Both become more difficult as the system moves to an intermediate point between order and disorder and therefore increases the effective complexity (Figure 2.1).

A brief model can sometimes describe a whole range of dynamic patterns. Compression of patterns into a brief model is much easier for a very ordered system since one river arrangement would not differ significantly from another. If the behaviour were very disordered, patterns would not have to be reproduced and a brief model would also be enough to recreate the same, almost random, behaviour (Gell-Mann, 1994). The ripple and

dune geometry model, described in section 5.8, for predicting the development of bed-forms from initial to an equilibrium state uses only a small number of equations. No more than a few equations are used because of the ordered nature of bed-form behaviour. However, their disordered nature produced by their varied and changing geometry makes it difficult to reduce the number of equations. The model therefore has high effective complexity.

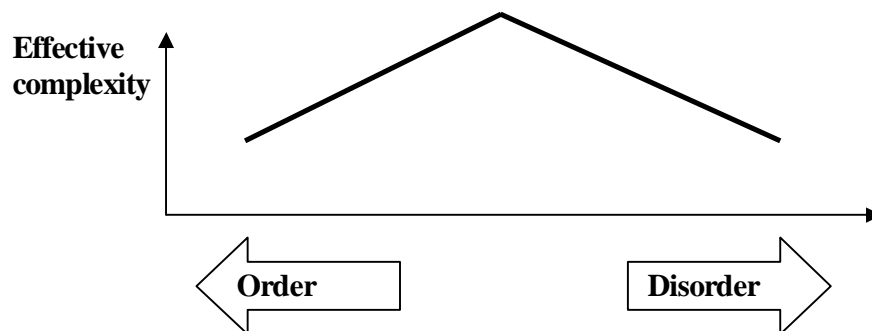


**Figure 2.1** A diagram showing the effective complexity varying as the system moves towards a state between order and disorder

A model may use only simple equations but the program procedure to run that equation may produce complex behaviour (Wolfram, 1984). For example, the Cellular Automata modelling, described in section 5.5, used to model sediment bar dynamics, uses a simple sediment routing formulation according to local bed slopes. The disordered nature of sand bar development as flow moves in many directions makes it very hard to apply this simple formulation and requires much computer code. The model therefore also has high effective complexity.

## **2.2 Reasons for river complexity**

The complexity of a system increases as the number of interacting processes increases (Cilliers, 2001). Rivers are complex since their behaviour involves many processes. “Process” in rivers refers to the dynamic series of actions or operations producing a particular river arrangement or distribution of biota (Habersack, 2000).

In a river, the water, sediment and vegetation processes interact. Vegetation and river form determine hydraulic conditions for a given discharge; hydraulic conditions and river form define habitat for vegetation establishment and growth; vegetation and hydraulics determine form by controlling the movement, trapping and storing of sediment (Figure 2.2) (Jordanova and James, 2003; Michaelides and Wainwright, 2004).

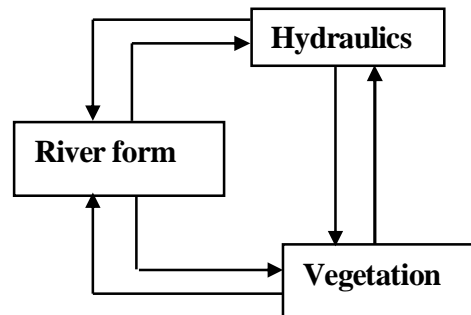


**Figure 2.2 Schematic showing sediment-hydraulics-vegetation interaction (James *et al*, 2001a)**

Patterns produced by sediment, hydraulics and vegetation processes can be observed over many scales within a river (Montgomery, 1999). Scale determines the units appropriate for observing patterns. It is characterised by grain and extent, and defines the upper and lower limits of resolution of the scale at which the model explains the process dynamics (Dollar *et al*, 2007). Figure 2.3 illustrates bed-forms observed at an extent of about 1 metre and a grain not much larger than 10 centimetres. Making the grain too large or extent too small will result in no distinguishable pattern being discerned.

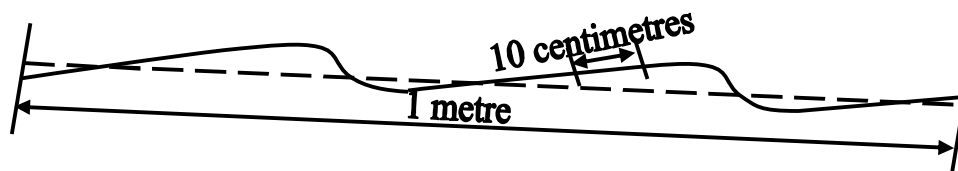


**Figure 2.3 Ripples observed at a particular scale**

As the range of scales over which observations are made increases, it becomes harder to compress the patterns, produced by processes, into models. For example, patterns produced by sediment process of a river can be found at a very large extent to include

planform patterns such as meandering or bar development. Stand-alone models for sediment dynamics do not exist over the entire range of scales over which these patterns are discerned. Increasing the extent therefore requires an increase in the number of models necessary to describe all the patterns that will be observed as a result (Haschenburger and Souch, 2004). In order to simulate the full range of river behaviour, separate models have to represent patterns produced by processes at all required scales (Lenaerts *et al*, 2002).

Hence, the effective complexity of rivers at a particular scale is high but increases even more as the extent increases and the grain decreases. Including interacting processes increases the effective complexity of rivers even more. The effects of these process interactions at the larger scales are non-linear. Non-linearity indicates that what happens at a smaller scale cannot be summed to produce larger scale effects, i.e. superposition does not apply. Non-linearity is prescribed by complex systems (Cilliers, 2001) and is outlined in section 2.4.

### **2.3 Hierarchical description**

Hierarchies are useful devices for organising models at various spatial and temporal scales or organisational levels (Wu and David, 2002). Hierarchy theory allows aspects of rivers to fit into naturally occurring levels that share similar time and space scales and interact in systematic ways (Jewitt and Görgens, 2000; Harrison, 2001; Favis-Mortlock, 2004). The higher levels are characterised by high perspective and low detail and the lower levels, by low perspective and high detail (Lane and Richards, 1997; Jewitt and Görgens, 2000). At coarse scales the effects of local heterogeneity are averaged out or coarse-grained, so that patterns appear to be more predictable (Wiens, 1998). Patterns forming at a particular scale within the hierarchy constitute an organisational level (O'Neill *et al*, 1989; Dollar *et al*, 2007) as shown by Figure 2.4.

Macro-reaches can be defined as stretches of river where flow and sediment regime influences are sufficiently uniform to result in similar channel-types. Within macro-reaches are a variety of channel-types (such as braided or meandering) and within each channel-

type are geomorphic units (Thorp *et al*, 2006). A channel-type is characterised by a particular combination of geomorphic units (van Niekerk and Heritage, 1993) and assumed to be representative of all similar stretches of the river. A geomorphic unit is a sedimentary or bedrock structure forming a feature in the river channel, e.g. a pool or a bar.

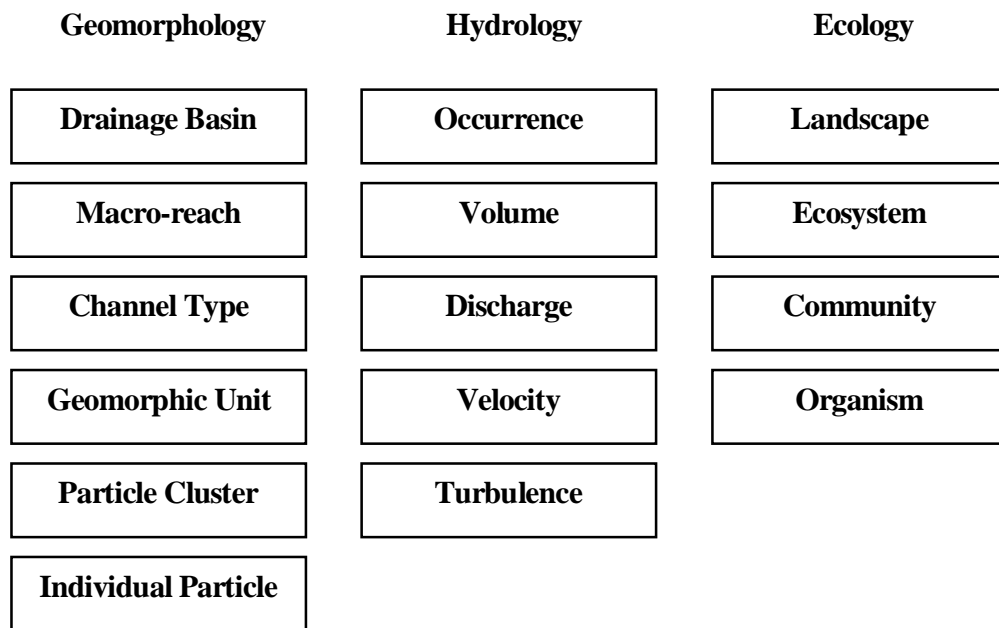


**Figure 2.4 Hierarchical descriptions of levels of organisation that characterise the geomorphological, hydrological and ecological subsystems of a river (Dollar *et al*, 2007)**

Vegetation at different scales is adequately represented through the ecology hierarchy (Barrett *et al*, 1997), and describes a plant population as a collection of interbreeding plants. Vegetation responses are observed at the spatial and temporal scales considered important by the experts studying them. At one extreme end of resolution, vegetation could be described as simply absent or present and at the other end by the number and size of individuals of a particular species and their location within the reach. It is also not practical to model vegetation dynamics at time steps as small as hours because the changes in vegetation structure would be too small to have significant effects on river form. Sensitivity analyses show that processes at very small time scales (such as plant growth) can be neglected at larger temporal scale, since changes in population distribution would appear stagnant (Jewitt and Görgens, 2000). Hydrology can be described at most spatial

and temporal scales and can easily be related to both vegetation and sediment organisational models.

Hierarchical descriptions can be integrated within a hierarchical framework as illustrated in Figure 2.5, which integrates different river processes to describe river form dynamics at various organisational levels.

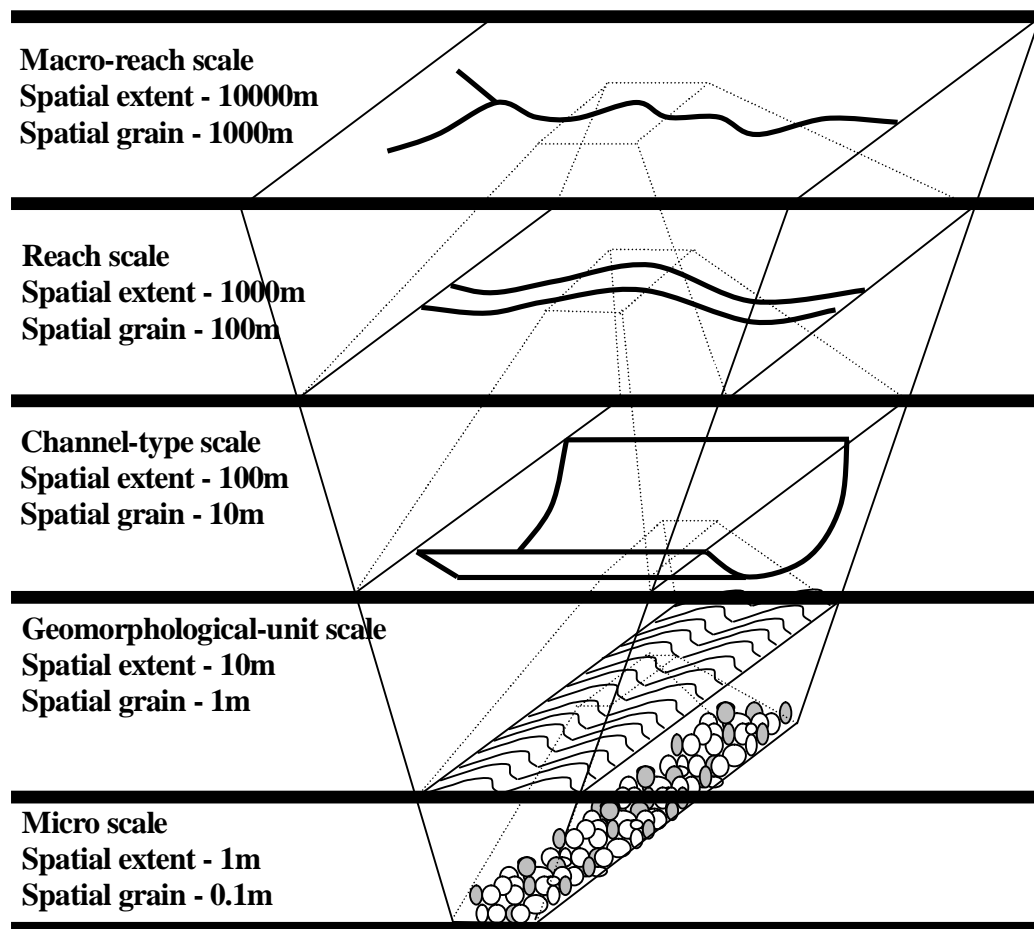


**Figure 2.5 Representation of river form linked through a hierarchical framework (adapted from Sear *et al.* 1995)**

The extent of a lower organisational level is represented at the grain of a higher organisational level. The organisational levels important for decadal geomorphology prediction are loosely the reach scale, channel-type scale and the geomorphological-unit



scale because at these temporal scales these organisational levels have the most tangible effects on geomorphological change. These organisational levels, however, should be adaptable and not fixed because pattern determines scale and not the other way around (Cilliers, 2001).

## **2.4 Non-linearity of river processes**

### **2.4.1 Up-scaling**

Up-scaling allows transference of small-scale variability to make large-scale predictions (Spedding, 1997). Up-scaling is needed for river management to assess the overall ecology and not just at the scales where important biotic aspects are observed (Habersack, 2000).

Statistical up-scaling focuses on how best to represent the spatial variability of small-scale properties at the large scales, taking advantage of strongly linearizable smaller scale properties. Statistical up-scaling embeds or reflects small-scale process effects but does not explain the relevant processes. Statistical up-scaling produces simple lumped models which may not be sufficient to capture the complexity produced by interacting river processes. Such models may agree with spatial behaviour but temporally still be unable to estimate geomorphological change to a consistently high level of accuracy (Haff, 1996). This is primarily due to the non-linear large-scale effects of these small-scale river processes. The non-linearity of river geomorphology is indicated through the presence of self-organisation and emergence within river systems (Haff, 1996). Self-organisation and emergence form part of non-linear theory used to characterise complex systems (Wu and David, 2002; Bogena and Diekkrüger, 2002).

A more effective up-scaling method than statistical up-scaling is presented in this study. This method uses a hierarchical modelling approach which is a “real time” up-scaling where small-scale processes are simulated concurrently and interact with the large-scale ones. This dynamic up-scaling approach uses the spatially averaged numerical outputs of models representing small-scale process.

## 2.4.2 Self-organisation

De Wolf and Holvoet (2004) proposed a working definition for self-organisation: “Self-organisation is a dynamical and adaptive process where systems acquire and maintain structure themselves, without external control.”

Self-organisation in rivers is closely related to the equilibrium concept (De Wolf and Holvoet, 2004). Equilibrium of river form is maintained by energy dissipation to tend to a point where the inputs and outputs of mass and energy into system are equal (Graf, 1988). The destabilisation of rivers typically occurs when the balance between controlling factors becomes altered. The controlling factors are discharge, sediment load, size of bed material, vegetation (riparian and/or upland species) and slope.

Any change in these controlling factors may result in new river form tending towards a new equilibrium state. It sets up a series of concurrent adjustments to seek a new equilibrium (Leopold *et al*, 1964). Hack (1960), used the term "dynamic equilibrium", referring to a system in which there is a continuous inflow of materials where the form or character of the system remains unchanged. Energy-dissipating functions are dependent on flow resistance coefficients, which adjust the river system's ability to balance the inputs and outputs of water and sediment (Phillips, 1996).

In the self-organised state of a fluvial system, the outflow would be equal to the inflow with no change in river form patterns. Pushing the fluvial system into disequilibrium causes the inflow and outflow of sediment to become different and adjust river form patterns. The adjustment would be rapid at first but would slow down as the system moved towards a self-organised state.

Self-organisation of river form can be observed at various organisational levels (Thorne and Welford, 1994; Eaton *et al*, 2004) such as drainage networks, slope morphology and bed-forms (Phillips, 1996). At the geomorphological-unit scale, ripples or dunes self-organise under the action of flowing water. A constant flow of water and sediment for long enough will cause bed-forms eventually to develop a constant length and height (Raudkivi, 1997). The bed-form might still move but the length would remain the same. This dynamic quality is referred to as “self-organised criticality”. Self-organised

criticality can be considered as a dynamic state of the pattern, describing the whole system, which maintains itself at a critical point (Bak, 1996, Fonstad and Marcus, 2003).

Bars may also self-organise critically by migrating within a channel. They may still appear to move but the amount of sediment stored in the system remains unchanged (Huang *et al*, 2004). At higher organisational levels, river geometry such as width, depth, sinuosity and longitudinal grain size distribution also self-organise critically (Stølum 1996; Sapozhnikov and Foufoula-Georgiou, 1996). It has been noted by Paola (2001) that this dynamic behaviour of river form stabilises as vegetation colonises the resulting template.

### **2.4.3 Emergence and emergent structures**

Emergence of river form patterns is important at various organisational levels (Church, 1996). An emergent phenomenon is seen as a large-scale, group behaviour of a system, which does not seem to have any clear explanation in terms of the system's constituent parts (Schweber, 1993; Darley, 1993). De Wolf and Holvoet (2004) proposed a working definition for emergence: "A system exhibits emergence when there are coherent emergents at the macro-level that dynamically arise from the interactions between the parts at the micro-level. Such emergents are novel with respect to the individual parts of the system."

A river may be considered as an emergent phenomenon. From a purely reductionist point of view, a river could be viewed as a continually fed flow of water molecules. It would not be considered a river but rather water molecules in motion. To view the river in this light would deny opportunities to increase the understanding of the river in its entirety, since much of the explanatory power would be lost. Such an opportunity would be to describe the river as used by its biota. To its biological inhabitants the river is a persistent feature of their environment. The river's emergence therefore lies not in the materials that drive the process but rather in the collection of processes that exists (Abbott, 2005).

De Wolf and Holvoet (2004) compared self-organisation to emergence and noted that a process can be characterised by self-organisation or emergence or both. Self-organisation is mostly associated with emergence. Emergence can exist without self-organisation when there is a micro-macro effect but no increase in order. Self-organisation can exist alone when there is an increase in order but no micro-macro effect. There are few similarities between emergence and self-organisation, other than that both arise from dynamic processes over time. Together, they constitute an emergent structure and can be used to integrate the many parts of complex systems (De Wolf and Holvoet, 2004; Inamdar, 2006). Micro-forms self-organise length and height to change flow resistance that emerges at larger scales. Bed-forms therefore display both self-organisation and emergence and can be considered to be emergent structures.

In rivers, emergent structures arise within organisational levels. Self-organisation at a lower level can affect self-organisation at a higher level through emergent structures. An example is the self-organisation of sediment bars observed at the channel-type scale. The manner in which a bar self-organises or arranges depends on the effect that other bars and vegetation within the same channel have on water flow, i.e. bars and vegetation provide feedback to create a particular pattern within the channel. Hence, when the system is viewed at the higher organisational level or, in this case, the channel-type scale, a particular pattern emerges that is made up of sediment bars self-organising towards an equilibrium state and becoming constant if controlling factors also remain constant. It is this emergent pattern that allows the channel-type to be classified. Figure 2.6 shows the feedback between river processes at a lower level allowing patterns at the larger scale to emerge.

From a reductionist point of view, river form can also be considered to be made up of sediment particles. However, that would exclude the way in which these particles are ordered. Observation of sediment organisation at increasing scales reveals the emergence of ordered patterns including bed-form, sediment bar and planform patterns. These patterns are discerned at various scales and can be described from the top down, using emergent laws. Baas and Emmeche (1997) summarised emergent laws as the general principles of the regularities produced by emergent structures. Ripple and dune formation on river beds,

for example, is an emergent phenomenon. These bed-form patterns can be described by emergent laws such as van Rijn's (1984) empirical equations. These laws are used to predict the length and height of bed-forms and the time it would take for these bed-forms to develop. An emergent property stemming from micro-forms is roughness, which determines how larger scale water flow is affected.

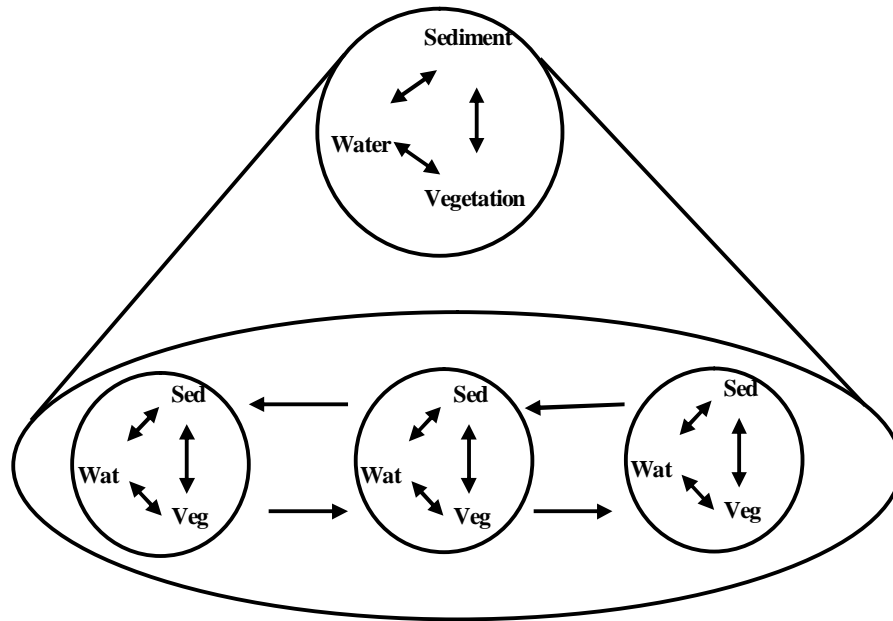


**Figure 2.6 Process models linked to produce self-organisation and emergence (an emergent structure) at a particular organisational level (Adapted from Baas and Emmeche, 1997)**

## 2.5 Conclusion

Dealing with complexity in river geomorphological modelling is vital to achieve reliable predictions over decadal time scales, especially when considering that small-scale processes are required to achieve this. It is largely the interacting processes of water, sediment and vegetation that contribute to river complexity. The non-linearity of river process interactions means that modelling has to allow for emergent structures at various organisational levels. It is therefore necessary to investigate the details of these interacting processes and the particulars of the feedbacks that affect river form.

The aim of this study is to further the predictive capability of geomorphological modelling by developing an approach that is able to deal with the complexity associated with rivers. In order to make better predictions over decadal time scales, the interactions across scales must be considered. The hierarchical modelling strategy links emergent structures forming at various organisational levels by using the coarse-grained predictions of water flow resistance at smaller scales to make predictions at larger scales. The predictions of material flows of water, sediment and biomass at larger scales form the boundary conditions around which the smaller scale predictions are made.

The following chapter describes river processes and the feedbacks affecting river geomorphology, in order to determine the modelling that is required.

# Chapter 3 - Processes affecting river geomorphology

---

River process interactions affect river geomorphology in various ways. These river processes include sediment, vegetation and water dynamics. Knowledge of these processes is essential for assessing the complexity of rivers and dealing with complexity is essential for making reliable predictions over decadal time scales. This chapter details process interactions that should be included in river geomorphological modelling used for prediction of river form and habitat at a decadal time scale.

## 3.1 Vegetation dynamics

### 3.1.1 Riparian vegetation

Rivers and streams, along with their adjacent floodplain areas, are referred to as riparian ecosystems. Riparian systems have been noted for their resilience, i.e. their ability to recover quickly from disturbance (Gecy and Wilson, 1990). Riparian species have developed response mechanisms, which allow them to adapt to a rapidly changing geomorphology. Even if a flood deposits a layer of sediment carried from upstream, the trees and reeds can quickly put out new shoots in this layer and continue growing on the same site (Rountree *et al*, 2000).

Riparian zones have considerable impact on the flow resistance and transport of sediment and therefore on the geomorphology (Baptist *et al*, 2002). At the reach scale, the flow regime is the primary source of disturbance in riparian zones and is considered to be the driving force behind riparian vegetation persistence and survival (Junk *et al*, 1989). A flow regime can be defined by its main components of magnitude, frequency, duration, timing and rate of change of discharge. Any flow regime has a natural range of variation in these five characteristics, due to seasonal or inter-annual variation in runoff (Poff *et al*, 1997). Other factors influencing riparian vegetation are channel hydraulics, fluvial

geomorphology and geotechnical considerations (Pollowy, 1998). As such, riparian zones are diverse and complex biophysical systems subject to disturbances at various scales.

The riparian corridor acts as a dissipative structure resisting water flow over various scales. Riparian vegetation contributes to the dissipation of the kinetic energy of floods through its high flow resistance to water flow. The role of the vegetation in determining overall flow resistance is of great importance (Bren, 1993). Dissipative effects of riparian vegetation during floods vary with the discharge and appear to vary according to the width of the riparian corridor in comparison with the channel width (Baptist *et al*, 2002).

Riparian vegetation controls hydraulic processes at the geomorphological-unit scale (Darby, 1999). The flow field in the river adjusts to the vertical and horizontal structures of the riparian vegetation (Tabacchi *et al*, 2000). This local control of riparian vegetation on water flow gives it the ability to entrap and retain sediment. Sediment deposition in turn provides sites for riparian-vegetation colonisation (Fetherston *et al*, 1995).

### **3.1.2 Vegetation establishment and succession**

At the geomorphological-unit scale, water flow influences vegetation dynamics by providing, or limiting, opportunities for processes such as seed production and dispersal, germination, survival and growth. Vegetation interacts with hydrological processes from the earliest stages of plant succession and can have significant impacts on hydraulic processes, particularly during periods of low flow, as well as at the beginning or at the end of flood periods (Thorne *et al*, 1997).

Disturbances initiated by floods of different magnitudes are fundamental influences on riparian vegetation. At the macro-reach scale, extreme floods act to reorganise the physical river template by eroding and depositing sediment, readjusting channel geometry and redistributing nutrients. Extreme floods also destroy established riparian vegetation and deposit woody debris (Parsons *et al*, 2003).

At smaller scales, frequent flooding discourages the establishment of terrestrial vegetation by surface erosion and scour and by the physiological effects of inundation (Gregory *et al*, 1991). The timing of floods is critical for successful plant performance and



most species tend to have a lower flooding tolerance during growth periods (Siebel and Blom, 1998). Thus, event timing is the critical parameter for the hydraulic response of riparian vegetation to flood events. The survival of riparian vegetation therefore depends significantly on elevation above the active channel of the river (Stromberg *et al*, 1993).

Through influencing river flow, geomorphology strongly influences spatial patterns of riparian vegetation (James *et al*, 1996). Other factors include light and nutrient availability, soil texture, and biotic properties of the soil. Riparian vegetation demonstrates a downstream zonation, which is greatly affected by the specific characteristics of the substrate present (du Plessis, 1997). Soils differ in their ability to support plant life in the riparian environment. The varying hydrologic settings of riparian environments (repeated flooding and drying), can destroy soil structure in silt and clay soils. When this happens soils may become too dense, not allowing seeds to germinate, or to persist even if they germinate, because the new roots are unable to penetrate through the compacted soil (Pollowy, 1998).

Seeds are transported and dispersed readily by wind and water and opportunistically colonise areas of the channel that are abandoned or exposed at low flows (Johnson, 2000). However, hydrology limits what plants will grow and where. It is known, for example, that water levels required for successful establishment may be quite different from optimum conditions for subsequent survival and growth and that the response to water levels may vary among species (Mahoney and Rood, 1998). Vegetation that is not removed while young, when the plants can be uprooted or buried by even minor flows, becomes stronger and increasingly resistant to erosion and removal by the flow (Tal *et al*, 2003).

Periods of drought lead to a reduction in flows that would otherwise flush out vegetation in its early stages (Johnson, 2000). Droughts cause dropping of the water table, which favours the establishment of vegetation that may not grow under normal conditions (Rountree *et al*, 2001). The colonisation of newly deposited sediments by vegetation helps to sustain high moisture levels in the upper sediment layers during dry periods (Tabacchi *et al*, 2000).

### 3.1.3 Flow resistance of vegetation

At the channel-type scale, riparian vegetation succession determines the way hydraulic processes are affected. A narrow strip of trees with sharp boundaries is expected to increase turbulence at the internal and external edges, thus enhancing the resistance to flow when the water level rises. A patchy, heterogeneous vegetation profile may distribute resistance to transverse flow, increasing the lateral spatial extent of turbulence (Tabacchi *et al*, 2000). Vegetation affecting the roughness of a channel may also influence channel change by altering the way in which sediment is moved through a reach, since it influences the velocity of the flow and the amount of energy available for transporting sediment (Dawson and Charlton, 1988).

The factors which influence the roughness of vegetation at both the channel-type scale and the geomorphological-unit scale include:

- n the height of vegetation relative to depth of flow (Dawson and Roberson, 1985),
- n the diameter, shape and surface texture of plant stems and leaves (Kouwen and Li, 1980),
- n the height and stiffness coefficient which is a composite parameter that includes the density, elasticity, shape and flexibility of the vegetation (Fathi-Maghadam and Kouwen, 1997),
- n the form resistance and the dimensions of the plant patch (Petryk and Bosmajian, 1975) and
- n the distribution and density of stems within the plant patch (Petryk and Bosmajian, 1975).

Roughness can be extremely dynamic and change significantly in a short space of time (Dawson and Charlton, 1988). The roughness of plants changes as water velocity changes. Increasing velocity first leads to a rippled pattern in the vegetation with some turbulence and then to flattening of plants with a reduction in turbulence. Patchy vegetation of differing height and flexibility increases the variability of the roughness coefficient (Bromley *et al*, 1997).

### **3.1.4 Large Woody debris**

Coarse or large woody debris in rivers presents large roughness elements that divert flowing water and influence the scour and deposition of sediment. Dead logs can initiate the formation of mid-channel bars (Malanson and Butler, 1990) or create a change in river form through log jams which cause the backing up of water in pools known as debris dams. Woody debris may cause significant channel migration or widening, and increase sediment storage. However, the geomorphic effects of woody debris vary with river size (Zimmerman *et al*, 1967).

Large woody debris in rivers results from trees that fall on banks or hillslopes. Processes that initiate tree-fall include windthrow, bank erosion, channel avulsion, tree mortality, mass wasting and land-use practices, such as logging (Nakamura and Swanson, 1993). In-channel debris affects the flow resistance, channel bank-stability, sediment routing and storage (Gregory, 1992).

## **3.2 Sediment dynamics**

### **3.2.1 Sediment movement**

River hydraulics affects sediment transport processes, causing changes in channel form at various scales (Richardson and Simons, 1976). Hydraulics is the branch of physics dealing with the mechanics of water and is concerned with the energy of moving water. In rivers, hydraulics is the main driver of sediment transport causing erosion or deposition (Polly, 1998). Sediment movement takes place through the action of hydraulic forces on single grains of the riverbed. At the micro scale, a condition is reached where a few grains here and there begin to move if water flow velocity over a flat surface of loose grains is gradually increased (Raudkivi, 1976). Generally, at higher velocities, transport of sediment occurs.

Changes in magnitude, duration, and timing of river flows affect sediment movement. Sediment movement includes erosion, transport and deposition, which may be discrete, episodic or continuous in time and isolated, patchy or uniform in space depending on the scales of observation used. Sediment transport capacity of a river is determined by the

channel competence and the physical properties of the bed material (size, density and shape) (Richardson and Simons, 1976).

Various factors affecting sediment transport are given in Table 3.1. A storm of given magnitude may transport a large volume of sediment, as suspended and bed-load material, whereas a later storm of the same magnitude, may transport less sediment, owing to the other controlling factors being modified by the first storm (van Sicle and Beschta, 1983).

The flow and transport processes in a river are governed by the geomorphology and the supply of water and sediment from the catchment. The supply of sediment from the catchment varies spatially and temporally. External inputs will depend on the degree of weathering and the frequency of overland and gully flow providing sediment to the river. Vegetative cover in the catchment also determines the sediment load delivered to the channel (Nicolson, 1999).

**Table 3.1 Factors affecting sediment transport (Heritage and van Niekerk, 1995)**

Discharge regime	Flow volumes Flow frequency Flow duration
Sediment supply	Land degradation rates Sediment translocation In-channel storage
Channel competence	Channel roughness Channel slope Channel shape

Once sediment has entered the channel, it is generally transported slowly downstream in a sporadic manner by a number of separate flow events of varying magnitude. The transport of sediment through a river reach depends on discharge and will therefore vary considerably through natural hydrological variations (Birkhead *et al*, 1998). Changes to the supply of sediment or the transport capacity of a river will eventually result in bed levels rising as sediment builds up, or falling as sediment is removed. Local inputs from bank

collapse or disruption of a channel storage area may lead to release and movement of previously stationary material downstream (Meigh, 1987).

The unsteadiness in bed-load transport rates has resulted in the identification of discrete quasi-periodic bed-load pulses (Hoey and Sutherland, 1991). Gomez (1991) regards pulsing as distinct temporal fluctuations in the transport rate, which need not be of statistically significant regularity. These regular pulses may reflect the development of dynamic sediment waves with length scales equivalent to the channel width (Griffiths, 1993) and are associated with scour and fill phenomena (Ashmore, 1988; Whiting *et al*, 1998). Unsteady transport also occurs at the scale of instantaneous particle interactions with the flow at temporal and spatial scales corresponding with turbulence (Williams, 1990). Such spatial and temporal organisation in bed-load may result in subtle temporal changes in bed elevation and bed roughness, which may modify local hydraulic conditions (Seminara *et al*, 1996).

### **3.2.2 Erosion and deposition**

Erosion occurs when water flow removes particles from the riverbank and/or riverbed. Erosion processes depend on the geotechnical properties of bank and bed material, for example the presence or absence of cohesion and the other parameters (Thorne, 1990).

River bank erosion drives temporal changes in river planform. Increasing hydraulic shear or increasing bank erodibility should result in increased rates of bank erosion and lateral river migration. River channels will naturally migrate because of erosion on the outside of bends and deposition on the inside. Through these processes, the meanders will migrate downstream at a rate controlled by the water's energy, the ability of the bank and bed material to resist erosion, bank height and the radius of curvature of the meander. Variables such as topography, geology and vegetation govern bank erosion (Howard, 1984).

Bed erosion can destabilise riverbanks by oversteepening the slope and undermining the bank toe, particularly after the level of the active channel incises below the root zone of the riparian vegetation, and/or after the channel erodes down to a more resistant substrate. The combination of increased energy within the channel and reduced bank-stability often leads

to rapid bank erosion. Toe erosion refers to all incidents of bank undermining and collapse due to water flow (ISPG, 2002).

Local scour is erosion at a specific location that is greater than erosion found at other nearby locations of the riverbed or bank. Local scour can occur on both the channel bank and bed (Simons and Senturk, 1992).

Deposition is the progressive accumulation of in-channel sediment resulting in increased channel bed elevation. Deposition is a response to channel system changes that reduces the channel's capacity to transport the sediment delivered to it. Generally, this occurs as result of increased sediment supply, increased grain size or diminished stream power (transport capacity).

Erosion and deposition produce sorting of sediment. Since most riverbeds consist of grains with a broad range of size fractions, sorting can produce variable sediment grading along the river. Transported sediment generally increases in volume downstream but decreases in particle size. In an erosion process, fine particles are entrained more easily and the bed surface will become progressively coarser. Ultimately, an armour coat of large particles is formed, stopping further degradation. During the deposition process layers of sediment will be deposited on the bed surface and the bed surface will be progressively finer. Local variations in geology and bank material, as well as depositional patterns, may result in highly variable sediment character (du Plessis, 1997).

### **3.2.3 River bank-stability**

Channel-width adjustment occurs in a wide variety of geomorphic contexts and is usually accompanied by changes in other morphological parameters, such as channel depth, roughness, bed material composition, riparian vegetation, energy slope and channel planform. The processes responsible for width adjustment are diverse and the adjustment process itself displays a wide variety of spatial and temporal patterns.

Channel-width increase occurs through mass failure, resulting from bank instability. Mass failure usually occurs by a combination of fluvial erosion of intact bank material and mass failure under gravity followed by basal clean-out of disturbed material. Mass failure is the

downward movement of large and intact masses of soil and rock. It occurs when the down-slope shear stress (weight) exceeds the shear strength (resistance to weight) of the earth material. Shear stress is the driving force from gravity and/or loads acting on the slope. Shear strength is the characteristic of soil (cohesive bonds between particles and aggregates), rock and root structure. Any cause that increases the shear stress or, conversely, decreases the shear strength will cause a mass failure. Most mass failures are triggered by water saturating a slide-prone slope (Turner and Schuster, 1996). Furthermore, mass failure can occur in combination with other mechanisms of failure such as toe erosion or subsurface entrainment (ISPG, 2002).

Bank drainage enhances bank-stability and is effected by riparian vegetation; vegetated banks are drier and better drained than unvegetated banks (Thorne, 1990). Vegetation can also contribute to bank-stability through canopy interception and evapotranspiration. These effects lead to drier, better-drained banks with reduced bulk unit weight, as well as lower positive pore pressures (Simon and Collison, 2002).

A critical condition for bank failure usually occurs during rapid draw-down of the water surface elevation on the riverside of the bank. The reason for this is that the riverbank might become saturated during high-flow conditions and that the phreatic surface of the infiltrated water in the bank does not recede at the same rate as the water level in the river. This leads to excess pore water pressures within the soil of the bank weakening the soil and providing cause for bank failure (Pollowy, 1998; Parkinson *et al*, 2003).

Riparian vegetation often enhances river bank-stability (Gregory, 1992). Vegetation effects on riverbank-stability, however, are complex and vegetation cannot be classed as simply a benefit or liability without detailed consideration of other factors, including the processes responsible for retreat or advance, bank material properties and bank geometry and the type, age, density and health of vegetation (Thorne, 1990).

### **3.2.4 Vegetation-sediment interaction**

Vegetation is an important agent in influencing fluvial geomorphology and sedimentary processes because it affects local hydraulics that determine sediment transport. Vegetation offers local resistance to flow by increasing drag and reducing velocity, thus decreasing the

shear stress available for erosion and transport (Carollo *et al.*, 2002; Jordanova and James, 2003). As vegetation slows water down, the tendency for sediment to settle under the action of gravity increases and leads to build-up of sedimentary features (Dawson and Charlton, 1988).

Vegetation changes flow patterns and alters the way in which sediment moves down through the channel (Nicolson, 1999). In-stream vegetation is therefore very effective in promoting sediment deposition (Abt *et al.*, 1994) since vegetation decreases the erosive force of water (Pollowy, 1998). Boundary shear stress is proportional to the square of near-bank velocity. Vegetation therefore reduces soil erodibility by retarding near-bank flow, which reduces forces of drag and lift on the bank surface. Vegetation also damps turbulence, which induces velocities 3x the mean for short sweeps (Smith, 1976).

Vegetation plays an important role in trapping fine material carried as wash load. Wash load is sediment carried by the river, which is finer than that commonly found in the bed. Wash load deposition can be significant on vegetated banks where dense strands or stalks and stems damp turbulence and filter out fine material. The addition of fine materials may increase the cohesion of the sedimentary deposits (Thorne, 1990).

Vegetation can grow dense root networks that bind sedimentary features and resist plant removal by flood scour (Nilsson *et al.*, 1989). Thus, vegetation acts as a sediment trap and confines erodible sediment particles; when the velocities do become higher the sand that would have been eroded is now kept in place. Vegetation also reinforces the soil to increase its apparent cohesion (Waldron, 1977; Hicken and Nanson, 1984).

Deep-rooted plants associated with woody vegetation are able to withstand larger erosive forces than grass and reed species can. More woody trees grow in areas where erosion represents the dominant morphogenic force. In comparison, shallow-rooted species are usually associated with areas of deposition; these species have roots that grow with the accumulation of sediment (Haslam, 1978).



### **3.3 River form**

#### **3.3.1 Effect of flooding on river form**

Floods may produce devastating impacts or only minor geomorphological changes. Geomorphological changes caused by floods are related to the magnitude of discharge and frequency of occurrence. Large floods are associated with much greater shear stress and stream power per unit boundary relative to the available resistance. They cause large-scale channel modification or floodplain stripping. In zones where high shear stresses occur, erosion may result with minimal geomorphic impacts occurring elsewhere (Magilligan *et al*, 1998; Parsons *et al*, 2003).

At the reach scale, the availability of sediment and the sequence of events may be as important as flood magnitudes in determining the effects of flooding. Extreme floods are also important geomorphologically because of their ability to erode the cohesive sediment deposited as consolidated sediment at the macro-reach scale (Birkhead *et al*, 1998).

At the channel-type scale, increased flooding may result in channel incision. Channel incision involves the progressive lowering of the channel bed relative to its floodplain elevation. Increased roughness can reduce conveyance over parts of the channel and force the flow into a smaller area (Johnson, 1994). Increased roughness may result in higher flow depths which can lead to greater flood potential as well as increased bed degradation (Tsujiimoto and Kitamura, 1996).

#### **3.3.2 Vegetation-river form interaction**

Vegetation plays a key role in stabilising riverbanks, dissipating energy and maintaining a stable channel form. Vegetation colonises large areas of the sedimentary features in rivers and plays an active role in determining the river form. Interrelationships of riparian vegetation and river form are often illustrated through the width-to-depth ratio of river channels. One of the most striking changes that occurs with increasing vegetation is a substantial reduction in the channel width, which can reduce the channel capacity and increase the risk of flooding (Eschner *et al*, 1983). Also, increased vegetation density is typically linked to a decrease in bank erosion and lateral migration rates (Smith, 1976).

Bank-vegetated channels are narrower and deeper than unvegetated channels (Charlton *et al.*, 1978). The width-to-depth ratios of rivers cutting through woodland are generally lower than those channels cutting through grassland (Zimmerman *et al.*, 1967). This can be attributed to the root depths of trees being deeper than those of grass, and increased resisting shear stress on the channel beds (Gregory, 1992).

At the macro-reach scale, vegetation has been recognized as a primary control on river planform, particularly as a determinant of whether a river will adopt a braided or single-thread pattern (Millar, 2000). For instance, vegetation is used to alter the stream flow direction and induce meandering in straight degraded river channels (Rowntree and Dollar, 1999). The vegetation around a bend effectively reduces erosion and induces bank accretion and lateral migration (Beeson and Doyle, 1995). Studies have shown that overall behaviour of the system correlates with vegetation type or density, shifting between a single-thread channel and a multi-thread system as vegetation changes (Goodwin, 1996; Ward and Tockner, 2000).

Vegetation responds to changes in river form (James *et al.*, 1996), so that vegetation survival is significantly related to elevation. At the reach scale, the river form represents an obvious environmental gradient, as flood duration decreases with increasing elevation. Significant relationships have been found between vegetation distribution and the elevation of the morphological features in rivers (Gill, 1970; van Coller *et al.*, 1997). Since such gradients represent changes in flooding frequency and duration as well as water availability, hydrology underlies these distribution patterns (Franz and Bazzaz, 1977; Nicolson, 1999). Spatial distribution patterns of riparian plant species depend on the interactions of hydrogeomorphic processes of the river with the topography (Hupp and Osterkamp, 1985). These vegetation distribution patterns are often described in relation to the strong vertical and lateral gradients, which characterise these riparian systems (Gregory *et al.*, 1991).

At the channel-type scale, vegetation distribution patterns are associated with geomorphological-units of channel bars, channel shelves, the floodplain and terraces (Hupp, 1988). The geomorphological-units thus strongly influence spatial patterns of

riparian vegetation but riparian vegetation also influences the evolution of geomorphic units. At similar scales vegetation affects river form through river bank-stability. Vegetation increases river bank-stability through root binding of the earth and increases the threshold shear stress needed to erode the sediment. Roots add tensile strength and elasticity, which help to distribute stresses, thus enhancing the bulk shear strength of the soil. Root-permeated soil, therefore, makes up a composite material that has enhanced strength (Thorne, 1990; Simon and Collison, 2002) although this effect remains poorly quantified (Micheli and Kirchner, 2002). Woody vegetation may also lead to instability of banks due to undercutting: although woody vegetation has deeper root systems than grassy vegetation has, the shallow roots of grasses increase surface shear strength and therefore enhance bank-stability (du Plessis, 1997).

The heterogeneity in the geomorphological structure controls vegetation development (Kalliola and Puhakka, 1988) and is reflected in the distribution of different vegetation types (Gregory *et al*, 1991). The establishment of different vegetation types and their growth is closely related to the geomorphic environment (van Coller, 1993; van Coller and Rogers, 1996), often showing patterns of vegetation zonation (Furness and Breen, 1980). Some species germinate only in particular geomorphic environments (van Coller, 1993).

### **3.3.3 Effect of geology on river form**

The form of a river is influenced to a large degree by the underlying geology and bedrock lithologies which determine whether rivers are predominantly bedrock or sediment controlled. The geology often produces complex fluvial geomorphological structures as a result of variable sediment deposition and erosion occurring down the course of the river in response to variable channel gradients resulting from different bedrock lithologies (Raudkivi, 1976; van Niekerk *et al*, 1996; Rountree *et al*, 2001).

The bedrock controls introduce additional variability into rivers owing to the sharp gradient changes upstream and downstream of the bedrock controls. Additional bedrock influence on geomorphological-units is present in such channels which will have an effect on both the

vegetation and hydrological characteristics of the bedrock influenced sections of the river (Rountree *et al.*, 2000).

The geology of the catchment determines to a large degree whether the river is bedrock-controlled or alluvial only. Bedrock-controlled river reaches are those which have substantial proportions of the boundary exposed to bedrock, or are covered by a veneer which is largely mobilised during high flows, so that underlying bedrock geometry strongly influences patterns of flow hydraulics and sediment movement (Tinkler and Wohl, 1998).

Alluvial reaches generally have smaller water surface slopes than bedrock reaches. These reaches contain sediment which may be eroded. The sediment size determines to a large degree whether a river will be straight, braided or meandering. Alluvial reaches which are fed by large amounts of coarse sediment develop unstable, wide, often braided channels, whereas those with a limited coarse sediment supply develop stable, much narrower, often meandering channels (Harvey, 1990). The mechanism of braiding streams involves multiple channels that intertwine in a pattern and quickly rearrange themselves. In some braided systems, a large number of channels forms an intricate arrangement that changes in an apparently random way while maintaining a statistically steady state (Paola and Foufoula-Georgiannou, 1991). Mid-channel bars are common on many active meandering gravel-bed rivers. High stream power, unconsolidated banks, non-uniform flow, bed topography and rapid rates of erosion and deposition characterise gravelly braided rivers. Sediment supply may be the most important control of channel pattern (Carson, 1984).

Channel responses in alluvial reaches can often be attributed to distinct causes. These include channel migration, incision, lateral migration and avulsion (Brewer and Lewin, 1998), which are most commonly observed in alluvial systems that are free to adjust their channel boundaries.

In comparison with alluvial reaches, bedrock reaches accommodate morphological change at very slow rates to increased levels of shear stress and stream power. High-magnitude flood events may effect limited wear and polish but not large morphological change. The slope is almost certainly well in excess of alluvial reaches. A relatively steep mean gradient is

consistent with the typical coexistence of gravel-bed and bedrock reaches and lateral or transverse bars along the channel (Tinkler and Wohl, 1998).

The gradient of the river is arrested upstream of the bedrock outcrop, although when it flows over the bedrock outcrop, the local gradient may become very steep. Such outcrops are known as bedrock controls, since they exert a local controlling influence on the gradient of both upstream and downstream alluvial sections of the river. Velocity is increased owing to the steeply sloping bedrock outcrop, and sediment load decreased because much is deposited in the low-gradient, slow-flowing backwaters upstream of the bedrock outcrop (James *et al*, 1996).

Transport capacity of grains over hard surfaces is larger than over loose grains of the same size as those in motion. Bedrock therefore increases sediment transport owing to rebound of sediment grains on hard bedrock. Unlike what takes place when grains impact on other grains of similar size, much of the momentum of the impacting grains is not lost to frictional losses and small displacement of bed grains. As a result, downstream transition from bedrock to alluvial bed can often be abrupt because of the sudden loss of mobility (Howard, 1987).

### **3.3.4 Bar formation**

There are three main causes of bar formation at the channel-type scale: a decrease in shear stress, the widening of the channel and tributary entrances. These factors all cause a flow divergence. Channel conditions that are likely to lead to stationary bars appear to be heterogeneous, coarse bed-load material, steep channel gradients, and shallow depths (Lisle *et al*, 1991).

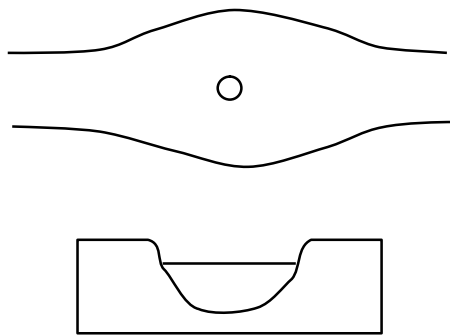
A combination of the following factors contributes to the creation of these deposits and prevents bar-head erosion (Lisle *et al*, 1991):

- n Coarse particles are carried into zones of decreasing boundary shear stress and are selectively deposited to form a highly armoured surface layer.
- n Shallow submergence of coarse particles further decreases their mobility.
- n Mutual interference between large grains concentrated by sorting and deposition enhances further accumulations.

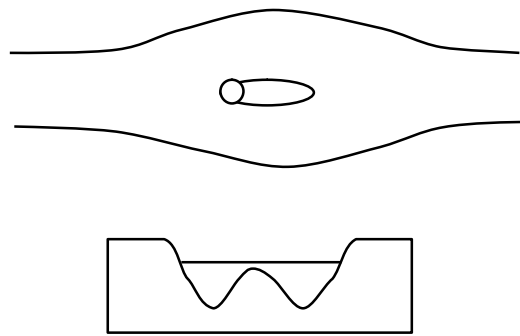
Most mid-channel bars are a result of flow divergence (i.e. channel widening causing loss of energy and deposition of a small shoal which divides the channel in two). Flow divergence is often caused by an obstruction, e.g. a log or tree (Hicken, 1984), or resistant coarse deposits, typically at the head of a bar. Figure 3.7 illustrates the sequence of mid-channel bar development. The resistant coarse deposits deflect flow and sediment transport around the bar and thereby stop bed-load transport over the bar surface downstream (Figure 3.7 - A).

There is usually a spatial gradation in size from the upstream to the downstream end, but this is less marked in early stages of bar development when material is very coarse and in latter stages when it is predominantly sand (Figure 3.7 - B) (Hooke, 1997).

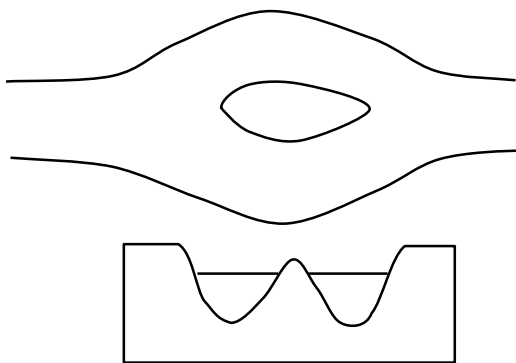
Vegetation influences and is influenced by the sedimentology and sedimentation of a bar. A bar provides conditions for the establishment and growth of vegetation, i.e. the occurrence of vegetation is the result of the bar as well as the cause. However, vegetation does play a role in the subsequent growth and development of existing bars that have been colonised (Figure 3.7 - C) (Hicken, 1984). Without vegetative stabilisation bars may form in the river and later be eroded by high flows. Bars will not be eroded until the vegetation has died or been stripped out by floods (Figure 3.7 - D) (Rowntree, 1991).



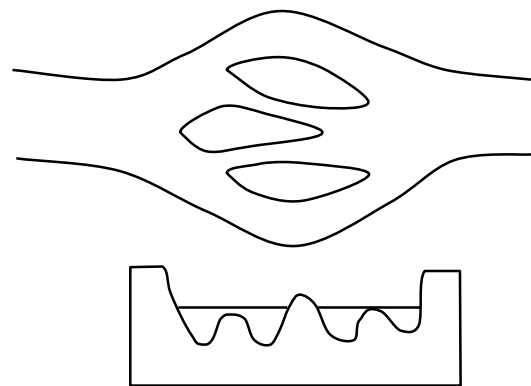
**A - Coarse lag stalls at flow expansion**



**B - Obstacle to flow promotes deposition**



**C - Bank erosion leads to bar emergence**



**D - Bar stabilised by fines and vegetation  
process repeated in anabranches**

**Figure 3.7 Mid-channel bar formation (Hooke, 1997)**

Over a period of several years, depending on the channel, flow on one side of a mid-channel bar may become more dominant and the bar can evolve asymmetrically to become a side bar (Figure 3.8) (Hooke, 1997).

Many types or variations of bars can be present in a river at the same time. The variations reflect their positions within the channel (i.e. mid-channel or side), their stages of development, and their shapes (i.e. whether they are longitudinal or transverse). Bar type depends on sediment supply and river gradient (Hooke, 1997).

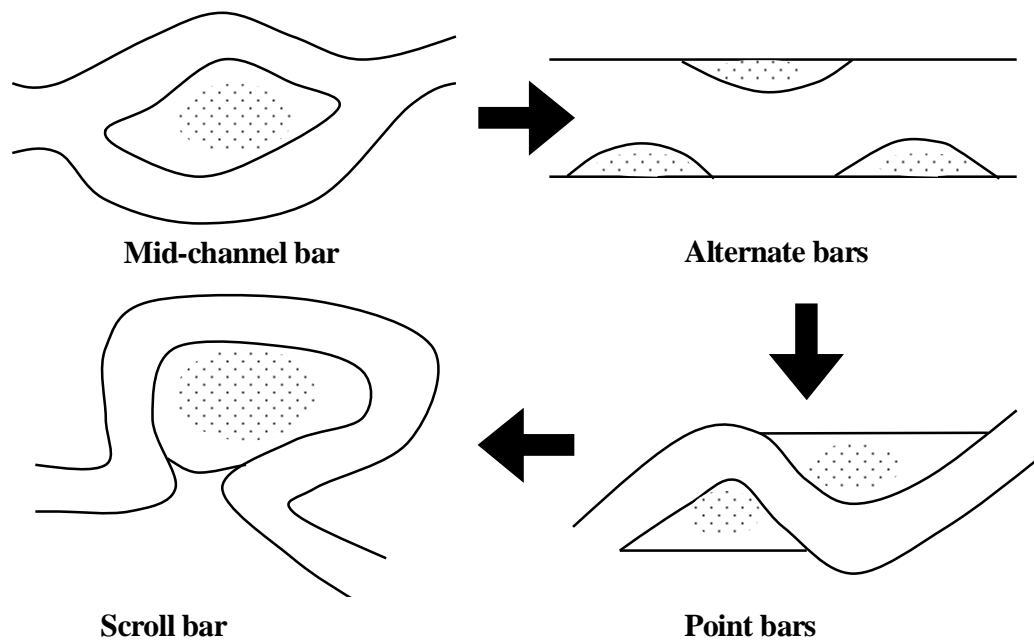


**Figure 3.8 Different types of alluvial bar. Increasing stability from mid-channel bar to scroll bar (Hooke, 1997)**

### 3.4 Conclusion

This chapter reviews river processes and the feedbacks affecting river geomorphology in order to arrive at fuller description, and thus highlights the complexity of river systems. Rivers can be considered as complex because not only do they include many interacting processes, but these processes interact to change river geomorphology at various spatial and temporal scales. The river processes of water sediment and vegetation are complex in themselves, holding implications for their modelling.

The organisational levels associated with a hierarchical description of rivers which are identified to be important for decadal prediction are the reach scale, channel-type scale and the geomorphological-unit scale. Apart from extreme floods resetting riparian corridors at the macro-reach scale, the organisational levels mainly associated with changes in river form at a decadal time scale are observed at the reach scale, the channel-type scale and the geomorphological-unit scale.



To model geomorphic changes over decades, the processes that must be described include:

- n Flood flows at the reach scale
- n Vegetation establishment and growth at the geomorphological-unit scale, vegetation succession at the channel-type scale and vertical distribution of vegetation at the reach scale
- n Resistance to water flow at various scales since different vegetation and channel competence characteristics come into effect at different scales
- n Erosion and deposition processes, using appropriate sediment transport rates appropriate to various spatial scales including local scour at the geomorphological-unit scale
- n Bar formation caused by flow diversion and therefore flow in two directions as well as sediment bar formation dynamics at the channel-type scale
- n The effect of vegetation on flow resistance, particularly at the channel-type scale since vegetation plays a large role in flow diversion and sediment trapping
- n Bedrock affecting river form
- n Geomorphological-unit scale sediment characteristics affecting water flow and therefore also sediment transport rates
- n River bank-stability, especially when cohesion plays a role in bank substrate

The following chapter explains how these individual processes can be modelled. River geomorphological modelling has to allow for feedback between interacting processes. Chapter 6 provides evidence of the extent to which feedback of interacting processes is included in modelling.

# Chapter 4 – Geomorphological modelling

---

This chapter discusses modelling used in river geomorphology. It reviews the available modelling methods and details of modelling identified processes at particular scales in order to select the best model for each organisational level for each individual process affecting river form. Since these processes are complex in themselves, the best models are those that simplify the dynamics they simulate but still provide realistic results. The review identifies the most suitable models for predicting river form change over decadal time scales and the gaps where suitable modelling of particular processes at particular scales does not exist. Where suitable modelling does not exist, the review guides the selection of the most appropriate modelling method and provides insight on the type of model formulations required.

More detail is given to certain existing models, including the following:

- 1) Models not employed in this study but deemed to be important, as ascertained in Chapter 3, for realistic modelling of river geomorphology over decades. These include 3-D CFD modelling, seedling recruitment modelling and bank-stability modelling.
- 2) Those adapted to provide the models used in this study, for example the braided river model of Murray and Paola (1994).

## 4.1 Modelling methods

### 4.1.1 Physical modelling

Modelling of river processes and interactions may be carried out using physical modelling techniques. In river geomorphology, scaled physical models have been used primarily to investigate sediment processes. Physical models allow the development of channel patterns and the effects of flow structure and bed-load transport on channel geometry to be studied. Physical models allow water flow and sediment movement to be examined in detail over

short reaches. Sediment processes that can effectively be simulated in a physical model with a movable bed include suspended load, bed-load, density currents, scour and deposition, and channel shifting, widening and meandering. Physical models can also be applied in studies of the feedback between channel morphology and bed-load transport, in mechanisms of anabranch avulsion and processes of fine-grained sediment deposition (Julien, 2002).

Experiments can be carried out in miniature laboratory models or scaled physical models to reproduce a river system at a small scale. Scaled physical models allow complex natural processes to be investigated in a controlled and simplified environment. In order to create a realistic physical model of the river system, scaling must be applied to ensure that the system characteristics are correctly represented. Scaling is based on the concept that complete similarity between model and prototype is achieved when the model displays geometric, kinematic, and dynamic similitude.

One example of physical modelling application is micro-scale loose bed hydraulic models. The United States Army Corps of Engineers has developed micro-models which are extremely small physical models. Such a model consists of five components: a hydraulic flume, a model-channel insert, an electronic flow controller, synthetic bed sediment and pervious steel mesh, for replicating dikes and other river-training structures representing the reach to be studied. Flow and sediment are recirculated through a submersible pump (Gains and Maynard, 2001).

Such micro-models have been used for channel response studies, such as establishing suitable alignment, depth and width for navigation channels. Other channel response studies include improving flow conditions at bridges for example. These studies, however, focus mainly on reducing maintenance in river channels. The models are also used to evaluate the likelihood of success of various channel control alternatives to obtain a desired channel configuration. They are also used to identify the overall flow patterns and channel form so that both surface velocity distributions and associated channel adjustment, are obtained (Gains and Maynard, 2001).

Since hierarchical modelling can be applied contextually only as computer programmes, physical modelling serves mainly as a tool for calibration and verification of computer programs. Physical models may provide data sets for computer programmes using, for example, rule-based models or artificial neural networks to make predictions.

#### **4.1.2 Numerical modelling**

Numerical models are developed to mimic the behaviour of natural systems as accurately as possible and allow representation of natural phenomena observed at a particular scale. This involves the construction of a numerical model based on a hypothesis, using identified variables and simplifying assumptions and boundary conditions (Thomas and Huggett, 1980). The primary source of error in numerical model predictions are the assumptions that are required to express the model mathematically. Numerical modelling demands a great deal of knowledge about these processes.

The identification of the appropriate variables for inclusion in a numerical model and the relationships between those variables is, to a certain degree, an inductive process. Dependent variables form the output obtained from relationships with independent variables or events that appear to contribute to explaining the phenomenon (Baker and Twidale, 1991). The model is calibrated to get dependent variables to be consistent with measured variables of the system. This is followed by verification to compare model predictions with field and experimental data (Thomas and Huggett, 1980).

Numerical models describe river processes using equations varying from relatively simple to highly complicated relationships, accounting for a wide range of interactions and organisational levels. River geometry and other parameters representing the river system also vary from very simplistic to highly complicated. An appropriate intersection of process and environment description is obtained to provide realistic simulations and model simplicity (Michaelides and Wainwright, 2004).

A numerical model is often presented as a sequence of procedures allowing one spatial or temporal step to be followed logically by another. The accuracy and reliability of numerical models applied to river geomorphology depends largely on the effectiveness of the numerical methods employed and the user's experience and skill. One application of

numerical models in representing fluvial systems is known as Computational Fluid Dynamics, which is discussed in detail in the following section.

#### **4.1.3 Computational fluid dynamics**

Computational Fluid Dynamics (CFD) models are used to simulate increasingly complicated cases. They represent flow and sediment dynamics in 1, 2 and 3 dimensions and simulate detailed processes such as non-equilibrium transport of sediment with non-uniform composition exchange between bed-load and suspended-load sediment movement in unsteady flow. CFD models can predict changes in bed elevation resulting from spatial differences in the predicted sediment flux fields, which are computed through numerical solution of the sediment continuity equation. The sediment continuity equation is usually simplified by neglecting either the longitudinal or the transverse sediment flux difference terms. These simplifications allow these models to describe phenomena at larger scales more realistically but limit their validity at smaller scales. For example, stream-wise and transverse sediment flux terms are significant in describing near-bank and bed topography changes at the geomorphological-unit scale (Darby and Thorne, 1992).

One-dimensional (1-D) models are used mainly to simulate long-term sediment transport processes in the general flow direction and are generally applied at the reach scale. Two-dimensional (2-D) and three-dimensional (3-D) models are used in studying local and detailed phenomena at the channel-type scale or the geomorphological-unit scale. Depth-averaged 2-D models resolve horizontal variations and provide many more details like the influence of changing cross-sections and irregular side boundaries. These are used for solving many practical problems over shorter river stretches, such as flow around sediment bars or near structures.

Many CFD models include grain-size sorting modelling, which employs the mixing layer theory. The mixing layer is the layer of bed material where sediment transport, for given grain-size of bed material and flow condition, occurs. The mixing layer or the active layer interacts with the bed surface or the inactive layer. During a deposition process some sediment particles will leave the active layer and enter the inactive layer. During the scour process, some particles originally in the inactive layer will enter the active layer.

According to this procedure, the thickness of the active layer is set equal to a preselected number of layers times the geometric mean of the largest size class used in the simulation. The active layer is defined as the bed material layer that can be worked or sorted through by the action of the flowing water (Lee and Hsieh, 2003).

1-D sediment routing procedures ignore transverse sediment fluxes and require various assumptions concerning the distribution of predicted changes in bed elevation across the channel cross-section (ASCE, 1998a). For example, Osman (1985) assumed that the bed level change is distributed evenly over the entire cross-section. In contrast, Alonso and Combs (1986), utilized various assumptions to distribute the scour and fill of sediment more realistically across the section.

Kassem and Chaudhry (2002) developed a 2-D model to predict the time variation of bed deformation in alluvial channel beds. The model uses depth-averaged unsteady water flow equations along with the sediment continuity equation. It employs a body-fitted coordinate system and uses an unsteady flow equation. The effective stresses associated with the flow equations are modelled by using a constant eddy viscosity approach. The model was used to investigate the process of evolution and stability of bed deformation in circular bends with uniform particle size.

Recently, several 3-D models for water flow and sediment transport have been developed. Some of these 3-D models also have the capability to predict the evolution of the channel bed. van Rijn (1987) proposed a quasi-3-D model in which the sediment transport is calculated in 3-D, while the horizontal mean flow is obtained solving the 2-D depth-averaged flow equations. His model assumes a vertical logarithmic velocity profile, which is valid only for gradually varying open channel flow. Gessler *et al.* (1999) developed a mobile-bed module for sand rivers. It accounted for the movement of non-uniform sediment mixtures through bed-load and suspended load. Their model is also capable of simulating bed evolution processes, such as aggradation scour and bed-material sorting.

Wu *et al.* (2000a) proposed a fully non-hydrostatic 3-D finite volume model, which included modules for both the suspended sediment and bed-load transport. Their modelling of the bed-load improved on the non-equilibrium method proposed by van Rijn (1987).

Wu *et al.* (2000a) also produced a 3-D CFD model solving the full Reynolds-averaged Navier-Stokes equations. The model simulated suspended-load transport through the general convection-diffusion equation with an empirical settling-velocity term. Bed-load transport is simulated with a non-equilibrium method and the bed deformation is obtained from an overall mass-balance equation. The suspended-load model is tested for channel flow situations with net entrainment from a loose bed and with net deposition.

CFD modelling is the most accurate way of modelling the complicated flow phenomena of water and sediment in rivers. However, it is very computationally intensive and the required computational effort increases with the increasing amount of detail that the models have to account for at decreasing scales. Numerical cellular automaton (CA) models of fluvial geomorphology are simplified or relaxed adaptations of the equations and numerical solutions of CFD modelling. This increases the speed at which these models run and therefore considerably increases computational efficiency. This also allows numerical CA models to be applied at larger scales. The increase in computational speed and simplicity also allows these models to include sediment processes between cells, allowing river form at smaller scales to be accounted for (Coulthard *et al.*, 2007).

#### **4.1.4 Rule-based modelling**

In rule-based models, the interactions between components of a system are not based strictly on established equations, but also, or exclusively, on rules that can take several forms. Rule-based models can be: 1) abstractions of basic physical laws; 2) syntheses of analyses, models, or observations of dynamics at scales smaller than those treated in the model; 3) based on observations of the natural system on relatively large scales; and/or 4) based on physical insight and intuition (Murray, 2003). Rule-based models enable the use of many variables, and because of their coarse-grained nature they can be used to describe general trends at large scale. By temporarily setting aside variables that are significant at smaller scales, they serve as powerful tools for general interrelationships at larger scales (Ebert and Mitchell, 1975). Rule-based modelling is therefore most appropriate for modelling vegetation dynamics at larger scales. Rule-based models are qualitative but, owing to the computational nature of the hierarchical strategy employed in this study, they

have to make quantitative descriptions. Expert systems are used to make quantitative descriptions.

An expert system is a computer-based system that employs rule-based modelling to reason using expert knowledge. Expert systems are built primarily for making the experience, understanding and problem solving capabilities of the expert in a particular subject area available to the non-expert. A typical layout of an expert system consists of a knowledge base, a database and an inference engine. The inference engine assigns a numerical value to the rule variables to allow computation of an expert's prediction (Anderson and McNeil, 1992). A fuzzy expert system is an expert system that uses fuzzy logic for inference of the rules (Klir and Yuan, 1995).

Fuzzy logic is viewed as a formal mathematical theory for the representation of uncertainty and deals with the concept of partial truth or truth-values between "completely true" and "completely false" (Bezdek, 1993). Fuzzy models allow working with imprecise or "fuzzy" information and exist in the form of rules (Kaufmann and Gupta, 1985). A fuzzy expert system is shown in Figure 4.9.

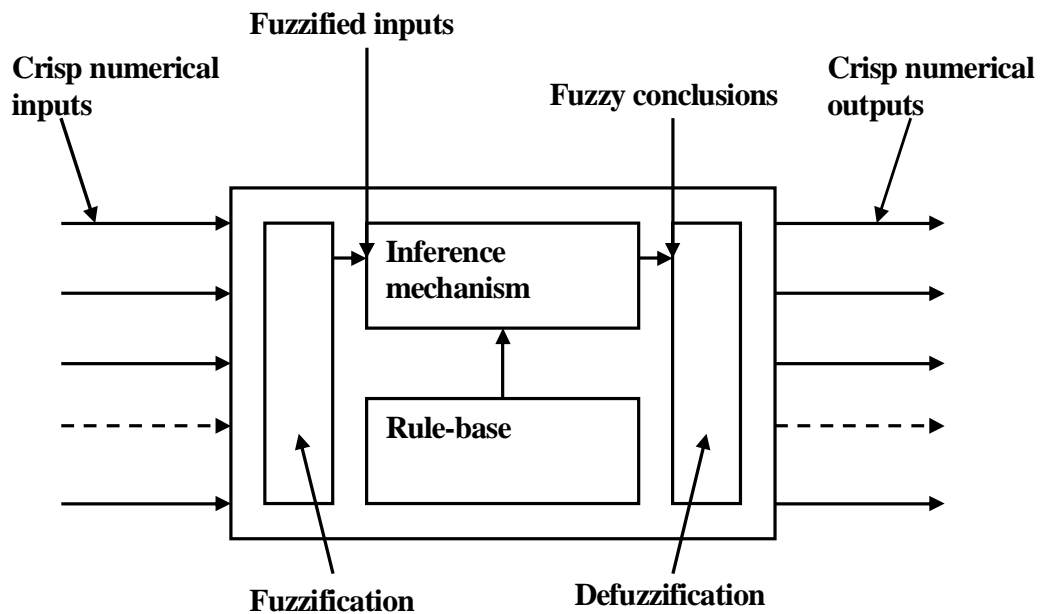


**Figure 4.9 Fuzzy expert system (Passino and Yurkovich, 1998)**

Artificial neural networks (ANN) offer an approach different from rule-based modelling. They try to provide a tool that programs itself and learns on its own. Neural networks are



structured to provide the ability to solve problems without the benefits of an expert. They can seek patterns in data and are self-learning mechanisms which don't require the traditional expertise on formulating models for prediction (Anderson and McNeil, 1992).

ANN allow predictions to be made based on a data set. Such a data set includes the information that can characterize the problem. It also requires an adequately sized data set to both train and test the network. Note, however, that they involve an empirical skill and intuitive feel to create an appropriate network to allow predictions to accord with data. With an understanding of the basic nature of the problem to be solved, a decision on creating the network can be made (Anderson and McNeil, 1992).

ANNs have been applied to larger scale geomorphological problems concerning prediction of catchment sediment yield (Sarangi and Bhattacharyaa, 2004), landslides (Ermini *et al.*, 2005) and river network characteristics (Strobl and Forte, 2007). ANN are not used in this study but would offer a good way to make large-scale predictions of vegetation population dynamics if a good data set were available.

#### **4.1.5 Cellular Automata modelling**

A cellular automata (CA) model consists of a cellular grid where the state of each cell is updated in time steps, according to a set of simple deterministic local interactions, relating the state of the cell to adjacent or neighbouring cells. The local interactions can be described with numerical formulations (e.g. Murray and Paola, 1994) or can be rule-based (e.g. Chen *et al.* 2000). The state of each cell changes in each time step, according to the imposed rules involving states of neighbouring cells.

CA modelling simulates spatial pattern formation, which arises from the interaction described by rules defining transfer between the cells (Packard and Wolfram, 1985). The application of these local rules creates larger scale patterns, which are not apparent when examining the rules for the interactions between cells. Although the concept of CA models is basic, the interaction between the cells can give rise to complex non-linear behaviour (Wolfram, 1984) and can demonstrate highly realistic physical behaviour (Malanson, 1999). Wolfram (1984) identified five key factors which briefly define cellular automata:

- n They consist of discrete cells
- n They evolve in discrete time steps
- n Each cell can take on a finite set of possible states
- n The state of each cell evolves according to the same deterministic laws
- n The laws for cell evolution depend only on interactions with immediately neighbouring cells

CA models are inherently spatial and are an effective means of simulating geomorphological processes that change through time. CA models can represent self-organising processes within a 2-D framework or lattice of grid cells. The spatial nature of geomorphological processes and the ease of applying gridded data are well suited to CA models.

Favis-Mortlock (1996) used a CA model to investigate the evolution of rill networks. The rill model described by him shows a degree of self-organisation by forming a channel network. The model simulates the impact of individual raindrops or 'run-off packets' on a semi-arid hillslope. These packets of rainfall erode the hillslope according to a stream power law and are routed to the lowest neighbour. Simulated planform and rill spacing compare well with field measurements.

Luo *et al.* (2003) described a simple CA model that simulates first order processes associated with sediment erosion. The model describes sediment erosion by iteratively applying a set of simplified rules to individual cells of a digital topographic grid. The model implements a rainfall event of a random size at a random location within a grid. Runoff from the rainfall event moves sediment from each cell to its lowest neighbour according to a sediment transport equation. This transport rate is dependent on the elevation difference between two adjacent cells. The model allows both erosion and deposition of sediment, depending on the difference between sediment input and output of a cell. When all runoff from a rainfall event has been routed across the grid a new rainstorm with a random area is applied at another random location and the whole process is repeated (Luo *et al.*, 2003).

Jimmenez-Hornero *et al.* (2003) described a 2-D CA model that is coupled with a Bathnagar, Groos, and Krook (BGK) version of the lattice Boltzmann model. The erosion and transport components of the model are coupled to the water flow. If the flow at any point is high, solid particles will be picked up and displaced, whereas if the velocity is low, the particles will either settle or remain at rest. Once flow is established, the number of particles that do not leave the site is determined on the basis of a probability calculated from the velocity components.

## 4.2 River process modelling

### 4.2.1 Sediment transport and bed evolution

#### 3-D CFD modelling

In chapter 3, sediment and water processes at the geomorphological-unit scale were identified as important for prediction of river geomorphology at decadal time scales. Three-dimensional (3-D) CFD modelling provides what are considered state-of-the-art means to simulate fluvial processes at these smaller scales. The large computational effort needed to solve the 3-D CFD modelling equations described in this section has resulted in the use of alternative, less computationally-intensive modelling to account for geomorphological-unit scale sediment and water processes.

Wang and Weiming (2004) provided details of 3-D model equations for river sedimentation and morphology modelling. A 3-D flow field can be described by the following Reynolds-averaged continuity and Navier-Stokes equations:

$$\frac{\partial u_i}{\partial x_i} = 0 \quad (4.1)$$

$$\frac{\partial u_i}{\partial t} + \frac{\partial (u_i u_j)}{\partial x_j} = F_i - \frac{1}{\rho} \frac{\partial p}{\partial x_i} + \frac{1}{\rho} \frac{\partial \tau_{ij}}{\partial x_j} \quad (4.2)$$

where  $u_i$  ( $i=1, 2, 3$ ) are the velocity components.  $F_i$  includes the external forces, including the gravity force per unit volume,  $p$  is the pressure and  $\tau_{ij}$  are the turbulent stresses, which is determined by using a turbulence model.  $\rho$  is the fluid density.

For the shallow water flow, the pressure is assumed hydrostatic and all the vertical components of fluid acceleration can be ignored, yielding the quasi 3-D governing equations as

$$\frac{\partial u}{\partial x} + \frac{\partial v}{\partial y} + \frac{\partial w}{\partial z} = 0 \quad (4.3)$$

$$\frac{\partial u}{\partial t} + \frac{\partial (uu)}{\partial x} + \frac{\partial (vu)}{\partial y} + \frac{\partial (wv)}{\partial z} = -g \frac{\partial z_s}{\partial x} + \frac{1}{r} \frac{\partial t_{xx}}{\partial x} + \frac{1}{r} \frac{\partial t_{xy}}{\partial y} + \frac{1}{r} \frac{\partial t_{xz}}{\partial z} + fv \quad (4.4)$$

$$\frac{\partial u}{\partial t} + \frac{\partial (uv)}{\partial x} + \frac{\partial (vv)}{\partial y} + \frac{\partial (wv)}{\partial z} = -g \frac{\partial z_s}{\partial y} + \frac{1}{r} \frac{\partial t_{yx}}{\partial x} + \frac{1}{r} \frac{\partial t_{yy}}{\partial y} + \frac{1}{r} \frac{\partial t_{yz}}{\partial z} - fu \quad (4.5)$$

where  $u$ ,  $v$  and  $w$  are the velocities in the  $x$ ,  $y$  and  $z$  directions respectively and  $f$  is the Coriolis coefficient.

The hydrostatic pressure assumption brings significant simplification to the full 3-D problem of equations (4.1) and (4.2). However, this assumption is valid only for gradually varying open-channel flows. A full 3-D model without the hydrostatic pressure assumption is used in the regions of the rapidly varying flows, such as flows around bridge piers. The 3-D models developed by Wang and Adeff (1986), and Casulli and Cheng (1992) are based on the hydrostatic pressure assumption while those developed by Wu *et al.* (2000a), and Jia *et al.* (2001), are not.

The turbulent shear stresses in 2-D and 3-D models are determined by turbulence models. Most of the common turbulence model for river flow is based on the Bossinesq's eddy viscosity concept:

$$t_{ij} = r\nu_{ti} \left( \frac{\partial u_i}{\partial x_j} + \frac{\partial u_j}{\partial x_i} \right) - \frac{2}{3} kd_{ij} \quad (4.6)$$

where  $k$  is the turbulent kinetic energy, which is omitted in the zero-equation turbulence models.  $\nu_t$  is the eddy viscosity usually determined by the parabolic eddy viscosity model, the mixing length model or the linear  $k$ - $\varepsilon$  turbulence model (Wang and Weiming, 2004).

The 3-D flow drives the sediment transport as shown in Figure 4.10. The sediment transport is divided into suspended-load and bed-load, and hence the flow domain is

divided into a bed-load layer with a thickness  $\delta_b$  and the suspended load layer above it with a thickness  $h - \delta_b$ . The exchange of sediment between the two layers is through downward sediment flux (deposition) at a rate of  $D_{bk}$  and upward flux (entrainment) from the bed-load layer at a rate of  $E_{bk}$ . The distribution of the sediment concentration in the suspended-load layer is determined by the following convection-diffusion equation:

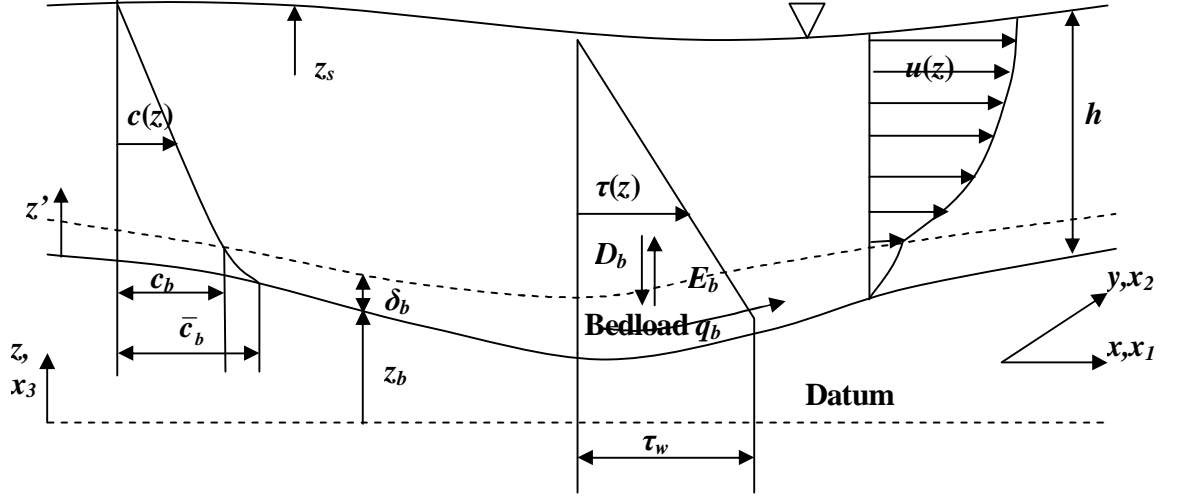


Figure 4.10 Flow configuration (Wang and Weiming, 2004)

$$\frac{\partial c_k}{\partial t} + \frac{\partial \left( (u_j - w_{sk} \delta_{j3}) c_k \right)}{\partial x_j} = \frac{\partial}{\partial x_j} \left( \frac{v_t}{s_c} \frac{\partial c_k}{\partial x_j} \right) \quad (4.7)$$

where  $c_k$  is the local concentration  $j$  of the  $k$ -th size class of suspended load.  $w_{sk}$  is the settling velocity.  $\delta_{j3}$  is the Kronecker delta with  $j = 3$  indicating the vertical direction. At the free surface, the vertical sediment flux is zero and hence the condition applied is:

$$\frac{v_t}{s_c} \frac{\partial c_k}{\partial z} + w_{sk} c_k = 0 \quad (4.8)$$

At the lower boundary of the suspended sediment layer, the deposition rate is  $D_{bk} = w_{sk} c_{bk}$  while the entrainment rate  $E_{bk}$  is:

$$E_{bk} = - \frac{v_t}{s_c} \frac{\partial c_k}{\partial z} = w_{sk} c_{bk} \quad (4.9)$$

where  $c_{bk}$  is the equilibrium concentration at the reference level  $z = z_b + \delta$ , which needs to be determined using an empirical relation.

The bed change can be determined by the exchange equation:

$$(1 - p'_m) \left( \frac{\int z_b}{\int t} \right)_k = D_{bk} - E_{bk} + \frac{1}{L_s} (q_b - q_{b^*}) \quad (4.10)$$

where  $L_s$  is the non-equilibrium adaptation length for bed-load transport and  $q_{b^*}$  is the bed-load transport under equilibrium conditions. The bed-load transport  $q_b$  is simulated using a formulation which is a function of flow hydraulics, bed composition and upstream sediment supply. These bedload transport formulations have varying levels of complexity in simulating non-equilibrium transport (Rahuel and Holly, 1989; Wu *et al*, 2000a; Wu and Vieira, 2002).

The overall sediment mass-balance equation integrated over the water depth  $h$  is

$$(1 - p'_m) \left( \frac{\int z_b}{\int t} \right)_k + \frac{\int (hC_{tk})}{\int t} + \frac{\int q_{tkx}}{\int x} + \frac{\int q_{tky}}{\int y} = 0 \quad (4.11)$$

$$q_{tky} = \alpha_{by} q_{bk} + \int_d^h \left( v c_k - \frac{v_t}{s_c} \frac{\int c_k}{\int y} \right) dz \quad (4.12)$$

$$q_{tkx} = \alpha_{bx} q_{bk} + \int_d^h \left( u c_k - \frac{v_t}{s_c} \frac{\int c_k}{\int x} \right) dz \quad (4.13)$$

where  $C_{tk}$  is the depth-averaged sediment concentration; and  $q_{tkx}$  and  $q_{tky}$  are the components of the total-load sediment-transport in  $x$ - and  $y$ -directions with  $\alpha_{bx}$  and  $\alpha_{by}$  being the direction cosines of the bed shear stress (Wang and Weiming, 2004).

### Local scour

Determination of local scour or scour at the geomorphological-unit scale is a highly complicated 3-D flow problem and requires the use of the 3-D CFD modelling equations described above because of the ability to present detailed flow characteristics required at this scale. These flow characteristics include downward flow, localized pressure gradient fluctuations, vorticity and turbulence intensity.

Richardson and Panchang (1998) obtained local scour by firstly, modelling the water flow field around an obstacle. The flow field provides the bed shear stress used to assess the potential erosion. The shape and size of the scour hole were predicted by including movement of the bed-load which forms a new geometry after some iteration.

Olsen and Melaaen (1993) simulated the scour process around a cylinder. They calculated sediment concentration for the bed elements with van Rijn's (1987) deterministic formula. Based on continuity for the bed sediment, erosion and deposition are calculated. Olsen and Melaaen's approach does not predict the scour hole depth when it reaches equilibrium. Olsen (1996) corrected this and used bed shear stress to compute the bed changes over a long time step with steady flow. This gave a scour hole shape very similar to what was obtained in a physical model study.

Hoffmans and Booij (1993) presented a scour model for the flow in a trench based on the solution of the 2-D Reynolds equation and the convection-diffusion sediment transport equation. The stochastic method proposed by van Rijn (1987) computed bed-load and suspended-load.

FHWA (1995) used appropriate sediment transport capacity formulas formulated especially for scour modelling, in conjunction with 1-D, 2-D and even 3-D flow models, to predict the maximum scour depth at the structures. These models simulate the details of the erosion process around in-stream structures especially under unsteady flow conditions. Empirical formulas determined the scour caused by particular in-stream structures (FHWA, 1995). Jia *et al.* (2001) and Wu and Wang (2004) provide examples of existing sediment transport formulas that simulate local scour near in-stream structures.

#### **4.2.2 Channel sedimentology and planform**

At the reach scale to the channel-type scale, the river is continuously evolving as fluvial sediments are transported through a moving bed or through suspended sediment transport. Numerical models account for sediment stores which adjust to changes in flow and sediment regimes causing channel aggradation and degradation. Models at these same scales simulate environmental sedimentology of river environments and stream planform characteristics.

### **Channel aggradation and degradation**

Channel aggradation and degradation is often modelled numerically using both width- and depth-averaged 1-D or 2-D models over a grid of cells. At each time step, transport capacity of the existing bed grain size distribution and sediment supply are used to compute the bed elevation and new grain size distribution. Operating over larger temporal and spatial scales there are a number of models designed to describe the river geometry and channel elevation change. These models are not concerned with the fine detail but only the general position and size of the channel.

Wiele and Franseen (2000) described a model that predicts the effects of variations in water discharge and sediment supply on deposition rates and magnitude. The model determines the effect of channel shape when aggradation and degradation changes occur. The model was developed to study bank erosion, bar formation and stability in gravel-bed rivers and has subsequently been extended to include suspended sediment transport.

The flow field is calculated with the vertically-averaged momentum and continuity equations for open channel flow. The model employs a 3-D advection-diffusion related to the local shear velocity quantifying the turbulent mixing. The product of the velocity and suspended sediment concentration is integrated vertically to calculate the local suspended sediment discharge. Calculation of the sediment transported as bedload includes the effect of local bed slope on transport rates. In areas with sufficient sediment thickness, local roughness and skin friction are calculated using the method of Bennett (1995) that relates bed-form dimensions to flow conditions and sediment size. In areas with little or no sediment, local channel roughness is calculated as a function of the spatial variability in the channel topography. Local change in bed elevation is then calculated using sediment continuity. The system is fully coupled as the bed changes induced by deposition or erosion affect the flow which, in turn influences sediment transport (Wiele and Franseen, 2000).



### **Braided river models**

Traditionally, researchers have opted for physical models to study braiding in gravel-bed rivers. Parker *et al.* (1982) performed experiments to model the transport mechanism of poorly sorted gravel at a scale of 1:10. Ashmore (1988) used small-scale physical models to examine channel forms and processes in braided gravel streams. He conducted laboratory modelling of braided river morphology and bed-load transport in river trays. Hoey and Sutherland (1991) developed a generic model at a scale of between 1:30 and 1:50 to examine braided channel morphology and bed-load transport of braided gravel-bed streams. Leddy *et al.* (1993) studied mechanisms of anabranch avulsion using a 1:20 scale model of the braided gravel-bed. Warburton and Davies (1994) determined variability in bed-load transport and channel morphology, in a 1:50 braided river model.

Murray and Paola (1994) modelled braiding using a simple non-linear relationship between flow strength and sediment transport with sediment flux increasing linearly with flow strength. The elevation of each cell is changed as sediment is moved downstream, cell by cell. Murray and Paola's model organises itself to form a visually realistic simulation of a braided channel. Flow strength is measured by bed shear stress, velocity, or the stream-power index, which is discharge multiplied by slope. Murray and Paola's model is a CA model that predicts braiding based on how river form and flow pattern interact through mutual feedback. During each time step, water is routed downstream from row to row within a rectangular grid. Water flow in a cell  $Q_o$  is distributed among the three downstream neighbour cells  $i$  as a function of the topographic gradients  $S_i$ :

$$Q_i = Q_o S_i^n / \sum_j S_j^n \quad (4.14)$$

where  $Q_i$  is the discharge from the cell in question into cell  $i$  and the sum is over the downstream neighbours. If none of the three downstream immediate neighbours is lower in elevation, the water is distributed to all three cells in a similar way, with more water flowing where the slopes are least negative (Murray and Paola, 1997).

Sediment transport fluxes  $Q_{si}$  are calculated as function of flow gradient and discharge described by:

$$Q_{si} = K(Q_i(S_i + C_s) - Th)^m \quad (4.15)$$

where  $K$ ,  $C_s$  and  $m$  are constants.  $m$  is based on empirical data on sediment transport according to stream power using reach-averaged slopes.  $Th$  is a sediment transport threshold. Since water depth is not defined in the model, Murray and Paola (1997) used bed slope as an approximation to water surface slope.  $C_s$ , however, still allows water to flow over regions with negative bed slopes causing sediment transport. Bed evolution occurs as cells in the model grid, representing the bed surface, change elevation (Murray, 2003).

In order for the sediment-transport process to maintain its dynamic behaviour indefinitely, a gravity-driven component of sediment transport that moves noncohesive sediment down lateral slopes was introduced. This is accounted for by a ‘lateral transport’ rule, based on that of Parker (1984), where sediment flux per unit width  $q_{sl}$  is transported down lateral slopes  $S_l$ :

$$q_{sl} = ((1 + mr) / m)(t_c / t)^{1/2} S_l q_s \quad (4.16)$$

$\mu$  is the dynamic coefficient of Coulomb friction,  $r$  is the ratio of lift to drag,  $t_c$  is the critical value of bed shear stress  $t$ , and  $q_s$  is the flow-driven sediment flux per unit width.

Figure 4.11 shows the routing of water and sediment fluxes, described above, to and from a given cell. The model produced a constantly migrating channel whose form and magnitude remain similar, displaying a form of dynamic equilibrium. The model also produces a non-linear sediment discharge, predicting pulses of sediment even though the water discharge is constant. The model predictions compared well with a laboratory-modelled river (Murray and Paola, 1997).

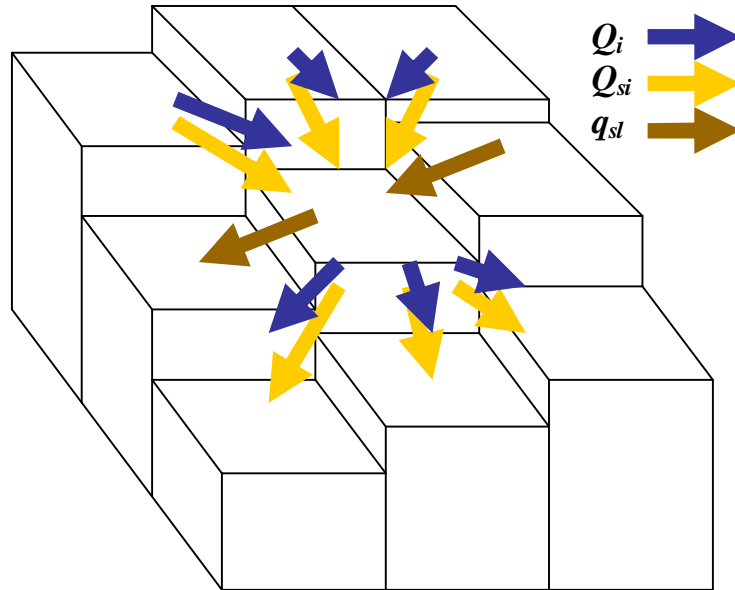


**Figure 4.11 Water and sediment routing in the Murray and Paola (1994) braided model. A given cell receives and distributes water from its neighbouring cells. Water flux is shown by blue arrows, direct sediment flux by yellow arrows and lateral sediment transport by brown arrows**

More recently, braiding has been modelled using the shallow water approximation of the Navier-Stokes equations (Murray, 2003). McArdell and Faeh (2001) developed a model that produces braiding including the emergence of mid-channel bars to form flow-dividing islands. They solved partial differential equations for water flow in a complex, radically changing channel, using ‘wetting and drying’ of model nodes. These flow equations were coupled to a sediment transport equation.

### **Meander models**

A few analytical models have been developed to predict the bed deformation in river bends. These models include that of Kikkawa *et al.* (1976), Zimmermann and Kennedy (1978), and Odgaard (1981). Such models are based on the balance of the dominant forces acting on a sediment particle moving along a radically inclined bed. The forces are fluid drag and particle submerged weight. When these forces become equal, an equilibrium transverse bed slope is achieved. These analytical models,

however, are applicable only to relatively simple bend flow conditions and do not provide the time variation of bend development.

A number of 2-D numerical models have been developed for computing bed deformation in meandering channels. These include those of Struiksma *et al.* (1985), and Shimizu and Itakura (1989). The numerical model developed by Shimizu and Itakura (1989) is used for the computation of time-independent 2-D bend deformation in alluvial rivers. Their model can be applied to channel geometry that can be modelled as a series of circular bends with constant width (Struiksma *et al.*, 1985). In addition, their model is applicable only to steady flow conditions. Shimizu and Itakura (1989) developed a 2-D model to calculate bed variation in channels under steady flow conditions. In their model, the governing equations of flow and sediment transport are solved in a cyclical coordinate system, which is valid only for a specific geometry.

Johannesson and Parker (1989), presented a physically-based model for meander dynamics, which was used to predict meander wavelength. Howard (1996) combined a meander evolution model based on that of Johannesson and Parker (1989) with a floodplain sedimentation model. He used this model to investigate the interaction between meander bend migration and floodplain sedimentation, and lithology. Stølum (1996) used a similar meander model to study the self-organising properties of an evolving meander train. He showed that such a system evolves towards a state of self-organised criticality resulting in sinuosity fluctuating through time. Nagata *et al.* (2000) presented a model that can be used to investigate both bed deformation and bankline shifting in 2-D meander plan form. The basic equations are used in a moving boundary-fitted coordinate system. They included a new formulation for non-equilibrium sediment transport to reproduce the channel processes.

Demuren and Rodi (1986) used 3-D simulations of the flow in meandering channels. Demuren (1989) extended this work to calculate suspended sediment transport. Demuren (1991) included a simple model for bed-load transport and calculated the flow and sediment transport in a 180-degree laboratory channel bend. Olsen (2003) used a fully

3-D non-hydrostatic model to predict the formation of the meandering pattern in an initially straight alluvial channel. His algorithm accounts for wetting and drying caused by channel erosion and deposition. Modules for both the suspended load and the bed-load were incorporated into the code.

#### **4.2.3 Modelling stable channel morphology**

River form, at the reach scale to the channel-type scale, can depend largely on riverbank failures and the long-term stability of riverbanks. There are various models that simulate the mechanisms whereby channel processes cause bank collapse. Such models predict the location of erosion and the rate of bankline shifting at critical locations.

##### **Bank-stability modelling**

The modelling employed in this study applies to non-cohesive sediment where the stability of the bank is accounted for by a simple formulation based on the angle of repose of sediments. Bank-stability modelling is important for realistic modelling of river geomorphology, as determined in Chapter 3, to include the effect of cohesion of fine grained sediments and the roots of vegetation.

Simon and Curini (1998) and Simon *et al.* (1999) produced a model to determine the stability of riverbanks. Their model is based on the wedge failure type models of Osman and Thorne (1988) and Simon *et al.* (1991). The model of Osman and Thorne (1988) employs an algorithm to analyse the stability of banks and calculates the factor of safety between the forces that drive and resist mass-bank failure. The model accounts for the geotechnical properties of the bank material, including soil shear strength (cohesion, angle of internal friction and unit weight) and positive and negative pore-water pressure (Simon and Curini, 1998; Simon *et al.*, 1999). In addition to positive and negative pore-water pressure, the model incorporates layered soils, changes in soil unit weight based on moisture content and external confining pressure from streamflow (Simon and Curini, 1998). Simon *et al.* (2000) proposed a more sophisticated bank-stability and toe erosion model, which considers wedge-shaped bank failures with several distinct bank material layers and user-defined bank geometry.

The wedge failure analysis entails use of the Mohr Coulomb Limit Equilibrium Criterion for the saturated portion of the wedge and the Fredlund *et al.* (1978) criterion for the unsaturated portion. In the unsaturated portion of the bank pores are filled with water and with air so that pore-water pressure is negative. The difference ( $\mu_a - \mu_w$ ) between the air pressure  $\mu_a$  and the water pressure in the pores  $\mu_w$  represents matric-suction  $\psi$ . The increase in shear strength due to an increase in matric suction is described by the angle  $\phi^b$ . Incorporating this effect into the standard Mohr Coulomb equation produces (Fredlund *et al.*, 1978):

$$S_r = c' + (s - m_a) \tan f' + (m_a - h_w) \tan f^b \quad (4.17)$$

where  $S_r$  is shear stress at failure,  $(\sigma - \mu_a)$  is net normal stress on the failure plane at failure. The value of  $\phi^b$  is generally between  $10^\circ$  and  $20^\circ$ , and increases with the degree of saturation. It attains a maximum value of  $\phi'$  under saturated conditions. The effects of matric suction on shear strength are reflected in the apparent or total cohesion  $c'$  term.

Negative pore-water pressures (positive  $\psi$ ) in the unsaturated zone provide an apparent cohesion over and above the effective cohesion, and thus, greater shearing resistance. In addition to this static model, there is also a dynamic version that uses a time series of pore-water pressure values to calculate the factor of safety (Simon *et al.*, 1999). The model was run using the simulated flow conditions as a driving input. The predicted bank profile was calculated on a daily basis and imported into the bank-stability model so that the stability of both the initial and the predicted bank profile could be assessed.

The bank-stability model used by Simon *et al.* (2003) incorporates the hydraulic effects of bank-toe erosion which increases the applicability and accuracy of the model in predicting critical conditions. A 2-D hydrology model is used to evaluate the effect of the simulated flow regime on streambank pore-water pressures. The bank-stability and toe-erosion model is used to investigate the effects of high flows on bank-toe scour and resulting bank geometry.

The bank-stability and toe-erosion model predicts the change in channel geometry that will result from exposure of bank and toe materials to flows of a given stage and duration. It

calculates erosion of cohesive soils using an excess shear-stress approach from the model of Partheniades (1965):

$$\varepsilon = k(\tau_o - \tau_c)^a \quad (4.18)$$

where  $\varepsilon$  is the erosion rate in m/s.  $k$  is an erodibility coefficient in  $\text{m}^3/\text{N}/\text{s}$ ;  $(\tau_o - \tau_c)$  is the excess shear stress in Pa.  $\tau_o$  is the average bed shear stress in Pa.  $\tau_c$  is the critical shear stress in Pa; and  $a$  is an exponent (often assumed = 1.0). The measure of material resistance to hydraulic stresses is a function of both  $\tau_c$  and  $k$ .  $k$  can be estimated as a function of  $\tau_c$  (Hanson and Simon, 2001):  $k = 0.1\tau_c^{-0.5}$  (4.19)

Resistance of non-cohesive materials is a function of surface roughness and particle size (weight) and is expressed in terms of the Shields criterion (Simon *et al*, 2003).

### **River widening and bank erosion modelling**

Bank erosion is the primary cause of river channel widening and meandering (Chang, 1980a). Many models make use of process-based and/or probabilistic bank-stability models to estimate the locations and sizes of active bank failures along streams (Darby and Thorne, 1996a). Inclusion of a method to predict the hydraulic shear erosion of cohesive bank materials is important in width-adjustment modelling because erosion directly influences the rate of retreat of the banks and also steepens the bank profile and promotes retreat. Widening models that attempt to account for river erosion of cohesive bank materials are often based on empirically based methods (i.e. Arulanandan *et al*, 1980).

Models of non-cohesive bank erosion employ sediment transport models in the near-bank zone, causing widening of river banks with homogeneous vertical structure. One such model is that of Li and Wang (1994), which simulates the bank erosion mechanism using a heuristic procedure. When bank slope exceeds the angle of repose of the boundary materials, a heuristic slumping model maintains an angle of repose onto the flow plain surface. Sediment above the failure plane is removed downslope, forming a deposit with a linear upper surface.

Most cohesive bank width adjustment modelling approaches have been based solely on analysis of planar failures. Mass failure of cohesive bank material, however, is discontinuous. Mass wasting algorithms for cohesive banks include that of Osman (1985), who accounts for the bank profile geometry associated with natural eroding river banks that are destabilised through a combination of lateral erosion and bed degradation (ASCE, 1998b). Darby and Thorne (1996b) developed a numerical model of bank erosion that introduces rotational slip and planar failure of the bank and applied it to model the geomorphological behaviour of a natural river.

#### **4.2.4 Equilibrium approaches**

Existing methods describing equilibrium river morphology entail the use of regime theory, power laws, extremal hypotheses and tractive force methods to describe a river at the macro-reach to the reach scale. These have been used to predict equilibrium river geometries. In general, width adjustment occurs simultaneously with changes in river geometry, roughness, slope, channel pattern etc. These adjust as the river approaches a dynamic state of equilibrium. Definition of the various forms of equilibrium is dependent upon the spatial and temporal scale under which the river is considered (Graf, 1988).

#### **Regime theory and Power law approach**

Regime theory is based on the tendency of a river system to obtain an equilibrium state under constant environmental conditions. Regime theory is based on empirical equations derived from regression of observed stable channel properties, such as width, depth, slope and meander length on flow and sediment properties. The theory suggests that principal channel characteristics remain stable for a period of years and that a change in the hydrologic or sediment regime results in erosion or deposition. River reaches that are “in regime” are able to move their sediment load through the system without net erosion or deposition and do not change their average shape and dimensions unless the long-term flow regime changes (Hey, 1997).

Geomorphologists have used data from natural rivers and laboratory flumes to develop power law hydraulic relations between channel top width, average depth, average velocity and bank full discharge (Leopold and Maddock, 1953). The regime equations of



Lindley (1919) and Blench (1969), are the most widely known. Semi-analytical work by Julien and Wargadalam (1995), has attempted to refine the regime approach within a framework based on the governing principles of open channel flow. These hydraulic geometry relations described adjustable characteristics of the river in terms of independent and dependent variables when the river is neither aggrading nor degrading. Rivers described as being "in regime" are considered "stable". Equations describing river geometry for stable mobile gravel-bed rivers were presented by Hey and Thorne (1986). Additional equations and discussion on stable river morphology were presented by Hey (1997).

Regime theory does not provide dimensionally homogeneous equations and their validity is limited to the catchments and data from which they were derived. Regime theory can give large errors when equations are applied to conditions that differ from those for which they were derived. Furthermore, regime equations are applicable to systems that have achieved equilibrium between sediment and water flow conditions (Brownlie, 1983).

### **Extremal hypothesis approach**

Extremal hypotheses argue that a river moves towards a state that is the most efficient. Although such a state may never be reached, a river is constantly adjusting itself in that direction (Chang, 1985). Extremal hypotheses predict channel geomorphology, using equations for sediment transport and alluvial friction in combination with a third relationship to predict regime or equilibrium geometry. The third relationship is used to maximize or minimize a parameter, such as stream power, energy dissipation rate or sediment concentration.

Extremal hypotheses that have been introduced and tested include minimum entropy production (Leopold and Langbein, 1962; Langbein, 1964), minimum energy dissipation rate (e.g. Brebner and Wilson, 1967; Yang and Song, 1979; Yang *et al*, 1981; Song and Yang, 1982; Yang, 1987), maximum sediment transporting capacity (e.g. Pickup, 1976; Farias, 1995; Qing Huang *et al*, 2002), minimum stream power (Chang, 1979; Chang, 1980a; Chang, 1980b; Millar and Quick, 1993; Millar and Quick, 1998), maximum friction factor (Davies and Sutherland, 1980;

Davies and Sutherland, 1983), and minimum Froude number (Jia, 1990; Yalin and Silva, 1999; Yalin and Silva, 2000).

Extremal hypotheses represent a general principle within the fluvial system and allow the selection of a single preferred cross-section out of many possibilities. The theoretical justification of extremal hypotheses lacks convincing physical explanation. The predictions based on extremal hypotheses, however, agree with a wide range of observations (Knighton, 1998).

### **Tractive force methods**

Tractive force or mechanistic methods use the basic laws of mechanics to obtain expressions that specify the geometry of stable channel cross-sections. The theory is founded on a fluid momentum balance to obtain the boundary shear stress and stability criterion for the sediment particles that make up the channel perimeter. Tractive force methods assume that the channel is straight, that there is negligible secondary flow and that sediment is non-cohesive and does not vary within the channel. With these assumptions a cosine profile is predicted for the stable cross-section (ASCE, 1998b).

### **4.2.5 Modelling spatial vegetation interaction**

For effective river management to be achieved it is important to model not only riparian vegetation dynamics but how the vegetation dynamics affects its habitat. Modelling riparian vegetation is different from modelling vegetation that is not riparian in that it is subject to a continually changing geomorphology and hydraulic regime. However, the resources that vegetation requires for establishment are the same. These resources include available sunlight, water, substrate and substances present in the soil. Plants use the resources available to sprout, survive, grow, and reproduce themselves and the resources also affect how the different individuals compete for them (Bandini and Pavesi, 2004). Most spatio-temporal vegetation models are described using partial differential equations (Berger and Hildenbrandth, 2000) but Chen *et al.* (2000) showed that the CA approach is good for modelling vegetation.

There are several examples of models predicting vegetation adjustment to alterations of hydrological regimes in regulated rivers (Rood and Mahoney, 1990; Auble *et al*, 1994; Richter *et al*, 1997; Friedman and Auble, 1999). These models are usually generated from long-term data of the reaction of vegetation dynamics to hydrological variation (Johansson and Nilsson, 2002). The interaction of riparian vegetation on its habitat, however, is less known.

Riparian vegetation changes its habitat by changing sediment transport indirectly owing to its effects on flow resistance. Sediment transport equations that describe sediment transport through vegetation are sparse because the interaction between sediment transport and riparian vegetation is to a large degree unknown. The effects of vegetation on sediment transport are validated by field and laboratory measurements to inform numerical modelling (Houwing *et al*, 2002; Madsen *et al*, 2001; Teeter *et al*, 2001; Jordanova and James, 2003).

### **Seedling recruitment modelling**

The vegetation modelling used in this study does not require detailed seedling recruitment modelling but, as discussed in Chapter 3, this process is an important process when vegetation establishment occurs primarily through seedlings and therefore it is described here in more detail.

Scott *et al*. (1996) developed a seedling recruitment model that predicts establishment and survival conditions necessary for cottonwood seedlings. The model determines the effects that hydraulic and geomorphic processes in river channels have on seedling recruitment. The model takes account of the physical requirements for seedling recruitment so that establishment occurs on sites that are bare, moist and relatively safe from physical disturbance.

The recruitment model couples with descriptions of geomorphological processes such as meandering, narrowing and flood deposition to produce different spatial and temporal patterns of riparian forest. The model deals with sediment deposition and erosion, which often produce or remove recruitment sites (Auble and Scott, 1998).

The operation of the model is illustrated below. The illustrations use typical bank geometry to show how tree recruitment patterns arise. Combinations of flood disturbance and suitable moisture conditions each year are produced in the wetted zone set out by summer peak flow and late summer base flow. No year-to-year change occurs when seedlings germinate in a zone adjacent to the channel which is disturbed by flooding (Figure 4.12) (Auble and Scott, 1998).

Some combination of flow variability and channel change that is different from the No Year-to-year change case in Figure 4.12 is necessary to produce successful tree recruitment. Peak floods produce bare, moist surfaces that are high above the channel bed and therefore relatively safe from future fluvial disturbance. Figure 4.13 shows a scenario resembling low flow years where flooding does not affect seedling establishment. Figure 4.14 shows the inclusion of geomorphological change in model predictions (Auble and Scott, 1998).

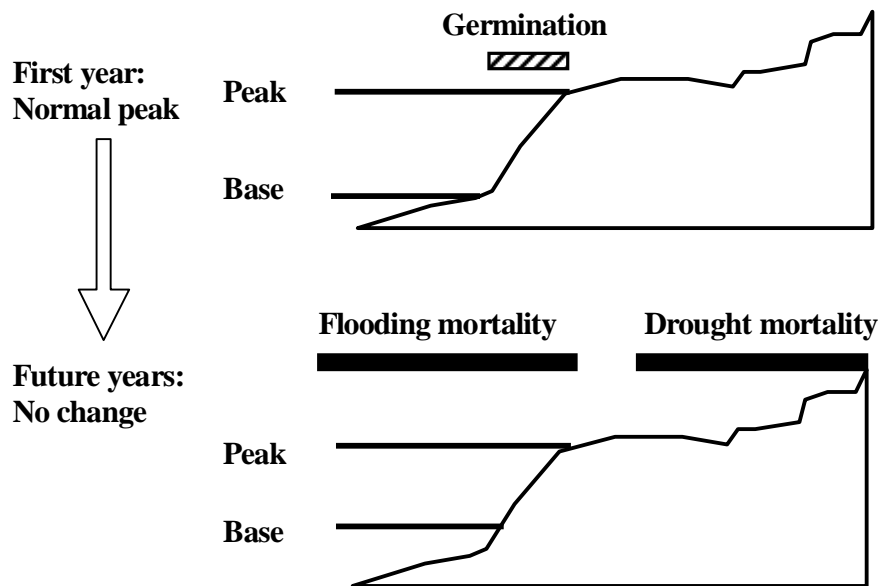


**Figure 4.12 No year-to year change in seedling recruitment due to germination falling in a zone where flooding occurs (Auble and Scott, 1998)**

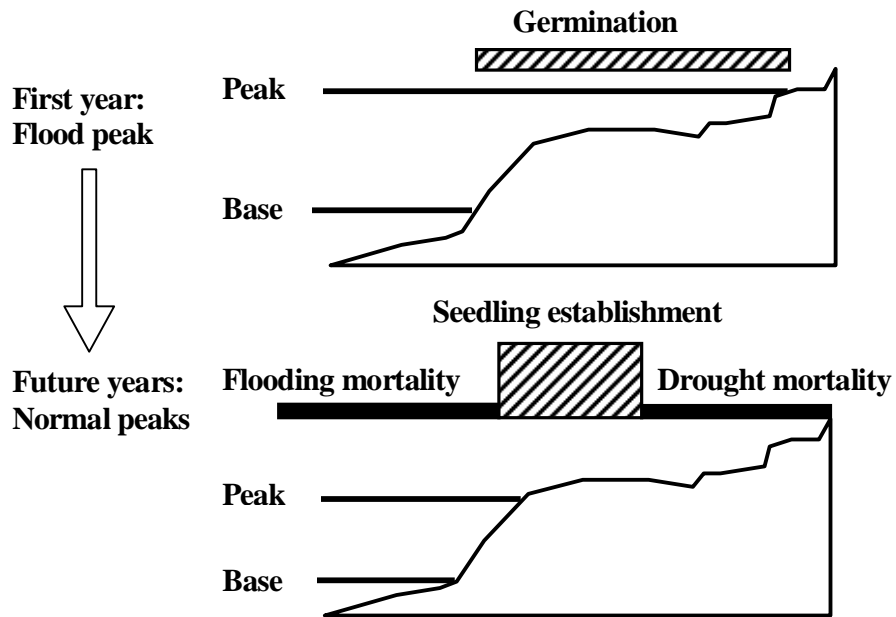


Figure 4.13 Seedling establishment in a zone where germination is unaffected by flooding and drought (Auble and Scott, 1998)

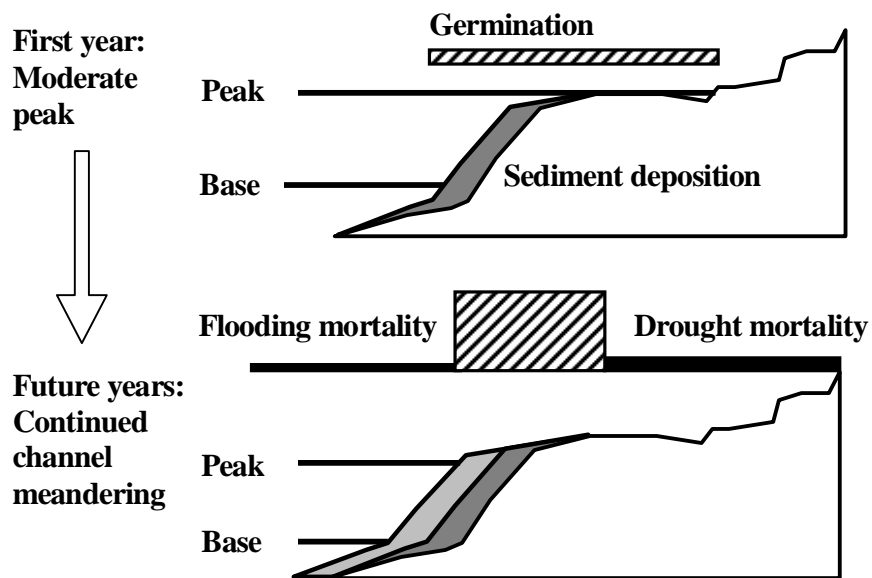


Figure 4.14 Inclusion of geomorphological change affecting seedling germination (Auble and Scott, 1998)

### **Growth and mortality modelling**

Growth and mortality modelling of riparian vegetation applies to the geomorphological-unit scale but in a special version of the GSTARS growth and mortality modelling is upscaled to represent the vegetation state at larger scales. GSTARS is a geomorphological code and will be discussed in more detail in the following section. The vegetation model is an addition to the 1-D simulation of river hydraulics, sediment transport and erosion/deposition of the GSTARS model. The model simulates the processes of vegetation growth and mortality as a function of species type, changing river stage, groundwater level, rate of root growth and the potential for scour velocity. The model assumes that vegetation will begin to grow at all points above the wetted channel that are free of existing vegetation (Wiele and Franseen, 1999).

The model applies a species-dependent growth rate to the plant roots and stem and tracks the root depth in relation to the groundwater level. If root growth is such that the roots stay below a falling capillary fringe caused by groundwater lowering, then the model assumes the vegetation can continue to grow. Otherwise, the model assumes that vegetation dies from desiccation. The model also takes account of the plant mortality due to drowning, velocity scour and burial. Furthermore, the model accounts for the initial vulnerability of seedlings becoming more resistant to plant stresses with time (Wiele and Franseen, 1999).

### **Cellular Automaton vegetation modelling**

Currently, the application of CA modelling is used mainly to model the growth and spatial evolution of single plant species at the channel-type scale. For example, Aassine and El Jaý (2002), developed an approach based on coupling of a local model for simulation of vegetation growth with a spatial evolution of vegetation described by CA modelling. The model takes account of local biomass growth, using partial differential equations. For describing the spatial evolution of vegetation, a CA model is used that employs 'transition rules'. For each cellular automaton, the 'transition rules' describe how the local growth dynamics affect space-time evolution of vegetation (Aassine and El Jaý, 2002).

Bandini and Pavesi (2004) however, presented a two-dimensional (2-D) CA model that simulates the evolution of heterogeneous plant populations, which include different perennial species in woods and forests. They used CA to model the interactions among single individuals and their associated competition for the resources available. Baltzer *et al.* (1998) also used CA to study vegetation dynamics of entire populations.

### **Rule-based vegetation modelling**

Baptist and Mosselman (2002) developed a rule-based model to determine the succession of three riparian vegetation types and the flow resistance caused by the vegetation at the reach scale. The model employs knowledge rules that are obtained from literature reviews. The knowledge rules are based on the suitability of environmental factors for vegetation growth and on directions and rates of vegetation succession. The rules are applied to every cell in a computational grid. The model predicts the path and rate of succession of the vegetation based on inundation time, the grazing intensity and changing river geomorphology. The input variable specified for inundation time includes the effects of inundation frequency and groundwater level (Baptist and Mosselman, 2002).

The vegetation mosaic is subdivided into low-lying, middle-lying and high-lying inundation classes based on their inundation time. Hence, changing geomorphology in the river changes the inundation classes of the vegetated cells leading to a shift in the way that succession takes place (Baptist *et al.*, 2002).

### **Sediment transport and vegetation**

To date, studies for the effect of vegetation were mainly at the geomorphological-unit scale based on modelling of the drag force of vegetation and its effect on the bed shear stress (Li and Shen, 1973; Tsujimoto, 1999; Bing *et al.*, 2001). Laboratory analyses that were done on sediment transport through vegetation include Abt *et al.* (1994), Prosser *et al.* (1995) and Jordanova and James (2003).

Baptist (2003) carried out a laboratory experiment in which turbulence characteristics and sediment transport were measured through submerged flexible vegetation. Measured profiles of velocity and turbulence were analysed and simulated with a 1-D flow model to

obtain estimates of the bed shear stress. The analysis of the bed level profiles gave rise to the hypothesis that the sediment transport through vegetation is mainly in the form of suspended transport. The increased turbulence levels in between the vegetation are capable of picking up the sediment more effectively and thus bringing the sediment in suspension (Baptist, 2003).

## **4.3 Geomorphic modelling codes**

### **4.3.1 One-dimensional codes**

One-dimensional (1-D) sediment transport models have become increasingly useful predictive tools to assess aggradation and degradation within channels. Where long-term predictions are required numerical models are the only way to simulate aggradation and degradation of the channel bed (Rathburn and Wohl, 2001). The 1-D models CCHE1D, FLUVIAL-12, HEC-6 and CONCEPTS apply at the reach to channel-type scale and are discussed below.

#### **CCHE1D**

The CCHE1D sediment transport model has been widely applied to the simulation of general sediment transport in rivers and reservoirs. CCHE1D simulates unsteady flow and nonuniform sediment transport in channel networks and can handle sediment selection, bed material hiding, exposing and armouring. This model can predict channel aggradation and degradation patterns as well as the sediment transport characteristics. CCHE1D simulates channel widening by modelling the river erosion at bank toes and the consequent bank mass failures.

The CCHE1D sediment transport model adopts the non-equilibrium approach for the total-load transport. The flow and sediment calculations are decoupled but a coupled procedure is adopted in the sediment module to solve the nonuniform sediment transport, bed change and bed material sorting equations simultaneously. The sediment transport capacity can be determined from the formula of Wu *et al.* (2000b), the SEDTRA module (Garbrecht *et al.*, 1995), the modified Ackers and White formula



(Proffitt and Sutherland, 1983) and the modified Engelund and Hansen formula (Wu and Vieira, 2002).

### **FLUVIAL-12**

FLUVIAL-12 is an erodible boundary model that can model changes in bed elevation as well as channel width and topography induced by channel curvature. This model has five major components (Chang, 1998):

- n Water routing,
- n Sediment routing,
- n Changes in channel width,
- n Changes in channel bed profile,
- n Lateral migration of the channel.

The sediment routing component for the FLUVIAL-12 model has the following major features (Chang, 1998):

- n Computation of sediment transport capacity using a suitable formula for the physical conditions.
- n Determination of actual sediment discharge by making corrections for sorting and diffusion.
- n Upstream conditions for sediment inflow.

### **HEC-6**

HEC-6 (Thomas and Prashum, 1977) is one of the most widely used commercially available sediment transport models. The model predicts scour and deposition within rivers and reservoirs. In river applications, HEC-6 simulates uniform changes in riverbed elevation over the entire width of the channel to account for erosion and deposition under subcritical flow. The model does not simulate lateral channel changes such as meander migration or lateral changes in bed slope. The governing equations in HEC-6 include the energy equation and conservation of mass for water and sediment. The model takes into account the effects of sediment gradation.

HEC-6 makes use of a discharge hydrograph, which is presented as a sequence of steady flows of variable duration. Water surface profiles are calculated for each flow using the

standard-step method to solve the energy and continuity equations. Friction loss is calculated by Manning's equation and expansion and contraction losses can be calculated. Geometry of the river system is represented by cross-sections which are specified by coordinate points and the distances between cross-sections. HEC-6 raises or lowers cross-section elevations to reflect deposition and scour.

Using continuity of sediment bed elevation changes are calculated with respect to time along the study reach. Inflowing sediment loads are related to water discharge using sediment-discharge curves. Sediment loads are provided at the upstream boundaries of the river reach, tributaries and local inflow points. HEC-6 allows a different gradation at each cross-section. Sediment is routed downstream for each time step after the backwater computations are made.

## **CONCEPTS**

The National Sedimentation Laboratory has developed the Conservational Channel Evolution and Pollutant Transport System (CONCEPTS) to simulate the evolution of rivers. CONCEPTS simulates unsteady 1-D flow, graded sediment transport and bank-erosion processes in river channels. CONCEPTS includes varying boundary roughness along a cross-section. It can predict the dynamic response of flow and sediment transport to in-stream hydraulic structures and computes channel evolution by determining bed elevation changes and channel widening. CONCEPTS simulates transport of cohesive and cohesionless sediments, both in suspension and on the bed, and selectively by size classes. For graded bed material, the sediment-transport rates depend on the bed material composition. For cohesive bed, material erosion rates are calculated following an excess shear-stress approach. The deposition rate is based on local shear stress and particle fall velocity (Langendoen, 2000).

CONCEPTS simulates channel-width adjustment by incorporating the fundamental physical processes responsible for bank retreat: firstly river erosion or entrainment of bank-material particles by flow, and secondly, bank mass failure due to gravity. Bank material may be cohesive or non-cohesive and may comprise numerous soil layers. CONCEPTS

performs stability analyses of planar slip failures and cantilever failures of overhanging banks (Langendoen, 2000).

### **4.3.2 Multi-dimensional codes**

Multi-dimensional models employ 2-D and 3-D and helical flow modelling coupled with mobile bed calculation. Helical flow is represented by quasi-2-D models which employ the stream tube concept developed to reflect the effect of lateral variations of the channel geometry. The following multi-dimensional models are discussed below: CCHE2D; GSTARS2.0; SEC-HY11 and Mike 21C. These models apply to the channel-type scale.

#### **CCHE2D**

CCHE2D is a depth-averaged 2-D model for flow and sediment transport in rivers. Similar to CCHE1D, CCHE2D includes nonuniform sediment transport modelling and bed material hiding, exposing and armouring. The model is able to simulate channel widening and meandering by considering the effect of secondary flow on main flow and sediment movement.

CCHE2D has two versions. One is based on EEM (Efficient Element Method) and the other FVM (Finite Volume Method). In both versions of CCHE2D, the nonuniform total-load transport is simulated using the non-equilibrium approach. The sediment transport capacity is determined by the formula of van Rijn (1987), the formula of Wu *et al* (2000b), the SEDTRA module (Garbrecht *et al*, 1995), the modified Ackers and White formula (Proffit and Sutherland, 1983), or the modified Engelund and Hansen formula (Wu and Vieira, 2002). The effect of secondary flow on the main flow and sediment transport in curved channels is considered in both versions.

The EEM-based version adopts a fully decoupled procedure for flow and sediment transport while the FVM-based version adopts the semi-coupled procedure similar to that used in CCHE1D model. The FVM-based CCHE2D model is capable of simulating the geomorphological change because of vegetation growth in the river. The vegetation effects are considered by including the drag force in the momentum equations and by the generation and dissipation of turbulent energy in the  $k-\varepsilon$  equations.

## **GSTARS2.0**

The GSTARS computer model (Generalized Stream Tube model for Alluvial River Simulation) was first developed by Molinas and Yang (1986), to simulate the flow conditions in a semi-2-D manner and the change of channel geometry in a semi-3-D manner. The governing equations are based on energy and conservation of mass for water and sediment. GSTARS is able to specify the number of stream tubes at each cross-section (Rathburn and Wohl, 2001). The GSTARS model was revised and enhanced by Yang *et al.* (1998) to be released as GSTARS 2.0.

GSTARS 2.0 is a quasi-2-D model that utilizes a stream tube concept to accommodate differential scour and deposition over the width of a cross-section. It employs stream tubes as conceptual tube-like surfaces whose walls are defined by streamlines. In GSTARS, hydraulic parameters and sediment routing computations are made for each stream tube, allowing the position and width of each stream tube to change. In this way, vertical and lateral variations in cross-sectional elevation are simulated.

Sediment routing, bed sorting and armouring computations are performed independently for each stream tube. The model has 13 transport functions for particle sizes ranging from clay to silt, sand, and gravel, including non-equilibrium transport and flows with a high concentration of wash load. The model is able to predict variations in channel width according to the theory of total stream power minimization (Chih and Francisco, 1998).

## **Mike 21C**

Mike 21C is a generalised numerical modelling system for the simulation of the hydrodynamics of vertically homogenous flows and for the simulation of sediment transport. Mike 21C predicts a 2-D free surface and sediment transport in rivers where an accurate description of flow along the banks as well as helical 3-D flow is important. The model can for example deal with sedimentation of water intakes, outlets, bridge tunnels and pipeline crossings.

Helical flow is calculated in connection with sediment transport to enable prediction of bend scour, confluence scour and in formation of point bars as well as alternating bars. The

model allows for both bed-load and suspended-load transport. After each time step, the eroded bank material is included in the solution of sediment continuity equation (<http://www.dhigroup.com/Software/WaterResources/MIKE21C.aspx>).

#### **4.4 Conclusion**

This chapter gives a review of various modelling methods that can be used to describe river processes and existing models of river processes at various organisational levels. CFD modelling in this study will be employed for water flow at various scales but numerical CA modelling will be employed to model sediment and vegetation processes at the channel-type scale to add flexibility to the modelling, which is required for the hierarchical strategy employed. CFD modelling of water flow at this scale provides the required accuracy and therefore it would not be necessary to develop a rule-based model, for example, to determine water flow at the channel-type scale. Rule-based modelling would be most suitable for vegetation population modelling at the reach scale but for vegetation growth dynamics at the geomorphological-unit scale, numerical modelling is more appropriate. The models used and developed within this study are described in Chapter 5.

The river geomorphological modelling packages reviewed in this chapter do not consider all the processes which affect river form, especially vegetation. These modelling packages also do not consider many of the processes operating at various organisational levels and therefore lack the predictive capability for river form at decadal time scales. Not only is small-scale river form required for river habitat management, but it also affects the rates at which river form changes at larger scales.

Effective integration of models for various interacting processes at various scales has to allow for feedback, which is vital for accurate simulation of rivers over a decade. Few models simulate interactively the impacts of flow on plants in river channels and their feedback effects (Hooke *et al*, 2005). Modelling integration is discussed in Chapter 6.

## Chapter 5 – Hierarchical modelling

---

In this chapter, each of the hierarchically nested models representing sediment, water and vegetation processes is described. Models are chosen or developed to apply at the reach scale, the channel-type scale and geomorphological-unit scale. These models have to be linked to allow feedback between models. Figure 5.1 illustrates the process models described in this chapter and also the feedback between these process models.

Trans-scale modelling linkage refers to the feedback across organisational levels and is applied through roughness coefficients and boundary conditions. A critical aspect of trans-scale linkage is to determine flow resistance coefficients. These resistance coefficients are specific to the models chosen to represent water at various organisational levels used in this study. Flow resistance formulations also have to incorporate the effect of sediment and vegetation processes on water flow. Trans-scale linkage therefore requires further explanation and is discussed in the following chapter.

Existing water flow models at the reach scale and the channel-type scale are used. The reach scale water flow model solves one-dimensional (1-D) Saint-Venant equations whereas the channel-type scale water flow model is governed by two-dimensional (2-D) Saint-Venant equations. The water flow model at the geomorphological-unit scale is not based on the actual physics of water flow but does account for the smaller scale variability of the water distribution.

The sediment model at the reach scale employs the Exner equation of sediment continuity in combination with the gravel-bed-load transport equations to determine changes in bed elevation. For the channel-type scale, a cellular automaton (CA) model was developed using the modelling concept of Murray and Paola (1994). At the geomorphological-unit scale, a combination of existing formulations is used to predict the dimensions and growth of bed-forms representing sediment dynamics.

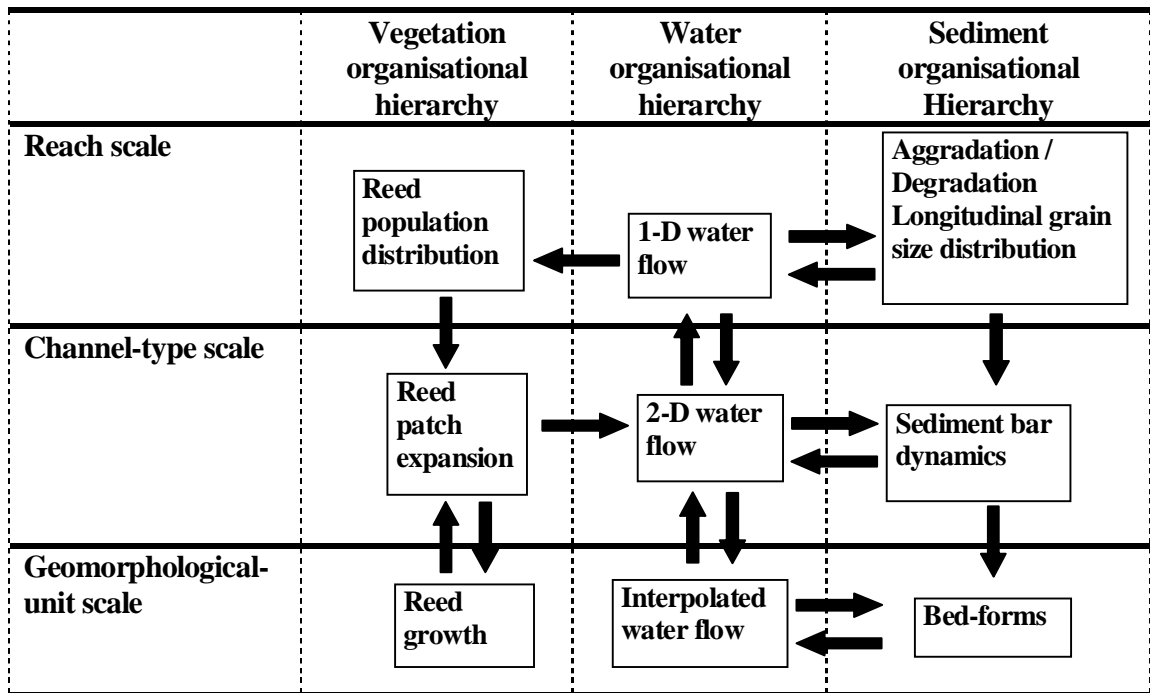


**Figure 5.1 Hierarchical models of sediment, water and vegetation processes across the reach scale, channel-type scale and geomorphological-unit scale. Downward arrows represent feedback through boundary conditions and upward arrows represent feedback through model parameters. Horizontal arrows represent feedback between water, sediment and reed processes**

In this study a shallow gravel-bed river was chosen to be modelled, which allows the important river process of river bank-stability, as outlined in Chapter 3, to be simplified. Another important river process identified in Chapter 3 is local scour, which is ignored within the modelling in this study. Local scour is a process at the geomorphological-unit scale which requires great computational effort and since the hierarchical modelling is inherently computationally intensive, local scour is ignored. Ignoring local scour may be acceptable since it is caused by the acceleration of flow and by vortices resulting from flow around an obstruction and it will therefore be assumed that no obstructions are present in the modelling scenarios.

The vegetation models at the reach scale and the channel-type scale were developed specifically to describe dynamics of common reeds or *Phragmites Australis*. Reeds were chosen for representing the effect of vegetation because of the large role they play as

geomorphological modifiers. This is a large simplification but is justified because the goal of this thesis, which is to deal with river complexity in order to make reliable predictions, will nevertheless be achieved. The reach scale model predicts the distribution of reed populations along the river bank gradient whereas the channel-type scale reed model is a CA model that predicts the expansion of patches within the population. The vegetation model at the geomorphological-unit scale is an existing model describing the growth of *Phragmites Australis* by integrating finite differential equations for biomass growth.

The spatial modelling resolution is 100 m for the reach scale, 5 m for the channel-type scale and 0.25 m for the geomorphological-unit scale. The models are decoupled and run at asynchronous time steps. Table 5.1 gives typical time steps used by each of the individual models.

**Table 5.1 Typical time steps used in the modelling at the various organisational levels for the vegetation, water and sediment hierarchies**

	<b>Vegetation organisational hierarchy</b>	<b>Water organisational Hierarchy</b>	<b>Sediment organisational hierarchy</b>
<b>Reach scale</b>	1 year	15 seconds	1 minute
<b>Channel-type scale</b>	20 days	0.2 seconds	5 seconds
<b>Geomorphological-unit scale</b>	1 day	-	0.1 second

Model equations and procedures were implemented in a MS-Excel workbook with Visual Basic for Applications (VBA). Modelling code is provided in the Appendixes.

## **5.1 Reach scale water flow**

### **5.1.1 One-dimensional Saint-Venant equations**

The dynamic model is governed by the 1-D Saint-Venant equations for open-channel flows with low sediment concentration:

$$\frac{\partial A}{\partial t} + \frac{\partial Q}{\partial x} = 0 \quad (5.1)$$



$$\frac{\partial}{\partial t} \left( \frac{Q}{A} \right) + \frac{\partial}{\partial x} \left( \frac{Q^2}{2A^2} \right) + g \frac{\partial y}{\partial x} + g S_f = 0 \quad (5.2)$$

where  $x$  and  $t$  are the spatial and temporal axes respectively;  $A$  is the flow area;  $Q$  is the flow discharge;  $y$  is water surface elevation;  $g$  is the gravitational acceleration; and  $S_f$  is the friction slope.

### 5.1.2 Flow resistance

The friction slope is defined as

$$S_f = \frac{n^2 Q^2}{A^2 R^{4/3}} \quad (5.3)$$

in which  $R$ , and  $n$  are respectively, the hydraulic radius and Manning's roughness coefficient. The Manning's  $n$  is stored at each computational node representing a cross-section within the reach.

### 5.1.3 The MacCormack method for solving 1-D flow

The equations are solved using the MacCormack method for solving finite difference equations. The MacCormack method is explicit, so that the value of each variable is calculated entirely from previously calculated values (Chaudhry, 1993).

Using the MacCormack method, each variable is calculated twice for each time step. In the first calculation, called the predictor step, depth,  $y^*$ , and velocity,  $u^*$ , are calculated with backward differences with respect to both  $x$  and  $t$ . In the second calculation, called the corrector step, depth,  $y^{**}$  and velocity,  $u^{**}$  are calculated using forward differences of the predictor step with respect to  $x$  and backward differences of the predictor step with respect to  $t$ . The final values are the arithmetic mean of the predictor and corrector values.

The following equations are given by Chaudhry (1993) and have been de-composed into finite difference equations:

$$A_j^* = A_j^{t-1} - \frac{\Delta t}{\Delta x} \left( (uA)_j^{t-1} - (uA)_{j-1}^{t-1} \right) \quad (5.4)$$

$$(uA)_j^* = (uA)_j^{t-1} - \frac{\Delta t}{\Delta x} \left( (u^2 A + gA\bar{y})_j^{t-1} - (u^2 A + gA\bar{y})_{j-1}^{t-1} \right) + g \cdot A \cdot \Delta t \cdot (S_0 - S_f)_j^{t-1} \quad (5.5)$$

$$A_j^{**} = A_j^{t-1} - \frac{\Delta t}{\Delta x} \left( (uA)_{j+1}^* - (uA)_j^* \right) \quad (5.6)$$

$$(uA)_j^* = (uA)_j^{t-1} - \frac{\Delta t}{\Delta x} \left( (u^2 A + gA\bar{y})_{j+1}^* - (u^2 A + gA\bar{y})_j^* \right) + g \cdot A \cdot \Delta t \cdot (S_0 - S_f)_j^* \quad (5.7)$$

$$A_j^t = \frac{1}{2} (A^* + A^{**}) \quad (5.8)$$

### 5.1.4 Stability Condition

The time interval  $Dt$  and distance step  $Dx$  is determined to ensure stability. The stability condition for most explicit finite difference methods is stated as:

$$C_n = \frac{|u| \pm c}{\Delta x / \Delta t} \leq 1 \quad (5.9)$$

where  $C_n$  is the Courant Number (Chaudhry, 1993), and  $c$  is calculated from:

$$c = \sqrt{g \cdot y} \quad (5.10)$$

Stability is ensured by increasing  $Dx$  or decreasing  $Dt$  for a maximum value of the numerator  $u + c$ .

## 5.2 Reach scale sediment flow and bed elevation

### 5.2.1 Model overview

The 1-D reach scale sediment model computes the change in river bed elevation  $h$ , based on total bed material load. The reach has length  $L$  over which bed sediment with grain size  $D$  and submerged specific gravity  $s$  is transported. Initially the channel has a uniform slope  $S$ . The bed elevation at the downstream end is assumed to be fixed. Changing the sediment feed rate  $G_f$  at the upstream end forces bed elevations to aggrade or degrade to move toward an equilibrium state over time  $t$ .

### 5.2.2 Intermittency

Most geomorphological change occurs during floods and flooding, which typically occurs only over a small portion of time throughout a year (Figure 5.2). This portion of time is

referred to as the Intermittency  $I_f$  of the river (Paola *et al*, 1992). Intermittency allows the time step to be increased to provide the total period over which the bed elevation changes.

After averaging over many floods, the relation between cumulative time in which the river has been in flood  $t_f$  and actual time  $t$  is  $t_f = I_f t$  (5.11)

The model is driven by input provided by the 1-D water flow model, which simulates the flood flows. These floods are episodic events and their duration, together with intermittency, determines their effect at the decadal time scales.

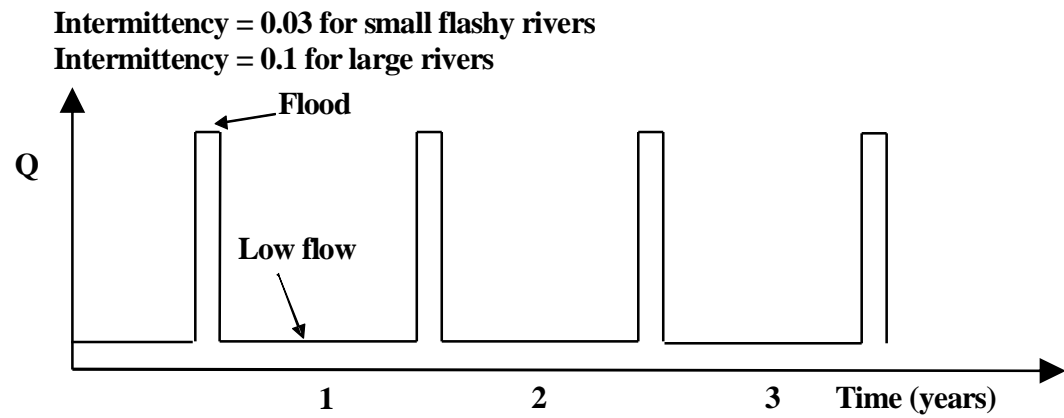


**Figure 5.2 Idealised hydrograph associated with intermittency**

### 5.2.3 Bed elevation computation

The Exner equation of sediment continuity takes the form

$$(1 - I_p) \frac{\partial h}{\partial t} = - \frac{\partial q_b}{\partial x} \quad (5.12)$$

where  $q_b$  refers to the bed-load sediment transport rate during flooding,  $h$  denotes bed elevation,  $I_p$  denotes the porosity of the bed deposit and  $t$  denotes time. Averaging over many floods, equation (5.12) is changed to

$$(1 - I_p) \frac{\partial h}{\partial t} = - \frac{\partial I_f q_b}{\partial x} \quad (5.13)$$

The numerical solution scheme for the Exner equation is described below.

### 5.2.4 Numerical solution scheme for the Exner equation

Figure 5.2 shows the numerical solution scheme for solving the finite difference form of the Exner equations. The reach is assumed to have length  $L$  and divided into  $M$  sub-reaches, each with length  $\Delta x$  which is given by

$$\Delta x = \frac{L}{M} \quad (5.14)$$

A ghost node is introduced to provide boundary conditions for backward difference applications.

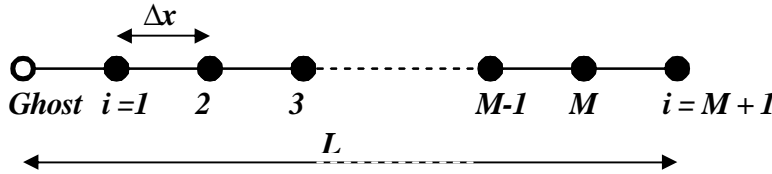


**Figure 5.3 Numerical solution scheme for the Exner equation of sediment continuity**

This defines  $M + 1$  node with the positions

$$x_i = (i - 1)\Delta x, i = 1..M + 1 \quad (5.15)$$

as noted in Figure 5.3. The initial bed elevations  $h_i$  are given as

$$h_i = S_l(L - x_i), i = 1..M + 1 \quad (5.16)$$

$S_l$  denotes the initial bed slope of the river.  $h$  is determined at all nodes allowing computation of the Shields number  $t^*$  at all nodes using equation (5.35). From the known values of  $t_i^*$  the sediment transport rate  $q_{b,i}$  can be computed from equation (5.22). The new bed elevation at the next time step is then given from a discretized version of equation (5.13).

$$h_i|_{t+\Delta t} = h_i|_t - \frac{1}{1 - I_p} \frac{\Delta q_{t,i}}{\Delta x} I_f \Delta t, i = 1..M + 1 \quad (5.17)$$

where  $\Delta t$  denotes the time step and

$$\frac{\Delta q_{t,i}}{\Delta x} = \begin{cases} a_u \frac{q_{t,i} - q_{t,i-1}}{\Delta x} + (1 - a_u) \frac{q_{t,i+1} - q_{t,i}}{\Delta x}, & i = 1..M \\ \frac{q_{t,i} - q_{t,i-1}}{\Delta x}, & i = M + 1 \end{cases} \quad (5.18)$$

In equation (5.18),  $a_u$  is a coefficient that can be set between 0 and 1. The setting  $a_u = 1$  yields a pure upwinding scheme, which gives stability at the cost of accuracy.  $a_u = 0.5$  yields a central difference scheme, which gives accuracy at the cost of stability.

### 5.2.5 Sediment feed

The bed-load sediment transport rate  $q_b$  in  $m^2/s$  is associated with the annual sediment yield  $G_t$  in tons/year given as

$$G_t r_s = q_b B I_f t_a \quad (5.19)$$

where  $t_a$  denotes the number of seconds in a year. Similarly, specifying the sediment feed rate  $G_{tf}$  at the upstream end of the river gives  $q_b$  as:

$$q_b = \frac{G_{tf}}{r_s B I_f t_a} \quad (5.20)$$

### 5.2.6 Sediment transport

The model implements the surface-based bed-load transport equations of Wilcock and Crowe (2003) developed for gravel-bed rivers described below. The equations and procedures recognise the role of the armour layer in regulating bed-load transport rates. The sediment transport include equations used apply the surface grain-size characteristics as inputs.

The bed-load transport relations use a dimensionless parameter  $W^*$  as a function of the transport stage

$$f = \frac{t}{t_r^*} \quad (5.21)$$

where  $t^*$  is the Shields stress and  $t_r^*$  is the reference Shields stress that produces a small but measurable transport rate. Bed-load transport rate per unit width  $q_b$  is determined according to  $W^*$

$$q_b = \frac{W^* r_s U^{*3}}{(s-1)g}$$

(5.22)

where  $s$  is the specific gravity of sediment determined from

$$s = \frac{r_s}{r} \quad (5.23)$$

where  $\rho_s$  is the density of sediment taken as  $2650 \text{ kg/m}^3$ ,  $\rho$  is the density of water.

$U^*$  is the shear velocity determined from:

$$U^* = \sqrt{(s-1)gD_{50}t^*} \quad (5.24)$$

where  $D_{50}$  is the midpoint of the distribution corresponding to the value for which half the sediment is finer is the median grain size.  $W^*$  is determined from relations described in section 5.2.8.

### 5.2.7 Grain size calculation

Representative samples of the bed surface-layer are required in order to develop a cumulative frequency distribution of the available grain sizes. Sample values are entered into the model as a cumulative frequency distribution of the percentage of particles finer than a given size  $D$  in millimetres.

For convenience, a  $\Phi$ -scale is also used to represent grain size. The  $\Phi$ -scale varies with the base 2 logarithm of the grain size:

$$\Phi = \log_2 D \quad (5.25)$$

where  $D$  is in millimetres.

The model calculates transport rates on the basis of discrete values of the grain size distribution  $D_i$  where the subscript  $i$  refers to an individual percentile of the grain size distribution. Sediment transport parameters are calculated from the full grain size distribution of the sample using individual values for each size class. Let  $D_1, D_2, \dots, D_{N+1}$  be the grain sizes associated with each of the  $N$  size classes, and let  $f_1, f_2, \dots, f_{N+1}$  be the fraction of the mass represented in each size class. The mean values of  $D_i$ ,  $\Phi_i$  and  $f_i$  for each class are calculated as follows:

$$\overline{D}_i = \sqrt{D_i D_{i+1}}, \quad \overline{\Phi} = \frac{\Phi_i + \Phi_{i+1}}{2}, \quad \overline{f} = f_{i+1} - f_i \quad (5.26a,b,c)$$

here the subscripts  $i$  and  $i + 1$  refer to adjacent size classes. The values obtained from equation (5.25) are used to estimate additional parameters,  $s_g = 2^s$ ,  $s = \sqrt{\sum_{i=1}^N (\Phi_i - \overline{\Phi})^2 f_i}$

$$\text{and } D_g = 2^{\overline{y}}, \quad \overline{\Phi} = \sum_{i=1}^N \overline{\Phi}_i f_i \quad (5.27a,b)$$

where  $\overline{\Phi}$  is the arithmetic mean in  $\Phi$  units,  $D_g$  is the geometric mean grain size in millimetres,  $\sigma$  is the arithmetic standard deviation in  $\Phi$  units and  $\sigma_g$  is the geometric standard deviation in millimetres.

### 5.2.8 The surface-based relation of Wilcock and Crowe (2003)

Wilcock and Crowe (2003) developed a transport relation based on the full grain size distribution of the bed surface including the sand. This relation includes an additional function that accounts for the non-linear effect of sand content on gravel transport rates. The basic form of the equation is as follows

$$W_i^* = 0.002f^{7.5} \quad \text{for } f < 1.35 \quad (5.28)$$

$$W_i^* = 14 \left( 1 - \frac{0.894}{f^{0.5}} \right)^{4.5} \quad \text{for } f \geq 1.35 \quad (5.29)$$

$$\text{where } t_{ri} = t_{r50} \left( \frac{D_i}{D_{50}} \right)^b, \quad t_r = \sum_{i=1}^N t_{ri} f_i \quad (5.30a,b)$$

and an empirical function that accounts for the variation in sand content

$$t_{r50} = 0.021 + 0.015 \exp(-20F_s) \quad (5.31)$$

where  $F_s$  is the percent of sand on the bed surface.

The exponent in the hiding function  $b$  is calculated from

$$b = \frac{0.67}{1 + \exp\left(1.5 - \frac{D_i}{D}\right)} \quad (5.32)$$

where  $D$  is the mean grain size of the bed surface. The reference shear stress for  $D$  is found using the Shields stress relation

$$t_r^* = \frac{t_r}{(s-1)gD} \quad (5.33)$$

## 5.2.9 Computation of the shear stress

The normal-flow formulation for boundary shear stress  $t_b$  and Shields number (Shields stress)  $t^*$  are the parameters used to compute sediment transport where

$$t_b = rU^{*2} = rgdS_f \quad (5.34)$$

and

$$t^* = \frac{t_b}{rRgD_g} = \frac{dS_f}{RD_g} \quad (5.35)$$

where  $S_f$  is the friction slope and  $d$  is the flow depth.

In order to calculate  $S_f$  the water surface elevation  $y$  average flow velocity  $U$  and bed slope  $S$  are required at each computational node  $i$  at interval distance  $\Delta x$  for the reach described by a numerical solution scheme.

$$S_{f_i} = \frac{\left( y_{i+1} + \frac{U_{i+1}^2}{2g} \right) - \left( y_{i-1} + \frac{U_{i-1}^2}{2g} \right)}{2\Delta x} + S \quad (5.36)$$

Values for these variables are obtained from the 1-D flow model described above.

## 5.3 Reach scale reed population dynamics

### 5.3.1 Model overview

The population distribution of common reeds (*Phragmites Australis*) up the river bank gradient at the reach scale is predicted by a fuzzy expert system. Fuzzy-rule-based modelling is well suited to prediction of the patterns of reed populations at the reach scale as affected by the flow regime since it is able to ignore the variation produced by smaller scale reed dynamics.

The model takes advantage of reed population data obtained by experienced scientists, as shown in Figure 5.4. The data are converted into a rule base for describing reed biomass affected by various flow regimes and related numerically using fuzzy logic. Fuzzy logic provides realistic numerical values for prediction, using rules that describe a dataset. It



provides a way of transforming linguistic variables such as the words “Low”, “Medium” and “Large” into numerical results.

Fuzzy-rule-based modelling extends the dataset to be generally applicable to intermediate and wider ranges of circumstances. This is especially important given that reeds at different elevations up along the river bank are affected differently by the same flow regime. The model also applies fuzzy-rule-based modelling to the prediction of reed biomass for flow regimes that are not included in the dataset.

The model runs at an annual time step and determines the percentage maximum biomass density of reeds that can potentially grow in a particular substrate. Hence, the reed biomass that can potentially grow at a given elevation on the river bank is determined. Rules are developed based on the maximum biomass density specified in the dataset. The maximum biomass density used in the model is particular to substrate within the reach and is specified by the user.

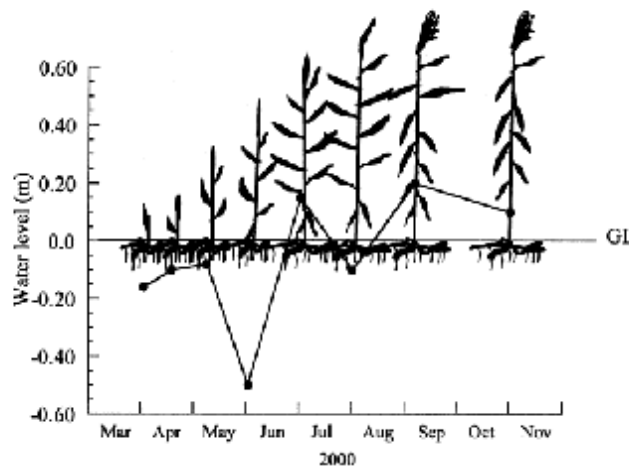


**Figure 5.4 Reed growth according to seasonal variation of water level in relation to ground level. Shoots are not drawn to scale (Karunaratne *et al*, 2003)**

Fuzzy logic is applied through the inference process. The general inference process proceeds in three steps: Fuzzification, Inference and Defuzzification. The inference procedure is outlined below.

The model utilizes relationships for reed biomass density ( $\text{kgDWT/m}^2$ ) and the yearly flow regime, which is represented by the yearly average flow and flow variability. The flow regime reflects the effect of the climatic regime (precipitation and temperature) and catchment controls on runoff on riparian vegetation. Under harsh flow conditions, reeds become stressed and develop to only a fraction of the full potential biomass density. Flow variability plays a role in reed expansion by supplying reeds on different elevations with water. Reeds require periodic inundation to supply water and nutrients to alluvial substrate of the bar. Variable flow depth is also important for seedling establishment at various elevations.

The average flow depths determined by the 1-D water flow model for every month of the year provide the mean yearly flow depth  $H_{ave}$ . These monthly average flows are also used for obtaining the coefficient of variance,  $COV_H$  ( $COV_H = \text{standard variance of flow depth} / H_{ave}$ ). The  $COV_H$  is useful when comparing data obtained for different flow regimes. The resultant  $COV_H$  is compared with that obtained from the data set using the inference procedure as set out by fuzzy logic.

The approach is novel and provides convincing outputs for reach scale reed population dynamics. This model has not been verified. Verification would require a wider range of flow variability and a longer period over which reed biomass is grown in the laboratory. The model also requires verification in terms of the maximum biomass density for a particular substrate.

## 5.3.2 Inference procedure

### **Fuzzification**

To perform inference, each rule must first be quantified with fuzzy logic. It allows conversion of numerical inputs into fuzzy membership functions. This process is termed fuzzification. Under fuzzification, the membership functions defined by the input variables are applied to their actual values to determine the degree of truth for a condition. To specify rules, linguistic descriptions were obtained from expert knowledge, which are needed for the inputs and their characteristics (Passino and Yurkovich, 1998). It is necessary to define appropriate membership functions for the input- and output variables to construct the rule base and to specify the fuzzy operators as well as the methods for calculating rule response and defuzzification. All of the membership functions assigned to each input variable are combined to form a single fuzzy membership function for each output variable (Klir and Folger, 1987).

### **Inference**

In the inference step, it is first required to determine the extent to which each rule is relevant to the current situation as characterised by the inputs. That is, the applicability of each rule is determined together with the conclusions reached. Based on the applicability of the individual rules the response of the system is calculated (Passino and Yurkovich, 1998).

Next, all the rules are checked for their degree of truth (DOT). In the inference sub-process, the truth-value for the condition of each rule is computed and applied to the conclusion part of each rule. This results in one fuzzy membership function to be applied to each output variable for each rule. For the evaluation of the fuzzy AND-operator in the rules the Min-Inference Method is used. The Min-Inference Method uses the lowest membership that is achieved for any condition within a given rule (Fischer *et al*, 2003). The output membership function is cut off at a height corresponding to the DOT computed as the minimum DOT for all the rule conditions. Different rules usually return different DOTs relating to different conclusions. In order to combine all these individual results, the fuzzy membership functions for the conclusions must be known (Klir and Folger, 1987).

## Defuzzification

Owing to the overlap of fuzzy input variables several rules with different DOTs can apply to a given condition. Therefore, a Defuzzification Method is specified, which defines how the conclusions of the corresponding THEN-parts are aggregated. Defuzzification Methods transform fuzzy outputs into crisp values (Schneider and Jorde, 2003).

In the model, the Centre Of Gravity (COG) method is used. In the COG method, the crisp value of the output variable is computed by finding the variable value of the COG of the membership function for the fuzzy value. If the output membership functions are not symmetric, then their centres, which are needed in the computation of the COG, will change depending on the membership value of the premise (Passino and Yurkovich, 1998). Simple geometry shows that the distance to the centre is

$$L = \frac{L_{crest} + w}{3} \quad (5.37)$$

for an asymmetrical triangle which peaks at 1 and has a width of  $w$ , shown in Figure 5.5.

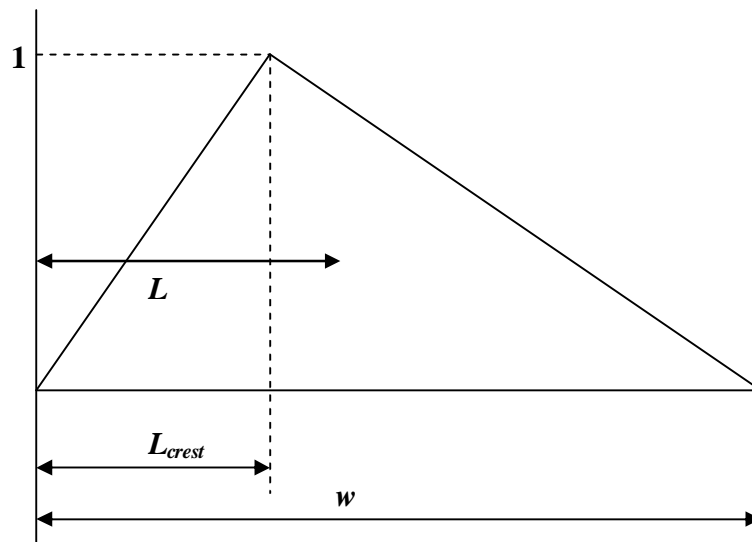


**Figure 5.5 Asymmetrical triangle, which peaks at 1 and has a width of  $w$**

The distance to the centre of the area formed when the triangle is chopped off at a height of  $h$  is equal to  $L_{centre}$  as shown in Figure 5.6.

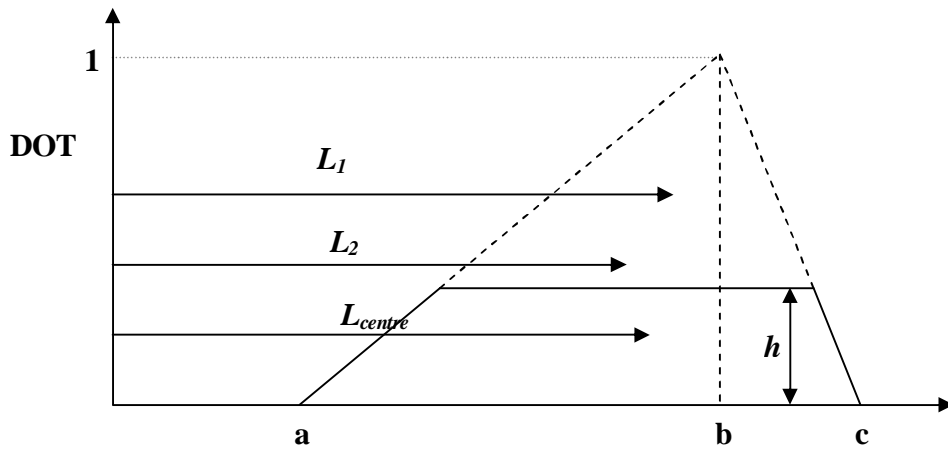


**Figure 5.6** Diagram indicating the distances to the centre of gravity

where

$$L_{centre} = \frac{L_1 A_1 - L_2 A_2}{A_1 - A_2} \quad (5.38)$$

The height  $h$  is the value of the DOT that is applicable to a conclusion, where

$$L_1 = \frac{a+b+c}{3} \quad (5.39)$$

$$L_2 = \frac{a+b+c-ha+2hb-hc}{3} \quad (5.40)$$

$$A_1 = 0.5(c-a) \quad (5.41)$$

and

$$A_2 = 0.5(c-a+ha-hc)(1-h) \quad (5.42)$$

The centre of gravity method computes the crisp value to be

$$u^{crisp} = \frac{\sum L_{centrei} A_i}{\sum A_i} \quad (5.43)$$

### 5.3.3 Reed biomass-elevation data

Deegan *et al.* (2007) ran an experiment to determine variations in biomass (gDWT) of *P. Australis* subjected to different water levels fluctuating at different elevations. They applied four amplitude fluctuations: Static;  $\pm 0.15$  m;  $\pm 0.30$ ; and  $\pm 0.45$  with water levels at 0.2; 0.4; and 0.6 m above bottom of an experimental pond. The results are shown in Figure 5.7. The data set shown in Table 5.2 which is used to develop rules for a fuzzy logic model were obtained directly from Figure 5.7. The dataset indicates the percentages of biomass obtained and maximum potential biomass taken as 400 gDWT. The experiment ran for 100 days.

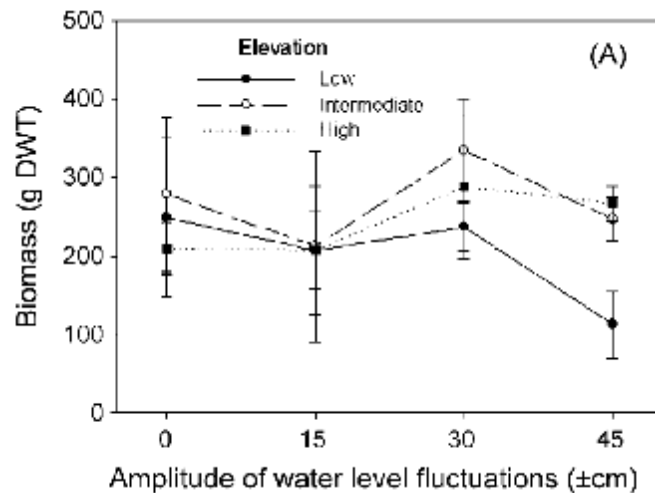


**Figure 5.7 Final biomass (gDWT) of reeds after being subjected to four amplitudes of water level fluctuation (static, 15, 30 and 45 cm) at three elevations (20, 40 and 60 cm) (Deegan *et al.*, 2007)**

**Table 5.2 Data set used to determine the rule base for finding the percentage of total biomass density given average flow depth and flow variability**

<b>Data line</b>	<b><math>H_{ave}</math> (m)</b>	<b><math>COV_H</math> (%)</b>	<b>Min</b>	<b>Biomass density (gDWT)</b>	<b>Max</b>
1	0.01	0	112	232	360
2	0.01	1108	52	188	296
3	0.01	2216	152	212	236
4	0.01	3323	48	116	152
5	0.2	0	212	288	440
6	0.2	55	104	244	384
7	0.2	111	224	272	304
8	0.2	166	72	136	176
9	0.4	0	216	328	416
10	0.4	28	140	256	332
11	0.4	55	304	400	440
12	0.4	83	244	292	316
13	0.6	0	176	244	280
14	0.6	18	176	248	292
15	0.6	37	232	332	456
16	0.6	55	268	308	340
17	0.8	0	52	80	92
18	0.8	14	56	92	112
19	0.8	28	72	140	192
20	0.8	42	64	80	88
21	1	0	20	36	40
22	1	11	36	60	68
23	1	22	36	72	96
24	1	33	8	12	12
25	1.2	0	20	28	32
26	1.2	9	12	16	20
27	1.2	18	4	4	8
28	1.2	28	0	0	0

### 5.3.4 Rule-base

The relationships between biomass density,  $H_{ave}$  and  $COV_H$  are expressed as rules describing reed growth according to flow regime. Linguistic variables define rules to form the knowledge base of the system. These variables as used in the rules are divided into low-resolution states appropriate to model the reeds at the reach scale.

The rules are usually of form: “if **A**, then **B**” where **A** and **B** are fuzzy membership functions, which in turn specifies to what degree a statement would be true (Klir and Yuan, 1995). **A** forms the condition that describes to what degree the rule applies, while **B** is the conclusion that assigns a membership function to the output variable.

Membership functions are used to quantify linguistic variables. Membership functions consist of fuzzy numbers. They have a peak or plateau with a maximum membership of 1. The membership function is increasing towards the peak and decreasing away from it. The value zero is used to represent complete non-membership. The value one is used to represent complete membership and a value in between represents an intermediate degree of truth (DOT) (Kaufmann and Gupta, 1985). The values obtained from the data in Table 5.2 are used to determine the range and DOT of the membership function for the conclusion to the rules.

Table 5.3 shows the rules used. The first rule provides that if  $H_{ave}$  = “Very Low” and  $COV_H$  = “Zero” then the membership for % *maximum biomass density* starts with DOT = 0 at 28 %, DOT = 1 at 58 % and ends with DOT = 0 at 90 %.

For the most part, the definition of a membership function is subjective rather than objective. At the very least, experts simply draw or otherwise specify different membership curves appropriate to a given problem. Membership functions are defined using fuzzy numbers with a variety of different shapes (Schneider and Jorde, 2003).

The percentage of maximum reed density as a conclusion is, therefore, described by linguistic variables. The number of rules used depends on the number of linguistic variables. The rules allow precise as well as imprecise information as input data to be processed (Klir and Folger, 1987). The number of linguistic variables can be related to the time step that is used in the model. The smaller the time step, for example, the smaller the observed changes in reed cover would be and the greater would be the number of linguistic variables. An increase in the number of linguistic variables leads to an increase in the number of rules.



**Table 5.3 Rule base for finding the percentage of total biomass density given average flow depth and flow variability**

<b>Rules</b>	<b><math>H_{ave}</math> (m)</b>	<b><math>COV_H</math> (%)</b>	<b>Range of % maximum biomass density</b>	<b>DOT of 1 for % maximum biomass density</b>
1	Very Low	Zero	28 to 90	58
2	Very Low	Low	13 to 74	47
3	Very Low	Medium	38 to 59	53
4	Very Low	High	12 to 38	29
5	Very Low	Zero	53 to 110	72
6	Very Low	Low	26 to 96	61
7	Very Low	Medium	56 to 76	68
8	Very Low	High	18 to 44	34
9	Low	Zero	54 to 104	82
10	Low	Low	35 to 83	64
11	Low	Medium	76 to 110	100
12	Low	High	61 to 79	73
13	Average	Zero	44 to 70	61
14	Average	Low	44 to 73	62
15	Average	Medium	58 to 114	83
16	Average	High	67 to 85	77
17	High	Zero	13 to 23	20
18	High	Low	14 to 28	23
19	High	Medium	18 to 48	35
20	High	High	16 to 22	20
21	Very High	Zero	5 to 10	9
22	Very High	Low	9 to 17	15
23	Very High	Medium	9 to 24	18
24	Very High	High	2 to 3	3
25	Very High	Zero	5 to 8	7
26	Very High	Low	3 to 5	4
27	Very High	Medium	1 to 2	1
28	Very High	High	0 to 0	0

To derive the maximum potential biomass density from values for given conditions ( $H_{ave}$ ,  $COV_H$ ), first the truth-values of the IF-parts are computed. Figure 5.8 shows the fuzzy membership function used for  $H_{ave}$  and includes what the imprecise expressions “Very low” or “High”, mean numerically. The information that is used to describe change in potential reed population distribution has linguistic variables such as “Very Low”  $H_{ave}$  which is between 0.01 and 0.4 or “High”  $H_{ave}$  which is between 0.6 and 1.0.

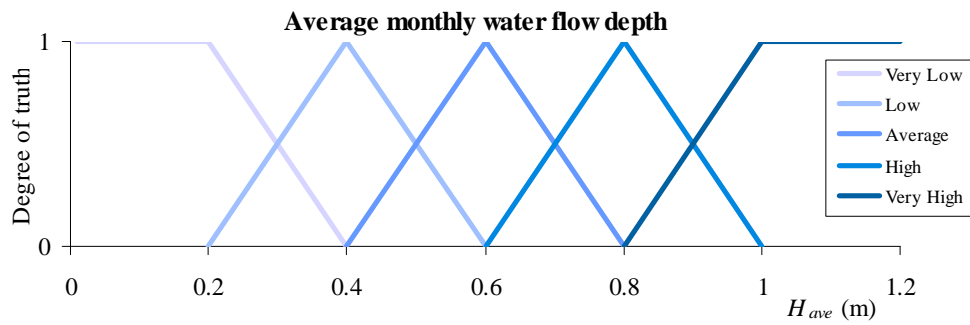


**Figure 5.8 Membership functions for Average Yearly Water Flow Depth**

The model applies variable membership functions as values for  $COV_H$  as  $H_{ave}$  increases. The membership function for  $COV_H$  therefore changes to specify new values for the linguistic variables of “Zero”, “Low”, “Medium” and “Large” appropriate to  $H_{ave}$  as for example shown in Figure 5.9 and Figure 5.10.

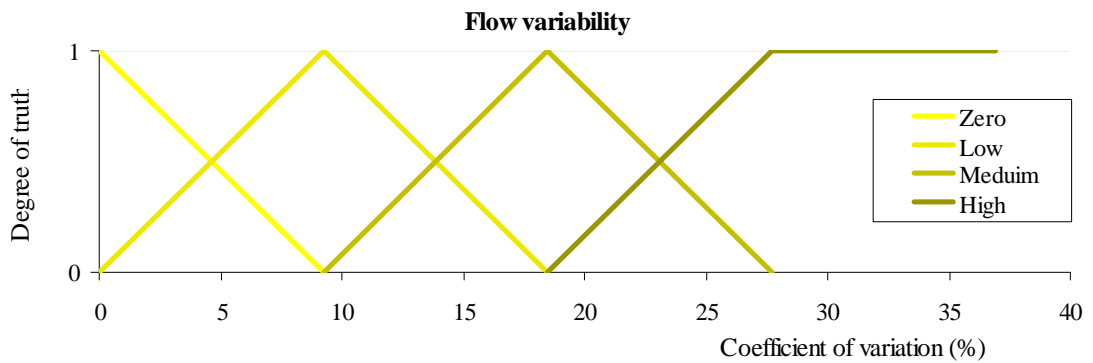


**Figure 5.9 Membership function for flow variability ( $COV_H$ ) for  $H_{ave}$  = “Very High”**

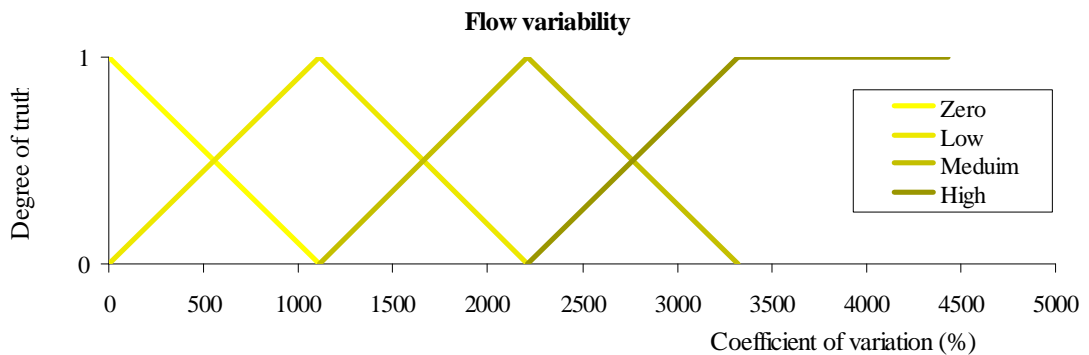


**Figure 5.10 Membership function for flow variability ( $COV_H$ ) for  $H_{ave}$  = “Very Low”**

The result for each rule is therefore a DOT between 0 and 1, which is obtained for each of the applicable rules.

### 5.3.5 Model Output

In order to show a typical output from the reach scale reed model at a given cross-section in the river, the following inputs for monthly water flow depths in Table 5.4 were used as an example. The model uses the  $H_{ave}$  and  $COV_H$  obtained from these data to determine the percentage of the maximum biomass density that can possibly grow at a given elevation.

**Table 5.4 Monthly flow depths at a point within the reach and associated Yearly Average and Covariance**

Month $z$ (m)	Jan	Feb	Mar	Apr	May	Jun	Jul	Aug	Sep	Oct	Nov	Dec	$H_{ave}$	$COV_H$
0	1.8	1.7	1.6	1.4	1.3	1.3	1.4	1.6	1.6	1.7	1.8	1.8	1.58	12
1.0	0.8	0.7	0.6	0.4	0.3	0.3	0.4	0.6	0.6	0.7	0.8	0.8	0.58	33

The monthly water flow depths are measured from the bottom of the river bed at  $z = 0$  which gives  $H_{ave} = 0.58$  m and  $COV_H = 33$  % at elevation  $z = 1$  m above bed. The applicable membership for  $H_{ave} = 0.58$  m is shown in Figure 5.11.

For **Low** yearly flow depths a DOT = 0.08 is obtained and for **Average** yearly flow depths the DOT = 0.92. Figure 5.11 shows the membership function for Flow variability interpolated linearly according  $COV_H$  and the rules shown in Table 5.3. The minimum, maximum and peak values for the membership of each conclusion to the applicable rules in Table 5.3 are obtained by linear interpolation using  $H_{ave}$  and the data in Table 5.2.

The rules in Table 5.3 show that for **Low** yearly flow depth and **Low** flow variability Rule 10 applies and for **Low** yearly flow depth and **Medium** flow variability Rule 11 applies. The range of the applicable membership of flow variability for Rule 10 starts at  $COV_H = 0$  to  $COV_H = 36.9$  with DOT = 1 at  $COV_H = 18.5$ .  $COV_H$  for DOT = 1 are determined from linearly interpolating the values from data lines 10 and 14 in Table 5.2 based on  $H_{ave}$  lying between 0.4 m and 0.6 m. Similarly, the membership range is obtained from data lines 9, 13, 11 and 15. Figure 5.12 shows that for **Low** flow variability a DOT = 0.24 is obtained and for **Medium** flow variability the DOT = 0.76. Rules 14 and 15 apply in the same way for **Average** yearly flow depth.

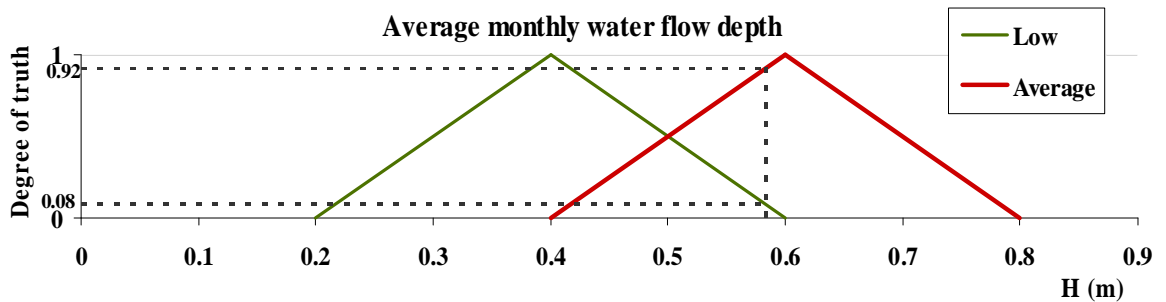


**Figure 5.11** Membership function for Average yearly water flow depth. The DOTs for  $H_{ave} = 0.58$  m are indicated by the dashed line

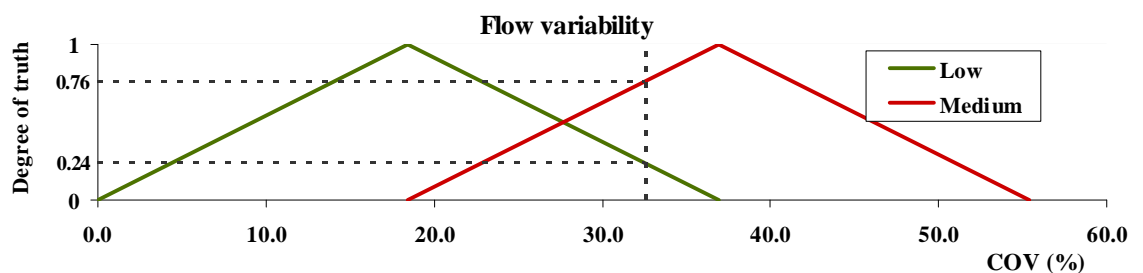


**Figure 5.12** Membership function for Flow variability associated with  $H_{ave} = 0.58$  m. The DOTs for COVH of 33 % are indicated by the dashed line

$COV_H = 33$  % at elevation above bed  $z = 1$  m gives, for **Average** yearly flow depth, a DOT = 0.16 for flow variability being **Low** and a DOT = 0.84 for flow variability being **Medium**. Figure 5.13 shows the membership function for the % of maximum biomass which is the conclusion to the applicable rules.

Rule 10 provides a minimum DOT of 0.08 and a membership range of % of maximum biomass ranging between 54.1 and 103.9 with DOT = 1 at 81.9. The values are obtained from data lines 9, 13, 10, 14, 11 and 15. Rule 11 also gives a minimum DOT of 0.08 where Rules 14 and 15 gives minimum DOTs of 24 and 76 respectively. Defuzzification of these values gives Reed biomass of 66.7 % of the Maximum Reed biomass as shown in Figure 5.14.

Figure 5.14 illustrates a typical output from the reach scale reed model at 0.25 m intervals up along the river bank. The dataset provided a maximum potential biomass of 400 gDWT which gives a maximum biomass of 268 gDWT allowed to grow at  $z = 1$  m above the river bed.

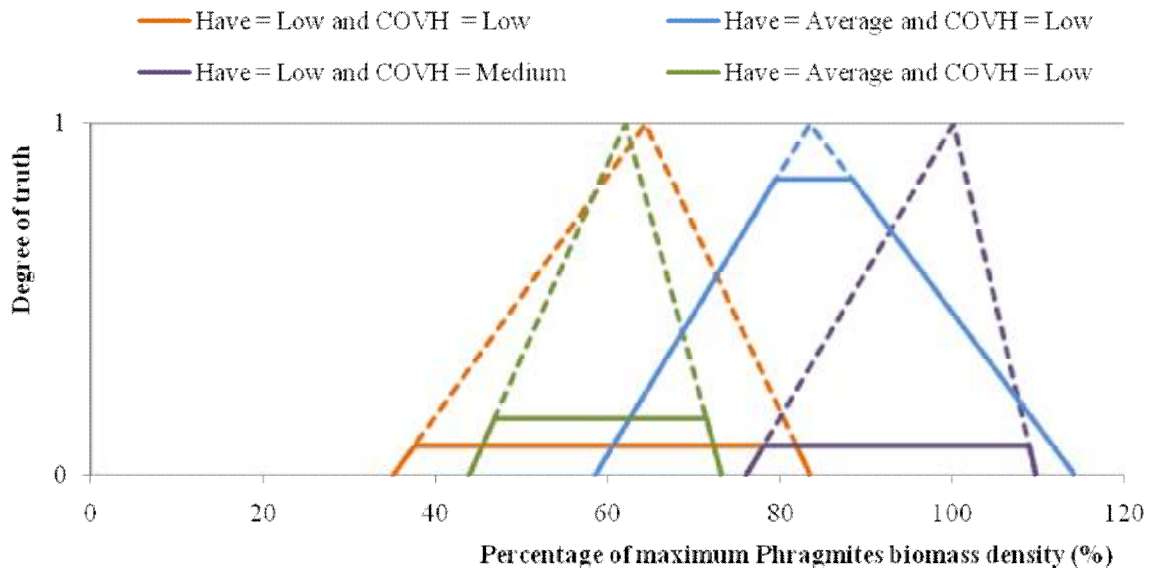


Figure 5.13 Membership function for % Maximum reed biomass associated with  $H_{ave} = 0.58$  m and  $COV_H = 33$  %

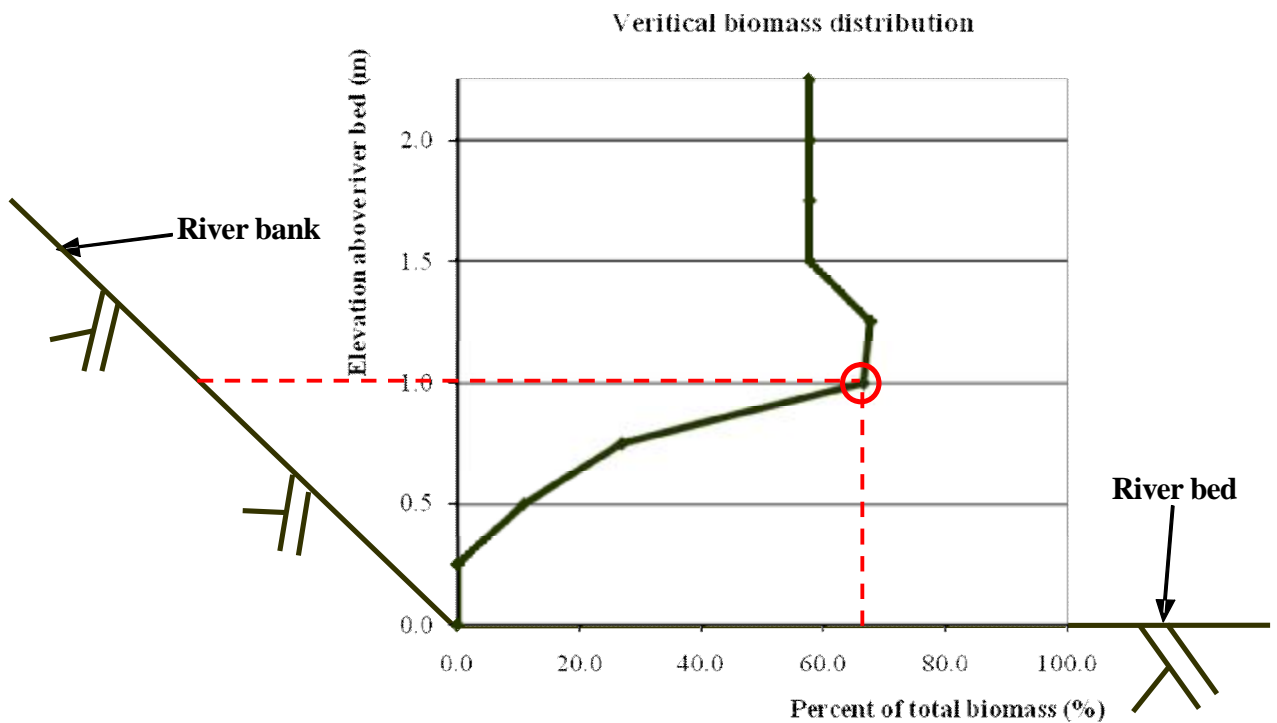


Figure 5.14 Typical model output providing the vertical distribution of percentage of the maximum *Phragmites* biomass density along the river bank. In the example above, a value of 66.7 % of the maximum possible biomass obtained at elevation above river bed  $z = 1$  m

## 5.4 Channel-type scale water flow

The water flow model at the channel-type scale provides average flow depth and the magnitude and direction of velocities in two dimensions (2-D). The model drives the sediment model, which in turn determines the distribution and flow of sediment accordingly. The model employs 2-D Saint-Venant equations and accounts for the resistance to flow specific to the channel-type scale.

### 5.4.1 2-D Saint-Venant equations

$$\frac{\partial H}{\partial t} + \frac{\partial}{\partial x}(UH) + \frac{\partial}{\partial y}(VH) = 0 \quad (5.44)$$

$$\frac{\partial U}{\partial t} + U \frac{\partial U}{\partial x} + V \frac{\partial U}{\partial y} = -g \frac{\partial z_w}{\partial x} - gS_{fx} + \frac{1}{H} \frac{\partial}{\partial x} \left( H \frac{\tau_{xx}}{r} \right) + \frac{1}{H} \frac{\partial}{\partial y} \left( H \frac{\tau_{xy}}{r} \right) \quad (5.45)$$

$$\frac{\partial V}{\partial t} + V \frac{\partial V}{\partial x} + U \frac{\partial V}{\partial y} = -g \frac{\partial z_w}{\partial y} - gS_{fy} + \frac{1}{H} \frac{\partial}{\partial x} \left( H \frac{\tau_{xy}}{r} \right) + \frac{1}{H} \frac{\partial}{\partial y} \left( H \frac{\tau_{yy}}{r} \right) \quad (5.46)$$

where  $H$  is the height of the water surface,  $U$  and  $V$  is the depth average velocities in the  $x$  and  $y$  directions. The friction terms,  $\tau_{xx}$ ,  $\tau_{xy}$ ,  $\tau_{yy}$ ,  $S_{fx}$  and  $S_{fy}$  are described below.

The Saint-Venant equations in the form of classical finite differences equations are solved using the MacCormack integration scheme. This method ensures second order precision in both space and time. It is written for a staggered grid, ensuring a resolution that is suited to mass and momentum conservation. The MacCormack integration scheme for 2-D water flow simulation on staggered mesh is described below.

### 5.4.2 Bed friction modelling

The hydraulic head losses due to bed friction,  $S_{fx}$  and  $S_{fy}$ , are expressed as energy slope components in the  $x$  and  $y$  directions. The friction slope terms depend on the bed shear stresses which are assumed to be related to the magnitude and direction of the depth averaged velocity. In the  $x$  direction, for example:

$$S_{fx} = \frac{\tau_{bx}}{rgd} = \frac{\sqrt{U^2 + V^2}}{gcd_s} U \quad (5.47)$$

where  $\tau_{bx}$  is the bed shear stress in the  $x$  direction and  $c_s$  is the nondimensional Chézy coefficient.  $c_s$  is related to the effective roughness height  $k_e$  of the boundary and the depth of flow  $d$  (Steffler and Blackburn, 2002) using:

$$c_s = 5.75 \log \left( 12 \frac{d}{k_e} \right) \quad (5.48)$$

$k_e$  is dependent on grain size and bed-form size which is obtained from models at the geomorphological-unit scale. The formulations used to determine  $k_e$  are described in section 6.3.2.

### 5.4.3 Turbulent shear stress modelling

Depth-averaged transverse turbulent shear stresses are modelled with a Boussinesq type eddy viscosity formulation. For the depth-averaged shear stresses, the Boussinesq assumption is expressed by the following equation:

$$\frac{t_{xx}}{r} = 2u_t \left( \frac{\mathcal{I}U}{\mathcal{I}x} \right) - \frac{2}{3}k \quad (5.49)$$

$$\frac{t_{xy}}{r} = \frac{t_{yx}}{r} = u_t \left( \frac{\mathcal{I}U}{\mathcal{I}y} + \frac{\mathcal{I}V}{\mathcal{I}x} \right) \quad (5.50)$$

$$\frac{t_{yy}}{r} = 2u_t \left( \frac{\mathcal{I}U}{\mathcal{I}y} \right) - \frac{2}{3}k \quad (5.51)$$

where  $v_t$  is the eddy viscosity coefficient. The turbulent kinetic energy  $k$  is estimated through the transport equation:

$$k = c_d / c_u (v_t / l_d) \quad (5.52)$$

where  $l_d$  is the turbulence length-scale.  $l_d$  is assumed to be proportional to the water depth  $d$ :

$$l_d = 0.1 d \quad (5.53)$$

where  $c_u = 0.09$  and  $c_d = 0.17$  are constants (Nadaoka and Yagi, 1998).

The eddy viscosity coefficient  $\nu_t$  is assumed to be composed of three components: a constant, a bed shear generated term, and a transverse shear generated term.

$$\nu_t = e_1 + e_2 \frac{H \sqrt{U^2 + V^2}}{C_s} + e_3 H^2 \sqrt{2 \frac{\partial U}{\partial x} + \left( \frac{\partial U}{\partial y} + \frac{\partial V}{\partial x} \right) + 2 \frac{\partial V}{\partial y}} \quad (5.54)$$

where  $e_1$ ,  $e_2$  and  $e_3$  are user-definable coefficients.

The default value for  $e_1$  is 0. This coefficient is used to stabilize the solution for very shallow flows when the second term in equation (5.54) may not adequately describe  $\nu_t$  for the flow. The default value for  $e_2$  is 0.5 but values of 0.2 to 1.0 are reasonable. Since most river turbulence is generated by bed shear, this term is usually the most important. For deep flow, or flows with high transverse velocity gradients, transverse shear may be the dominant turbulence generation mechanism. When strong recirculation regions are important examples,  $e_3$  becomes important. The third term is essentially a 2-D horizontal mixing length model. The mixing length is assumed to be proportional to the depth of flow. A typical value for  $e_3$  is 0.1 (Steffler and Blackburn, 2002).

#### 5.4.5 The MacCormack Method for solving 2-D flow

The spatial discretisation makes use of a staggered "marker-and-cell" (MAC) mesh (Harlow and Welsh, 1965). Figure 5.15 presents the MacCormack scheme for solving 2-D flow. The MAC mesh allows the velocities  $U$  and  $V$  to be defined for positions situated at a middle distance between the points where the bed level  $z$  are defined. These values  $z_b$  are given for points located at the centre of squares formed by 4 points where the water-level value  $z$  is defined. This location enables an easy estimation of the bed level value at any point of interest ( $z$ ,  $U$ ,  $V$ ), using a linear interpolation method. The MAC mesh provides a good coupling between the velocities and the water depth ensuring a very good mass and momentum conservation (Ferziger and Peric, 1996). The discretisation includes associated stability criterion and boundary conditions.

In order to facilitate the programming, the fractional indices from Figure 5.15 are replaced by entire values. Additionally, the value of the viscosity,  $\nu_t$  is defined at the same locations as the water level  $z$ .



Each equation described above is then discretised with a computational cell centred on the location where the value varying with the time is defined. The first order derivatives in the momentum equations are written using in alternation a forward and a backward difference operator, corresponding respectively to the predictor and the corrector steps of the MacCormack scheme. The first order derivatives in the continuity equation and the second order derivatives (diffusion terms) are written using centred difference operator. The value of a variable is interpolated from adjacent values (Bousmar, 2002).

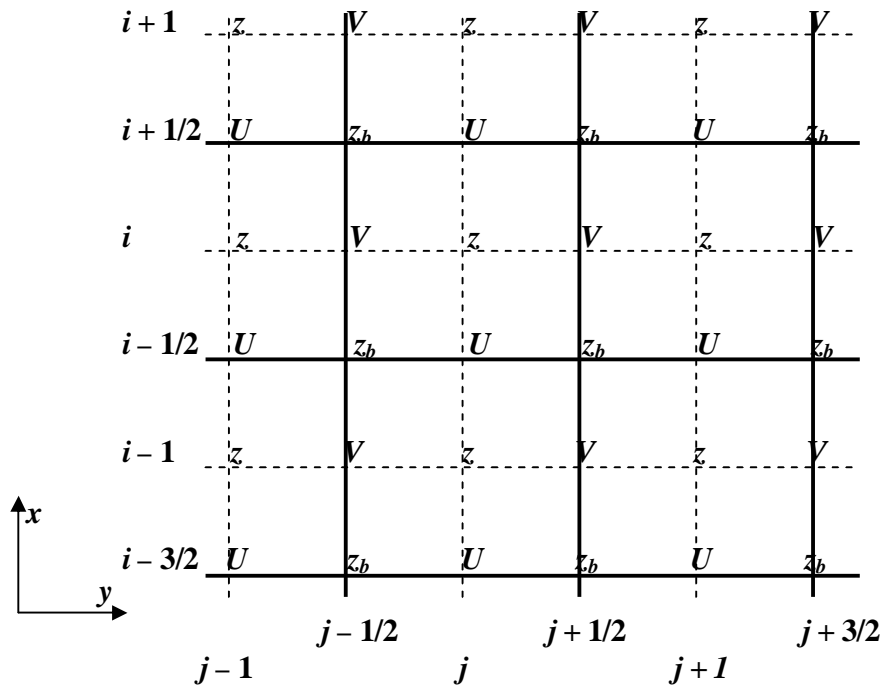


Figure 5.15 Staggered "MAC" mesh definition for 2-D shallow-water flow modelling

Accordingly, the discretised continuity equation (5.44) writes at the node  $(i, j)$ :

$$\frac{\partial z_{ij}}{\partial t} + \frac{1}{\Delta x} (H_{i+1,j}^U U_{i+1,j} - H_{i,j}^U U_{i,j}) + \frac{1}{\Delta y} (H_{i,j+1}^V V_{i,j+1} - H_{i,j}^V V_{i,j}) = 0 \quad (5.55)$$

where  $H_{i,j}^U$  and  $H_{i,j}^V$  stands for interpolated values of the water-depth at the definition points of  $U$  and  $V$ :

$$H_{i,j}^U = \frac{1}{2} (z_{i-1,j} + z_{i,j}) - \frac{1}{2} (z_{bi,j} + z_{bi,j+1}) \quad (5.56)$$

$$H_{i,j}^U = \frac{1}{2}(z_{i,j-1} + z_{i,j}) - \frac{1}{2}(z_{bi,j} + z_{bi+1,j}) \quad (5.57)$$

and where the temporal derivative  $\partial H_{ij} / \partial t$  becomes  $\partial z_{ij} / \partial t$ , as the bed level  $z_b$  remains constant.

The momentum equations (5.45) and (5.46) and the shear-stress equation (5.47) are discretised in a similar way. For the predictor step (forward difference operator), these equations write:

$$\begin{aligned} & \frac{\partial U_{i,j}}{\partial t} + \frac{1}{\Delta x} U_{i,j} (U_{i+1,j} - U_{i,j}) + \frac{1}{\Delta y} V_{i,j}^m (U_{i,j+1} - U_{i,j}) \\ &= -\frac{1}{\Delta x} g (z_{i,j} - z_{i-1,j}) - g S_{fxi,j} \\ &+ \left( \frac{1}{\Delta x} \right)^2 \frac{1}{H_{i,j}^U} (2H_{i,j}^Z \mathbf{u}_{i,j} (U_{i+1,j} - U_{i,j}) - 2H_{i-1,j}^Z \mathbf{u}_{i-1,j} (U_{i,j} - U_{i-1,j})) \\ &+ \frac{1}{\Delta x} \frac{1}{H_{i,j}^U} \left( \frac{2}{3} H_{i,j}^Z k_{i,j} - \frac{2}{3} H_{i-1,j}^Z k_{i-1,j} \right) \\ &+ \left( \frac{1}{\Delta y} \right)^2 \frac{1}{H_{i,j}^U} (H_{i,j+1}^B \mathbf{u}_{i,j+1}^m (U_{i,j+1} - U_{i,j}) - H_{i,j}^B \mathbf{u}_{i,j}^m (U_{i,j} - U_{i,j-1})) \\ &+ \frac{1}{\Delta x \Delta y} \frac{1}{H_{i,j}^U} (H_{i,j+1}^B \mathbf{u}_{i,j+1}^m (V_{i,j+1} - V_{i-1,j+1}) - H_{i,j}^B \mathbf{u}_{i,j}^m (V_{i,j} - V_{i-1,j})) \end{aligned} \quad (5.58)$$

$$\begin{aligned}
& \frac{\partial V_{i,j}}{\partial i} + \frac{1}{\Delta x} U_{i,j} (V_{i+1,j} - V_{i,j}) + \frac{1}{\Delta y} V_{i,j}^m (V_{i,j+1} - V_{i,j}) \\
&= -\frac{1}{\Delta y} g(z_{i,j} - z_{i,j-1}) - gS_{f_{i,j}} \\
&+ \frac{1}{\Delta x \Delta y} \frac{1}{H_{i,j}^V} (H_{i+1,j}^B \mathbf{u}_{i+1,j}^m (U_{i+1,j} - U_{i+1,j-1}) - H_{i,j}^B \mathbf{u}_{i,j}^m (U_{i,j} - U_{i,j-1})) \\
&+ \left(\frac{1}{\Delta X}\right)^2 \frac{1}{H_{i,j}^V} (H_{i+1,j}^B \mathbf{u}_{i+1,j}^m (V_{i+1,j} - V_{i,j}) - H_{i,j}^B \mathbf{u}_{i,j}^m (V_{i,j} - V_{i-1,j})) \\
&+ \left(\frac{1}{\Delta y}\right)^2 \frac{1}{H_{i,j}^V} (2H_{i,j}^Z \mathbf{u}_{i,j}^m (V_{i,j+1} - V_{i,j}) - 2H_{i,j-1}^Z \mathbf{u}_{i,j-1}^m (V_{i,j} - V_{i,j-1})) \\
&+ \frac{1}{\Delta y} \frac{1}{H_{i,j}^V} \left( \frac{2}{3} H_{i,j}^Z k_{i,j} - \frac{2}{3} H_{i,j-1}^Z k_{i,j-1} \right)
\end{aligned} \tag{5.59}$$

where the values of  $S_{f_{i,j}}$  and  $S_{f_{i,j}}$  are estimated using equations (5.49), (5.50) and (5.51) with the velocity values  $(U_{i,j}, V_{i,j}^m)$  and  $(U_{i,j}^m, V_{i,j})$  respectively;

$$U_{i,j}^m = \frac{1}{4} (U_{ij} + U_{i,j-1} + U_{i+1,j} + U_{i+1,j-1}) \tag{5.60}$$

$$V_{i,j}^m = \frac{1}{4} (V_{ij} + V_{i,j+1} + V_{i-1,j} + V_{i-1,j+1}) \tag{5.61}$$

$$\mathbf{u}_{i,j}^m = \frac{1}{4} (\mathbf{u}_{t_{ij}} + \mathbf{u}_{t_{i,j-1}} + \mathbf{u}_{t_{i-1,j}} + \mathbf{u}_{t_{i-1,j-1}}) \tag{5.62}$$

$H_{i,j}^Z$  and  $H_{i,j}^B$  stands for interpolated values of the water-depth at the definition points of  $z$  and  $z_b$ :

$$H_{i,j}^Z = z_{i,j} - \frac{1}{4} (z_{b_{i,j}} + z_{b_{i,j+1}} + z_{b_{i+1,j}} + z_{b_{i+1,j+1}}) \tag{5.63}$$

$$H_{i,j}^B = \frac{1}{4} (z_{i,j} + z_{i,j-1} + z_{i-1,j} + z_{i-1,j-1}) - z_{b_{i,j}} \tag{5.64}$$

The discretisation of the turbulent kinetic-energy transport equation (5.54) is obtained similarly centred on the  $z$  point:

$$v_i = \mathbf{e}_1 + \mathbf{e}_2 H_Z \frac{\sqrt{U_{ij}^m + V_{ij}^m}}{C_s} + \mathbf{e}_3^2 H_Z^2 \sqrt{2 \left( \frac{1}{\Delta x} (U_{i+1,j} - U_{ij}) \right)^2 + 2 \left( \frac{1}{\Delta y} (V_{i+1,j} - V_{ij}) \right)^2 + \left( \frac{1}{2\Delta y} \left( \frac{U_{i,j+1} - U_{i+1,j+1}}{2} - \frac{U_{i,j-1} - U_{i+1,j-1}}{2} \right) \right)^2 + \frac{1}{2\Delta x} \left( \frac{V_{i+1,j} - V_{i+1,j+1}}{2} - \frac{V_{i,j-1} - V_{i-1,j+1}}{2} \right) \right)^2} \quad (5.65)$$

The 2-D MacCormack scheme employs the following condition (Yulistiyanto, 1997):

$$\Delta t \leq \frac{1}{\frac{U + \sqrt{gH}}{Dx} + \frac{V + \sqrt{gH}}{Dy} + \frac{2u_i}{(Dx)^2} + \frac{2u_i}{(Dy)^2}} \quad (5.66)$$

The no-slip condition is used to assign a zero velocity value at the wall and provides a fictitious node behind the wall. The value  $U_{j=-1}$  at this fictitious node is obtained thanks to Taylor-series developments (Peyret and Taylor, 1983) that give

$$U_{j=-1} = \frac{1}{3} (U_{j+1} - 6U_{j=0} + 8U_{wall}) \quad (5.67)$$

where  $U_{wall} = 0$  is the velocity at the wall.

## 5.5 Channel-type scale bar evolution

### 5.5.1 Sediment routing

The channel-type scale bar evolution model is a cellular automaton model which routes sediment based on numerical rules for the sediment storage states of upstream and downstream cells. A certain volume of cohesionless sediment is fed into the first row of cells representing the upstream end of the river. The amount of sediment fed into the model depends on the sediment inflow rate and the time step that is specified by the user. The sediment inflow rate is obtained from the reach scale sediment model described above. Sediment moves cell-by-cell according to sediment flow relationships between cells. Figure 5.16 shows the procedure for routing sediment.

The flow chart in Figure 5.16 shows the modelling procedure. The model requires water flow velocity, flow depth, height differences between upstream and downstream cells, sediment inflow, local slope and 2-D flow direction for each cell in the cellular grid. Each cell in the grid receives a sediment inflow starting upstream. The water flow velocity and depth are used to determine the potential sediment that can be stored within the cell or storage state  $S_s$ . The  $S_s$  for the cell together with the sediment inflow from the upstream cells and height differences between upstream and downstream cells are used to determine how much sediment would flow out of the specific cell. The out-flowing sediment is allocated to the downstream cells according to local slope. This is repeated for all the cells within the cellular grid. The procedure is repeated for the next time step and is carried out for the duration of the flood.

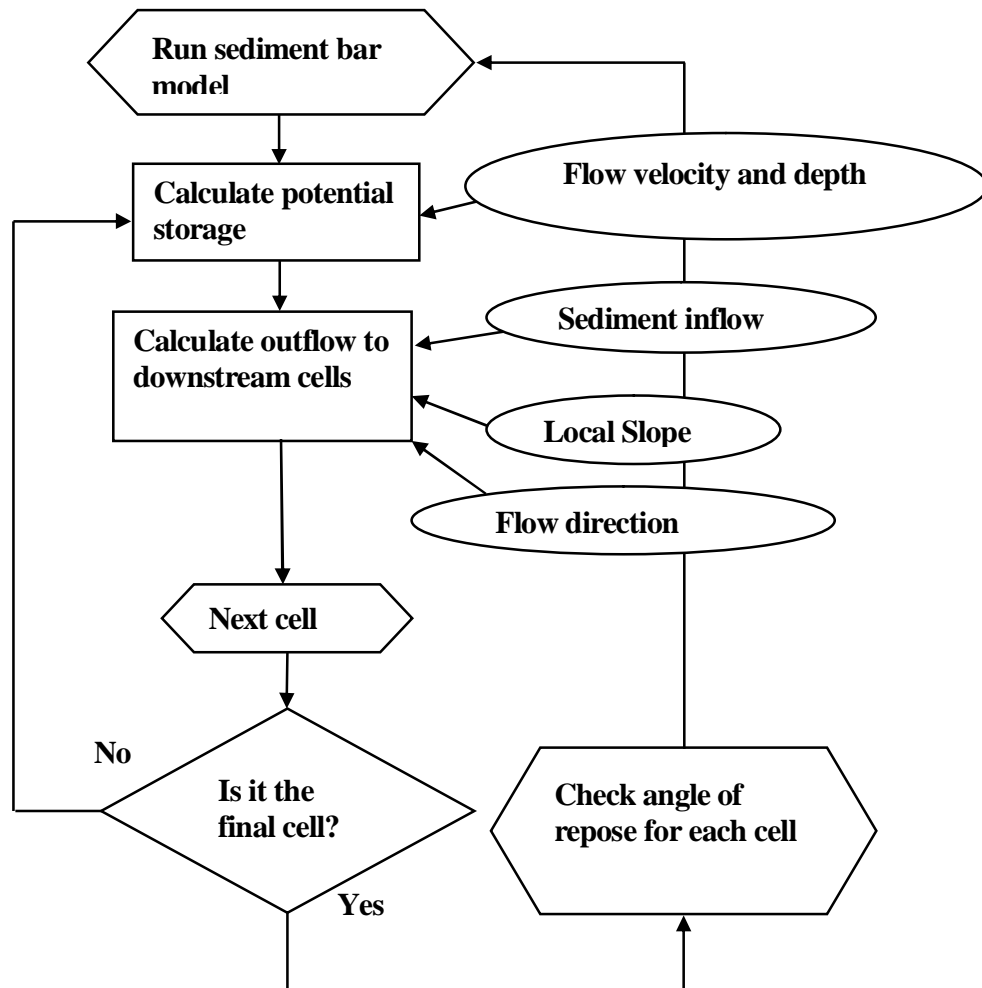


**Figure 5.16** Flow chart of the procedure for the sediment model at the channel-type scale

Iteration begins when sediment enters the upstream end of the cellular grid and ends when outflow has been calculated for the cells at the downstream end of the grid. There is no net loss or gain of sediment as sediment remains budgeted for during simulation. Sediment is routed along the flow direction within a computational cell. Figure 5.17 shows sediment routed in the direction of the flow moving sediment from upstream cells to three downstream neighbours.

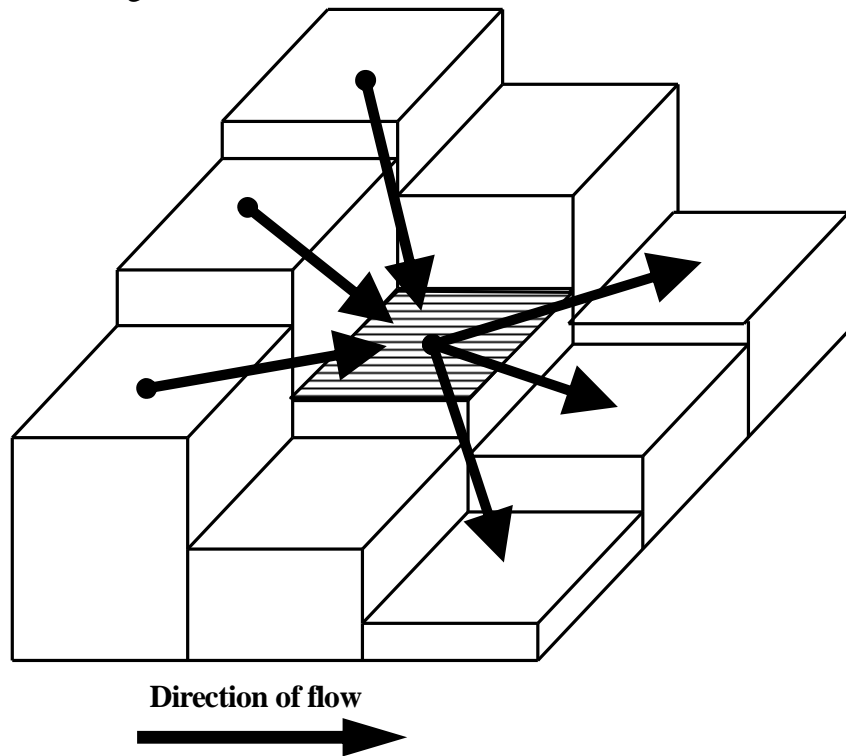


**Figure 5.17 Movement of sediment through a cell in a rectangular gridded computational domain**

### **5.5.2 Sediment allocation according to local slope**

The amount of sediment that will flow from the upstream to a downstream cell depends on the fraction of the local slope between the upstream and downstream cell and the sum of the slopes of all the downstream cells to which sediment would flow (Murray and Paola, 1994). Downstream from a cell may be in any direction following the direction of water flow as simulated by the 2-D flow model described above.

$$SO_i = \frac{m_i}{m_i + m_{i+1} + m_{i+2}} Outflow \quad (5.68)$$

$SO_i$  is the sediment flow to a particular downstream cell. *Outflow* is the total sediment that flows from an upstream cell.  $m_i$ ,  $m_{i+1}$  and  $m_{i+2}$  are the weighted factors indicating relative slope values. When considering the three downstream cells to which sediment may possibly flow, a lower downstream cell will have a larger fraction of the total outflow from the upstream cell allocated to it.

In rivers, water can flow uphill when the surface slope is positive and there is enough momentum (Murray and Paola, 1994). This means that if one or more of the slopes are negative, flow of sediment may still occur. Because slopes can be negative, sediment moving towards upstream cells is achieved by adding the lowest negative slope to the other slopes, making the lowest slope equal to zero and other slopes positive. The sediment outflow for uphill flow is then allocated the same way as for when flow is simply downhill, i.e. according to the fraction that the slope to the downstream cell makes to the total of all the downstream cells.

### 5.5.3 Sediment storage

Sediment storage is ideal for modelling sediment organisation at the channel-type scale since sediment supply is often limited. Sediment flow is determined based on how much sediment can potentially be stored.

Sediment Continuity states that the input from upstream and the sediment transport  $Q_s$  can be used to solve the change in storage  $\Delta Storage$ :

$$\Delta Storage = Q_{sin} - Q_{sout} \quad (5.69)$$

James *et al.* (2001b) introduced an alternative modelling method that applies sediment continuity as an inverted equation:

$$Q_{sout} = Q_{sin} - \Delta Storage \quad (5.70)$$

This form of the equation requires sediment input from upstream and a calculated storage to determine the amount of outflow. It allows for lower resolution modelling to be used to make predictions at much coarser scales.

The volume of sediment that can potentially be stored in a cell or  $\Delta Storage$  is related to the flow depth and shear velocity in that cell. It is therefore possible to determine the storage state  $S_s$  after a given time, based on the amount of sediment removed from a cell. The sediment inflow and  $S_s$  are used to determine the full possible outflow to a downstream cell as shown in Figure 5.18.

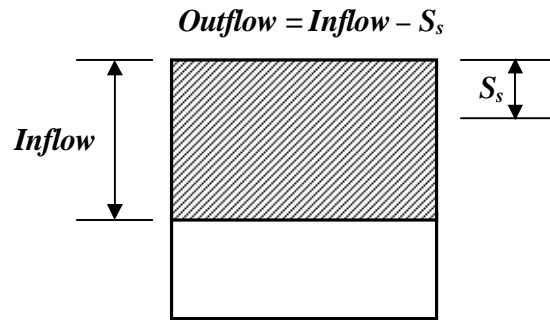


**Figure 5.18 Sediment outflow determined from the Storage State  $S_s$  and the sediment inflow for a given cell**

The  $S_s$  is the elevation difference between the upstream and the downstream cells disregarding sediment flowing in and after sediment has flowed out. The  $S_s$  is determined from the change in cell volume after sediment is removed according to a bed-load transport equation to arrive at the lowest possible elevation of the cell after a time step  $\Delta t$  used by the cellular model.

$$S_s = \frac{q_b \Delta t}{\Delta x} \quad (5.71)$$

where  $q_b$  is the bed-load transport in  $m^2/s$  and  $\Delta x$  are the cell length and width in metres. It is assumed the effect of the energy slope remains unchanged during  $\Delta t$ .

$q_b$  is determined by the Bagnold equation (Bagnold, 1980). The Bagnold equation applies since it represents a statement of the bulk displacement of sediment by the shearing action of the water. The Bagnold equation is described below. The formulation simplifies to such a degree the actual physics of the grain movements under the influence of water flow that it can be regarded as no more than a scale correlation.



### 5.5.4 Bagnold's empirical bed-load formula

The Bagnold empirical bed-load formula is used to predict the amount of sediment that will be transported within a computational cell described in section 5.5.1. His bedload formulation reads as follows (Martin and Church, 2000):

$$i_b = \frac{1}{s-1} i_{b\_ref} \left( \frac{w-w_o}{(w-w_o)_{ref}} \right)^{3/2} (d/d_{ref})^{-2/3} (D/D_{ref})^{-1/2} \quad (5.72)$$

where

$$i_{b\_ref} = 0.1; (w-w_o)_{ref} = 0.5; d_{ref} = 0.1; D_{ref} = 0.0011 \quad (5.73)$$

wherein  $i_b$  is specific bedload transport rate in kg/m/s,  $s$  is the specific gravity of sediment,  $\omega = \rho g d S U = \tau U$  is specific stream power,  $\rho$  is fluid density,  $g$  is the acceleration of gravity,  $d$  is flow depth,  $S_e$  is the energy gradient of the flow,  $U$  is the mean velocity of the flow,  $\tau$  is shear stress exerted by the fluid at the bed.  $\omega_o$  is critical specific stream power,  $D$  is characteristic particle size denoted in mixtures by  $D_{50}$ .

$$w_o = 5.75 \left( (t^*)_c (s-1)r \right)^{3/2} (g/r)^{1/2} D^{3/2} \log(12d/D) \quad (5.74)$$

$(\tau^*)_c$  is the Shields entrainment number. The threshold stream power for bedload transport,  $\omega_o$  depends on depth and grain size. The value of  $\omega_o$  critically affects the transport rate as it dictates the lowest value of stream power at which transport is detected.

The volumetric bedload transport rate is determined as:

$$q_b = \frac{i_b}{rs(1-p)} \quad (5.75)$$

where  $p$  is the porosity of the bed material.

### 5.5.5 Angle of repose

After a model iteration, the angle of repose rule is implemented (Nield *et al*, 2002) in order to simulate bank erosion and not allowing unnatural steep slopes to develop. The angle of repose is the critical angle at which sediment moves down hill. The model allows avalanches to occur so that height differences between cells are lower than the angle of repose stipulates. Each cell collapses, allowing sediment to move to neighbouring cells and

slopes between neighbouring cells to be at the angle of repose. This angle of repose rule is not implemented within cells occupied by reeds, in order to simulate cohesion provided by roots. van Rijn (1993) provided angle of repose values for stable channels as seen in Table 5.5.

**Table 5.5 Angle of repose for various sediment sizes (van Rijn, 1993)**

Sediment size ( $D$ ) (mm)	Angle of repose (degrees)
< 1	30-35
5	32-37
10	35-40
50	37-42
> 100	40-45

## 5.6 Channel-type scale reed expansion

### 5.6.1 Model overview

The reed model at the channel-type scale combines both the top-down effect of the flow regime as well as the bottom-up effect of reed growth determined by the climate. It is a cellular automaton model that predicts expansion of reeds according to their propensity to spread primarily by growth of surface runners and underground rhizomes. Expansion occurs through interactions based on biomass density of reeds among cells within a cellular grid. The model attempts to deal with *Phragmites* growth as characterised by (Philips and Field, 2005):

- 1) Initial establishment
- 2) Unrestricted development
- 3) Restricted development by water or other patches of *Phragmites*

Expansion accords with a specific reed front advancement rate. Reed front advancement rates were obtained from a *Phragmites* patch study done by Alvarez-Cobelas and Cirujano (2007). They gave reed front advancement rates as high as 9 m/month for the summer to as low as 0.3 m/month in winter. The time step is determined from the Reed front advancement rate and the cell length  $\Delta t$ .

$$\Delta t = \Delta x / (\text{Reed front advancement rate}) \quad (5.76)$$

Reed expansion depends on the growth rate. If the threshold biomass density is reached within  $\Delta t$ , the associated reed front advancement rate will be achieved. Hence, reeds would expand to neighbouring cells at every time step should the reeds grow denser than the reed density threshold within that time step.

The reed model at the geomorphological-unit scale provides the growth rate specific to the time of year. The growth rate is specific to a cell because the onset of reed growth for each cell may be different. Cells may therefore be at different stages of the growth cycle affecting their expansion rate. In addition to the growth cycle, the air temperatures, radiation for photosynthesis and sun angle for a particular month of the year give rise to variable growth rates and thus variable expansion rates.

The effect that water level fluctuations in the river have on reed expansion is provided by the reach scale reed model, giving the percentage of maximum reed density for a particular cell elevation. The maximum reed density is specified by the user. By limiting the biomass density within a cell, the threshold biomass density may not be reached and so reed expansion halts.

### 5.6.2 Model outputs

Particular cell elevations provided in a sediment bar simulation at the channel-type scale provides a particular arrangement of maximum possible biomass density. For each of the 5 by 5 m cells, a maximum possible biomass density is obtained using the result of the reach scale reed model. The outputs of the reach scale model provided in Figure 5.14 multiplied by a maximum reed biomass density of 6 kg/m<sup>2</sup> dry weight were used for determining the maximum possible densities shown in Figure 5.20. Reed expansion was simulated according to the maximum possible densities and the elevation above the river resulting from the sediment distribution given in Figure 5.19.

Figure 5.21 shows a sequence of simulated reed expansion given for the maximum reed biomass allowed for the cells shown in Figure 5.20. The top down constraints from the reach scale reed model are also evident in confining reed expansion. Depending on the

time of year and when growth within a cell started, the reed biomass within that cell will grow at a rate provided by the geomorphological-unit scale reed model. The modelling in this study used the temperature values shown in Table 5.6 as indication of summer and winter months.

**Channel type scale sediment distribution**

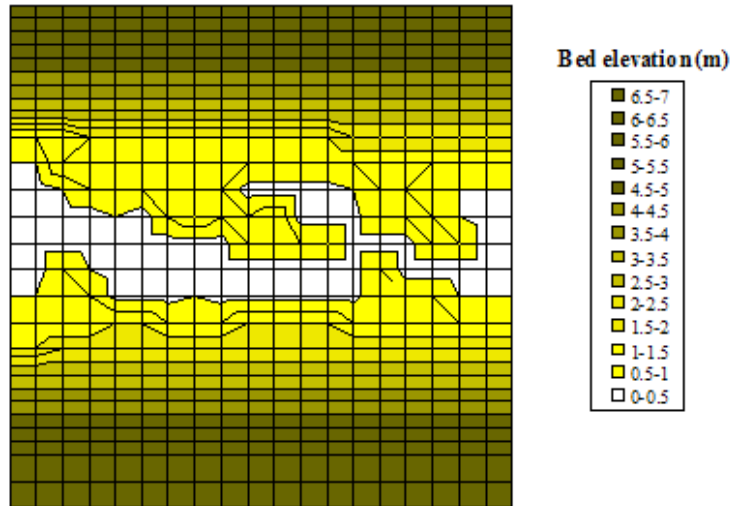


**Figure 5.19 Sediment distribution provided by a simulation of the sediment model at the channel-type scale**

**Table 5.6 Monthly average daily temperature**

Month	Daily Average Temperature $T$ (C°)
1	4
2	8
3	10
4	14
5	18
6	20
7	22
8	20
9	18
10	16
11	11
12	6

Irradiance, sun angle and average daily temperature specified to change every month therefore affects the reed growth rate at a particular time of year. These values are described in further detail in section 5.9.3, because they are specific to the reed growth model at the geomorphological-unit scale. Figure 5.21 shows that biomass density and biomass expansion decrease during the winter months because irradiance, sun angle and average daily temperature are lower.

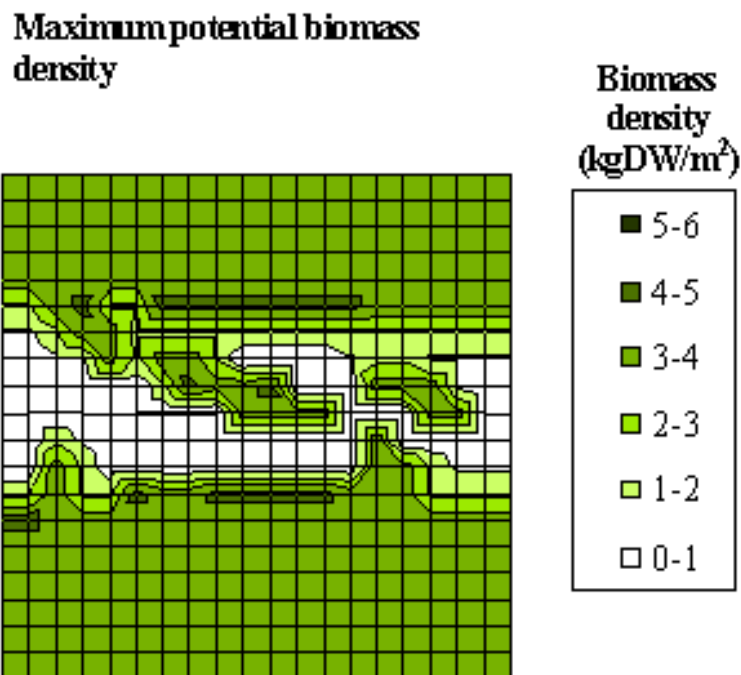


**Figure 5.20 Maximum potential biomass for given cell elevations**

The growth events also occur at different times of the year, resulting in an even more varied growth rate. This growth rate determines how fast the threshold biomass density of  $2.6 \text{ kg/m}^2$  dry weight within a cell is reached and therefore how fast expansion occurs. Figure 5.21 illustrates this, with reed expansion decreasing during winter months at the end of the year. Once this threshold density is reached, rhizome biomass is transferred to neighbouring cells with smaller biomass densities.

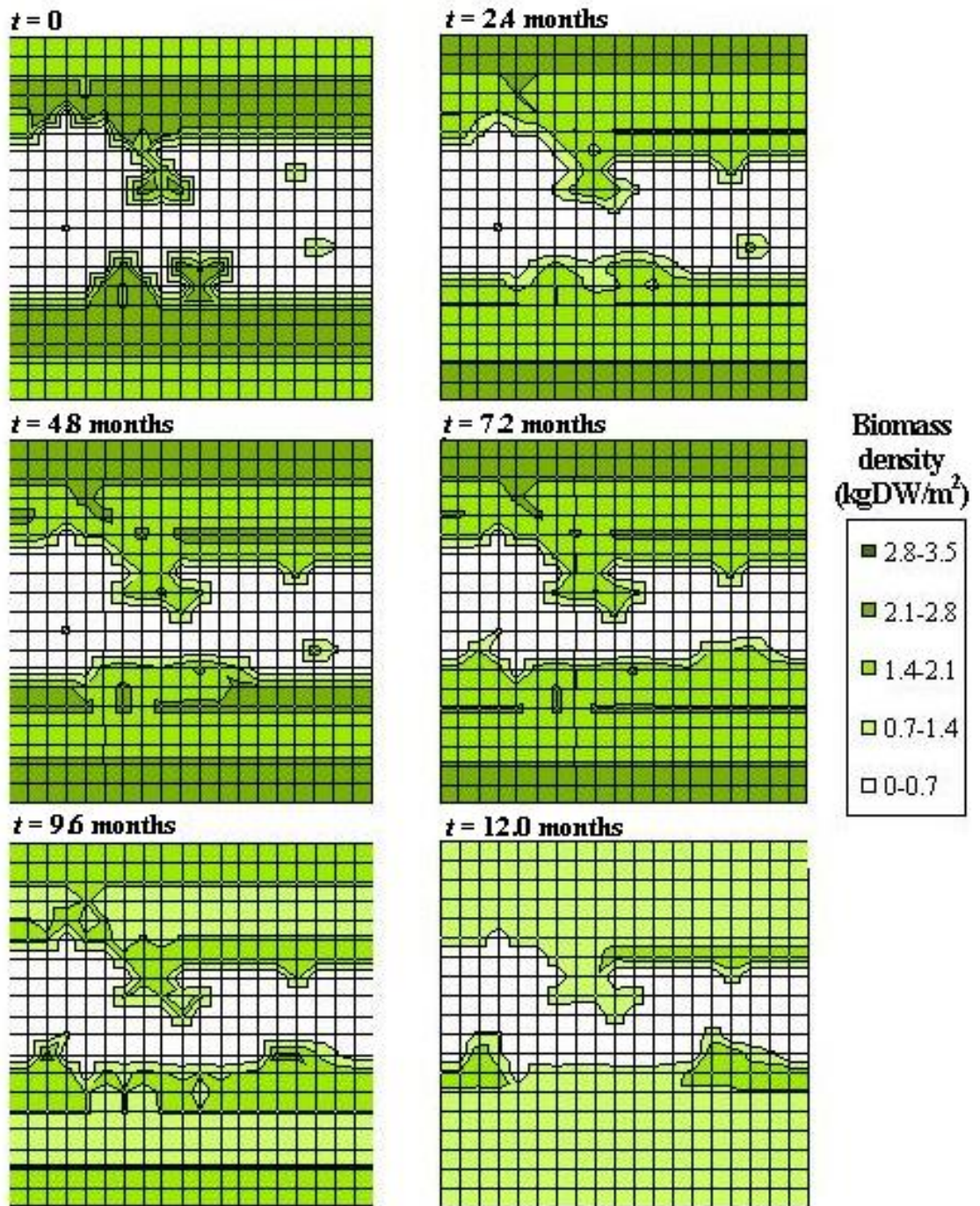


Figure 5.21 Typical reed expansion at the channel-type scale. Rapid growth of reeds during summer months increases biomass density quickly, allowing expansion, which slows down during winter months when reed growth decreases. Expansion occurs after a biomass density of 2.6 kg/m<sup>2</sup> dry weight is reached

The model only simulates expansion of reeds assuming no occurrences of reed removal through mortality, washout and being covered with sediment. These can be implemented by the user. The modelling in this study does not require a mechanism for removing biomass in cells since the biomass will start as stripped out and it will be assumed that no extreme flood, which may remove reed biomass from the reach, will occur during the period of simulation.

## **5.7 Geomorphological-unit scale water flow**

### **5.7.1 Model overview**

The geomorphological-unit scale water flow model uses boundary conditions provided in terms of flow velocities and depths by the 2-D water model at the channel-type scale to interpolate flow velocities and depths at a 0.25 m resolution.

Spatial variability of flow at small scales produces non-linear changes to resistance to flow emerging at larger scales (Bathurst, 1982). It is therefore necessary to predict the water flow distribution at the geomorphological-unit scale. State-of-the-art models of bed-forms and skin friction require detailed flow modelling to make predictions (Coleman *et al*, 2006), since roughness depends on both the geometry of bed-forms and skin friction. The bed-forms and skin friction modelling used in this study do not require detailed three-dimensional (3-D) water flow modelling such as that described in section 4.2.1. Bed-form and skin friction is estimated from larger scale flow characteristics, which for determining river evolution over decadal time scales is acceptable.

A steady state was therefore assumed to produce simple finite difference equations that are solved iteratively, using the residual method. The Jacobi residual method was used to interpolate intermediate values for the flow distribution. These values are used to determine the bed-form for each 0.25 by 0.25 m cell at the geomorphological-unit scale (Section 5.8). The method is described below.

The water flow distribution determined using this method is a first step toward reliable simulation for water flow at the geomorphological-unit scale. The model has the ability to

deal with obstacles such as large boulders or a tree by treating the obstacle as a boundary and specifying boundary flow characteristics.

### 5.7.2 The residual method

Two-dimensional steady-state flow is solved by assuming that the flow characteristics between adjacent cells vary linearly.

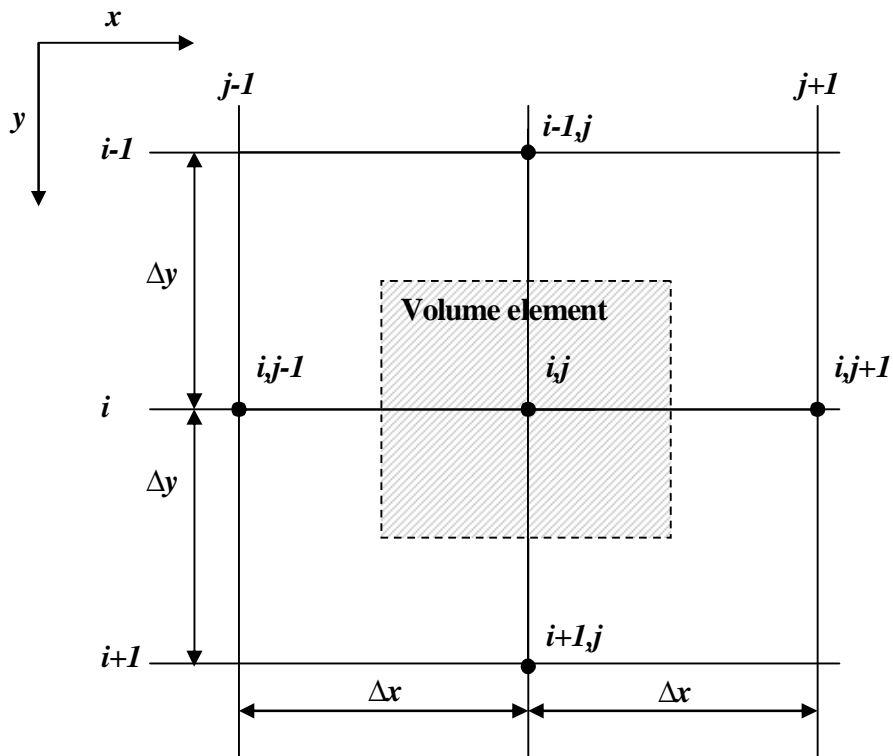


**Figure 5.22** Volume element of a general interior cell  $i, j$  for two-dimensional flow in rectangular coordinates

The flow characteristics at an interior cell then simplify to:

$$X'_{i,j} = X_{i,j} + \frac{X_{i-1,j} + X_{i,j+1} + X_{i+1,j} + X_{i,j-1} - 4X_{i,j}}{4} \quad (5.77)$$

Initial approximate values are given to  $X_{i,j}$ . At each stage in order to make further iteration, each  $X_{i,j}$  is updated. Updating proceeds sequentially. The updated value  $X'_{i,j}$  is based on the previous iterate, where  $X$  denotes flow depth,  $d$ , velocities,  $U$  and,  $V$  in the  $x$  and  $y$  directions. The model can be extended to three-dimensional flow in such a way that the interior nodes have six neighbouring nodes instead of four and introducing velocity  $W$  in



the  $z$  direction. It would also require boundary conditions specified at the water surface and bed.

## 5.8 Geomorphological-unit scale bed-form development

The bed-form geometry is determined for each 0.25 by 0.25 m cell at the geomorphological-unit scale from the shear stress obtained from the water flow model described above. Coleman *et al.* (2005) formulated a power law relating bed-form geometry (lengths or heights) to time, assuming that flow is sub-critical.

$$\left( \frac{P - P_i}{P_e - P_i} \right) = \left( \frac{t}{t_e} \right)^\gamma \quad (5.78)$$

The relation describes ripple or dune growth with time to approach equilibrium size at equilibrium time  $t_e$  with  $P$  denoting ripple or dune length  $L_b$  or height  $H_b$ .  $i$  refers to initial state of the bed-form. The exponent  $\gamma$  for bed-form length:

$$g_L = 0.14D_*^{0.33} \quad (5.79)$$

and bed-form height:

$$g_H = 0.22D_*^{0.22} \quad (5.80)$$

where

$$D_* = D \left( \frac{g(s-1)}{n^2} \right)^{1/3} \quad (5.81)$$

$D$  is characteristic particle size denoted in mixtures by the median grain size  $D_{50}$ . The initial length is given by Coleman and Melville (1996):

$$L_{bi} = 175D^{0.75} \quad (5.82)$$

and initial bed-form height is determined from (Engelund and Hansen, 1967):

$$H_{bi} = \frac{fL_{bi}}{1.88} \quad (5.83)$$

$f$  represents the flow resistance due to the sediment grains and is determined by the Colebrook-White formula for turbulent flow (Chanson, 1999) expressed by the following equation.

$$\frac{1}{\sqrt{f}} = -2.0 \log \left( \frac{k_s}{3.71D_H} + \frac{2.51}{\text{Re}\sqrt{f}} \right) \quad (5.84)$$

$$\text{Ripples: } t_e = 2.08 \times 10^8 \left( \frac{t_*}{(t_*)_c} \right)^{-2.42} \left( \frac{D}{U_*} \right) \quad (5.85)$$

$$\text{Dunes: } t_e = 2.05 \times 10^{-2} \left( \frac{D}{d} \right)^{-3.5} \left( \frac{t_*}{(t_*)_c} \right)^{-1.12} \left( \frac{D}{U_*} \right) \quad (5.86)$$

where equilibrium bed-form height,  $H_{be}$

$$H_{be} = 0.11d \left( \frac{D}{d} \right)^{0.3} \left( 1 - \exp \left( -0.5 \left( \frac{t_b}{(t_b)_c} - 1 \right) \right) \right) \left( 25 - \left( \frac{t_b}{(t_b)_c} - 1 \right) \right) \quad (5.87)$$

and equilibrium bed-form length,  $L_{be}$

$$L_{be} = 7.33d \quad (5.88)$$

where

$$U_* = \frac{f}{8} U^2 \quad (5.89)$$

$$t_b = rU_* \quad (5.90)$$

$$t_* = \frac{t_b}{r(s-1)gD} \quad (5.91)$$

and

$$(t_b)_c = r(s-1)gD(t_*)_c \quad (5.92)$$

(Chanson, 1999).

$(\tau)_c^*$  is the Shields entrainment number determined by the following relations (Cao *et al*, 2006):

$$\mathbf{R}_s = \left( D \left( \frac{sg}{u^2} \right)^{1/3} \right)^{3/2} \quad (5.93)$$

$$(\tau_*)_c = 0.1414 \mathbf{R}_s^{-0.2306} \quad \text{For } \mathbf{R}_s < 6.61 \quad (5.94)$$

$$(\tau_*)_c = 0.045 \quad \text{For } \mathbf{R}_s > 282.84 \quad (5.95)$$

$$(\tau_*)_c = \frac{\left( 1 + (0.0223 \mathbf{R}_s)^{2.8358} \right)^{0.3542}}{3.0946 \mathbf{R}_s^{0.6769}} \quad \text{For } 6.61 > \mathbf{R}_s > 282.84 \quad (5.96)$$

## 5.9 Geomorphological-unit scale reed growth

### 5.9.1 Model overview

The reed model at the geomorphological-unit scale provides reed biomass density to the channel-type scale reed model, which is used to simulate reed cover expansion. This model also provides the flow resistance attributes (stem spacing and diameter), which is correlated to the shoot biomass determined in the model. The flow resistance formulations are described in section 6.3.2.

The model of Asaeda and Karunaratne (2000) was selected to model the growth of a monospecific stand of *P. Australis*. Biomass of shoots, inflorescence, roots, old rhizomes and new rhizomes were described using finite differential equations:

$$\frac{\mathcal{I}B_{sh}}{\mathcal{I}t} = Ph_{sh} - R_{sh} - D_{sh} + (1 - x_{frac}) f_{rhi} Rhif - \varepsilon_{sh} f_{sh} B_{sh} - \varepsilon_{ph} f_{ph} Ph_{sh} - (p_{frac} B_{sh} + k_{frac} Ph_{sh}) f_f - f_{rt} G_{rt} \quad (5.97)$$

$$\frac{\mathcal{I}B_{rhi}}{\mathcal{I}t} = -R_{rhi} - D_{rhi} - f_{rhi} Rhif + y_{frac} f_{sh} e_{sh} B_{sh} + y_{frac} f_{ph} e_{ph} Ph_{sh} \quad (5.98)$$

$$\frac{\mathcal{I}B_n}{\mathcal{I}t} = -R_n - D_n + (1 - y_{frac}) e_{sh} f_{sh} B_{sh} + (1 - y_{frac}) e_{ph} f_{ph} Ph_{sh} \quad (5.99)$$

$$\frac{\partial B_{rt}}{\partial t} = G_{rt} f_{rt} - R_{rt} - D_{rt} + x_{frac} f_{rhi} Rhif \quad (5.100)$$

$$\frac{\partial B_p}{\partial t} = -R_p - D_p + k_{frac} f_f Ph_{sh} + p_{frac} f_f B_{sh} \quad (5.101)$$

where  $B_a$  and  $b_a$  are biomasses in gram ash-free dry weight with  $a$  representing subscripts  $sh$ ,  $rhi$ ,  $n$ ,  $rt$ , and  $p$  which are shoots, rhizomes, newly-formed rhizomes, roots and panicles, respectively.  $k_{frac}$  and  $p_{frac}$  are the fractions of contribution of the current photosynthesis and accumulated shoot dry matter to the formation of panicles.  $Rhif$  is the mobilization of stored material from rhizome to roots and shoots during the initial stage of growth.  $x_{frac}$  is the fraction of  $Rhif$  allocated for root growth and the rest for shoots.  $y_{frac}$  is the fraction of shoot assimilates for old rhizomes.

The factor  $f_a$  is made 1 when a growth event occurs or 0 when the event ends. For example,  $f_{rhi} = 1$  when rhizomes dynamics occur. The occurrence of growth events and parameter values are given in Figure 5.23 and Table 5.7 respectively. The equations were solved using the Fourth order Runge-Kutta integration.

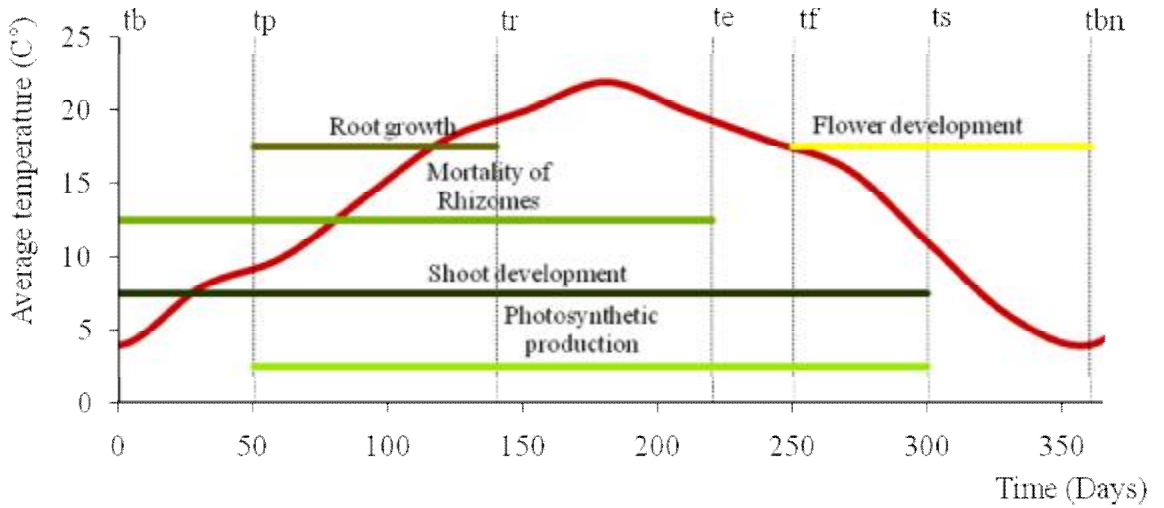


**Figure 5.23 Growth events and average air temperature used as inputs to the reed growth model**

**Table 5.7 Parameters used in the reed growth model at geomorphological-unit scale (Asaeda and Karunaratne, 2000)**

Parameter	Value	Units
Maximum specific growth rate of roots at 20C° ( $g_m$ )	0.007	gg <sup>-1</sup> per day
Specific respiration rate of roots at 20C° ( $R_{sh}$ )	0.007	gg <sup>-1</sup> per day
Specific respiration rate of shoots at 20C° ( $R_r$ )	0.002	gg <sup>-1</sup> per day
Specific respiration rate of old rhizomes at 20C° ( $R_{rhi}$ )	0.002	gg <sup>-1</sup> per day
Specific respiration rate of new rhizomes at 20C° ( $R_n$ )	0.003	gg <sup>-1</sup> per day
Specific respiration rate of panicles at 20C° ( $R_p$ )	0.003	gg <sup>-1</sup> per day
Specific mortality rate of shoots from $t_b$ - $t_p$ at 20C° ( $\gamma_{sh}$ )	0.0025	gg <sup>-1</sup> per day
Specific mortality rate of shoots from $tp$ - $ts$ at 20C° ( $\gamma_{sh}$ )	0.003	gg <sup>-1</sup> per day
Specific mortality rate of shoots after $ts$ at 20C° ( $\gamma_{sh}$ )	0.1	gg <sup>-1</sup> per day
Specific mortality rate of panicles from $tp$ - $ts$ at 20C° ( $\gamma_p$ )	0.003	gg <sup>-1</sup> per day
Specific mortality rate of panicles after $ts$ at 20C° ( $\gamma_p$ )	0.04	gg <sup>-1</sup> per day
Specific mortality rate of roots at 20C° ( $\gamma_n$ )	0.0002	gg <sup>-1</sup> per day
Specific mortality rate of old rhizomes at 20C° ( $\gamma_{rhi}$ )	0.0002	gg <sup>-1</sup> per day
Specific mortality rate of new rhizomes at 20C° ( $\gamma_n$ )	0.0002	gg <sup>-1</sup> per day
Fraction of current photosynthesis translocation to below ground structures ( $\epsilon_{ph}$ )	0.42	
Fraction of shoot assimilates translocation to below ground structures ( $\epsilon_{sh}$ )	0.026	
Fraction of shoot assimilates translocation for old rhizomes ( $\gamma_{frac}$ )	0.6	
Fraction of shoot assimilates translocation for inflorescence ( $p_{frac}$ )	0.0003	
Fraction fo current photosynthesis translocation to inflorescence ( $k_{frac}$ )	0.025	
Fraction of shoot biomass for elongation ( $q_{frac}$ )	0.41	
Fraction mobilized from rhizomes for root formation ( $x_{frac}$ )	0.1	
Maximum specific net daily photosynthesis rate at 20C° ( $P_m$ )	0.33	mg CO <sub>2</sub> gm <sup>-2</sup> per day
Half saturation constant of age for shoot photosynthesis ( $K_{age}$ )	125	d
Half saturation constant of PAR for shoot photosynthesis ( $K_{PAR}$ )	1E+07	micmol m <sup>-2</sup> per day
Half saturation constant of age for root growth ( $K_r$ )	50	d
Temperature constant ( $\theta$ )	1.09	
Conversion constant of carbon dioxide to ash-free dry weight ( $k_{co}$ )	0.65	gg <sup>-1</sup> CO <sub>2</sub>

## 5.9.2 Model closures

Model parameters are satisfied by the following equations (Asaeda and Karunaratne, 2000):

$$Rhif = a_{rhi}^{(T-20)} B_{rhi} \quad (5.102)$$

where  $\alpha_{rhi}$  is the specific transfer rate of rhizome biomass and  $T$  is daily average temperature in C° shown in Figure 5.23.

$$\alpha_{rhi} = 0.5B_{rhi_{initial}}^{-0.5} \quad (5.103)$$

The supply of photosynthesized material for root growth  $G_{rt}$  is given by

$$G_{rt} = g_m q^{(T-20)} \frac{K_{rt}}{K_{rt} + Age_{rt}} B_{rt} \quad (5.104)$$

where  $g_m$  is the maximum specific growth rate of roots at 20 C°;  $K_{rt}$  is the half saturation coefficient of root age, and  $Age_{rt}$  is the age of roots in days from the start of root growth.

$$R_a = b_a q^{(T-20)} B_a \quad (5.105)$$

$$D_a = g_a q^{(T-20)} B_a \quad (5.106)$$

A constant shoot elongation rate was assumed, even though it increases from the start of the growing season until the end of the rapid growth period and then declines. The shoot elongation per day in metres is given by

$$\text{New Shoot Height} = \text{Initial Shoot Height} \left( \frac{1 + (B_{shl} - B_{shlo})q}{B_{shl} - (B_{shl} - B_{shlo})q} \right) \quad (5.107)$$

where  $q$  is the fraction of biomass contributed to shoot elongation from each layer.

Net plant photosynthesis was assumed to be restricted by irradiance, mean air temperature and the age of assimilatory apparatus. Nutrient stress was ignored. The net daily plant photosynthesis ( $\text{gm}^{-2}$  per day) is given by a form of the Michaelis–Menten equation:

$$Ph_{shl} = P_m k_{co} q^{(T-20)} \frac{I_{PAR}}{K_{PAR} + I_{PAR}} \frac{K_{AGE}}{K_{AGE} + Age_{shl}} B_{shl} \quad (5.108)$$

where  $Ph_{shl}$  is the photosynthesis of shoots ( $\text{gm}^{-2}$  per day) and  $P_m$  is the maximum specific net daily photosynthesis rate of the plant top at 20°C in the absence of light and nutrient limitations.  $k_{co}$  is the conversion constant of carbon dioxide to ash-free dry weight.  $I_{PAR}$  is the photosynthetically active radiation.  $Age_{shl}$  is the age of shoots from the start of growth, and  $K_{PAR}$  and  $K_{AGE}$  are the half saturation coefficients of Photosynthetically Active Radiation (PAR) and age, respectively.  $I_{PAR}$  is the PAR in the open and  $I_{PAR}$  is the PAR in the stand, i.e.

$$I_{iPAR} = I_{PAR} e^{-k_i LAI} \quad (5.109)$$

where  $k_{ij}$  is the light extinction coefficient and  $LAI$  is the Leaf Area Index.

$$I_{PAR} = 0.45(\text{Global radiation}) \quad (5.110)$$

The following relationship between leaf biomass  $B_{leaf}$  and shoot biomass  $B_{sho}$  were used to calculate the  $LAI$  in the plant stand.

$$B_{leaf} = 0.25B_{sho} \quad (5.111)$$

where  $B_{leaf}$  is the leaf biomass.

$$LAI = 0.01355 B_{leaf}^{1.02} \quad (5.112)$$

The relationship between the  $k_{ij}$  and the sun elevation,  $\theta$  was obtained from Karunaratne *et al.* (2003):

$$k_{ij} = -0.0008 \theta^2 + 0.0706 \theta - 0.4 \quad (5.113)$$

The inputs for sun angle  $\theta$  and **Global radiation** used in the model are provided in Table 5.8.

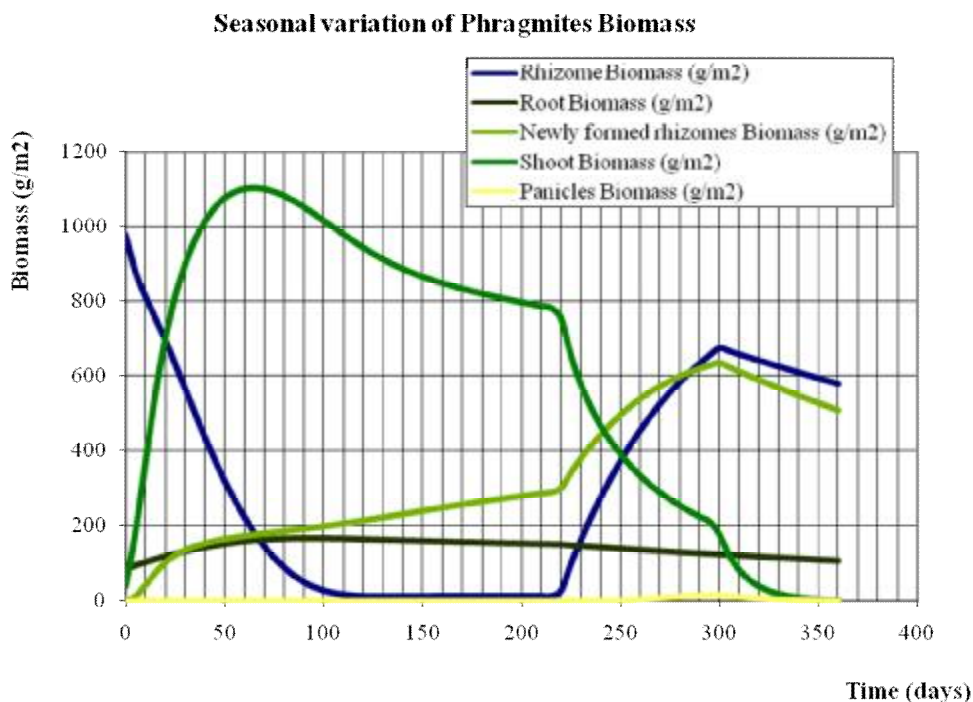
**Table 5.8 Monthly global radiation and sun angle inputs to the reed growth model**

Month	Global radiation (micromol /m <sup>2</sup> per day)	Sun Angle $\theta$ (degrees)
January	106398000	55
February	92460000	58
March	73416000	61
April	53590000	64
May	38042000	67
June	30130000	70
July	36248000	67
August	45816000	64
September	63526000	61
October	80638000	58
November	96232000	55
December	106398000	52

### 5.9.3 Model Output

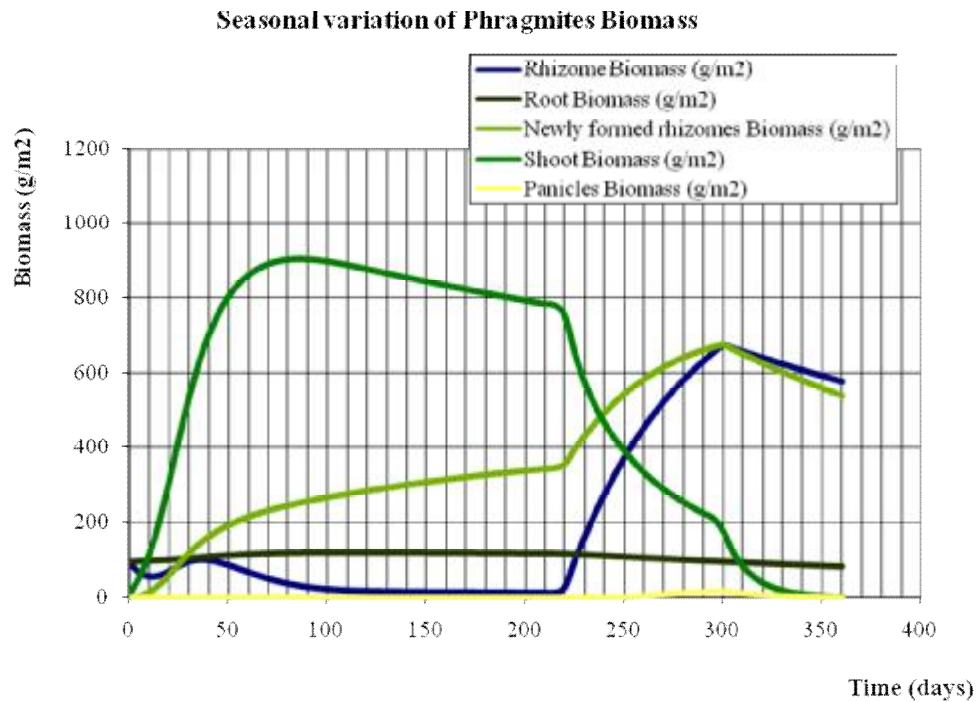
In the beginning of the growth year, each 5 by 5 m cell at the channel-type scale occupied by reeds has a certain amount of Root and Rhizome Biomass. The Rhizome Biomass allows growth of the other biomass variables of Root, Newly formed rhizomes, Shoot and Panicle according to the individual growth events. The Shoot Biomass is especially important for the flow modelling in this study, since it gives an indication of resistance to flow that the reeds will have.

Figure 5.24 and Figure 5.25 show a typical output for reed biomass throughout the year for a particular cell. It is assumed that no expansion occurs and therefore no exchanges of Rhizome Biomass to and from neighbouring cells. The reeds in this cell are growing at 100 % of their maximum potential biomass and are not constrained in terms of the flow regime. The initial rhizome biomass value impacts on reed growth, as indicated by the difference in biomass in Figure 5.24 and Figure 5.25.



**Figure 5.24 Typical model output showing seasonal variation of *Phragmites* biomass (ash free dry weight) of shoots, inflorescence, roots, old rhizomes and new rhizomes**





**Figure 5.25 Geomorphological-unit scale reed model output with a change in initial rhizome biomass**

### 5.10 Conclusion

Models for water flow, sediment and reed processes at each organisational level were developed to represent the most important aspects of rivers required for decadal prediction of the river state. At the reach scale, bed-elevation is simulated using sediment continuity according to water flow determined by a 1-D flow model and associated flow resistance. A fuzzy-rule-based model predicts the reed population distribution at the same scale. The sediment model at this scale is driven by flood flows which is responsible for the most significant geomorphological changes to the river channel, whereas the reed model is affected by the flow regime. At the channel-type scale a cellular automata model for both sediment routing and reed expansion is used. This sediment model simulates bar dynamics driven by a 2-D flow model as affected by the dynamic state of reed patches described by the reed expansion model. The changing reed state influences sediment behaviour in each episodic sediment model application through its effect on flow resistance. At the

geomorphological-unit scale, a sediment model predicts the geometry of bed-forms through a statistical approach but accounts for dynamic behaviour using a power law describing the bed-form evolution with respect to time. The water flow model at this scale interpolates the water flow distribution obtained by the flow model at the channel-type scale to produce a flow distribution which is used to drive bed-form development also at the geomorphological-unit scale. The reed model at the geomorphological-unit scale describes the growth of reed biomass using finite difference equations.

# Chapter 6 – Organisational modelling integration

---

Chapter 2 shows that a river system can be divided up into parts in order to better deal with its complexity and non-linearity. The parts reflect different river processes and the scales at which these processes operate. These parts interact and have to be integrated to provide feedback within a hierarchical modelling structure.

Modelling integration entails specifying the location for feedback. Process models simulating sediment, water and vegetation dynamics within a specific organisational level can be coupled since they share the same spatial scale. Models of the same process, producing patterns at various organisational levels, are linked to share model information across organisational levels.

This chapter gives examples of coupled models of interacting processes to provide feedback at the same scale, and integration of the same processes to provide feedback across scales. The latter is more difficult since the integration involves parameterisation and the imposing of boundary conditions to allow congruency of the particular river process across scales.

## 6.1 Process coupling

Process interactions (between sediment, water and vegetation) within the same spatial extent (physical domain) can be achieved by selecting a particular spatial grain.

Dollar *et al.* (2007) used a flow chain model to represent river processes at a particular spatial scale. Note that their flow chain model concept was originally intended to cross organisational levels. The flow chain model in Figure 6.1 was adapted to represent the effect that sediment and vegetation dynamics have on river geomorphology within a specific organisational level. The three interacting sub-systems of vegetation, water flow

and sediment are linked at an appropriate organisational level, to enable solution of the problem of vegetation affecting sediment dynamics, which produces changes in river form.

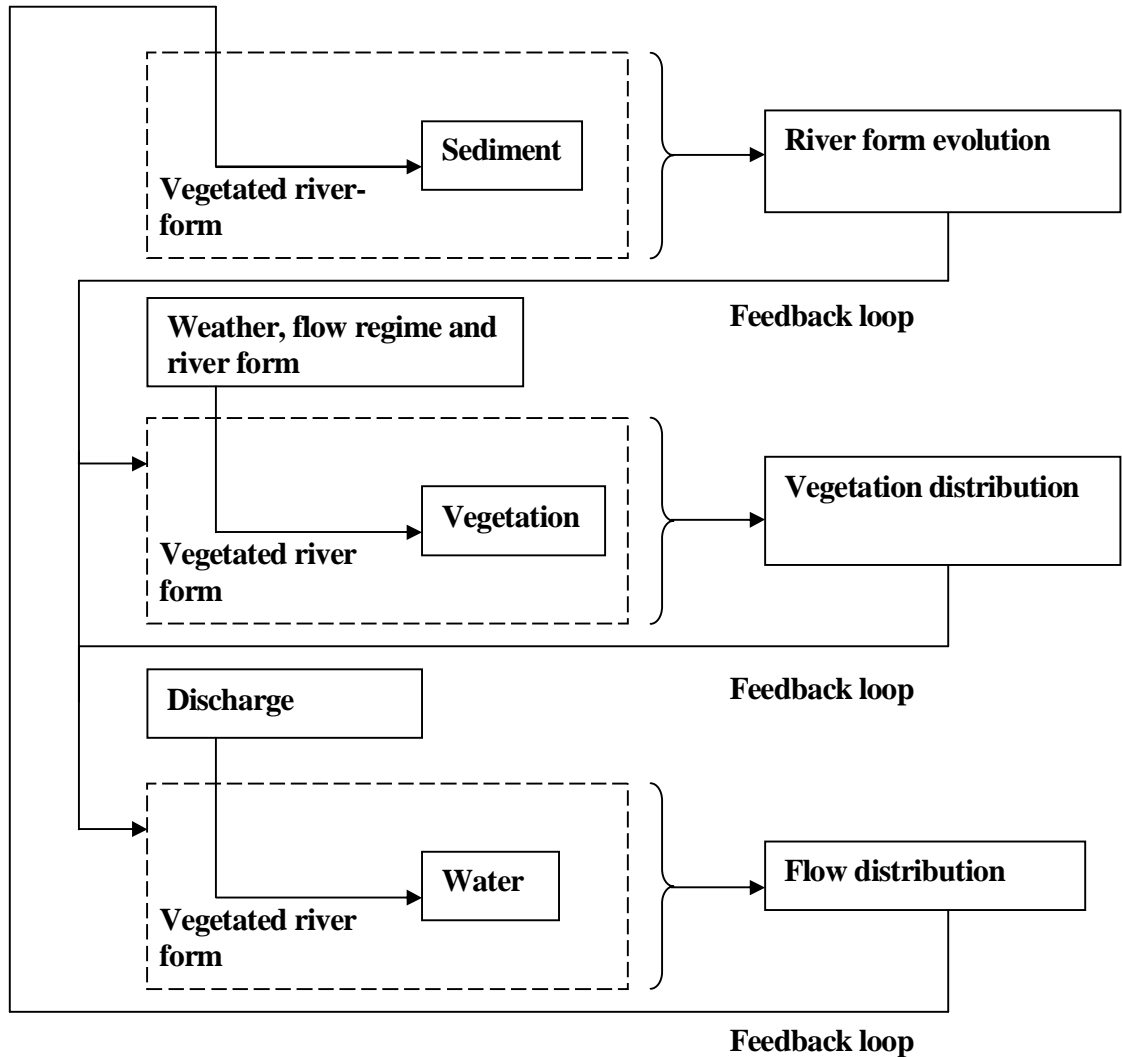


**Figure 6.1 A flow chain model, representing the integration of models providing output associated with a particular organisational level. The models are linked to provide feedback between sediment, water flow and vegetation processes (after Dollar *et al*, 2007)**

The connection between models for river flow, sediment organisation and riverine vegetation is made for each organisational level. All of these models in Figure 6.1 have the same spatial extent, representing processes at the appropriate organisational level. In order

to predict changes in river form when affected by vegetation, the sediment dynamics driven by water flow has to be incorporated. The sediment model, therefore, has to produce sediment organisation patterns resulting from river flow at the same spatial scales, where patterns for vegetation dynamics also affect these sediment patterns.

Figure 6.1 indicates that riparian vegetation dynamics is a responder to the weather, the flow regime and river form. Water flow dynamics is a responder to vegetated channel form driven by discharge. Sediment dynamics responds to river form and is driven by the flow distribution. An example is the evolution of a sediment bar in a river at the channel-type scale. The bar may form the substrate for reeds to grow on. The reeds slow down water flow velocities on and around it. This creates an opportunity for sediment to be deposited on and around the bar, allowing the bar to grow in order to create more substrate on which the reeds can become established. A further increase in reeds on that bar may further increase the size of the bar. However, feedback from the water flow may result as an increase in the bar size decreases the flow area, which may possibly increase flow strength, which may in turn erode the bar. The bar will therefore self-organise to reach a constant size under constant flow conditions.

Hierarchical modelling enables models for the interacting processes of water, sediment and vegetation to allow feedback between them at various points in time. The temporal scales between the models of vegetation and sediment dynamics can differ considerably. The use of asynchronous time steps allows the models to simulate important processes at time scales appropriate to those processes and not at some predetermined arbitrary time scale. However, the prerequisite for including the effect of processes that are described at dissimilar temporal scales is that they can provide feedback at the same spatial scale (Bendix, 1994).

Baptist and Mosselman (2002) coupled processes of sediment, water and vegetation to predict the medium- to long-term developments of geomorphology, vegetation and fish habitats for secondary channels in the Rhine River. In this study, state-of-the-art models for 2-D flow model and morphodynamics were used in combination with a rule-based vegetation model that is coupled to the spatial output to predict vegetation types,

succession and flow resistance. Coupling has been made between the changing flow resistance of vegetation and its effects on the hydrodynamics and morphodynamics. The hydrodynamics and morphodynamics are computed using a 2-D application of the numerical model Delft3D. Delft3D is a two-dimensional (2-D) and three-dimensional (3-D) flow and sediment transport model for tidal and riverine problems. The changing flow resistance is fed back to Delft3D, to account for the changes in vegetation composition (Baptist and Mosselman, 2002).

In the model, the flow resistance of vegetation is defined in terms of a Nikuradse equivalent roughness height  $k_e$  in metres. The flow resistance of each vegetation type in a grid cell is calculated by the weighted average of the roughness height with its percentage cover as weights. The succession of vegetation and its resulting change in flow resistance results in a change in flow velocities for a given discharge. The model in turn predicts changes in river geomorphology from the changing flow velocities in the river. The model results showed a gradual increase of forest cover bringing about increased roughness and producing aggradation in the river (Baptist *et al*, 2002).

Chen (2004) developed a cellular automata model that simulates algal blooms. Algal blooming is affected by hydrodynamic, physical, chemical and biological processes and species physiology. These factors are input into a fuzzy logic model using ecological rules for interactions between cells. The fuzzy logic model predicts algal biomass on the basis of the calculated nutrient concentrations, using the linked water quality and hydrodynamic modules of Delft3-WAQ. Delft3-WAQ is used for tidal and coastal flow and water quality prediction and determines the fate of nitrogen and phosphorus concentrations within a cellular grid. The combined CA and fuzzy logic model determines algal growth and spread by including nutrient processes and uptake as assimilated by algae (Chen, 2004).

## **6.2 Trans-scale linkage**

Models representing behaviour of a process at multiple organisational levels can share model outputs by linking them across scales. This trans-scale linkage allows incorporation of behaviour for the same process at different organisational levels.

The multiblock algorithm described by Wang and Weiming (2004) resembles model coupling using such principles. The multiblock method divides the solution domain into several sub-domains, or blocks, and generates a structured mesh for each individual sub-domain independently. The governing equations are solved block by block. During the solution process, the information updated at each time step or iteration step is transferred between the blocks. The interface treatment and information exchange between blocks are important and affect the solution accuracy and computation efficiency. The multiblock algorithm is often used with parallel computation (Wang and Weiming, 2004). Trans-scale linkage refers to this parallel computation using the multiblock algorithm. It allows model parameters to be continuously updated, using information from higher and lower organisational level blocks.

Figure 6.2 represents trans-scale linkage of models at various organisational levels. It requires links through parameters and boundary conditions that describe spatial phenomena of lower-level organisational models. This linkage is described in more detail in the following section. The number of arrows refers to the amount of spatial detail required for a particular organisational level i.e. the number of dimensions required for water flow modelling. Grain and extent for higher and lower organisational level models have to overlap to couple Lagrangian reference frameworks creating a new synthesis.

Similarly, trans-scale linkage of biological systems is found in Micro-Macro Link theory. According to the Micro-Macro Link theory, behaviour at the individual level generates higher-level structures (bottom-up process), which feed back to the lower level (top-down), reinforcing the producing behaviour either directly or indirectly (Conte *et al*, 2006). Vegetation is modelled on the same principles. Trans-scale integration of models for vegetation allows connecting of habitat units over space and time between organisational levels. For example, biomass growth according to the weather (lower organisational level) is determined within available habitat according to the river flow regime (higher organisational level) within the vegetation hierarchy.

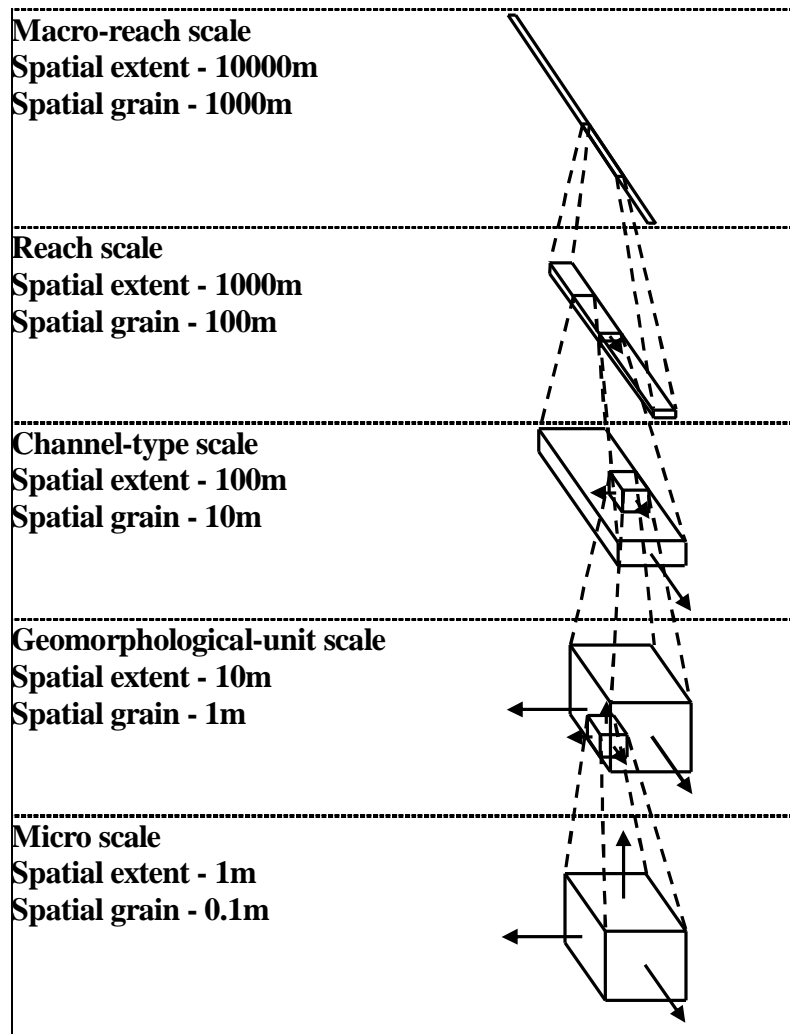


**Figure 6.2 Representation of trans-scale linkage where information produced by models representing the same physical processes (sediment, water and vegetation) at various organisational levels is shared. The grain of the higher-level model forms the extent of the lower-level model**

Wang and Weiming, (2004) suggested coupling of one-dimensional (1-D), two-dimensional (2-D) and three-dimensional (3-D) water and sediment models. Note that water and sediment models are coupled at the same scale but that 1-D, 2-D and 3-D models are linked across scales. Trans-scale linkage entails conserving the flow flux, momentum and energy as well as sediment flux, bed change and bed material gradation at interfaces between model subdomains. This approach can be used to apply 1-D models and 2-D models to examine change over a whole domain, and then a physical model for a detailed study of local problems of critical importance. The computational models provide boundary conditions for the physical model (Wang and Weiming, 2004).



Wu and Vieira, (2002) integrated CCHE1D and the catchment models AGNPS and SWAT. This integrated catchment-channel modelling system includes three components: landscape analysis, catchment modelling and channel simulation. The landscape analysis program is used to extract the channel network and its corresponding sub-catchments based on the elevation data from a Digital Elevation Model. The catchment models compute daily runoff and sediment yield for each sub-catchment. The channel model simulates the flow and sediment routing in the channel network using the boundary conditions provided by the catchment models (Wang and Weiming, 2004).

Bdour and Papanicolaou (2003) also integrated catchment process models with river process models. Their approach incorporates information regarding catchment and in-stream process interactions with a sediment transport model. Sediment influx and upland soil erosion from the catchment is obtained using the Geospatial Interface of Water Erosion Prediction Project model (GeoWEPP). GeoWEPP determines sediment load into the river and the upstream boundary condition for in-stream sediment transport modelling. The outcomes from GeoWEPP are coupled with a 2-D numerical model that predicts multifractional sediment transport, bed evolution and grain size distribution changes in mountain streams. Hence, the modelling system does not only perform detailed 2-D sediment transport but forms part of a coupled system of numerical models. These models also include models that simulate hydrologic and hydrodynamic phenomena from local to sub-regional to regional scale (Bdour and Papanicolaou, 2003).

## **6.3 Modelling integration**

### **6.3.1 Scale dependent variability of roughness**

Coarse-graining is achieved by averaging process outcomes at increasing scales. Coarse-graining can be applied to make models simple because high frequency contributions of lower scale process to the higher scale process will be eliminated by the averaging operation (Kavvas, 1999). Kavvas (1999) argued that coarse-graining allows a clearer view of an individual river process at a particular scale by eliminating the high frequency contributions of the smaller scale process by the averaging

operation. Therefore, the resulting models are free from the effects of the high frequency components of smaller scale processes and can still be quite simple.

When processes that are effective over longer time-scales and larger space-scales are dominant, the detail of high-frequency process variation at shorter time-scales and smaller space-scales is capable of incorporation through model parameters (Lane and Richards, 1997). Model parameters can therefore be determined through upward integration of small-scale processes to represent temporal fluctuations in small-scale patterns. Harrison (2001) stated that by integrating high-frequency and short-wavelength variables of a many-body system, parameters are able to describe the dynamics within large-scale systems. This is done through “coarse-graining”. For example, real time measurements of shear stress caused by the flow of water can fluctuate considerably over lengths in the order of millimetres and the time steps used by a water flow model. Larger scale flow models would use a roughness coefficient to determine the coarse-grained average to represent the shear stress caused by the flow of water at the resolution used by the model. Therefore, the average shear stress at the lower organisational level can be used to determine the flow resistance factor for a higher organisational level.

River models use friction and sedimentary characteristics for parameterisation representing the spatial environment over which water flows. Lane (2005) implies that the resistance coefficients used in water flow modelling represent the topography over which water flows that has to be calibrated, rather than having any meaning in the value itself. For example a Manning's  $n$  value in one model may be different from a Manning's  $n$  in another even though both predict the same flow phenomena. The difference lies in the resolutions for which the models apply. As the spatial scale of consideration changes, the amount of topography that must be dealt with implicitly changes.

Bathurst (1982) related various flow resistance coefficients to flow conditions and noted that a "single roughness size may not allow for the full resistance effects of a change in bed material size. This is because the wake eddies which are shed by the elements and which interact with the flow turbulence depend on the absolute size of the elements". With this in mind, flow resistance coefficients do have meaning in terms of the magnitude of the shear stress resisting the flow of water. It is assumed that the

average shear stress over a model extent can be carried up to higher organisational levels to determine the flow resistance coefficients at the grain of these higher organisational levels.

It is typical for flow resistance to change constantly for a particular location in a river. Flow resistance changes as a result of: the geological condition, such as sediment size and distribution and bed rock outcrops; channel geometry, such as depth and width; longitudinal profile, such as geomorphological-units (slope, riffles, pools, etc.) and the stream patterns (meandering, straight and braided); and vegetation distribution, such as patchiness and flow-retarding attributes (leaves and stems). These factors determine the rates at which flow resistance adjusts through all the organisational levels considered. Therefore, changing flow resistance due to factors varying at lower organisational levels has to be coarse-grained to account for flow resistance at higher organisational levels. Accounting for changing alluvial bed flow resistance is still very new.

### 6.3.2 Flow resistance formulations

#### Flow resistance at the geomorphological-unit scale

The shear stress at the geomorphological-unit scale is partitioned by the sum of the shear stress caused by the grain and form resistance.

Grain (or "skin") resistance is due to the presence of small, distributed irregularities such as bed-substrate. The average of the skin friction shear stress over model extent at the geomorphological-unit scale is calculated with the dimensionless Darcy–Weisbach friction coefficient  $f$  (Chanson, 1999):

$$\bar{t}_s = \frac{\sum \frac{f\rho V^2}{8}}{no} \quad (6.1)$$

where  $V$  is the depth-average flow velocity,  $no$  is the number of cells within the modelling domain for which water flow is computed,  $\rho$  is the density of water,  $f$  represents the flow resistance due to the sediment grains and is determined by the Colebrook-White formula for turbulent flow (Chanson, 1999) expressed by equation (5.84).

Form resistance due to the larger-scale internal deformation in the flow field is imposed by channel bed irregularities such as bed-forms. Shear stress as a result of form resistance due to the modelled 2-D bed-forms is determined using:

$$\overline{t}_{bf} = \frac{\sum \frac{1}{8} rV^2 \frac{\overline{H}_b^2}{\overline{L}d}}{no} \quad (6.2)$$

where  $\overline{H}_b$  and  $\overline{L}$  respectively are the average height and length of the bed-form determined at the extent of the geomorphological-unit scale (Chanson, 1999).

The average shear stress over the extent at the channel-type scale,  $\tau_o$ , is often considered to be composed of linearly additive components of shear stress attributable to these different aspects of flow resistance (Chanson, 1999). The total shear stress at geomorphological-unit scale:

$$t_o = \overline{t}_s + \overline{t}_{bf} \quad (6.3)$$

### Flow resistance at the channel-type scale

The friction slope depends on the bed shear stress which is assumed to be related to the magnitude and direction of the depth-average velocity (Steffler and Blackburn, 2002). The resistance model is based on the non-dimensional Chézy coefficient  $c_s$ .

$$S_f = \frac{t_o}{rgd} = \frac{(U^2 + V^2)}{gdc_s^2} \quad (6.4)$$

by rearranging

$$c_s = \sqrt{\frac{r(U^2 + V^2)}{t_o}} \quad (6.5)$$

$c_s$  is related to the effective flow resistance height  $k_e$  of the boundary and the depth of the flow through (Steffler and Blackburn, 2002) using:

$$c_s = 5.75 \log \left( 12 \frac{d}{k_e} \right) \quad (6.6)$$

Hence,  $k_e$  for a computational cell at the channel-type scale can be determined from  $c_s$ .

$$k_e = \frac{12d}{10^{c_s/5.75}} \quad (6.7)$$

### Flow resistance at the reach scale

Substituting the Manning equation into the Du Buoy's Equation ( $\tau_o = \rho g d S_f$ ) produces shear stress which varies linearly with the square of velocity. The end result is shear stress expressed as a function of Manning's  $n$  (Chaudhry, 1993):

$$t_o = n^2 \frac{rgdQ^2}{A^2 R^{4/3}} \quad (6.8)$$

in which  $R$  is hydraulic radius,  $A$  is flow area,  $Q$  is flow discharge and  $g$  is gravitational acceleration. To find Manning's  $n$  for each cross-section at reach scale, the average shear stress at the extent of the channel-type is determined from an average  $k_e$  and  $d$  (Steffler and Blackburn, 2002):

$$t_o = \frac{rU^2}{c_s^2} = \frac{rU^2}{\left(5.75 \text{Log} \left(12 \frac{\sum d}{\sum k_e}\right)\right)^2} \quad (6.9)$$

Manning's  $n$  as flow resistance coefficient at the reach scale is

$$n = \sqrt{\frac{t_o A^2 R^{4/3}}{rgdQ^2}} \quad (6.10)$$

### Flow resistance by reeds

A simple resistance relationship for flow velocity was used to represent flow through emergent reeds (Jordanova *et al*, 2006).

$$V = \frac{1}{F} \sqrt{S} \quad (6.11)$$

in which  $F$  is a resistance coefficient dependent on stem diameter  $D_{stem}$ , stem spacing  $a$  and drag coefficient  $C_D$ .

The following relationship for  $F$  has been derived for the conditions listed in Table 6.1:

$$F = 1.885 \left(\frac{a}{D_{stem}}\right)^{-0.65} \left(\frac{D_{stem}}{y}\right)^{0.07} C_D^{0.48} \quad (6.12)$$

**Table 6.1 Range of variables for which the resistance equation (6.12) is applicable (Jordanova *et al*, 2006)**

Variable	Range
Discharge, $q$ ( $\text{m}^3 \text{s}^{-1} \text{m}^{-1}$ )	0.005-0.5
Bed slope, $S$	0.0005-0.002
Stem diameter, $D$ (mm)	5.0-20.0
Stem spacing, $a$ (m)	0.05-0.1

The drag coefficient  $C_D$  depends on the stem size and shape and the Reynolds number  $\mathbf{Re}$  expressed in terms of stem diameter  $D_{stem}$ .

$$\mathbf{Re} = \frac{VD_{stem}}{\nu} \quad (6.13)$$

The relationship between  $C_D$ , and stem Reynolds number  $\mathbf{Re}$  can be represented by

$$C_D = a \mathbf{Re}^b \quad (6.14)$$

Best-fit values of coefficients  $a$  and  $b$  for the experimental conditions are listed in Table 6.2.

**Table 6.2 Values of  $a$  and  $b$  coefficients for estimation of the drag coefficient as a function of the stem Reynolds number (Jordanova *et al*, 2006)**

Description	$a$	$b$
Stem only	30.3	-0.38
3 – 6 leaves	999.58	-0.80
Fully Foliage	209.9	-0.58
Upper limit	1241.2	-0.79
Lower limit	10.35	-0.28
Average	114.79	-0.62

### 6.3.3 Boundary conditions

Boundary conditions are the constraints that a larger scale and more slowly changing environment imposes on a smaller scale and faster acting process. Over the temporal grain used to model these small-scale processes, boundary conditions supplied by larger scale models are assumed to be stationary since they change so slowly that they appear to stand still. Lower-level organisational models describe process reactions within the boundary conditions (defined by process models at higher levels of organisation) and result in a product that defines the template for process models at the next lower-level.

Organisational models share boundary conditions in two ways. In the first, models at higher organisational levels provide the rates of material flows at the upstream and downstream ends of the computational domain of the lower organisational level model. For this modelling, material flows are water, sediment and reed biomass. In the second, large-scale models provide the template or modelling sub-domain where smaller scale model descriptions apply. The grain of higher-level organisational models is related to the lower organisational levels by providing spatial information such as average slope. Thus, river features at higher organisational levels determine the location at which lower-level organisational models make predictions. For example, the deviation of elevation of the riverbed at the reach scale forms the average elevation around which sandbar dynamics at the channel-type scale is modelled. The elevation of such a sandbar would in turn represent the average around which bed-forms elevations fluctuate at the geomorphological-unit scale.

### **6.3.4 Linkage procedure**

Flow chain models of sediment, water and vegetation processes are shown in Figure 6.3, which illustrates the modelling linkage. The organisation levels selected are the reach scale, channel-type scale and the geomorphological-unit scale. The models are linked, providing feedback across these organisational levels.

The linkage modelling procedure is illustrated in Figure 6.4 to Figure 6.8 and proceeds as follows:

- 1) At the reach scale, the monthly flow depths from the water flow model are used by the reed model to determine the reed population distribution after every year. The reach scale reed distribution model determines a maximum biomass density for a given elevation on the river bank. The 1-D water flow model predicts the monthly flow depths from which the coefficient of variance and average yearly flow depth is determined and used to predict the maximum biomass density growing at a given elevation.
- 2) The reed model at the channel-type scale predicts the manner in which patches of reeds expand within a cellular grid, based on the bed elevations of cells and the corresponding maximum biomass density provided by the reach scale reed model.
- 3) The 1-D water flow model at the reach scale provides the boundary conditions for the water flow at the channel-type scale. The intermediate 2-D depth-average flow

distribution at the grain of the channel-type scale is determined given the average flow velocity and depth, at the grain of the reach scale, forming the boundary conditions. The 1-D water flow model also provides the inputs to the sediment model at the reach scale.

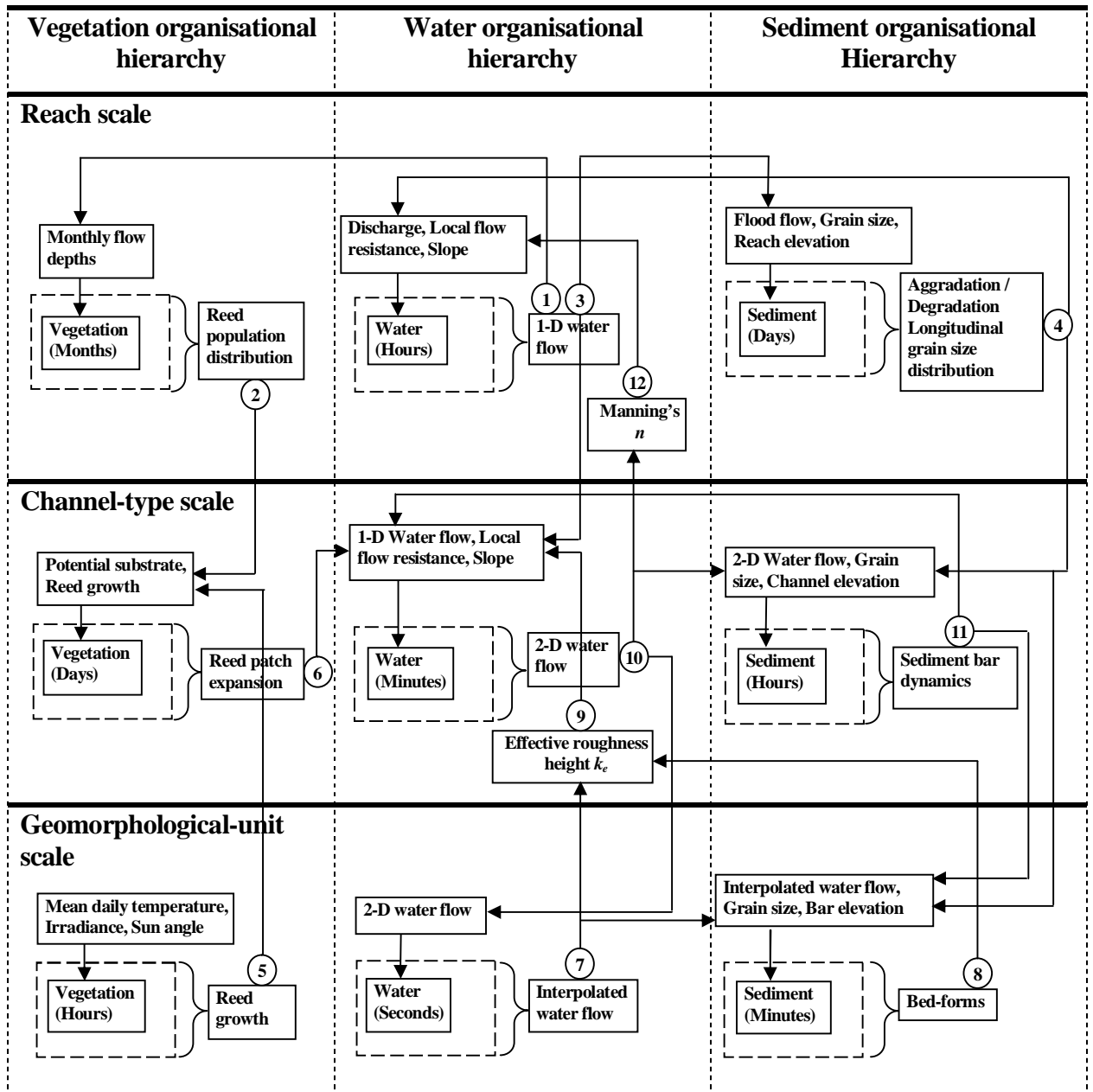


Figure 6.3 Hierarchical modelling integration of sediment, water and vegetation processes across the reach scale, channel-type scale and geomorphological-unit scale. Arrows represent feedback through provision of model inputs, boundary conditions and parameters



- 4) The bed elevation determined by the reach scale sediment model is fed back to the 1-D water flow model and determines the resulting water flow distribution. The reach scale sediment model provides the template on which sediment bars and erosion at the channel type scale are determined. The same model also provides the grain size to the sediment models at the channel-type and geomorphological-unit scale.
- 5) The reed model at the channel-type scale predicts the expansion of reed patches according to biomass growth determined at the geomorphological-unit scale.
- 6) The reed patch dynamics model provides the flow resistance to water flow through cells occupied by reeds.
- 7) At the grain of geomorphological-unit scale, the flow distribution is interpolated, allowing bed-form length and height to be estimated by the sediment model. The coarse-grained shear stress at the extent of the geomorphological-unit scale is used to determine the effective roughness height  $k_e$  at the grain of the channel-type scale.
- 8) The bed-form length and height also affect flow resistance values determined at the grain of the channel-type scale.
- 9) The resulting  $k_e$  values are used in the 2-D water flow model simulations. The sediment and water models at the geomorphological-unit scale run 3 times by specifying the interval for running the modelling procedure to allow the  $k_e$  values to be updated.
- 10) The 2-D depth-average velocity and flow depth drives the sediment bar model. The same model provides the boundary conditions at the extent of the geomorphological-unit scale. The shear stresses due to flow resistance at the extent of the channel-type scale are further coarse-grained to determine flow resistance values at the grain of the reach scale.
- 11) The sediment bar model predicts new cell elevations, which are updated in the 2-D water flow model to result in a new 2-D flow distribution. In so doing, these models are providing continuous feedback. The same model also provides the template for predicting bed-forms at the geomorphological-unit scale.
- 12) The coarse-grained shear stresses due to the flow resistance channel-type scale provide the Manning's  $n$  values at the grain of the reach scale used by the 1-D water flow model to determine the new flow distribution.

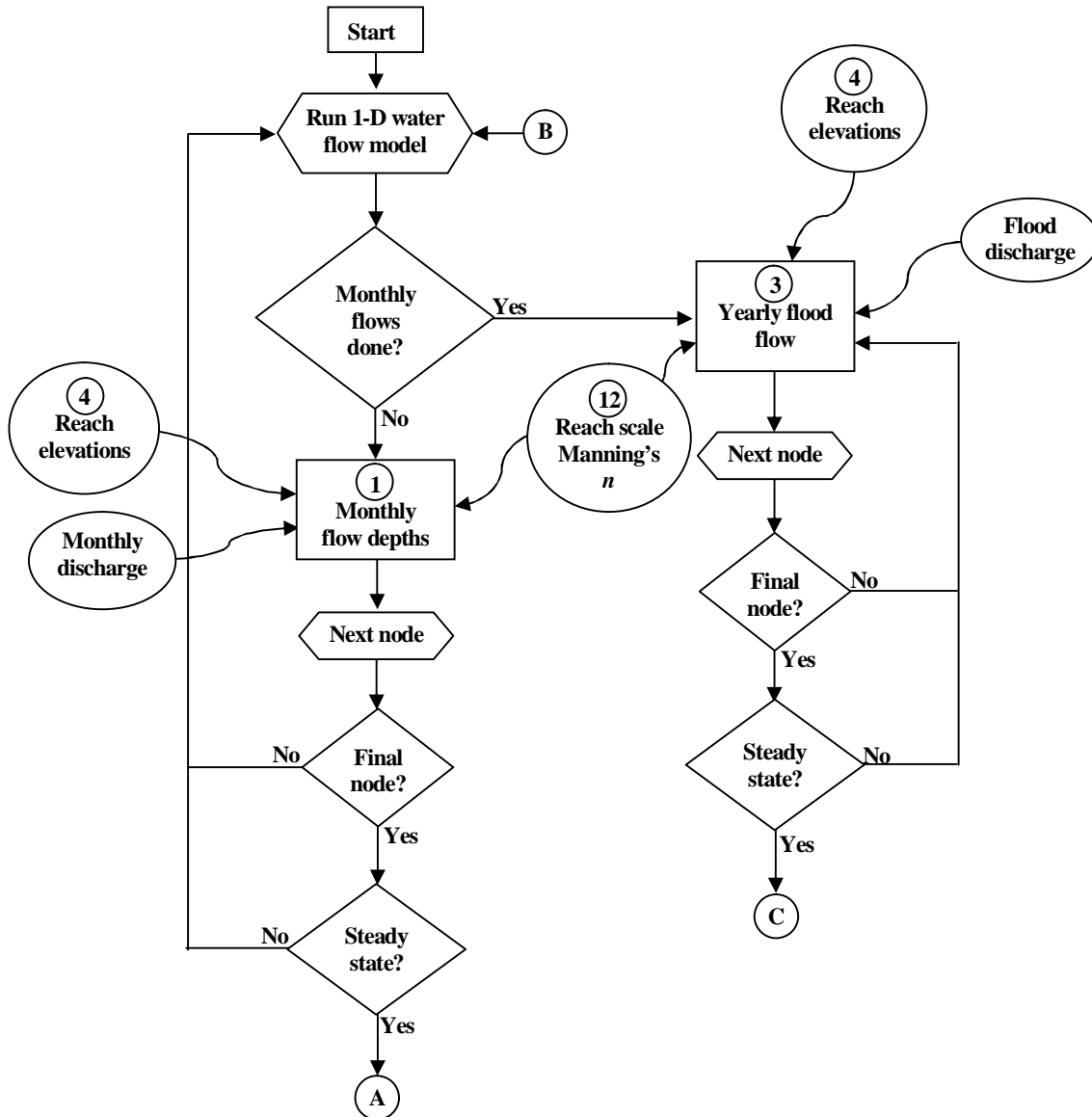


Figure 6.4 Sub-procedure for water flow modelling at the reach scale

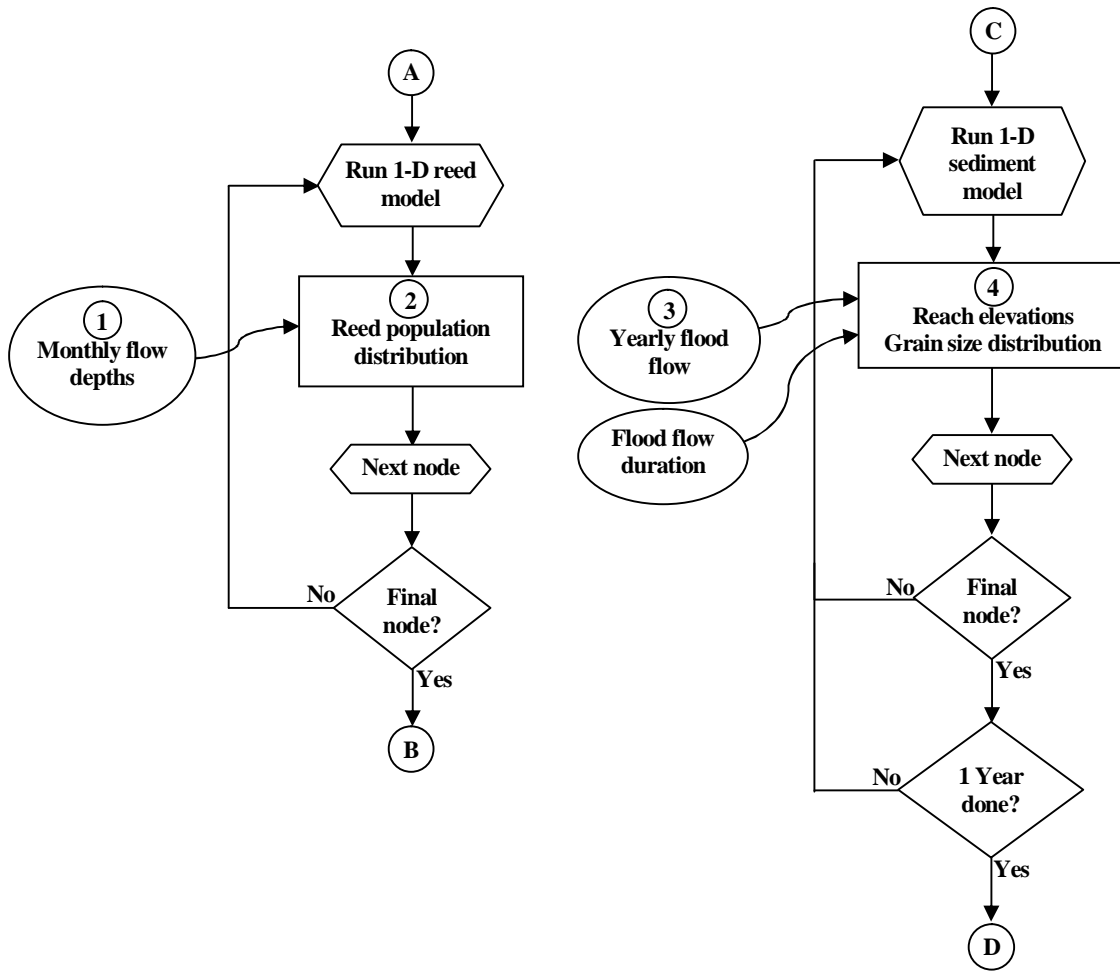


Figure 6.5 Sub-procedures for reed and sediment modelling at the reach scale

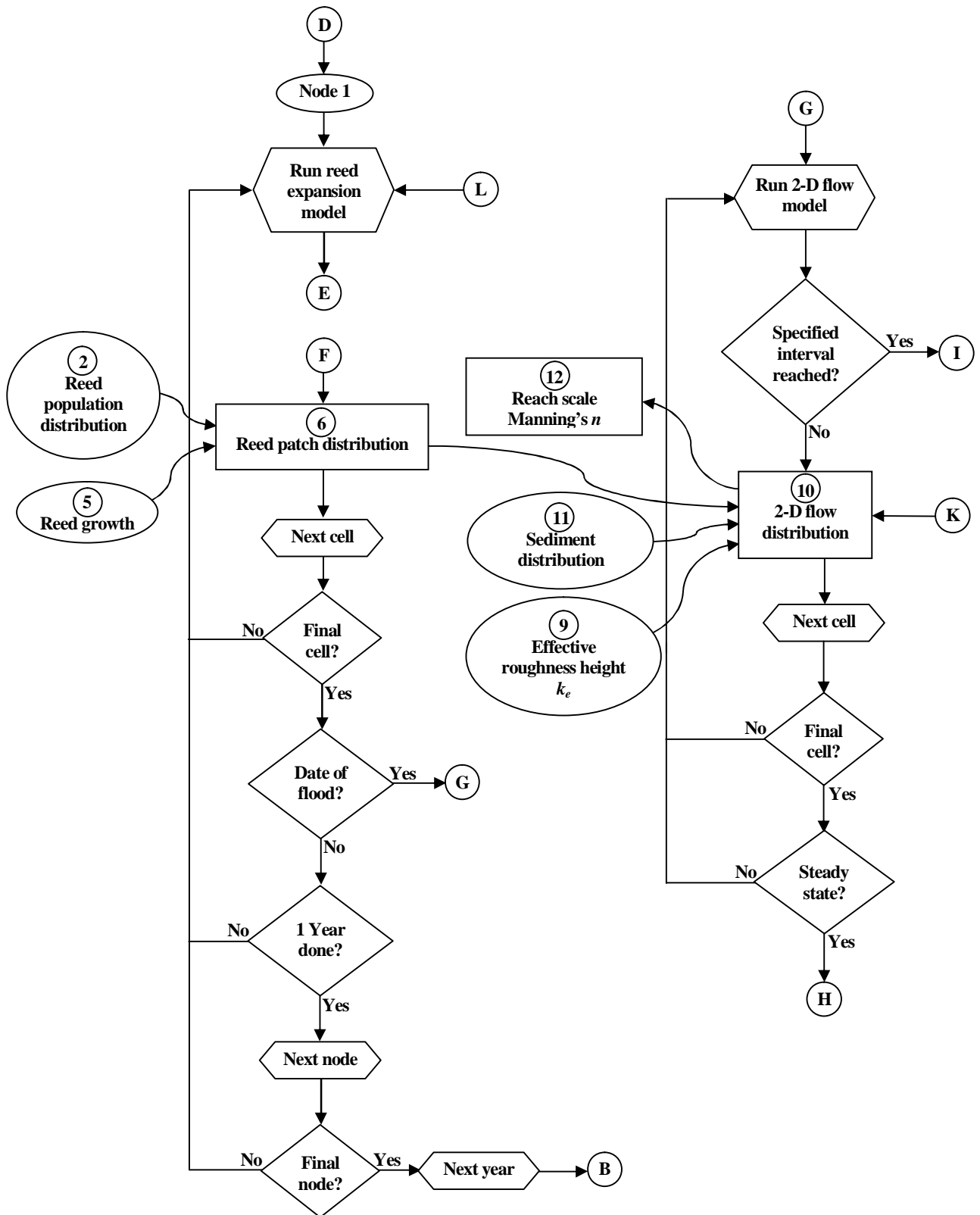


Figure 6.6 Sub-procedures for reed and water flow modelling at the channel-type scale

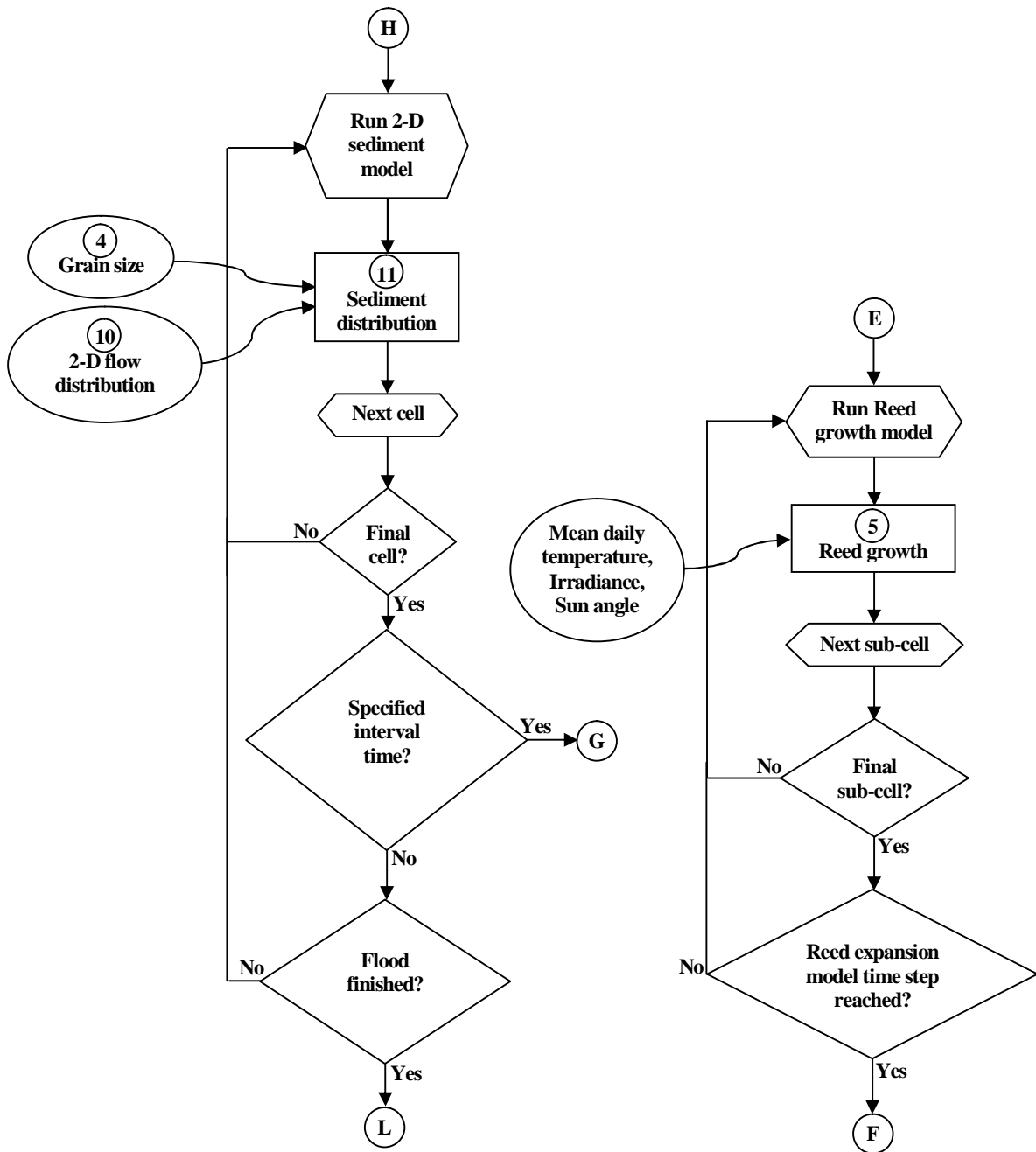


Figure 6.7 Sub-procedures for sediment modelling at the channel-type scale and reed modelling at the geomorphological-unit scale

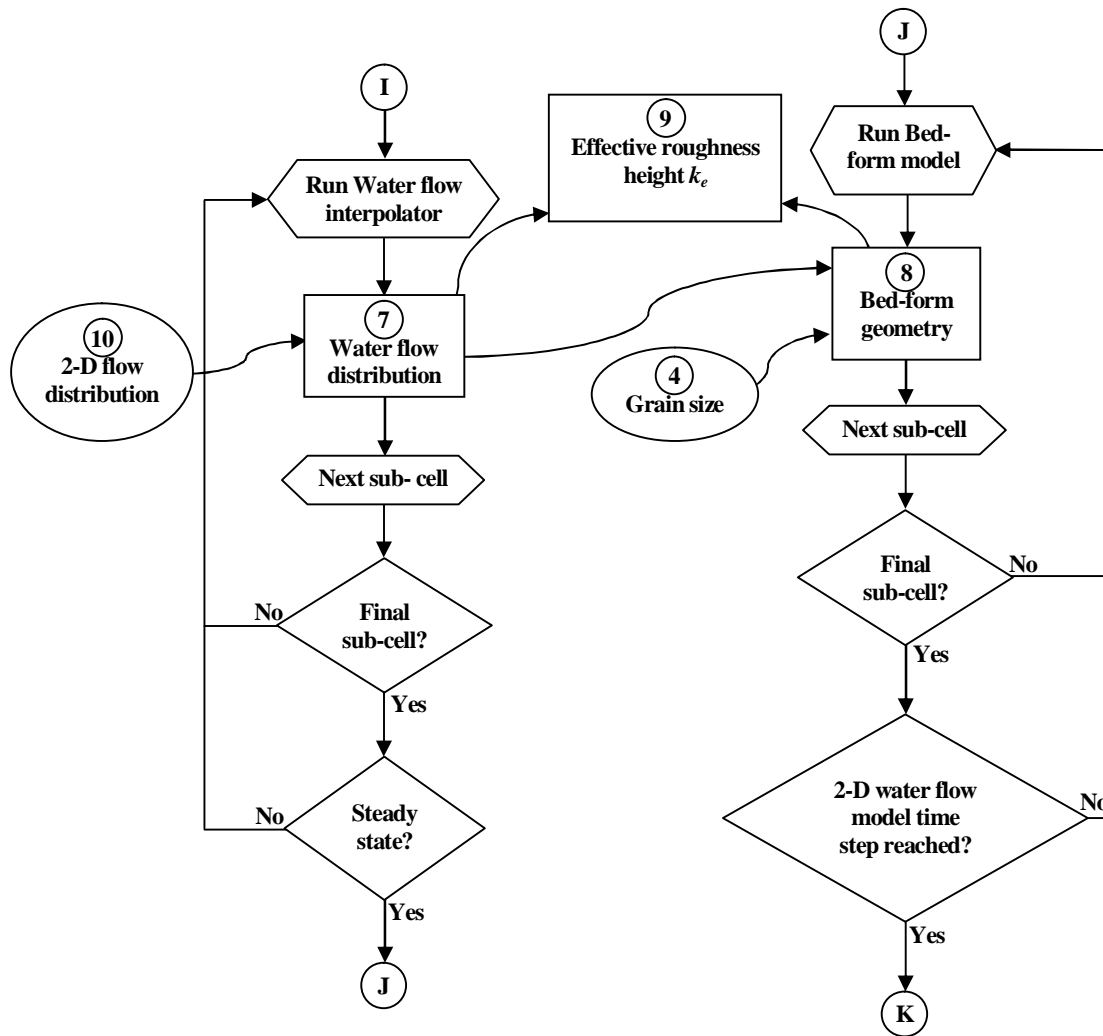


Figure 6.8 Sub-procedures for water flow and sediment modelling at the geomorphological-unit scale

## 6.4 Conclusion

Simulation across organisational level while incorporating process interactions, has rarely before been attempted. A new way of linking models across scale has been implemented to integrate models in a hierarchical framework. It allows integration of the interacting water, sediment and vegetation process models across scales to allow feedback between them. The models are linked to share outputs which provide boundary conditions and values for model parameters at specific locations within the modelling domain. A hierarchical framework allows prediction of small-scale geomorphology and accounts for its variability at the large-scale.

## Chapter 7 – Modelling results

---

River geomorphological modelling was performed to show the effects of dynamic processes regarding the interaction of sediment, water and reeds at various scales for a period of 10 years. An important aspect of the modelling is to simulate sequences of events and conditions and to incorporate feedback so that the changes in geomorphology from one event have an influence upon the impact of the next event.

Great algorithmic effort is needed for the numerical solutions to the model equations representing the river processes. Model integration therefore proved very computationally intensive because feedback between models at different organisational levels was required. 1 run took approximately 1 week. Because the computational cost of the hierarchical modelling approach is so high, only 3 river geomorphological scenarios were modelled. The points in time when feedback is transferred to higher organisational levels were selected to be effective and representative, but were reduced to save on the computational demand.

The sequence of model feedback proceeded as follows. The geomorphological-unit scale reed model is called up for every cell and time step of the channel-type scale reed model. After 6 months of a reed patch simulation at the channel-type scale, the sediment and water flow models at the same scale are called on to simulate a 30 minute flood event. These models provide boundary conditions for the models at the geomorphological-unit scale. The water flow and sediment models at geomorphological-unit scale are called up 3 times during the 30 minute flood flow simulation to supply coarse-grained flow resistance values at the grain of the channel-type scale. Each time new flow resistance values are determined, the resulting water flow distribution at the channel-type scale is simulated to drive the sediment model at the same scale for another interval of the flood duration. This is repeated for each of the 100 m sections over a 2000 m reach. The average of the 3 times when the coarse-grained shear stresses are obtained for water flow runs at the channel-type scale are used to determine Manning's  $n$  values. The new Manning's  $n$  values are used in the

reach scale water flow runs for the following year. The reach scale water flow distribution drives the sediment model and reed model at the same scale. After every yearly run, the outputs of all 3 reach scale models are used as boundary conditions by lower organisational level models.

All the modelling scenarios are on essentially the same hypothetical river but with two significant differences. Scenario 1 has a larger sediment feed rate than scenarios 2 and 3. Scenario 3 includes the effect of bedrock. Modelling results are compared for the cases where flow resistance is linked across organisational levels and the case where no linkage is made, but a typical flow resistance value is used. The simulation was rerun without integrated smaller scale modelling using the resulting Manning's  $n$  values from simulations with integrated small scale models.

## 7.1 Modelling Scenarios

In order to set up realistic modelling scenarios, the regime method of Julien and Wargadalam (1995) was used to determine general channel geometry. The method allows determination of the river geometry providing average flow depth  $h$  in metres and channel top width  $W$  in metres for bank full flow conditions given channel slope  $S$ , median grain size  $D_{50}$  in metres and dominant discharge  $Q$  in  $\text{m}^3/\text{s}$ . The following channel geometry relations were used:

$$W = 1.33Q^{(2+4m)/(5+6m)} D_{50}^{-4m/(5+6m)} S^{(-1-2m)/(5+6m)} \quad (7.1)$$

$$h = 0.2Q^{2(5+6m)} D_{50}^{6m/(5+6m)} S^{-1/(5+6m)} \quad (7.2)$$

$$\text{where } m = 1 / \ln(12.2h / D_{50}) \quad (7.3)$$

A typical Entrenchment Ratio (Rosgen, 1994) for a gravel-bed river was chosen. The Entrenchment Ratio provides a measure of how deep the river runs through the valley. The Entrenchment Ratio is defined as the Flood-Prone Width divided by the top width  $W$  where the Flood-Prone Width is taken to be twice the bank full depth  $h$ . Given the Entrenchment Ratio, the channel lateral slope  $S_l$  was determined. The model assumes a trapezoidal shaped channel. Figure 7.1 shows the variables describing the channel geometry.



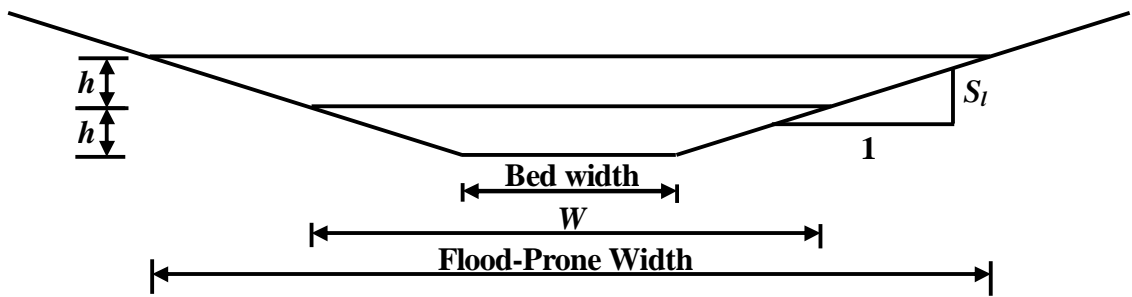


**Figure 7.1 Schematic showing variables describing the channel dimensions. A trapezoidal channel was assumed**

River type B4 described by Rosgen (1996) was used for representation by this modelling. This stream type is narrow, moderately entrenched, occasionally well vegetated and the channel material is dominated by gravel with lesser amounts of cobble and sand (Rosgen, 1996).

It was assumed that the flood responsible for moving most of the sediment at a steady discharge  $Q_f$  lasted for 30 minutes, as shown in Figure 7.2. This flood duration does not involve the Intermittency value  $I_f$  and was chosen purely for computational reasons.

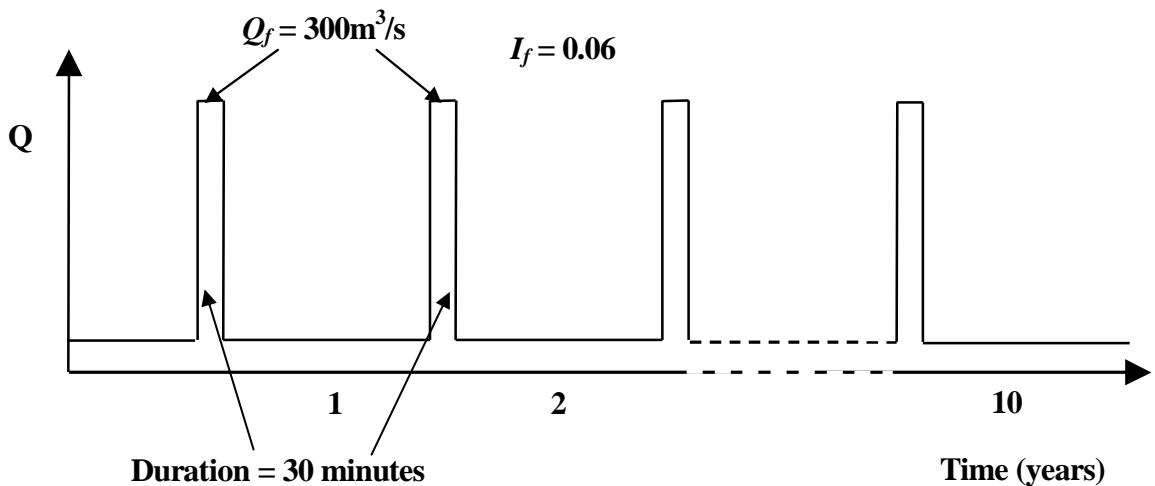


**Figure 7.2 Flow regime specified for the particular modelling scenarios**

The following values were used to determine and describe the channel dimensions for inputs in the modelling:

$$\begin{aligned}
 Q_f &= 300 \text{ m}^3/\text{s} \\
 I_f &= 0.06 \\
 Q &= 18 \text{ m}^3/\text{s} \\
 D_{50} &= 0.011 \text{ m} \\
 S &= 0.004 \text{ m/m} \\
 h &= 0.70 \text{ m} \\
 W &= 25.0 \text{ m} \\
 \text{Entrenchment ratio} &= 1.6 \\
 \text{Flood prone width} &= 40.0 \text{ m} \\
 \text{Side slope} &= 0.088 \text{ m/m} \\
 \text{Bed width} &= 10.2 \text{ m}
 \end{aligned}$$

The above values are used for description of the initial river state. The objective was to examine the effect of much larger average flows on river form. Larger flow in reality can, and often do, result from numerous river and catchment alterations (dams, levees, channelization, land use changes, etc.).  $Q_f$  drives the sediment model at the reach scale whereas the initial state of the river has been based on  $Q$ . The monthly flows in Table 7.1 were used by the 1-D flow model to determine the monthly flow depth used by the reed model.

**Table 7.1 Monthly discharges input data into the 1-D water flow model to predict the monthly flow depths used by reach scale reed model to predict the maximum biomass density growing at a given elevation**

Month	Average monthly discharge (m <sup>3</sup> /s)
January	170
February	150
March	130
April	110
May	100
June	110
July	120
August	130
September	140
October	150
November	160
December	170

The following parameters were implemented in the cellular automata reed model to predict the expansion of reeds at the channel-type scale:

Reed front advancement rate = 7 m/month  
 Time step ( $\Delta t$ ) = 21 days  
 Maximum reed density = 6 kg DWT/m<sup>2</sup>  
 Reed density before expansion occurs = 2.6 kg DWT/m<sup>2</sup>

Figure 7.3 shows the representative particle size distribution for both feed and substrate for the river type chosen to model, as obtained from Rosgen (1996) and input into the reach scale sediment model.

The 3 scenarios were modelled using the attributes provided above except that a sediment feed rate of  $3 \times 10^{-4}$  m<sup>2</sup>/s per unit width was specified for scenario 1 whereas  $3 \times 10^{-6}$  m<sup>2</sup>/s was specified for scenarios 2 and 3.

Scenario 3 incorporated the effect of bedrock. Bedrock was specified at 2 metres below the sediment surface at the start of simulation and random bedrock outcrops shown in Figure 7.4 were implemented to allow for the heterogeneity that is associated with bedrock at the channel-type scale.

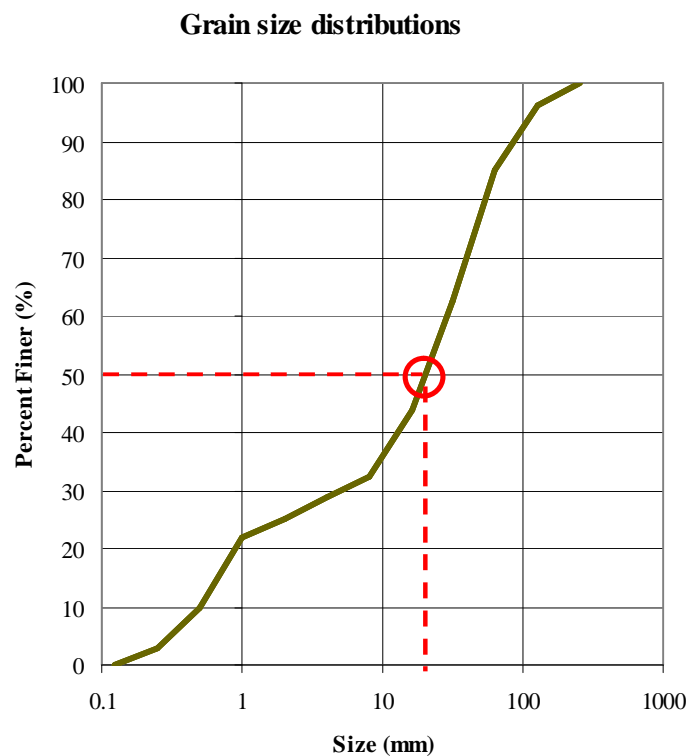


**Figure 7.3 Grain size distribution for feed and substrate typical for the stream type modelled (Rosgen, 1996). The initial  $D_{50}$  of 0.011 m is indicated**

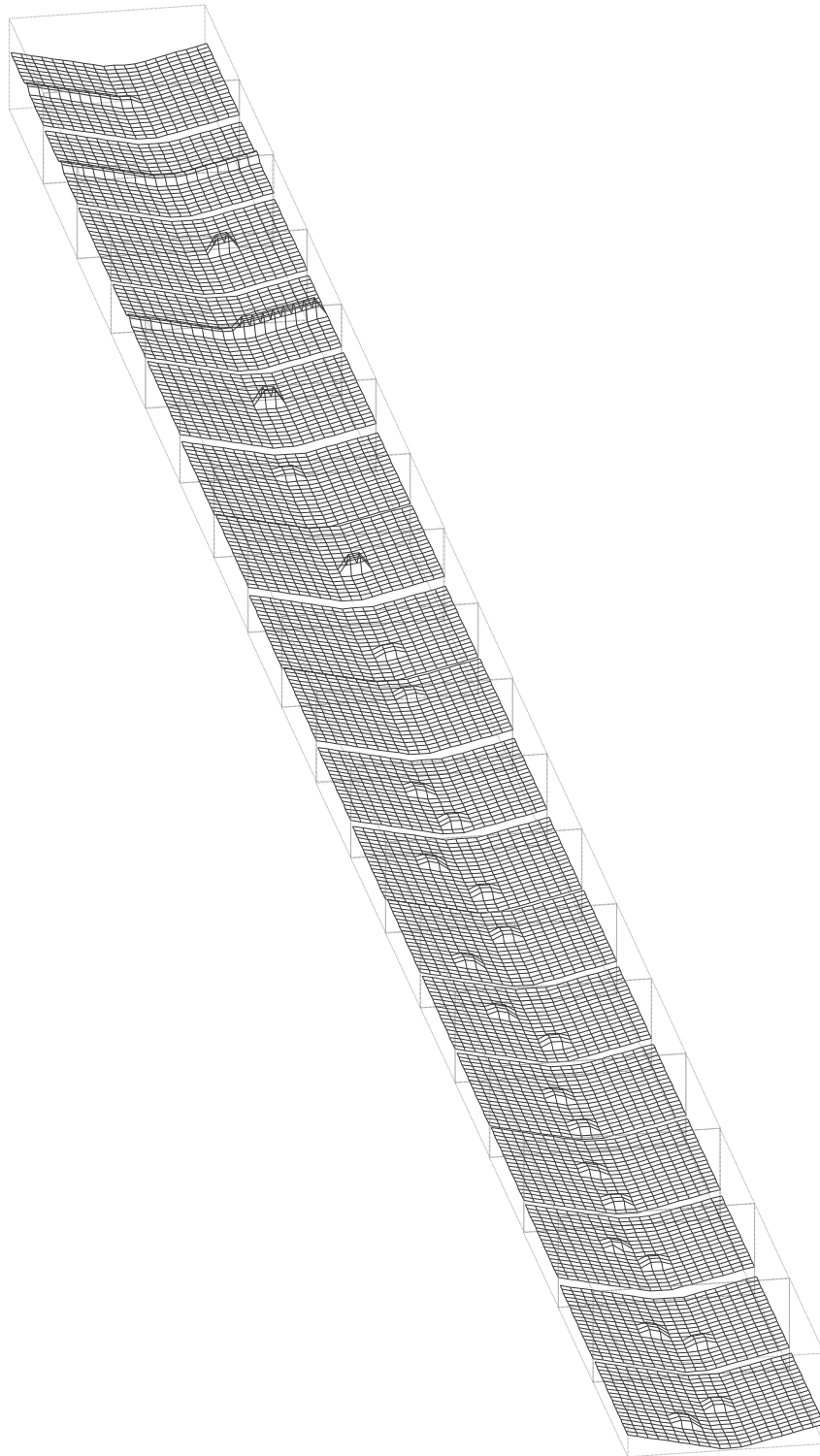


**Figure 7.4 Bedrock outcrops specified for scenario 3**

A Manning's  $n$  value of 0.029 was used to provide an initial estimate and is typical of gravel-bed rivers (Yen, 1991). This value was used for the first year of simulation, after which linked smaller scale water flow models provided values for Manning's  $n$ . Two simulation were performed which did not include smaller scale modelling integration. The Manning's  $n$  of 0.029 was used throughout for the first. A second simulation was

performed which not include smaller scale modelling integration using the Manning's  $n$  values obtained from year 10 for the run that did include smaller scale modelling. The resulting elevations are shown in Figure 7.10, Figure 7.13 and Figure 7.17.

## 7.2 Results and discussion

The unvarying sediment and water flow input or the reach scale sediment modelling for scenario 1 resulted in the bed elevation of the 2000 metre reach self-organizing at a 100 m resolution. The gradual decrease in bed elevation change as the river moves to an equilibrium state is shown in Figure 7.5 and Figure 7.6, indicating self-organisation.

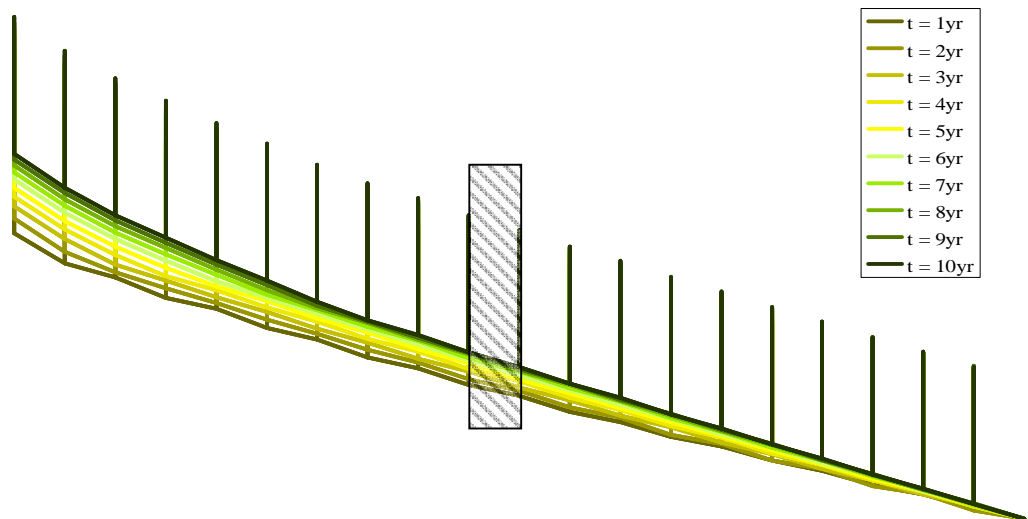


**Figure 7.5 Self-organisation of bed elevations for scenario 1 at the reach scale. Self-organisation at the channel-type scale is shown for the hatched section in Figure 7.8**

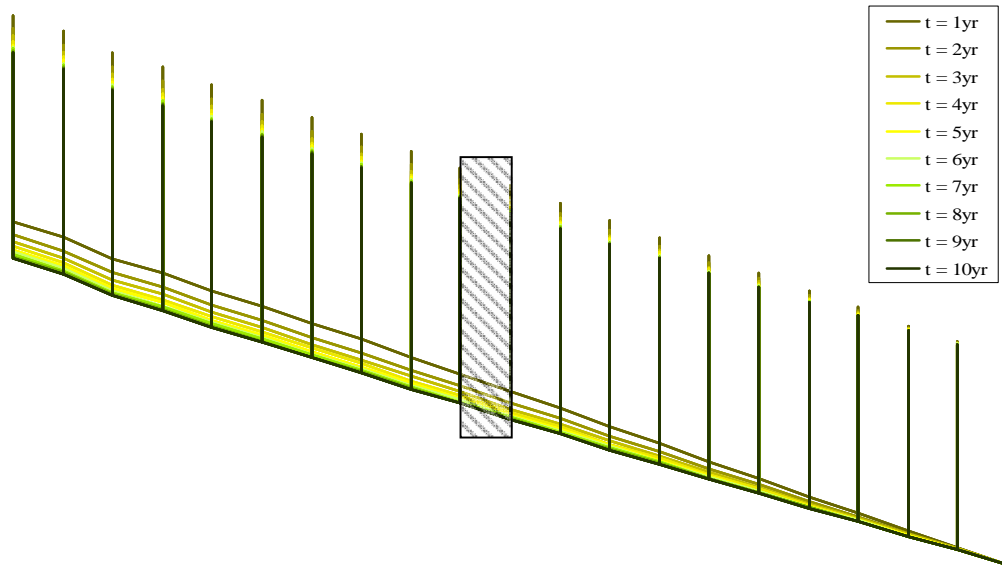


**Figure 7.6 Self-organisation of bed elevations for scenario 2 at the reach scale. Self-organisation at the channel-type scale is shown for the hatched section in Figure 7.9**

The resulting bed slope affects the flow depth, which determines the maximum potential reed biomass that can possibly grow at a given elevation as shown in Figure 7.7. The available reed habitat on the bank determined by the reach scale reed model is given as the maximum potential reed biomass that can grow at a given elevation on the river bank. The reach scale reed model therefore determines how the reeds could expand, which in turn affects how sediment at the channel-type scale organises. Simulating the growth of reeds at the geomorphological-unit scale allows determination of the properties of higher-level reed patches so that population distribution patterns emerge. The kinks at the upstream ends of the reaches are due to boundary conditions which affect the flow model used to predict the monthly flow depths for the reed model.

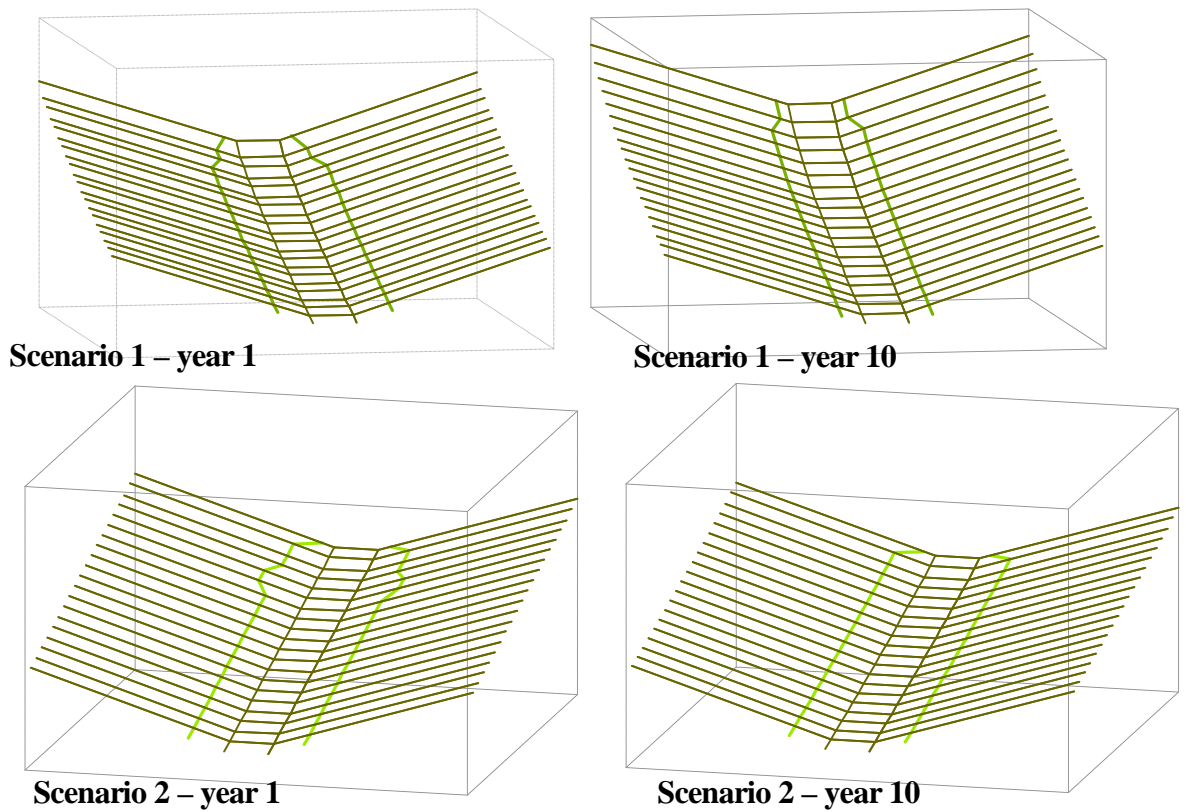


**Figure 7.7 The available reed habitat on the river bank lying on the entire area above the green line determined by the reach scale reed model for scenario 1 and 2**

Within the 100 by 100 m modelling domain representing the river at the channel-type scale, the process models describe interactions between water and sediment for every 5 by 5 m cell. Figure 7.8 and Figure 7.9 show that, as with bed elevations at the reach scale, the constant sediment and water inflow for the 30 minute event results in bed elevation changing towards a self-organized state. The bed elevations changed rapidly initially and slowed down to change much less from 15 to 30 minutes. The 2-D river flow was updated every 5 minutes, adjusting to the changing bed elevations to reach a steady state.

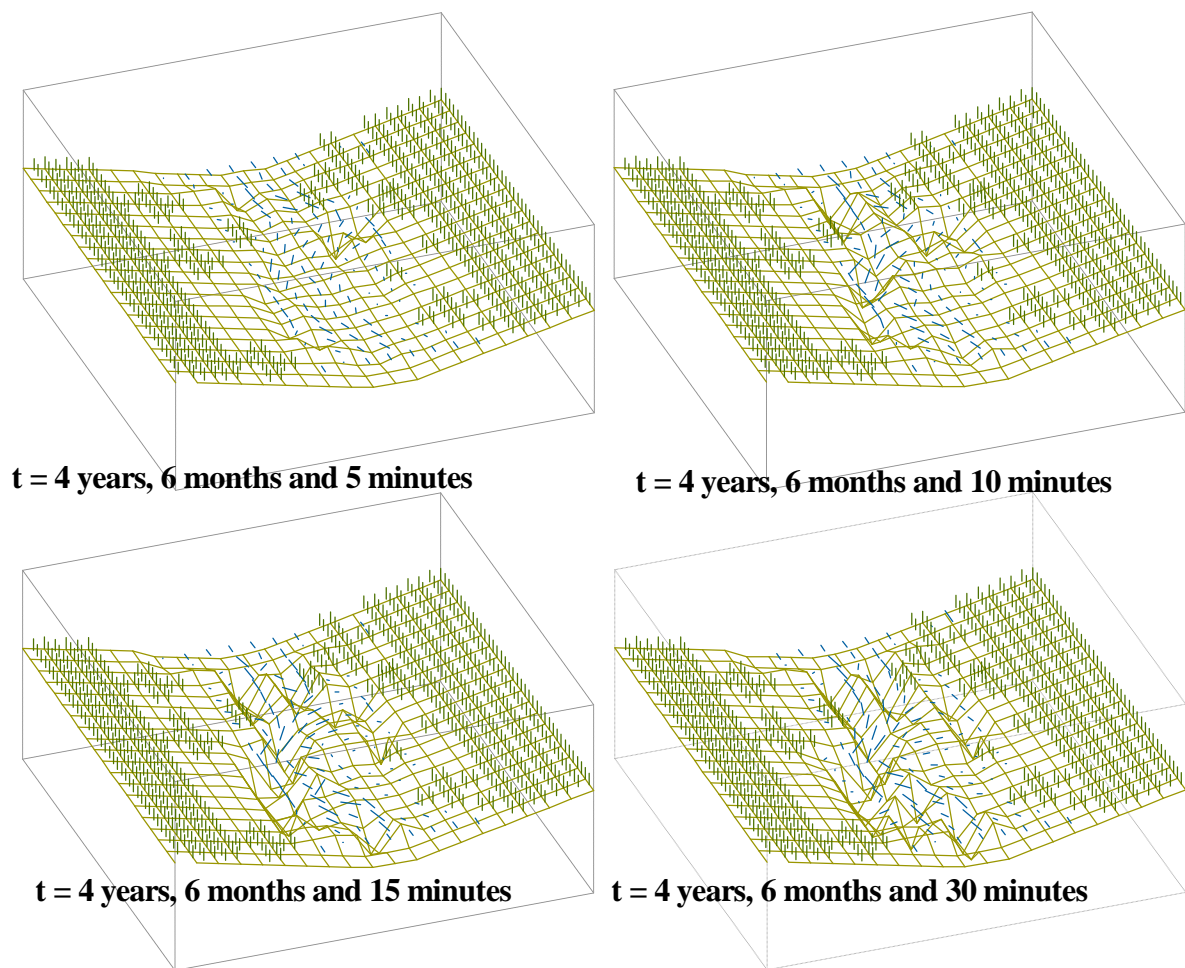


**Figure 7.8 Self-organisation of bed elevation for scenario 1 at the channel-type scale. The river between 900 m and 1000 m is shown for a 30 minute flood event beginning at 4 years and 6 months. The blue lines indicate the velocity vectors of the water flow and are placed at the water surface**

The lower-level self-organisation affected the higher-level self-organisation through material (sediment, water and biomass) flow, which implies the existence of emergent structures. More specifically, the smaller scale processes such as reed growth and bed-form development, which determine flow resistance, produce emergence. Following from the water flow models at lower levels, shear stress resisting water flow is aggregated at the reach scale, producing new Manning's  $n$  values. These new Manning's  $n$  values affect reach scale water flow and therefore reach scale sediment flow. The resulting water flow depth and velocity are transferred as boundary conditions to smaller scale models to again affect the shear stresses resisting water flow at these smaller scales.



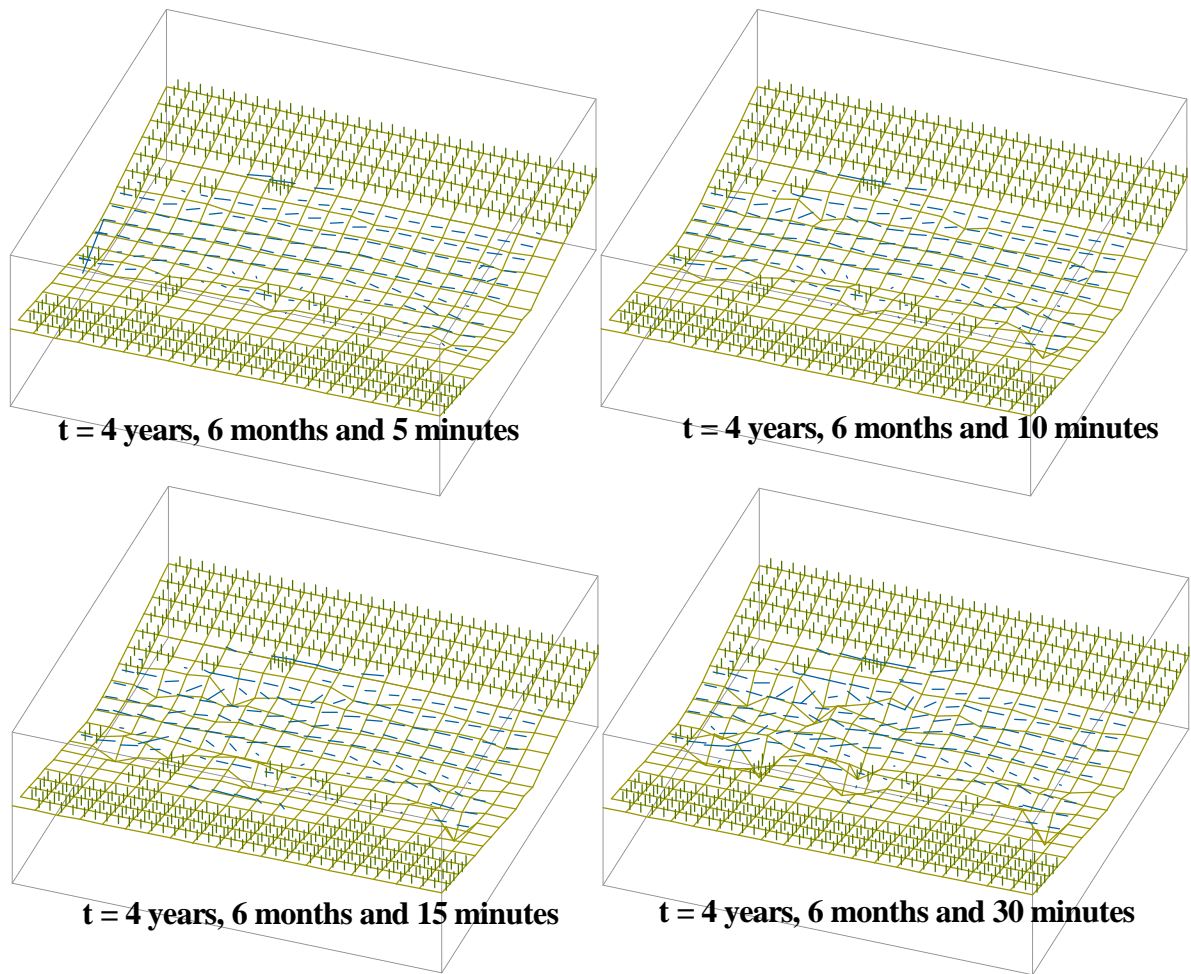


**Figure 7.9 Self-organisation of bed elevation for scenario 2 between 900 m and 1000 m beginning at 4 years and 6 months**

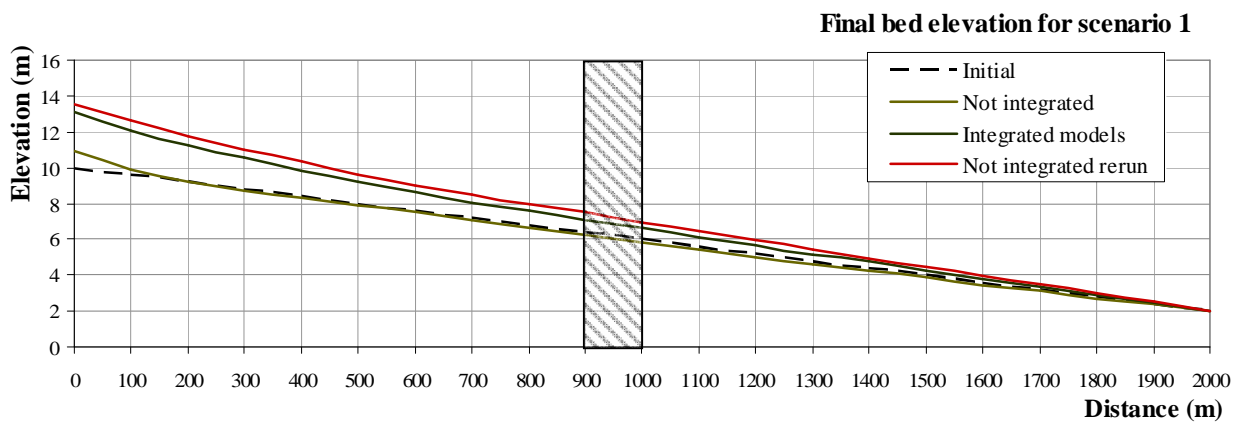


**Figure 7.10 Initial and 10 year reach scale bed elevations for scenario 1 with and without integrated smaller scale models. Details of the modelling results at the channel-type scale are shown for the hatched section in Figure 7.12**

Figure 7.11 shows Manning's  $n$  values determined from lower organisational level modelling with an initial Manning's  $n$  of 0.029 for gravel-bed rivers obtained in literature. The increased reed cover is shown in Figure 7.12, Figure 7.15 and Figure 7.19 is generally associated with increased flow resistance.

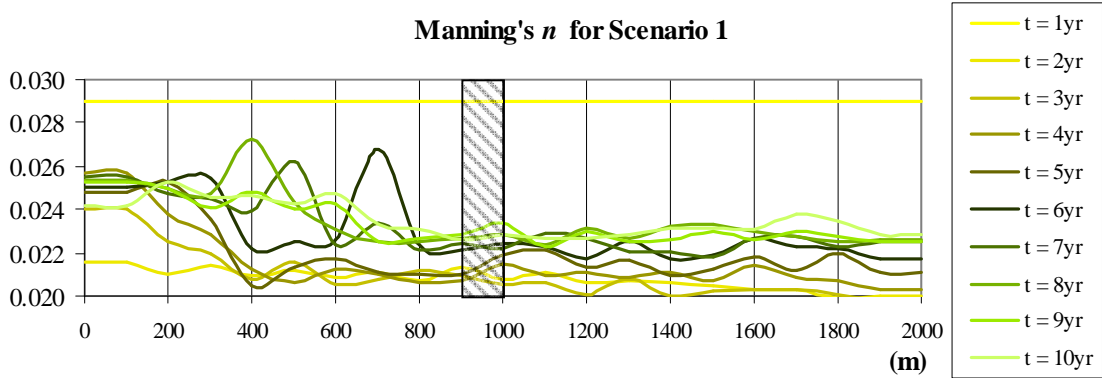


**Figure 7.11 Reach scale Manning's  $n$  values along the river after every year for scenario 1 obtained from integrated smaller scale models. Details of the modelling results at the channel-type scale are shown for the hatched section in Figure 7.12**

The increasing reed cover resulted in increasing flow resistance, which in turn increases the shear stress opposing water flow at the channel-type scale and manifests as larger Manning's  $n$  values at the reach scale. The larger Manning's  $n$  values results in water backing up, producing different flow conditions at the reach scale, which in turn provides the boundary conditions for flow modelling at the channel-type scale. The emergence of flow resistance at the reach scale is therefore a result of constant feedback from lower-level models.

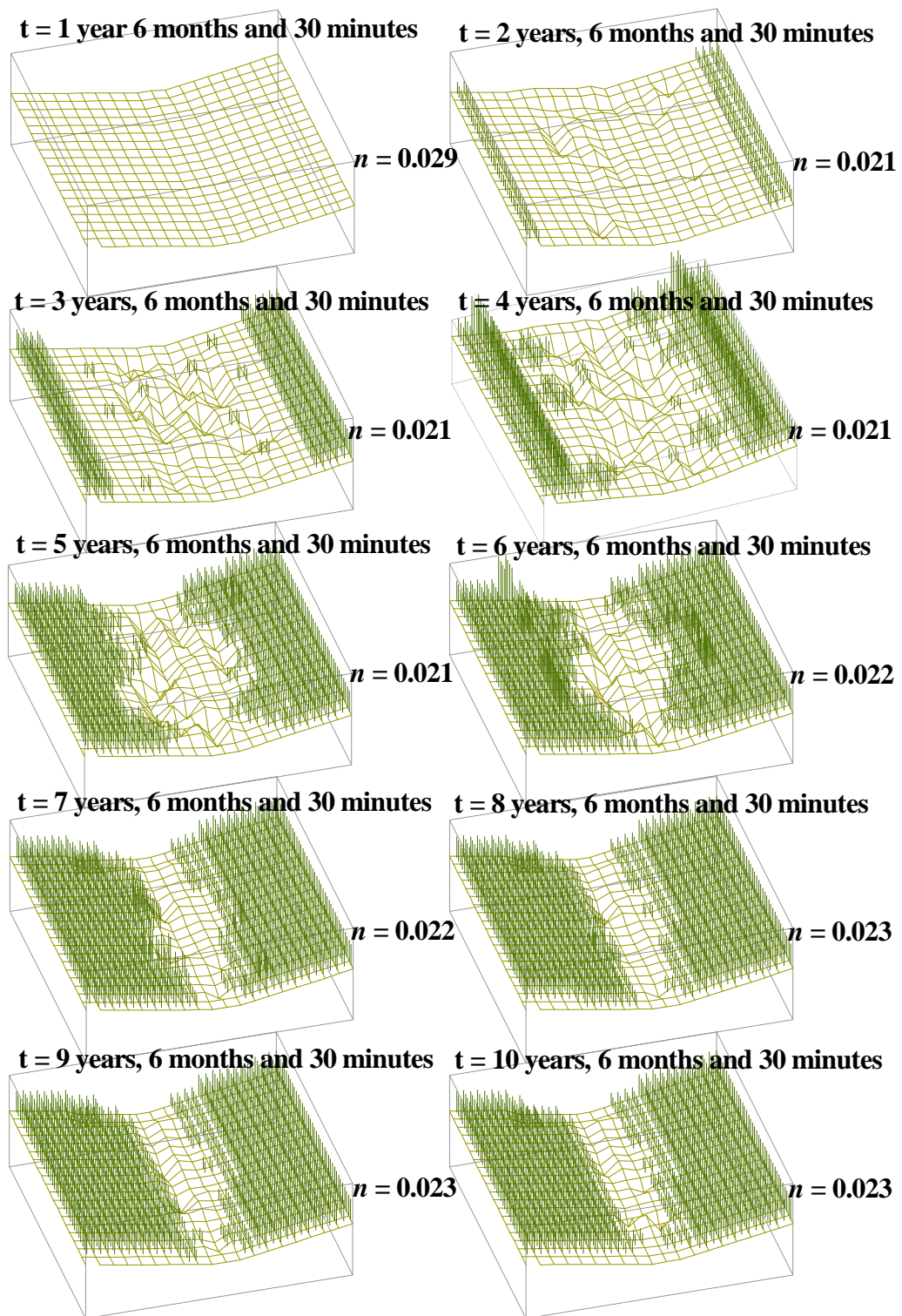
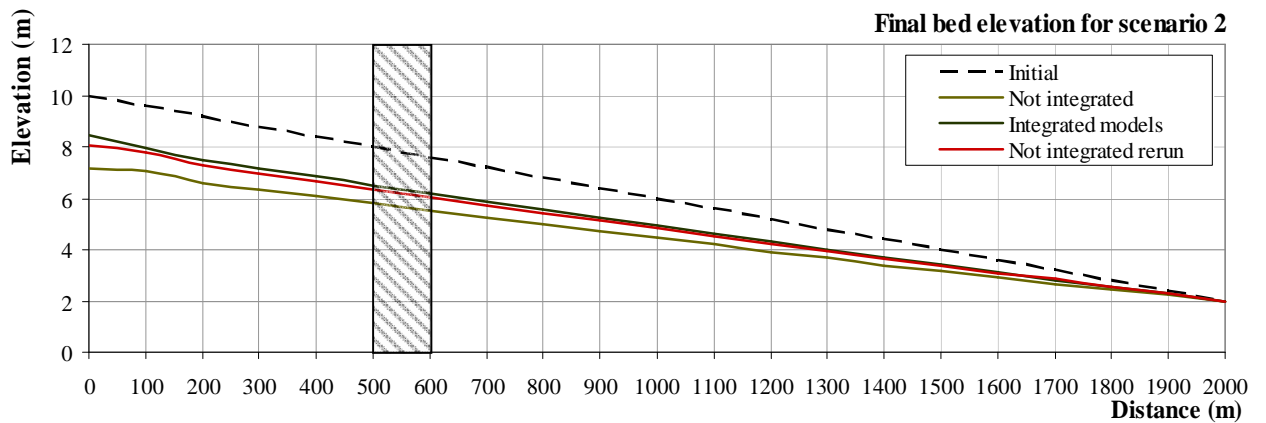


Figure 7.12 The yearly modelled river between distance 900 m and 1000 m for scenario 1

Variability in the water flow distribution forced by varying sediment bars, reeds and bedrock at the cross-sections produce variable Manning's  $n$  values. This is especially evident for scenario 3, where significantly larger Manning's  $n$  values resulted at the top of the reach (0 to 700 m) where bedrock outcrops are higher and larger.

Figure 7.13 also shows a large difference in the bed elevation obtained after the 10 year modelling period. Figure 7.14 shows the adjusted Manning's  $n$  values for scenario 2 at the reach scale, which was obtained from integrated smaller scale models.



**Figure 7.13 Initial and 10 year bed elevations for scenario 2 with, and without integrated smaller scale models. Details of the modelling results at the channel-type scale are shown for the hatched section in Figure 7.15**

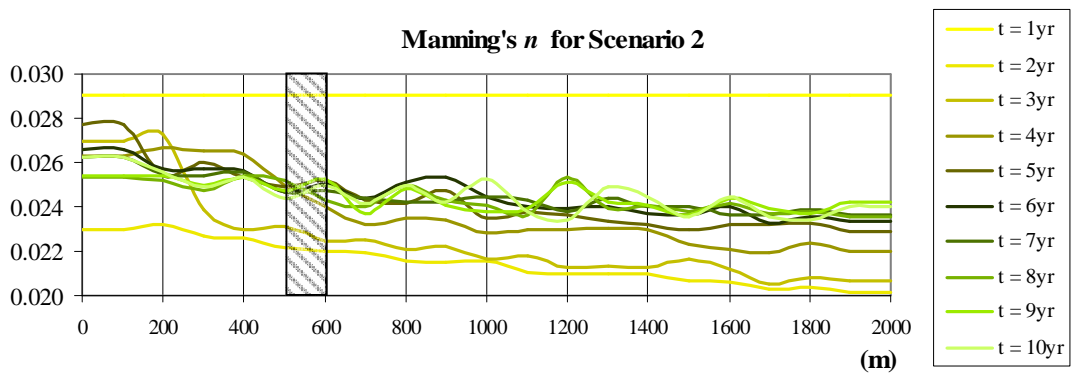


**Figure 7.14 Reach scale Manning's  $n$  values for scenario 2 obtained from integrated smaller scale models. Details of the modelling results at the channel-type scale are shown for the hatched section in Figure 7.15**

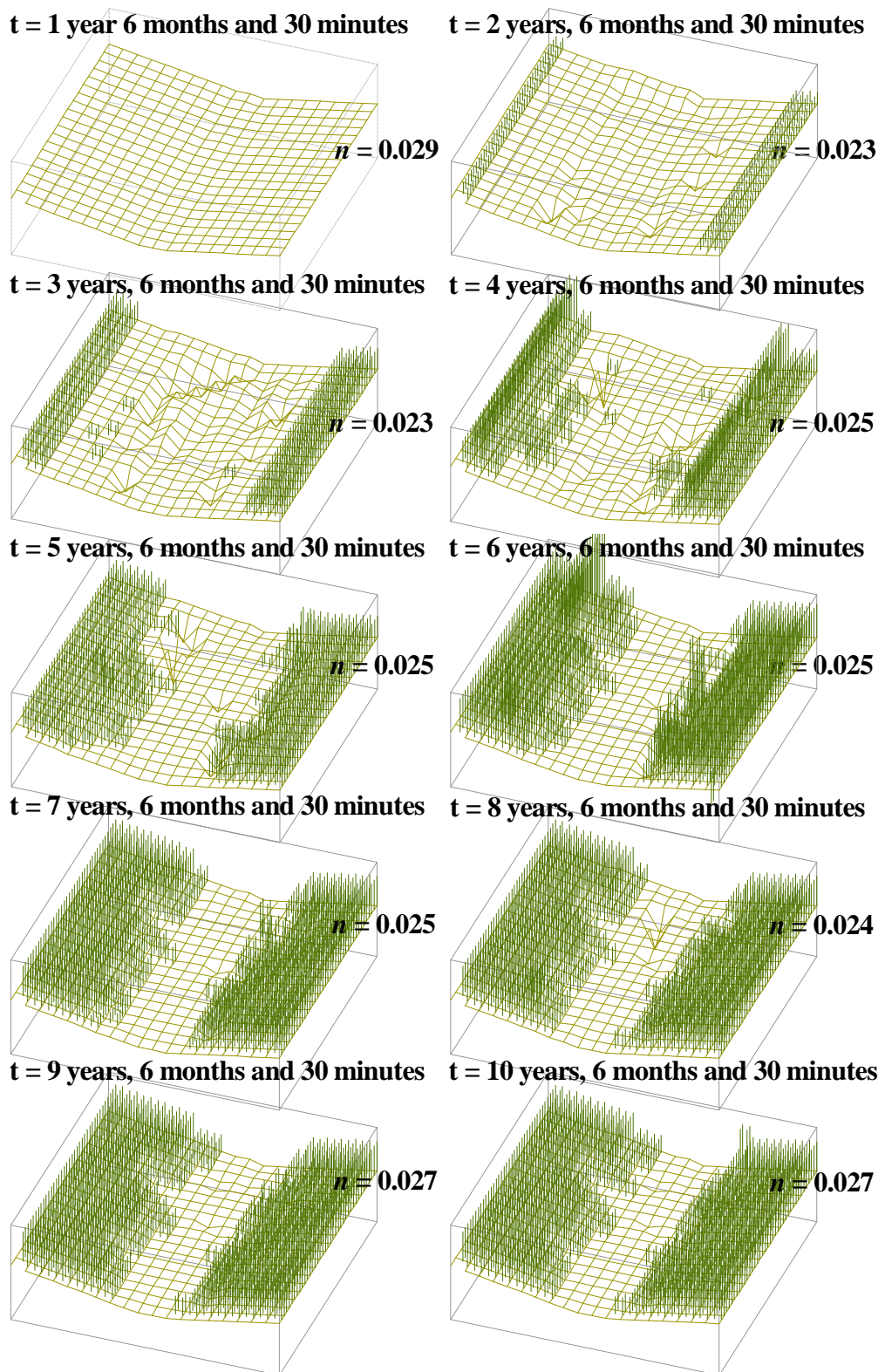
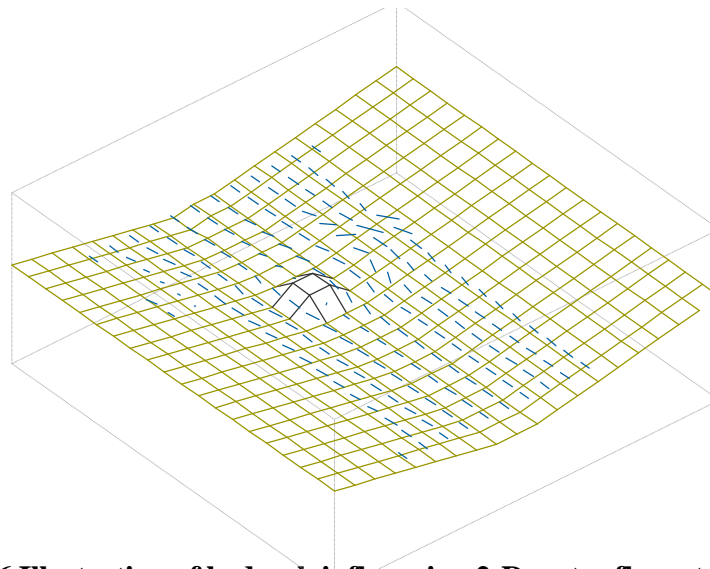


Figure 7.15 The yearly modelled river between distance 500 m and 600 m for scenario 2

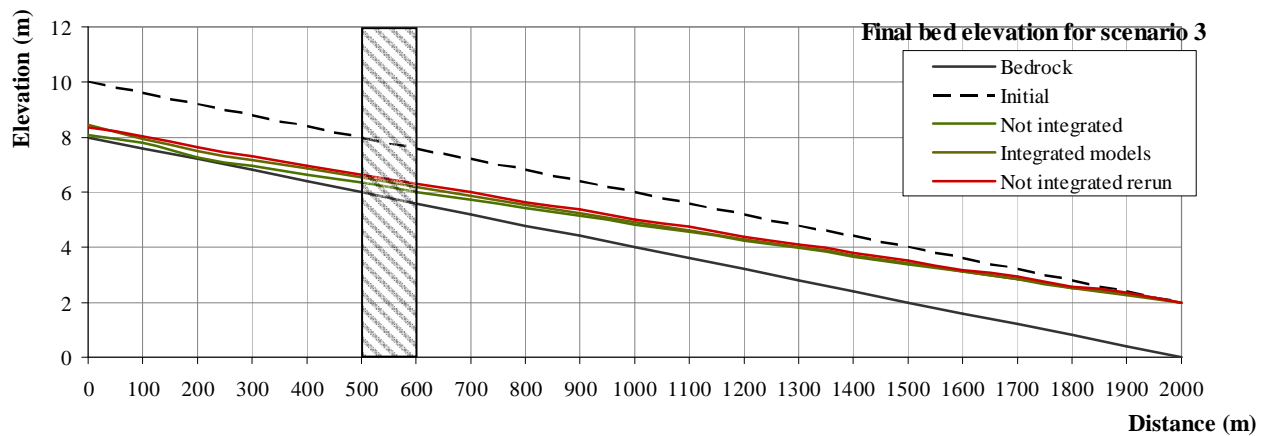
The modelling accounts for the self-organisation of bed-forms from initial geometry to geometry following the flood event. Bed-form sizes have been determined for each of the cells within the sediment model at the channel-type scale. The bed-forms were allowed to grow towards their equilibrium sizes throughout the storm event to affect the equivalent roughness or  $k_e$  values, which affects the flow distribution at the channel-type scale. The non-linear effect of increasing bed-form size on shear stresses resisting water flow in turn affects organisation of the bed elevation at the channel-type scale.

Changes in the water flow distribution affected bed-form size in such a way that bedrock, reeds and river bed elevation changes all contributed. Figure 7.16 shows scenario 3 with bedrock influencing water flow at the channel-type scale.

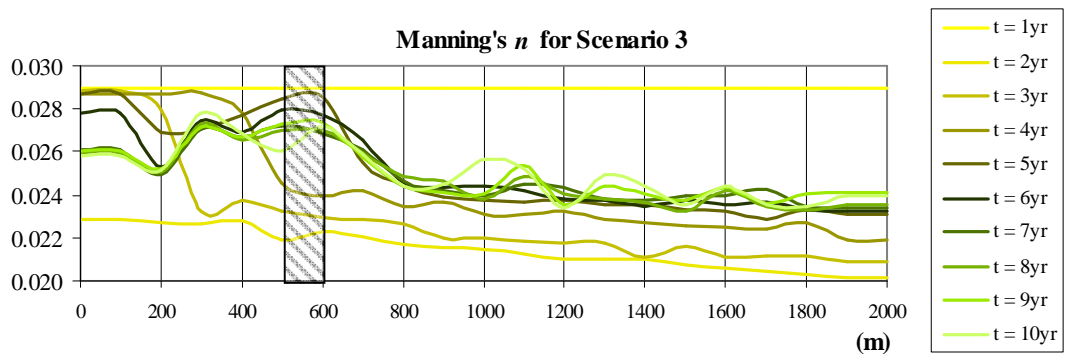


**Figure 7.16 Illustration of bedrock influencing 2-D water flow at the channel-type scale. The modelled river between distance 500 m and 600 m for scenario 3 is shown**

Figure 7.17 shows the results of simulations with and without integrated smaller scale models for scenario 3. No significant difference in the bed elevation at the reach scale was obtained after 10 years. The bedrock constrained any significant difference in bed elevation. Figure 7.17 shows the bedrock below the bed because it is outcropping locally above this level. Figure 7.18 shows Manning's  $n$  values which are larger in the upstream part of the river owing to bedrock influence being more pronounced.

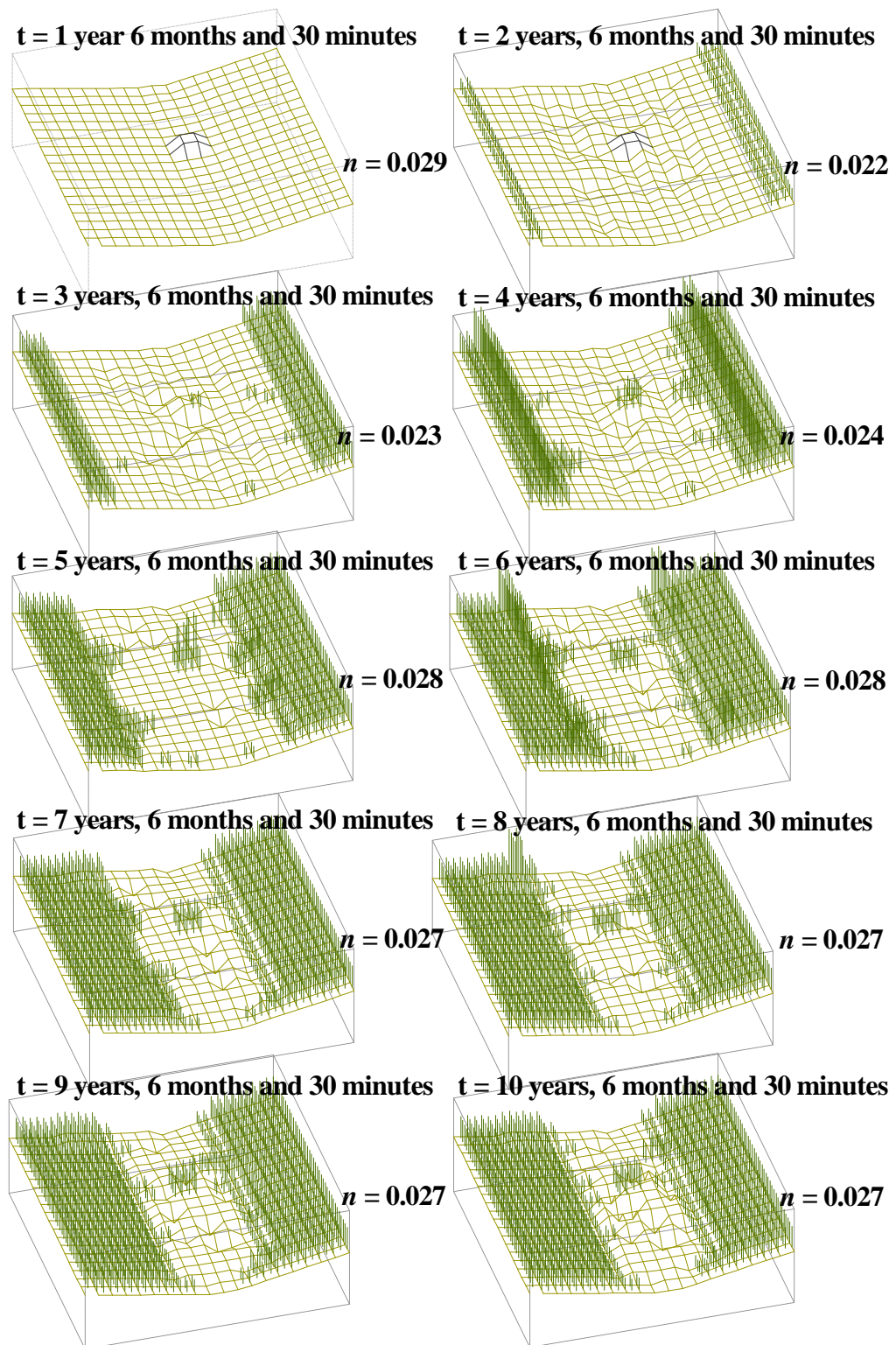


**Figure 7.17** Initial and 10 year bed elevations for scenario 3 with, and without integrated smaller scale models. Details of the modelling results at the channel-type scale are shown for the hatched section in Figure 7.19



**Figure 7.18** Reach scale Manning's  $n$  values for scenario 3 obtained from integrated smaller scale models. Details of the modelling results at the channel-type scale are shown for the hatched section in Figure 7.19

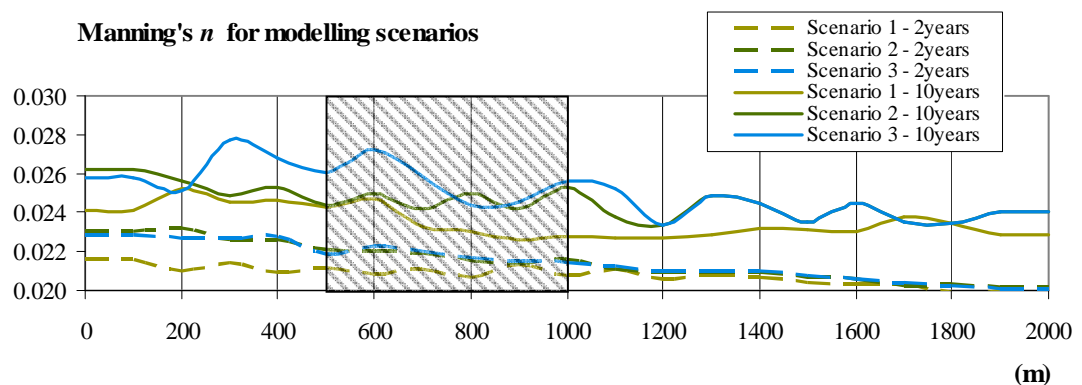
Figure 7.19 illustrates how changing Manning's  $n$  values at the reach scale correspond to the changing geomorphology at the channel-type scale as affected by bedrock. The effect of bedrock is distinct in the way sediment and reeds, at the channel-type scale, are organised in Figure 7.22 and Figure 7.24. This distinction appears in the Manning's  $n$  values at the reach scale obtained. The effect of bedrock is illustrated in scenario 3, producing a wider, shallower river configuration. The difference in scenario 1 lies in the reeds that are encroaching more on the river channel and causing the channel to become more incised.



**Figure 7.19** The yearly modelled river between distance 500 m and 600 m for Scenario 3

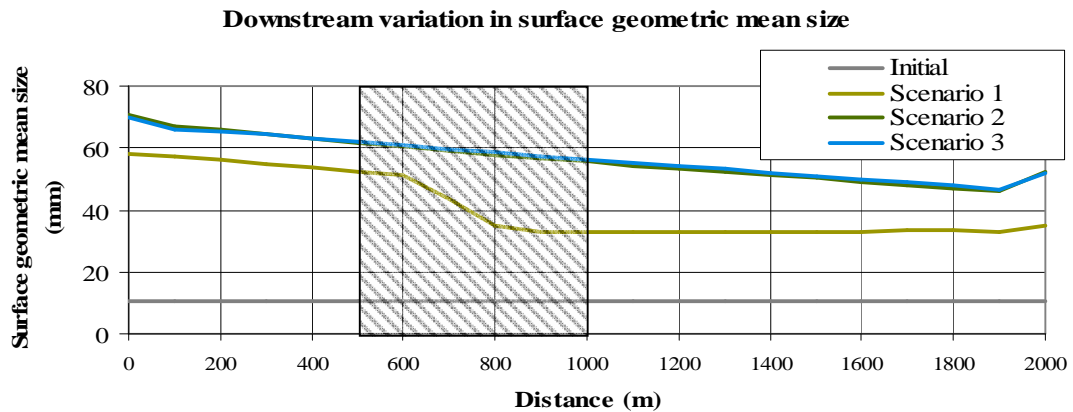


Figure 7.20 shows that all scenarios produced general increases in Manning's  $n$  from year 2. Reeds and bed-form size have increased. The resulting increase in shear stresses resisting flow at the channel-type scale was aggregated at the reach scale to present larger Manning's  $n$  values. Flow continuity at the channel-type scale was not strictly preserved. The flow resistance formulations accounting for reeds that were implemented in the 2-D water flow model resulted in flow being slightly less than that set out by the boundary conditions supplied by the 1-D flow model. This difference in water flow is increased as the flow velocities are reduced with greater reed cover. Preservation of flow continuity is expected to yield increased flow velocities and shear stresses in areas of little or no reed cover. Thus, the magnitudes of Manning's  $n$  values obtained may have been larger.



**Figure 7.20 Reach scale Manning's  $n$  values for all the modelling scenarios after year 2 and year 10. The scenarios gave significantly different Manning's  $n$  values. Details of the modelling results at the channel-type scale are shown for the hatched section in Figure 7.22, Figure 7.23 and Figure 7.24**

The Manning's  $n$  values for scenario 2 and 3 were larger than for Scenario 1, since different flow patterns resulted from the influence of bed-forms, bedrock and reeds. Bed-form size depends on grain size, shown in Figure 7.21, and its effect on shear stress resisting water flow gives larger Manning's  $n$  values at the upper part of the reach where grain sizes are higher. In general, the reach is coarsening for all the scenarios because the fines are removed during flood events. This coarsening occurs at a much slower rate for scenario 1 because a larger amount of sediment was fed to the reach. Grain size for scenario 1 has not reached an equilibrium state, as indicated by the sudden decrease in grain size for reach distance 600 m to 800 m along the river reach.



**Figure 7.21 Downstream variation of  $D_{50}$  for modelling scenarios initially and for year 10. Details of the modelling results at the channel-type scale are shown for the hatched section in Figure 7.22, Figure 7.23 and Figure 7.24**

The similar grain-size distributions obtained for scenarios 1 and 2 show the connection between Manning's  $n$  and grain size. Grain size affects the dimensions of bed-forms and therefore also contributes to shear stress caused by the resistance to water flow. This effect is translated to reach scale modelling to affect the Manning's  $n$ .

Figure 7.22, Figure 7.23 and Figure 7.24 show the extent to which the river behaviour can differ for smaller sediment inflow and bedrock influence. It would not be easy to find a statistical up-scaling of flow resistance to account for the interactions of these smaller scale processes at larger scales, which requires detailed and explicit modelling.

The modelling cannot be verified because no data set exists for geomorphology over the wide range of spatial and temporal scales required for modelling verification. The aim is not to provide exact predictions of river bed elevations at precise positions, but to give the type of impact and order of magnitude, and the approximate type of spatial distribution. The focus is not on the models themselves but on demonstrating the effect of trans-scale interactions and whether the modelling can allow for self-organisation and emergence, which are necessary to achieve prediction that is accurate.

River bed elevation was predicted over a range of organisational levels which is important for river habitat management. The model can simulate 'what if' scenarios to examine the effect that management decisions have on habitat conditions at various resolutions.

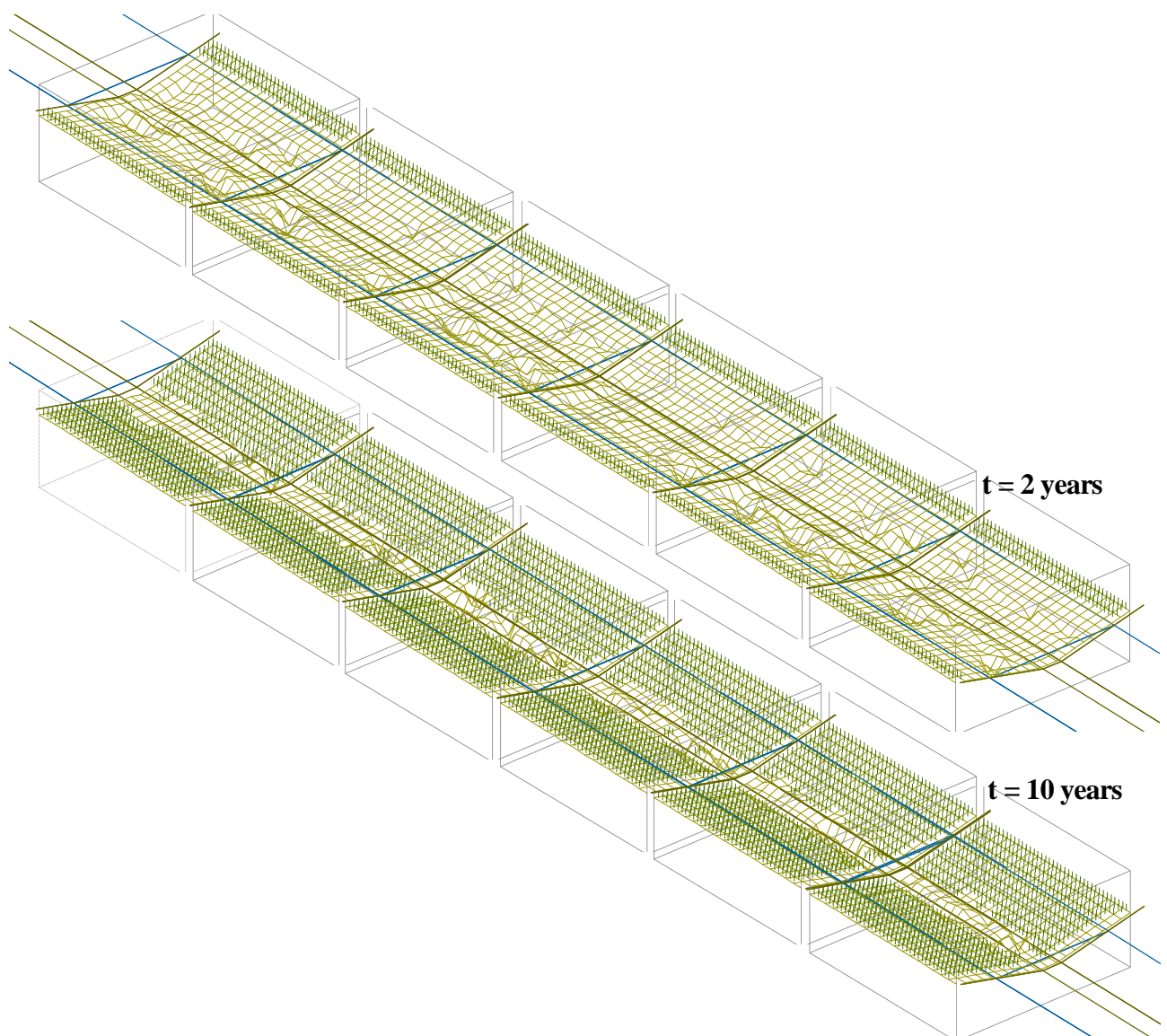


**Figure 7.22 The modelled river for scenario 1 between 400 m and 1000 m showing the template provided by the reach scale sediment model and flow depth provided by the reach scale water flow model**

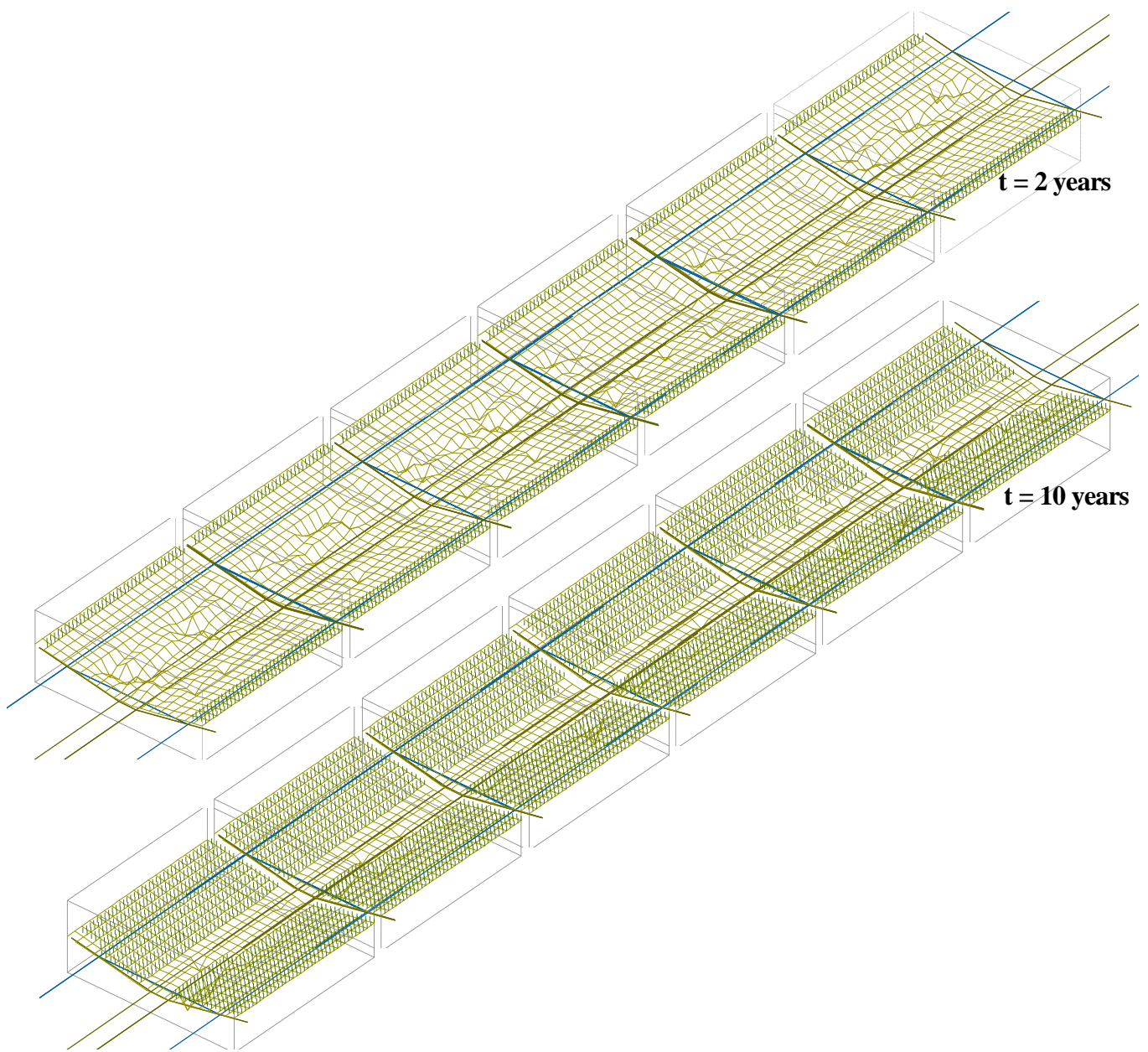


**Figure 7.23 Modelled river scenario 2 between 400 m and 1000 m**

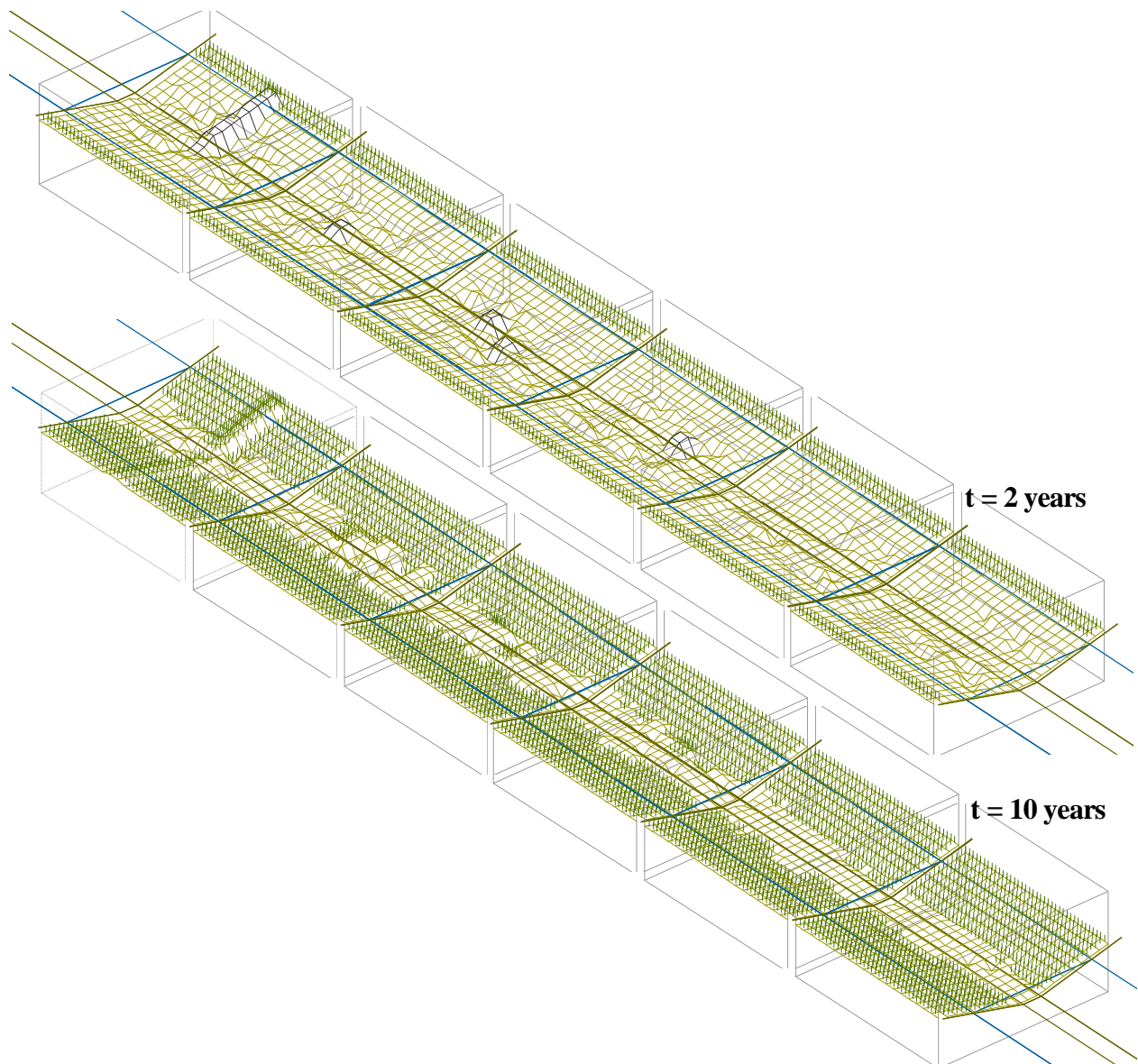


**Figure 7.24 Modelled river scenario 3 between 400 m and 1000 m**

Figure 7.8 to Figure 7.30 show the elevations of selected 100 m channel reaches as sediment self-organises. The associated reed height, water velocity and effective flow resistance height  $k_e$  distribution at the end of flood flow modelling of year 4 are shown. Eventhough the effective flow resistance height  $k_e$  remain similar throughout the flood flow modelling, its variability changes.

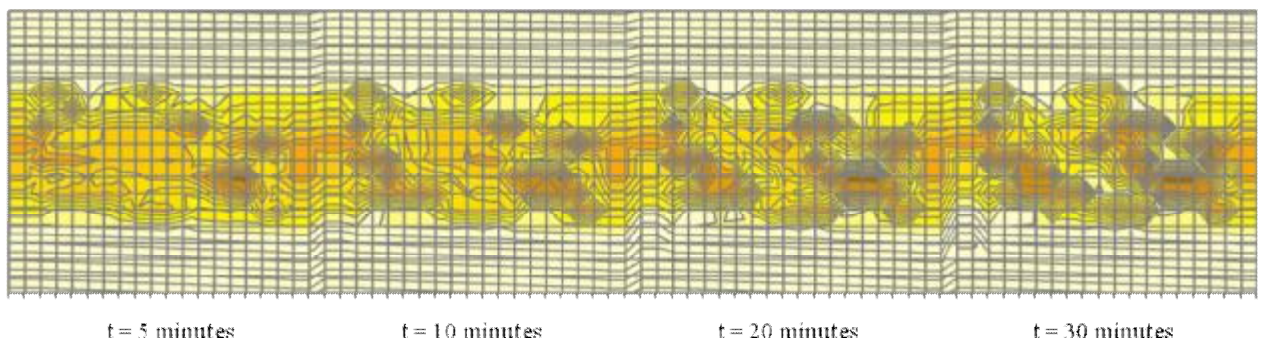
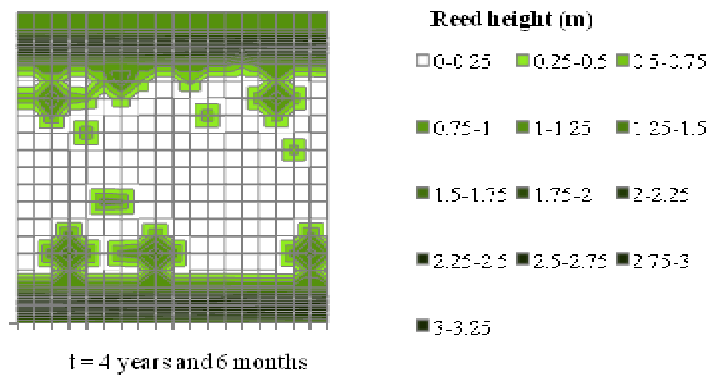


**Figure 7.25 Reed height (m) and bed elevation (m) distribution for the flood flow modelling of scenario 1 in year 4. The river between 900 m and 1000 m is shown.**

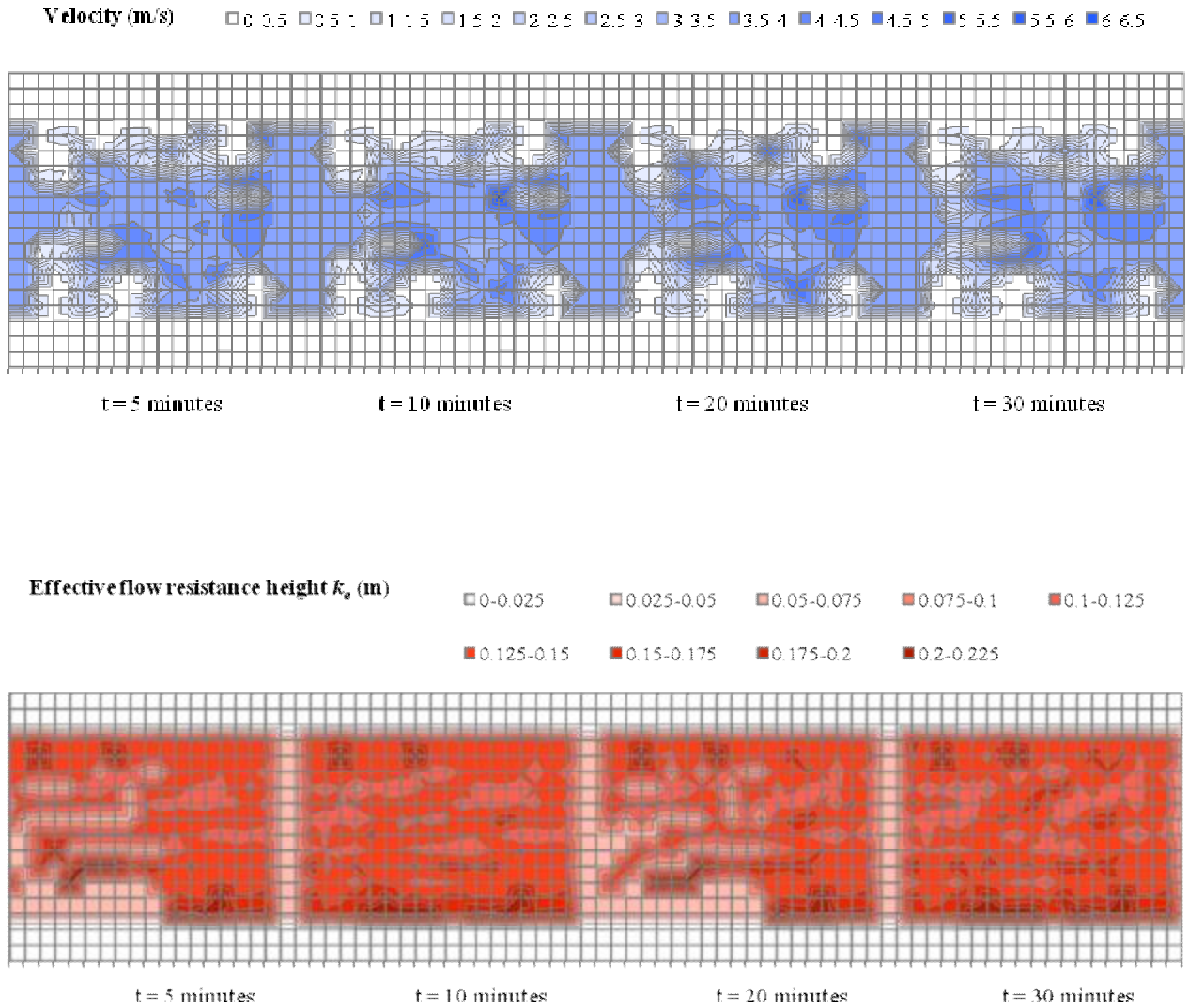


**Figure 7.26 Velocity (m/s) and effective flow resistance height  $k_e$  (m) distribution for the flood flow modelling of scenario 1 in year 4. The river between 900 m and 1000 m is shown.**

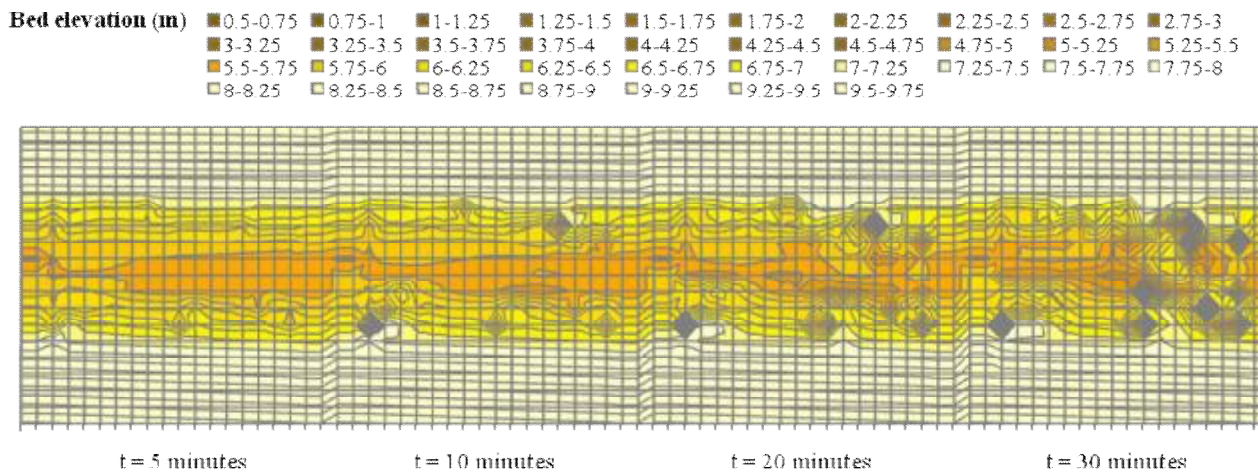
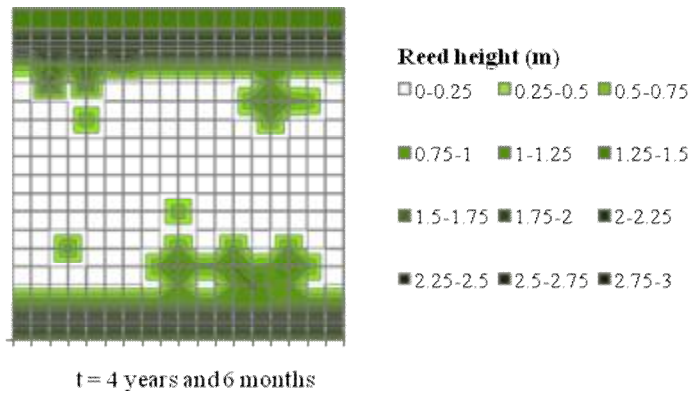


**Figure 7.27 Reed height (m) and bed elevation (m) distribution for the flood flow modelling of scenario 2 in year 4. The river between 900 m and 1000 m is shown.**



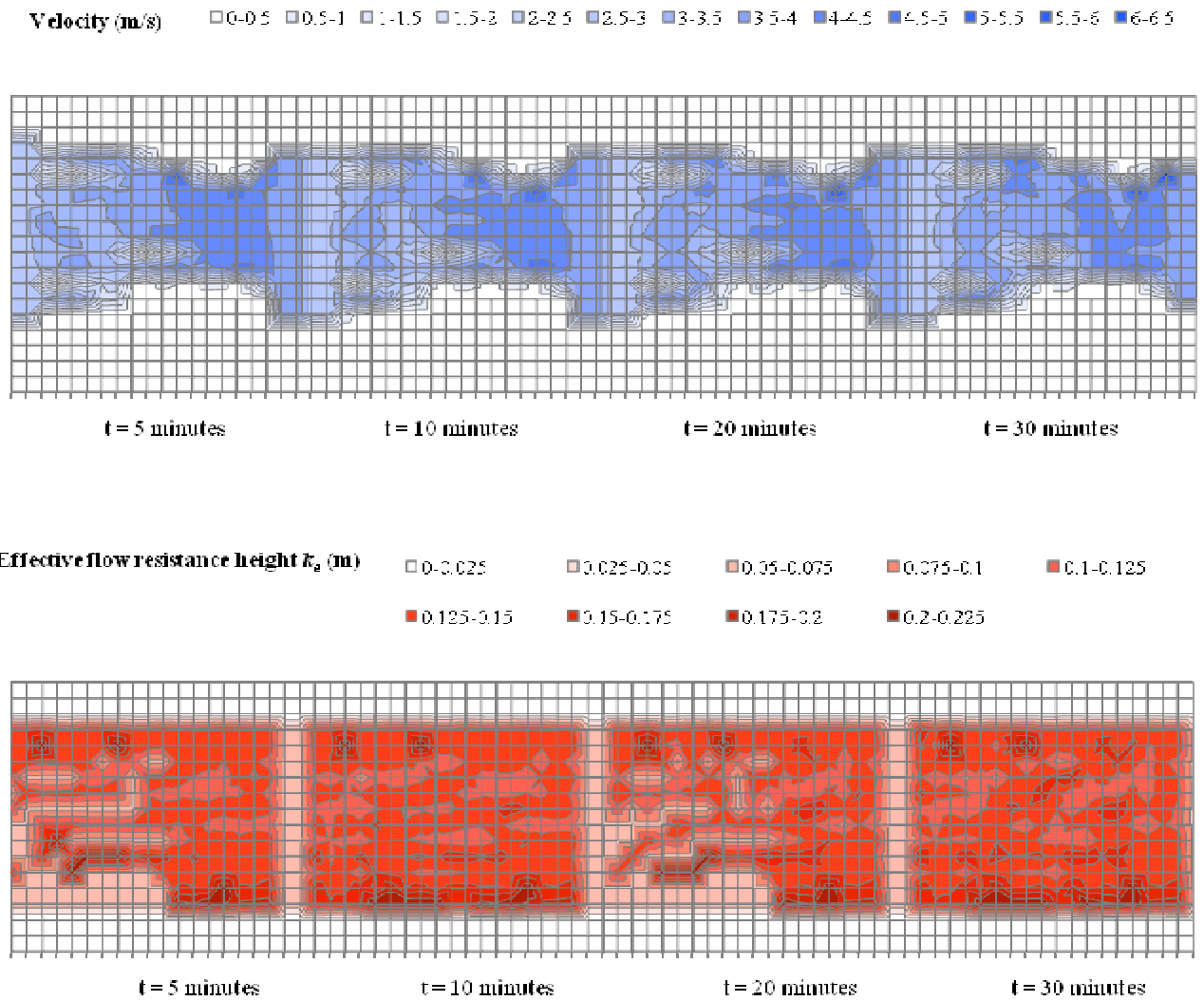


**Figure 7.28 Velocity (m/s) and effective flow resistance height  $k_e$  (m) distribution for the flood flow modelling of scenario 2 in year 4. The river between 900 m and 1000 m is shown.**

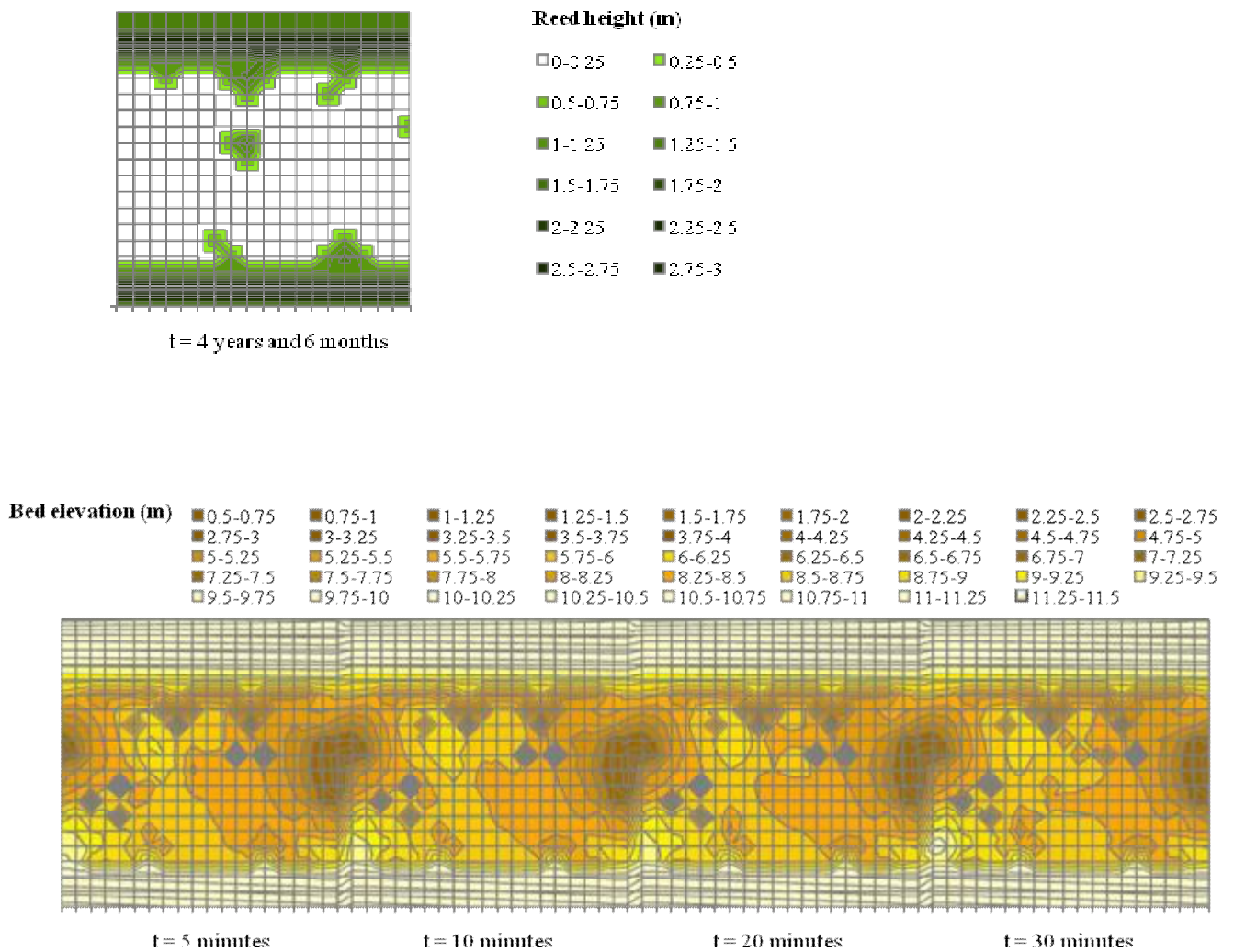
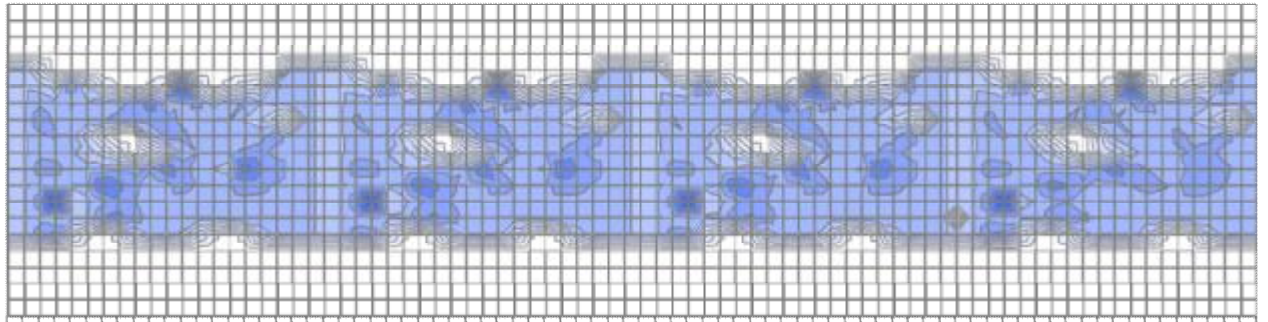


**Figure 7.29 Reed height (m) and bed elevation (m) distribution for the flood flow modelling of scenario 3 in year 4. The river between 500 m and 600 m is shown.**

Velocity (m/s)    0-0.5   0.5-1   1-1.5   1.5-2   2-2.5   2.5-3   3-3.5   3.5-4   4-4.5   4.5-5   5-5.5   5.5-6   6-6.5



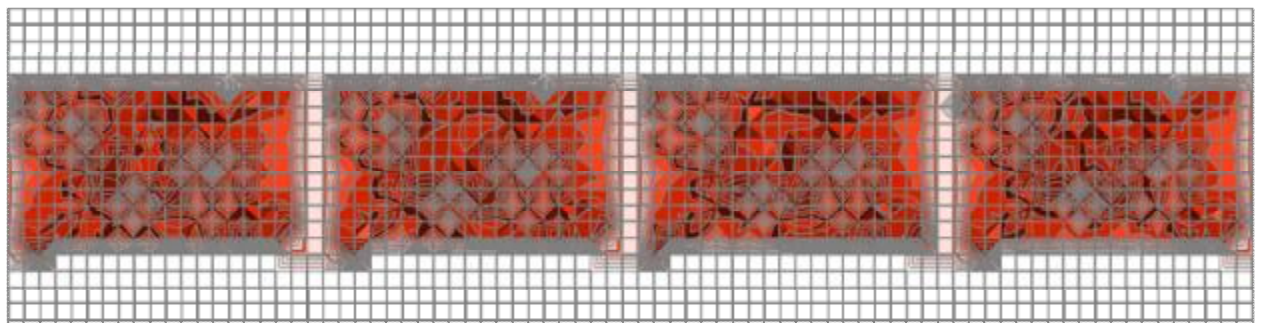
t = 5 minutes

t = 10 minutes

t = 20 minutes

t = 30 minutes

Effective flow resistance height  $k_e$  (m)    0-0.025   0.025-0.05   0.05-0.075   0.075-0.1   0.1-0.125   0.125-0.15  
 0.15-0.175   0.175-0.2   0.2-0.225   0.225-0.25   0.25-0.275   0.275-0.3  
 0.3-0.325   0.325-0.35   0.35-0.375   0.375-0.4   0.4-0.425



t = 5 minutes

t = 10 minutes

t = 20 minutes

t = 30 minutes

**Figure 7.30 Velocity (m/s) and effective flow resistance height  $k_e$  (m) distribution for the flood flow modelling of scenario 3 in year 4. The river between 500 m and 600 m is shown.**

To further the discussion on the findings of this study, it was compared to that of Hooke *et al.* (2005) who developed one of the most sophisticated contributions to river modelling at the time. The modelling simulated the interaction of flows with sediment and vegetation and the outcomes in terms of erosion, deposition, morphology, sediment cover, vegetation cover and plant survival at decadal time scales. Their modeling focused primarily on interactions at the channel-type scale (100 m channel reach).

Hooke *et al.* (2005) scaled down reach scale water flow modelling to the channel-type scale, by interpolating cross-sectional velocities to the cells in which vegetation were modelled. Similarly, catchment sediment loading was applied to each cell in order to determine erosion or deposition without routing sediment through the channel reach. The water flow modelling of Hooke *et al.* (2005) used Manning's  $n$  values from literature, which as shown above, may be different to those obtained from smaller scale modelling.

The following vegetation related processes were included in the modelling of Hooke *et al.* (2005) but not in modelling of this study:

- n Expansion of various vegetation groups (herbs, shrubs and phreatophytes);
- n Removal and burial of vegetation;
- n Substrate moisture modelling.

Hooke *et al.* (2005) used up scaled parameters for vegetation growth and stress processes allowing vegetation model application at the channel-type scale.

Hooke *et al.* (2005) included sediment size distribution at the channel-type scale through a 2 layer model by which a thin deposited layer is underlain by the original size of material. In this study, sediment size distribution is not modelled at the channel-type scale but rather scaled down linearly from the sediment size distribution produced at the reach scale. If sediment size distribution modelling at the channel-type scale were included in the modelling of this study, more realistic variability of the effective flow resistance height  $k_e$  and bed-form size would be achieved. These would impact on the Manning's  $n$  values determined at the reach scale.

Table 5.8 to Table 7.4 give the average bed-form length, bed-form height, skin shear stress, bed-form shear stress and effective flow resistance height  $k_e$  for selected 100 m channel reaches determined for the yearly flood flow modelling of all scenarios.

**Table 7.2 Average values for water flow and channel sediment attributes that impact on Manning's  $n$  values for scenario 1 between 900 m and 1000 m at various points in time**

Time	Average bed-form length (m)	Average bed-form height (mm)	Average shear stress $\tau_o$ (N/m <sup>2</sup> )	Average effective flow resistance height $k_e$ (mm)	Manning's $n$
t = 1 yr	1.79	64	57	106	0.029
t = 2 yr	1.98	79	42	125	0.021
t = 3 yr	2.00	72	28	127	0.021
t = 4 yr	1.84	63	38	127	0.021
t = 5 yr	2.02	65	55	122	0.021
t = 6 yr	1.97	60	39	127	0.022
t = 7 yr	1.94	58	84	120	0.022
t = 8 yr	1.93	69	56	112	0.023
t = 9 yr	1.93	53	79	116	0.023
t = 10 yr	1.95	53	97	118	0.023

Grain size for scenario 1 between 900 m and 1000 m remain similar throughout the simulation giving small change in the average bed-form size of the channel reach. The Manning's  $n$  values indicate no direct dependence on the the smaller scale water flow and channel sediment attributes. The variability of these attributes and the interaction of water flow with increased reed cover give rise to the increasing Manning's  $n$  values.

The modelling of Hooke *et al.* (2005) can simulate the effects of floods upon river form and the interaction with vegetation. However, the entire river is connected so that changes in one channel reach can affect adjustment in another, which in turn provides a feedback mechanism whereby the original river response predicted by Hooke *et al.* (2005) may be altered. At a decadel time scale, the boundary conditions to the modelling of Hooke *et al.* (2005) may therefore change considerably. For example, the initial response to base level lowering owing to a decrease in sediment load, as in scenarios 2 and 3, may lead to river degradation. This degradation leads to larger bed-forms because grain size and water depth increases. The modelling results given in

Table 7.3 and Table 7.4 show that these larger bed-forms add to the resulting larger Manning's  $n$  values. The larger Manning's  $n$  values amount to a decrease in water flow velocity which reduces degradation at the reach scale.

**Table 7.3 Average values for water flow and channel sediment attributes that impact on Manning's  $n$  values for scenario 2 between 900 m and 1000 m at various points in time**

Time	Average bed-form length (m)	Average bed-form height (mm)	Average shear stress $\tau_o$ (N/m <sup>2</sup> )	Average effective flow resistance height $k_e$ (mm)	Manning's $n$
t = 1 yr	2.01	73	67	149	0.029
t = 2 yr	2.23	86	71	154	0.021
t = 3 yr	2.44	100	56	196	0.023
t = 4 yr	2.40	104	55	184	0.023
t = 5 yr	2.71	124	89	250	0.025
t = 6 yr	2.77	138	101	196	0.025
t = 7 yr	2.85	118	125	261	0.025
t = 8 yr	2.89	118	89	219	0.024
t = 9 yr	2.94	114	93	254	0.027
t = 10 yr	2.94	119	100	256	0.027

**Table 7.4 Average values for water flow and channel sediment attributes that impact on Manning's  $n$  values for scenario between 500 m and 600 m at various points in time**

Time	Average bed-form length (m)	Average bed-form height (mm)	Average shear stress $\tau_o$ (N/m <sup>2</sup> )	Average effective flow resistance height $k_e$ (mm)	Manning's $n$
t = 1 yr	2.23	88	71	179	0.029
t = 2 yr	2.54	107	110	218	0.022
t = 3 yr	2.64	123	99	196	0.023
t = 4 yr	2.62	132	120	244	0.025
t = 5 yr	2.93	184	147	306	0.028
t = 6 yr	2.97	204	129	196	0.028
t = 7 yr	3.07	236	160	304	0.027
t = 8 yr	3.06	221	112	306	0.027
t = 9 yr	3.01	203	126	277	0.027
t = 10 yr	2.94	199	91	286	0.027

Degradation of the river at the reach scale, as in scenarios 2 and 3, increases the sediment inflow at the channel-type scale. The sediment transport rates simulated at the

reach scale is shown in Figure 7.31 to Figure 7.33. The channel-type scale sediment model uses these rates for the upstream sediment inflows.

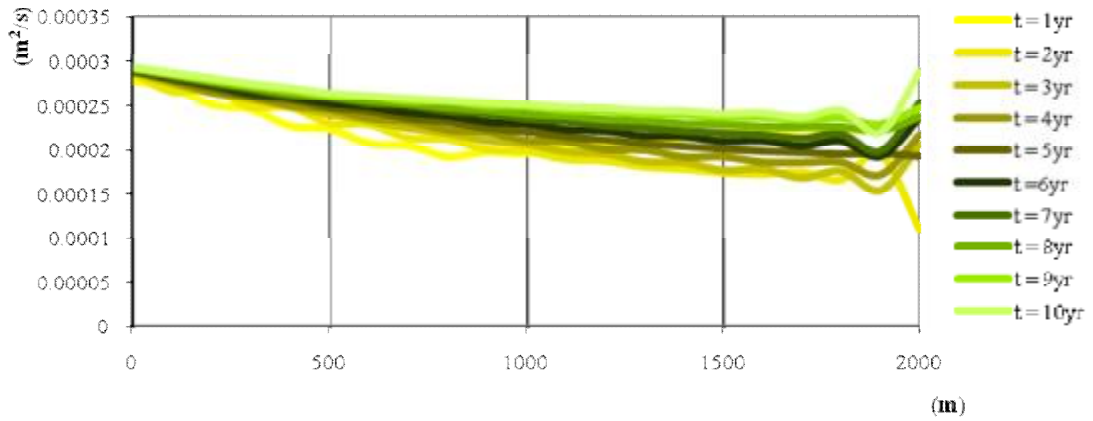


**Figure 7.31 Reach scale sediment transport rates along the river after every year for scenario 1**

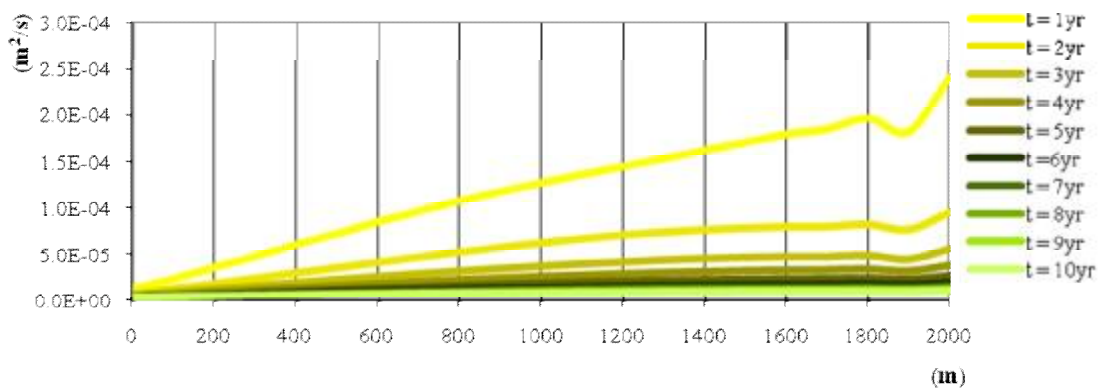


**Figure 7.32 Reach scale sediment transport rates along the river after every year for scenario 2**

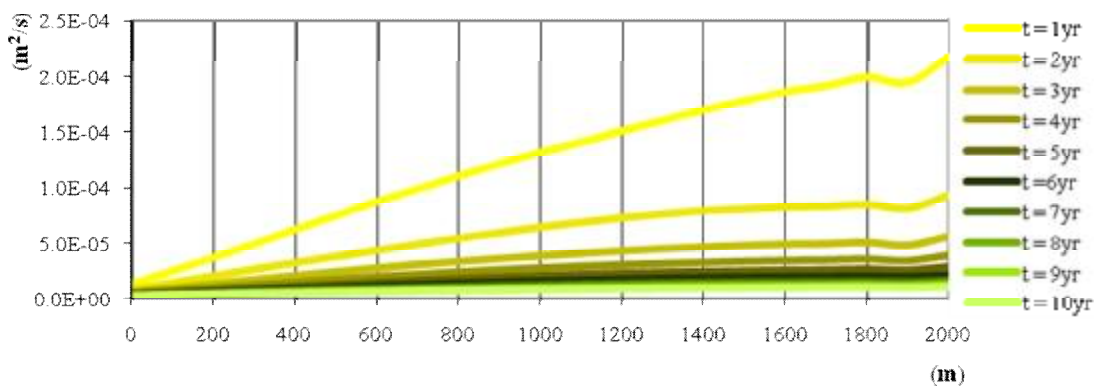


**Figure 7.33 Reach scale sediment transport rates along the river after every year for scenario 3**

The increased sediment inflow at the channel-type scale coupled with the slope flattening owing to the past degradation, result in sediment build up at the same organisational level. Sediment build up at the channel-type scale will in turn impact on sediment bar dynamics and therefore vegetation distribution. Such multiple responses is referred to as complex response (Schumm, 1977) which requires the inclusion of contributions from processes at various organisational levels. The hierarchical strategy presented in this study allows for precise contributions of each of these processes to be included in modeling river adjustment. Modelling the interaction of these processes coupled with the potential to deal with complex response makes effective river management achievable.

### **7.3 Conclusion**

Simulation included the interaction of channel components including sediment, water, reeds and bedrock at various organisational levels. The effect of sediment size and frequency of the flood event moving sediment, together with typical channel geometry, is provided for the scenarios chosen for modelling.

The sediment feed rate specified for scenario 1 was much higher than that for scenarios 2 and 3. Decreases in sediment feed rates occur, for example, after the construction of a dam. Dams also affect flow discharges but the effect on river geomorphology has not been considered in this study because of the computational cost of the modelling. It may, however, be expected that larger flows would be required to transport larger amounts of sediment going into the river system. Thus, larger flows may have an effect on geomorphology similar to that of lower sediment feed rates.

Emergence was indicated by the channel aggrading more for modelling with, than without the inclusion of the effect of smaller scale river process interactions. Emergence was also found in changing flow resistance to affect the river bed elevation at the reach scale. The changing flow resistance resulted from small-scale processes such as water flow affected by bed-forms or reeds. Bed-forms and reeds affected the energy loss to a large extent and provided a strong coupling between the flow and the river bed elevation.



Up-scaling using statistical formulations to account for small-scale models may, as shown above, not be suitable for dealing with river complexity for decadal prediction because interacting processes may greatly influence river dynamics at larger scales. The non-linearity of the effects of small-scale processes necessitates hierarchical modelling, as opposed to providing a statistical account at the larger scale. Smaller scale processes such as sediment bar development and reed expansion have to be modelled explicitly in order to allow for the non-linearity produced by these process interactions which, as substantiated by Chapter 2, is the requirement for dealing better with river complexity.

Reliable estimation of Manning's  $n$  values is required for realistic prediction of the river bed elevation at the reach scale. At the reach scale, the Manning's  $n$  values include the resistance to water flow caused by the bed characteristics, bar forms and reed cover at smaller scales. The Manning's  $n$  values are strongly dependent on the roughness formulations used in the smaller scale modelling. The accuracy of these flow resistance formulations is crucial because they affect the shear stresses opposing the water flow which is subsequently used in determining the Manning's  $n$  values. Smaller than expected Manning's  $n$  values obtained in the modelling could be attributed to flow continuity that was not strictly preserved across organisational levels.

Analysis showed that the flow resistance has a significant effect on the river bed elevation at reach scale. The use of a Manning's  $n$  value of 0.029 along the reach yielded significantly different bed elevations in comparison with the use of the final Manning's  $n$  values obtained from integrated smaller scale modelling. The determination of Manning's  $n$  values throughout the simulation is essential because the bed characteristics, bar forms and reed cover, which affect the Manning's  $n$  values, constantly undergo changes during simulation. The Manning's  $n$  values influence the rates at which smaller scale processes adjust and hence also the distributions of water, sediment and reeds. These distributions, therefore, affect and are affected by the Manning's  $n$  values. These distributions emerge as the habitat which is of interest to river managers. Therefore, the habitat predicted over decades using Manning's  $n$  values that are not determined from smaller scale modelling is questionable.

The hierarchical modelling approach proposed in this study could allow collaboration across disciplinary boundaries. Detailed qualitative and quantitative models existing in many fields of study can be integrated using such a hierarchical modelling strategy. It

is suggested that this modelling framework could be applied to a variety of complex adaptive systems (CAS) on earth. These earthly systems connect life whereby one system emerges to others. Models of low-level fast processes and high-level slow processes that are detailed to each specialty field may slot into one another by confirming rates and providing boundary conditions for material flows.

The continued improvement in computing power would decrease constraint placed on the number of organisational levels that may be included in the modelling. At the same time, greater demands will be placed on the data requirements of such integrated modelling systems. Real world data-sets that encompasses the perspectives of all considered organisational levels will be required for validation of both individual process models and integrated modelling. Regardless of the model integration used, the limitations of an individual model and their subsequent inherent uncertainties with respect to predicting the behavior of these complex systems, should be recognized. Such considerations are critical in the future development of CAS modelling to cope with issues and problems associated with human-environment interactions.

Hierarchical modelling allows more realistic prediction of river geomorphology after a decade since emergence and self-organisation is dealt with. The modelling showed that incorporating emergent structures provides the basis for dealing with the non-linearity of river processes across organisational levels, assuming that the models are reliable as stand-alone models.

## Chapter 8 – Conclusion

---

The prediction of river geomorphology at a decadal time scale using modelling is essential for effective river management. Realistic model predictions at decadal time scales require smaller scale variability to be integrated into larger scale modelling. The variability is attributed to processes that can be hierarchically organised based on the spatial scales at which they operate. At a decadal time scale, the spatial scale that extends across the organisational levels of the reach scale, the channel-type and the geomorphological-unit scale, is deemed important. The small-scale variability caused by riparian vegetation growth, for example, influences reach scale river geomorphology at a decadal time scale. Trans-organisational feedback translates such variability to higher organisational levels but also constrains variability according to the limits imposed by patterns at higher organisational levels.

River processes affecting river geomorphology are complex in nature. The main drivers for river geomorphological change include sediment, water and vegetation processes. These processes produce patterns that affect river geomorphology across the various organisational levels. River complexity demands lengthier model descriptions to explain the formation of patterns. The model descriptions are lengthened in order to include feedback from interacting processes and the non-linearity of the effects of these processes.

Riparian vegetation change is often neglected in studies. However, it plays a major role in affecting resistance to water flow. Riparian vegetation change has, as a result, a significant impact on river morphodynamics. Reed growth, in particular, is regarded as a major geomorphological agent, for example, in the Sabie River in the Kruger National Park. Hence, *Phragmites* was chosen to represent the riparian vegetation processes required in this modelling.

A review of current geomorphological modelling was carried out in order to select models which best represent river processes of water, sediment and vegetation at the

various organisational levels. On the basis of the review, the following models at the respective organisational levels were used:

§ At reach scale:

§ a 1-D water flow model,

§ the Exner equation to determine longitudinal bed elevation and grain size distribution, and

§ a fuzzy-rule-based model for *Phragmites* population distribution.

§ At channel-type scale:

§ a 2-D water flow model,

§ a cellular automata model for sediment routing, and

§ a cellular automata model for *Phragmites* expansion.

§ At geomorphological-unit scale:

§ a steady-state flow variability model,

§ a power law equation in combination with statistical bed-form geometry relations, and

§ partial differential equations for *Phragmites* biomass growth.

The models at various organisational levels were integrated through stipulating the bottom-up model parameters and the top-down boundary conditions. Particular consideration of the flow resistance coefficients was required in order to include the feedback between interacting processes in the modelling. This trans-organisational feedback enabled flow resistance parameters at the various organisational levels to be determined simultaneously. The flow resistance coefficients at higher organisational levels were determined using coarse-grained shear stresses which resist water flow at smaller scales.

A gravel-bed river reach of 2 kilometres was modelled. Model simulations were carried out for 3 scenarios: an aggradating reach and a degradating reach and a degradating bedrock reach. The modelling outputs achieved were at spatial resolutions of 100 metres, 5 metres and 0.25 metres for the reach scale, the channel-type scale and the geomorphological-unit scale respectively.

Non-linearity is characterised by self-organisation and emergence. This non-linearity that exists at each organisational level is dealt with by trans-organisational modelling, as indicated by the results. The changes in reed state influence sediment behaviour in

each periodic model application. At the reach scale, the bed elevation self-organised according to flooding simulated using the 1-D water flow model. At the channel-type scale, sediment bars self-organised according to the 2-D water flow model distribution which is affected by the patchiness of reeds. Similarly, the modelled water flow distribution allowed the prediction of bed-form self-organisation at the geomorphological-unit scale. The patchiness of reeds self-organises within the boundary conditions supplied by the reach scale population distribution at a rate and density supplied by reed biomass growth at the geomorphological-unit scale. The effects of the constantly changing bed-forms, sediment bars and reed state are translated across organisational levels to affect flow resistance at the reach scale. This flow resistance in turn affects the rate of self-organisation of the bed elevation. Hence, emergence of small-scale variability at higher organisational levels was achieved.

The results differ significantly for modelling with trans-organisational feedback and that without. This difference is a result of the emergence produced by small-scale dynamic processes at larger scales. The modelling results clearly illustrate changing riparian vegetation habitat at various organisational levels. The modelling, therefore, enables river managers to predict the changes in habitat for riverine biota. Trans-organisational feedback allows the habitat at a particular organisational level to be adjusted within the modelling so that the associated changes in habitat at other scales can be included in decision-making. Stripping of reeds that occurs during extreme flooding, for example, may be explored.

Further development of the modelling includes verification of the reed models at the reach scale and the channel-type scale and of the sediment model at the channel-type scale. The CFD models used may employ more sophisticated numerical solving techniques to allow improved computing efficiency and accuracy. More efficient programming code in general will increase computation speed, allowing more frequent accounts of the effects of smaller scale processes. The modelling can also include more detail in terms of the river processes at various organisational levels, such as scour at the geomorphological-unit scale and river bank stability at the channel-type scale. The preservation of flow continuity across various organisational levels through the application of boundary conditions requires greater effort. This will improve flow resistance estimations determined at larger scales. Trans-organisational modelling is set

in a robust hierarchical framework which can be used to incorporate additional river modifiers, including water quality, fauna and flora.

The modelling added the effect of smaller scale variability which statistical up-scaling cannot account for, owing to the non-linearity of river processes. The non-linearity of the river processes is addressed through the linkage of models within a progressively nested hierarchical modelling structure. The modelling dealt with the added complexity produced by multiple interacting river processes, such as the effect of riparian vegetation on water flow and water flow feedback on sediment. The hierarchical modelling structure allows for congruent and concurrent interaction of models that represent river processes at various organisational levels. Alone, each model tells a single story; together, they can simulate river morphodynamics.

## References

- Aassine, S. and El Jai, M.C. (2002) Vegetation dynamics modelling: a method for coupling local and space dynamics. *Ecological Modelling*, 154: 237-249.
- Abbott, R. (2005) Challenges for biologically-inspired computing. Proceedings of the 2005 Workshop on Genetic and Evolutionary Computation, Washington, D.C.
- Abt, S.R., Clary, W.P. and Thorton, C.O. (1994) Sediment deposition and entrapment in vegetated streambeds. *Journal of Irrigation and Drainage Engineering*, ASCE, 120(6): 1098-1111.
- Albert, M.R. (2000) Notes on current techniques in modeling spatial heterogeneity. 57th Eastern Snow Conference Syracuse, New York, USA.
- Alonso, C.V. and Combs, S.T. (1986) Channel width adjustment in straight alluvial streams. Proceedings of the 4th Fed. Interagency Sedimentation Conference., U.S. GPOI Washington D.C., 5(31): 5-40.
- Anderson, D. and McNeil, G. (1992) Artificial Neural Networks Technology: Data and Analysis Centre for Software, Rome, NY.
- Arulanandan, K., Gillogley, E. and Tully, R. (1980) Development of a quantitative method to predict critical shear stress and state of erosion of naturally undisturbed cohesive soils. Report no: G1-80-5, U. S. Army Waterway, Experiment station, Vicksburg, Miss.
- Asaeda, T. and Karunaratne, S. (2000) Dynamic modeling of the growth of *Phragmites Australis*: model description. *Aquatic Botany*, 67: 301-318.
- ASCE, Task Committee on Hydraulics (1998a) Bank mechanics and modelling of river width adjustment. I: Processes and mechanisms. *Journal of Hydraulic Engineering*, 124(9): 881-902.
- ASCE, Task Committee on Hydraulics (1998b) Bank mechanics and modelling of river width adjustment. II: Modeling. *Journal of Hydraulic Engineering*, 124(9): 903-917.

- Ashmore, P. (1988) Bed-load transport in gravel-bed stream models. *Earth Surface Processes and Landforms*, 13: 677-695.
- Auble, G.T. and Scott, M.L. (1998) Fluvial disturbance patches and cottonwood recruitment along the upper Missouri River, Montana. *Journal of the Society of Wetland Scientists*, 18(4): 546-556.
- Auble, G.T., Friedman, J.M. and Scott, M.L. (1994) Relating riparian vegetation to present and future streamflows. *Ecological Applications*, 4: 544-554.
- Avarez-Cobelas, M. and Cirujano, S. (2007) Multilevel responses of emergent vegetation to environmental factors in a semi-arid floodplain. *Aquatic Botany*, 67: 49-60.
- Baas, N.A. and Emmeche, C. (1997) On emergence and explanation. Working Papers: 97-02-008, Santa Fe Institute.
- Bagnold, R.A. (1980) An empirical correlation of bedload transport rates in flumes and natural rivers. *Proceedings of the Royal Society of London, Series A*, 372: 453-473.
- Bak, P. (1996) *How Nature Works*. Copernicus, New York.
- Baker, V.R. and Twidale, C.R. (1991) The reenchantment of geomorphology. *Geomorphology*, 4: 73-100.
- Baltzer, H., Braun, W.P. and Kohler, W. (1998) Cellular automata models for vegetation dynamics. *Ecological Modelling*, 107: 113-125.
- Bandini, S. and Pavesi, G. (2004) A model based on cellular automata for the simulation of the dynamics of plant populations. In *Complexity and Integrated Resources Management*, edited by C. Pahl-Wostl, S. Schmidt, A.E. Rizzoli, and A.J. Jakeman, Transactions of the Second Biennial Meeting of the International Environmental Modelling and Software Society, iEMSs: Manno, Switzerland, 277-282.
- Baptist, M.J. (2003) A flume experiment on sediment transport with flexible, submerged vegetation. International Workshop on Riparian Forest Vegetated



Channels: Hydraulic, Morphological and Ecological Aspects, 20 – 22 February 2003, Trento, Italy.

Baptist, M.J. and Mosselman, E. (2002). Biogeomorphological modelling of secondary channels in the Waal River. River Flow 2002 Symposium: 773-782, Louvain-la-Neuve, Belgium.

Baptist, M.J., van der Lee, G.E.M., Kerle, F. and Mosselman, E. (2002) Modelling of morphodynamics, vegetation development and fish habitat in man-made secondary channels in the River Rhine, the Netherlands. Environmental Flows for River Systems Working Conference and Fourth International Ecohydraulics Symposium: 1-29, Cape Town, South Africa.

Barrett, G.W., Peles, J.D. and Odum, W.P. (1997) Transcending processes and the levels of organisation concept. Bioscience, 47: 531-535.

Bathurst, J.C. (1982) Theoretical aspects of flow resistance. In Gravel-Bed Rivers, edited by R.J. Hey, J.C. Bathurst and C.R. Thorne, John Wiley and Sons, New York; 83-108.

Bdour, A. and Papanicolaou, A.N. (2003) Coupling a two-dimensional hydrodynamic/sediment routing model in a mountainous catchment. The Sixteenth ASCE Engineering Mechanics Conference, Seattle, WA, USA.

Beeson, C.E. and Doyle, P.F. (1995) Comparison of bank erosion at vegetated and non-vegetated channel bends. Water Resources Bulletin, 31: 983-990.

Bendix, J. (1994) Scale direction and pattern in riparian vegetation environment. Annals of the Association of American Geographers, 84(4): 652-665.

Bennett, J.P. (1995) Algorithm for resistance to flow and transport in sand-bed channels. Journal of Hydraulic Engineering, 121(8): 578-590.

Berger, U. and Hildenbrandth, H. (2000) A new approach to spatially explicit modelling of forest dynamics: spacing, ageing and neighbourhood competition of mangrove trees. Ecological Modelling, 132: 287-302.

- Bezdek, J.C. (1993) Fuzzy models. What are they, and why? *IEEE Transactions on Fuzzy Systems*, 1(1): 1-6.
- Bing, S., Shuyou, C. and Guifen, L. (2001) Effect of vegetation on river width adjustment. *Proceedings of IAHR-Conference, Beijing 2001*.
- Birkhead, A.L. and James, C.S. (2000) Modelling geomorphic change in the Sabie River, South Africa. *Australian Journal of Water Resources*, 4(2): 131-138.
- Birkhead, A.L., Heritage, G.L., James, C.S., Rogers, K.H. and van Niekerk, A.W. (1998) Geomorphological change models for the Sabie River in the Kruger National Park. WRC Report No. 782/1/98. Water Research Commission, Pretoria.
- Blench, T. (1969) *Mobile-Bed Fluvialology*. University of Alberta Press, Edmonton.
- Bogena, H. and B. Diekkrüger, (2002) Modelling solute and sediment transport at different spatial and temporal scales. *Earth Surface Processes and Landforms*, 27: 1475-1489.
- Bousmar, D. (2002) Flow modelling in compound channels - Momentum transfer between main channel and prismatic or non-prismatic floodplains. Ph.D Thesis, Université catholique de Louvain-la-Neuve, Belgium.
- Brebner, A. and Wilson, K.C. (1967) Determination of the regime equation from relationships for pressurised flow by use of the principle of minimum energy degradation. *Proceedings of the Institute of Civil Engineers, London*, 36: 47-62.
- Bren, L.J. (1993) Riparian zone, stream, and floodplain issues: a review. *Journal of Hydrology*, 150: 227-299.
- Brewer, P.A. and Lewin, J. (1998) Planform cyclicality in an unstable reach: complex fluvial response to environmental change. *Earth Surface Processes and Landforms*, 23: 989-1008.
- Bromley, J., Brouwer, J., Barker, A.P., Gaze, S.R. and Valentin, C. (1997) The role of surface water redistribution in an area of patterned vegetation in a semi-arid environment, South-West Niger. *Journal of Hydrology*, 198: 1-29.

- Brownlie, W.R. (1983) Flow depth in sand-bed channels. *Journal of Hydraulic Engineering*, 109(7): 959-990.
- Cao, Z., Pender, G. and Meng, J. (2006) Explicit formulation of the Shields diagram for incipient motion of sediment. *Journal of Hydraulic Engineering*, 132(10): 1097-1099.
- Carollo, F.G., Ferro, V. and Termini, D. (2002) Flow velocity measurements in vegetated channels. *Journal of Hydraulic Engineering*, 128: 664-673.
- Carson, M.A. (1984) The meandering-braided river threshold: a reappraisal. *Journal of Hydrology*, 73: 315-334.
- Casulli, V. and Cheng, R.T. (1992) Semi-implicit finite difference methods for 3-D shallow water flow. *International Journal for Numerical Methods in Fluids*, 15: 629-648.
- Chang, H.H. (1979) Geometry of rivers in regime. *Journal of the Hydraulics Division, ASCE*, 105(HY6): 691-706.
- Chang, H.H. (1980a) Stable alluvial canal design. *Journal of the Hydraulics Division, ASCE*, 106(HY5): 873-891.
- Chang, H.H. (1980b) Geometry of gravel streams. *Journal of the Hydraulics Division, ASCE*, 106(HY5): 1443-1456.
- Chang, H.H. (1982) Mathematical model for erodible channels. *Journal of the Hydraulics Division, ASCE*, 108(HY5): 678-689.
- Chang, H.H. (1985) Channel width adjustment during scour and fill. *Journal of Hydraulic Engineering*, 111(10): 1368-1370.
- Chang, H.H. (1998) FLUVIAL-12, Generalized computer program. Mathematical model for erodible channels, Users Manual, Updated Version, San Diego, California.
- Chanson, H. (1999) *The Hydraulics of Open Channel Flow. An Introduction*. Butterworth-Heinemann, Oxford.

Charlton, F.G., Brown, P.M. and Benson, R.W. (1978) The hydraulic geometry of some gravel-bed rivers in Britain. Report INT-180, Wallingford, Hydraulic Research Station.

Chaudhry, M.H. (1993) Open Channel Flow. Prentice Hall, New Jersey.

Chen, Q. (2004) Cellular Automata and Artificial Intelligence in Ecohydraulics Modelling. Taylor & Francis Group plc, London, UK.

Chen, Q., Mynett, A.E. and Minns, A.W. (2000) Application of cellular automata to modelling competitive growths of two underwater species. *Chara aspera* and *Potamogeton pectinatus* in Lake Veluwe. *Ecological Modelling*, 147: 253-265.

Chih, T.Y. and Francisco, J.M.S. (1998) Simulation and prediction of river morphological changes using GSTARS 2.0. 3rd International Conference on Hydro-Science and -Engineering, Cottbus/Berlin, Germany, Aug. 31-Sep.

Church, M. (1996) Space time and the mountain – how do we order what we see? In *The Scientific Nature of Geomorphology*, edited by B.L. Rhoads and C.E. Thorn, Wiley, 147-170.

Cilliers, P. (2001) Boundaries, hierarchies and networks in complex systems. *International Journal of Innovation Management*, 5(2):135-147.

Coleman, S.E. and B.W. Melville, (1996) Initiation of bed-forms on a flat sand bed. *Journal of Hydraulic Engineering*, 122(6): 301-310.

Coleman, S.E., Nikora, V.I., McLean, S.R., Clunie, T.M., Schlicke, T. and Melville, B.W. (2006) Equilibrium hydrodynamics concept for developing dunes. *Physics of Fluids*, 18(10): 105104-105104-12.

Coleman, S.E., Zhang, M.H. and Clunie, T.M. (2005), Sediment-wave development in subcritical water flow. *Journal of Hydraulic Engineering*, 131(2): 106-111.

Conte, R., Paolucci, M. and Di Tosto, G. (2006) Vampire bats and the micro-macro link. In *Agent-based Computational Modelling - Applications in Demography, Social, Economic and Environmental Sciences*, edited by F.C. Billari, T. Fent, A. Prskawetz, J. Scheffran, Physica-verlag HD, Springer, 173-195.

- Coulthard, T.J., Hicks, D.M. and Van De Wiel, M.J. (2007) Cellular modelling of river catchments and reaches: Advantages, limitations and prospects. *Geomorphology*, 90: 192-207.
- Darby, S. (1999) Effect of riparian vegetation on flow resistance and flood potential. *Journal of Hydrological Engineering*, 125(5): 443-453.
- Darby, S.E. and Thorne, C.R. (1992) Simulation of near bank aggradation and degradation for width adjustment modeling. *Hydraulic and environmental modeling: Estuarine and River Water*, edited by R. A. Falconerm, K. Shiono, and R. G. S. Mathews, M. Ashgate, Aldershot, England, 431-442.
- Darby, S.E. and Thorne, C.R. (1996a) Stability analysis for steep, eroding, cohesive riverbanks. *Journal of Hydraulic Engineering*, 122: 443-454.
- Darby, S.E. and Thorne, C.R. (1996b) Numerical simulation of widening and bed deformation of straight sandbed rivers. I: Model development. *Journal of Hydraulic Engineering*, 122: 184-193.
- Darley, V. (1993) Emergent phenomena and complexity. Nikos Drakos, Computer Based Learning Unit, University of Leeds.
- Davies, T.R.H. and Sutherland, A.J. (1980) Resistance to flow past deformable boundaries. *Earth Surface Processes*, 5: 175-179.
- Davies, T.R.H. and Sutherland, A.J. (1983) Extremal hypotheses for river behavior. *Water Resources Research*, 19: 141-148.
- Dawson, F.H. and Charlton, F.G. (1988) Bibliography on the hydraulic resistance of roughness of vegetated watercourses. *Freshwater Biological Association, Occasional Publication*, Number 25.
- Dawson, F.H. and Roberson, W.N. (1985) Submerged macrophytes and the hydraulic roughness of a lowland chalk stream. *Verhandlungen der Inrenationnaem Vereinigung fur Theoretische und Angewandte Limnologie*, 22: 1944-1948.
- De Wolf, T. and Holvoet, T. (2004) Emergence versus self-organisation: different concepts but promising when combined. *Engineering Self-Organising Systems*, 1-15.

- Deegan, B.M. White, S.D. and Ganf, G.G. (2007) The influence of water level fluctuations on the growth of four emergent macrophyte species. *Aquatic Botany*, 86: 309-315.
- Demuren, A.O. (1989) Calculation of sediment transport in meandering channels. Tech, Session A, Proceedings of the 23rd IAHR Congress, International Association for Hydraulic Research, Delth, The Netherlands.
- Demuren, A.O. (1991) Development of a mathematical model for sediment transport in meandering rivers. Report No: 1693, Institute for Hydromechanics, University of Karlsruhe, Germany.
- Demuren, A.O. and Rodi, W. (1986) Calculation of flow and pollutant dispersion in meandering channels. *Journal Fluid Mechanics*, Cambridge, U.K., 172: 63-92.
- Dollar, E.S.J., James, C.S., Rogers, K.H. and Thoms, M.C. (2007) A framework for interdisciplinary understanding of rivers as ecosystems. *Geomorphology*, 89: 147-162.
- du Plessis, A.J.E. (1997) Interrelationships between morphological change and riparian vegetation as a response to interbasin transfers in the Orange-Fish River interbasin transfer scheme. A research proposal submitted as a departmental requirement for the degree of Master Science in the Department of Geography, Rhodes University.
- Eaton, B.C., Church, M. and Millar, R.G. (2004). Rational regime model of alluvial channel morphology and response. *Earth Surface Processes and Landforms*, 29: 511-529.
- Ebert, R. and Mitchell, T.R. (1975) *Organizational Decision Processes: Concepts and Analysis*. New York: Crane, Russell & Company.
- Engelund, F. and Hansen, E. (1967) A monograph on sediment transport in alluvial streams. Teknisk Forlag, Copenhagen, Denmark.
- Ermini, L., Catani, F. and Casagli, N. (2005) Artificial neural networks applied to landslide susceptibility assessment. *Geomorphology*, 66(1-4): 327-343.

Eschner, T.R., Hadley, R.F. and Crowley, K.D. (1983) Hydrologic and morphologic changes in channels of the Platte River basin in Colorado, Wyoming, and Nebraska: A historical perspective. U.S. Geological Survey, A1-A39.

Farias, H.D. (1995) Physical and mathematical modelling of alluvial channels in regime. Proceedings of the XXVIth Congress of the International Association for Hydraulic Research, 1, Thomas Telford, London, 348-353.

Fathi-Maghadam, M. and Kouwen, N. (1997) Nonrigid, nonsubmerged, vegetative roughness on floodplains. *Journal of Hydraulic Engineering*, 123(1): 51-57.

Favis-Mortlock, D.T. (1996). An evolutionary approach to the simulation of rill initiation and development. Proceedings of the 1st International Conference on Geocomputation, edited by R.J. Abrahart, 1: 248-281.

Favis-Mortlock, D.T. (2004) Self-organisation and cellular automata models. In *Environmental Modelling: Finding Simplicity in Complexity*, edited by J. Wainwright and M. Mulligan, John Wiley and Sons, Ltd, 349-369.

Ferziger, J.H. and Peric, M. (1996). *Computational Methods for Fluid Dynamics*. Springer, Berlin.

Fetherston, K.L., Naiman, R.J. and Bilby, R.E. (1995) Large woody debris, physical process, and riparian forest development in Montane River networks of the Pacific Northwest. *Geomorphology*, 13:133-144.

FHWA, (1995) *Evaluating scour at bridges*, HEC-18, Third edition. Federal Highway Administration, U.S. Department of Transportation, Publication No FHWA-IP-90-017.

Fischer, C., Hirsemann, A. and Matejka, H. (2003) Rule-based modelling of soil-water interactions influenced by subsidence caused by mining activities. Institute of Geotechnical Engineering and Mine Surveying, Technical University of Clausthal.

Fonstad, M. and Marcus, W.A. (2003) Self-organized criticality in riverbank systems. *Annals of the Association of American Geographers*, 93: 281-296.

- Franz, E.H. and Bazzaz, F.A. (1977) Simulation of vegetation response of modified hydrologic regimes a probabilistic model based on niche differentiation in a floodplain forest. *Ecology*, 58: 176-183.
- Fredlund, D.G., Morgenstern, N.R. and Widger, R.A. (1978) The shear strength of unsaturated soils. *Canadian Geotechnical Journal*, 15: 313-321.
- Friedman, J.M. and Auble, G.T. (1999) Mortality of riparian box elder from sediment mobilization and extended inundation. *Regulated Rivers: Research and Management*, 15: 463-476.
- Furness, H.D. and Breen, C.M. (1980) The vegetation of seasonally flooded areas of the Pongolo River floodplain. *Bothalia*, 13 (1+2): 217-231.
- Gains, R.A. and Maynard, S.T. (2001) Microscale loose-bed hydraulic models. *Journal of Hydraulic Engineering*, 127(5): 335-338.
- Garbrecht, J., Kuhnle, R. and Alonso, C. (1995) A sediment transport capacity formulation for application to large channel networks. *Journal of Soil and Water Conservation*, 50(5): 527-529.
- Gecy, J.L. and Wilson, M.V. (1990) Initial establishment of riparian vegetation after disturbance by debris flows in Oregon. *American Midland Naturalist*, 123: 282-291.
- Gell-Mann, M. (1994) *The Quark and the Jaguar: Adventures in the Simple and the Complex*. Abacus, London.
- Gessler, D., Hall, B., Spasojevic, M., Holly, F., Pourtaheri, H. and Raphelt, N. (1999) Application of a 3D mobile bed, hydrodynamic model. *Journal of Hydraulic Engineering*, 125: 737-749.
- Gill, C.J. (1970) The flooding tolerance of woody species, a review. *Forestry Abstracts*, 31(4): 617-688.
- Gomez, B. (1991) Bedload transport. *Earth Science Reviews*, 31: 89-132.
- Goodwin, C.N. (1996) Channel widening and bank erosion processes on a cobble-bed river. *Geological Society, Am. Abstr. Programs*, 28: 262 p.



- Graf, W.L. (1988) *Fluvial Processes in Dryland Rivers*. Springer-Verlag, Inc., New York, NY.
- Gregory, K.J. (1992) Vegetation and river channel process interactions. In *River Conservation and Management*, edited by P.J. Boon, P. Calow, and G.E. Petts, Wiley: Chichester, 255-269.
- Gregory, S.V., Swanson F.J., McKee, W.A. and Cummins, K.W. (1991) An ecosystem perspective of riparian zones. *Bioscience*, 41: 540-551.
- Griffiths, G.A. (1993) Sediment translation waves in braided gravel-bed rivers. *Journal of Hydraulic Engineering*, 119(8): 924-937.
- Habersack, H.M. (2000) The river-scaling concept (RSC): a basis for ecological assessments. *Hydrobiologia*, 422/423: 49-60.
- Hack, J.T. (1960) Interpretation of erosional topography in humid temperate regions. *American Journal of Science*, 258A: 80-97.
- Haff, P.K. (1996) Limitations on predictive modelling in geomorphology. In *The Scientific Nature of Geomorphology*, edited by B.L. Rhoads and C.E. Thorn, Wiley, 337-358.
- Hanson, G.J. and Simon, A. (2001) Erodibility of cohesive streambeds in the loess area of the midwestern USA. *Hydrological Processes*, 15(1): 23-38.
- Harlow, F.H. and Welsh, J.E. (1965) Numerical calculation of time dependent viscous incompressible flow with free surface. *Physics of Fluids*, 8: 2182-2189.
- Harrison, S. (2001) On reductionism and emergence in geomorphology. *Transactions of the Institute of British Geographers*, 26: 327-39.
- Harvey, A.M. (1990) The influence of sediment supply on the channel morphology of upland streams: Howgill Fells, Northwest England. *Earth Surface Processes and Landforms*, 16: 675-684.

- Haschenburger, J.K. and Souch, C. (2004) Contributions to the understanding of geomorphic landscapes. *Annals of the Association of American Geographers*, 94(4): 771-793.
- Haslam, S.M. (1978) *River Plants*. Cambridge University Press, Cambridge.
- Heritage, G.L. and van Niekerk A.W. (1995) Drought conditions and sediment transport in the Sabie River. *Koedoe*, 38(2): 1-9.
- Heritage, G.L., van Niekerk, A.W., Moon, B.P., Broadhurst, L.J., Rogers, K.H. and James, C.S. (1997) The geomorphological response to changing flow regimes of the Sabie River and Letaba River systems. WRC Report, No 376/1/97.
- Hey, R.D. (1997) Stable river morphology. In *Applied Fluvial Geomorphology for River Engineering and Management*, edited by C.R. Thorne, R.D. Hey and M.D. Newson, John Wiley and Sons, New York, NY, 223-236.
- Hey, R.D. and Thorne, C.R. (1986) Stable channels with mobile gravel beds. *Journal of Hydraulic Engineering*, 112(8): 671-689.
- Hicken, E.J. (1984) Vegetation and river channel dynamics. *Canadian Geographer*, 28: 111-128.
- Hicken, E.J. and Nanson, G.C. (1984) Lateral migration rates of river bends. *Journal of Hydraulic Engineering*, 110(11): 1557-1567.
- Hoey, T.B. and Sutherland, A.J. (1991) Channel morphology and bedload pulses in braided rivers: a laboratory study. *Earth Surface Process and Landforms*, 16: 447-462.
- Hoffmans, G.J.C.M. and Booij, R. (1993) Two dimensional mathematical modeling of local scour holes. *Journal of Hydraulic Research*, 31(5): 615-634.
- Hooke, J.M. (1997) Styles of channel change. In *Applied Fluvial Geomorphology for River Engineering and Management*, edited by C.R. Thorne, R.D. Hey and M.D. Newson, John Wiley and Sons, West Sussex, England, 237-268.

Hooke, J.M., Brookes, C.J., Duane, W. and Mant, J.M. (2005). A simulation model of morphological, vegetation and sediment changes in ephemeral streams. *Earth Surface Process and Landforms*, 30: 845-66.

Houwing, E.J., Tanczos, I.C., Kroon, A. and de Vries, M.B. (2002) Interaction of submerged vegetation, hydrodynamics and turbidity; analysis of field and laboratory studies, Elsevier, *Proceedings in Marine Science*, 5, *Fine Sediment Dynamics in the Marine Environment*, edited by J.C. Winterwerp, and C. Kranenburg.

Howard, A. (1984) Sufficient conditions for river meandering: a simulation approach. *Water Resources Research*, 20(11): 1659-1667.

Howard, A.D. (1987) Modelling fluvial systems: rock-, gravel and sand bed channels. In *River Channels, Environment and Process*, edited by K. Richards, Institute of British Geographers, New York, 69-94.

Howard, A.D. (1996) Modelling channel evolution and floodplain morphology. In *Floodplain Processes*, edited by M.G. Anderson, D.E. Walling and P.D. Bates, Wiley, Chichester, 15-62.

Huang, H.Q., Chang, H.H. and Nanson, G.C. (2004) Minimum energy as the general form of critical flow and maximum flow efficiency and for explaining variations in river channel pattern. *Water Resources Research*, 40(4): W04502.

Hupp, C.R. (1988) Plant ecological aspects of flood geomorphology and paleoflood history. In *Flood Geomorphology*, edited by V. Baker, R. Kochel and P. Patton, John Wiley, New York, 335-356.

Hupp, C.R. and Osterkamp, W.R. (1985) Bottomland vegetation distribution along Passage Creek, Virginia. In relation to fluvial landforms. *Ecology*, 66(3): 670-681.

Inamdar, S.P. (2006) Challenges in modelling hydrologic and water quality processes in riparian zones. *Journal of the American Water Resources Association*, 42(1): 5-14.

ISPG (2002) Integrated streambank protection guidelines. Washington State Aquatic Habitat Guidelines Program.

James, C.S., Birkhead, A.L., Jordanova, A.A., Kotchy, K.A., Nicolson, C.R. and Makoa, M.J. (2001a) Interaction of reeds, hydraulics and river morphology. WRC Report No. 856/1/01, Water Research Commission, Pretoria.

James, C.S., Nicolson C.R., van Niekerk A.W. and Heritage G.L. (1996) Modeling the response of river geomorphology and riverain vegetation to water resources development in the Sabie River, South Africa. Ecohydraulics 2000, Proceedings of the 2<sup>nd</sup> International Symposium on Hydraulics and Habitats, Quebec, A: 331-341.

James, C.S., Odiyo, J.O. and Lambert, M.F. (2001b) Modelling sediment movement and storage in semi-arid, bedrock controlled rivers. 7th International Conference on Fluvial Sedimentology, Lincoln, Nebraska, U.S.A.

Jewitt, G.P.W. and Görgens, A.H.M. (2000) Scale and model interfaces in the context of integrated water resources management for the rivers of KNP. Water Research Commission report No: 627/1/00.

Jia, Y. (1990) Minimum Froude number and the equilibrium of alluvial sand rivers. *Earth Surface Processes and Landforms*, 15: 199-209.

Jia, Y., Kitamura, T. and Wang, S.S.Y. (2001) Simulation of scour process in plunging pool of loose bed material. *Journal of Hydraulic Engineering*, 127(3): 219-229.

Jimmenez-Hornero, F.J., Giraldez, J.W. and Laguna, A. (2003) A description of water and sediment flow in the presence of obstacles with a two dimensional lattice BGK cellular automata model. *Water Resources Research*, 39(12): 1396 p.

Johannesson, H. and Parker, G. (1989) Velocity redistribution in meandering rivers. *Journal of Hydraulic Engineering*, 115(8): 1019-1039.

Johansson, M.E. and Nilsson, C. (2002) Responses of riparian plants to flooding in free-flowing and regulated boreal rivers: an experimental study. *Journal of Applied Ecology*, 39: 971-986

Johnson, W.C. (2000) Tree recruitment and survival in rivers: Influence of hydrological processes. *Hydrological Processes*, 14: 3051-3074.

- Johnson, W.C. (1994) Woodland expansion in the Platte River, Nebraska: patterns and causes. *Ecological Monographs*, 46: 59-84.
- Jordanova, A.A. and James, C.S. (2003) Experimental study of bed-load transport through emergent vegetation. *Journal of Hydraulic Engineering*, 129(6): 474-478.
- Jordanova, A.A., James, C.S. and Birkhead, A.L. (2006) Practical resistance estimation for flow through emergent vegetation. *Water Management*, 159(WM3): 173-181.
- Julien, P.Y. (2002) *River Mechanics*. Cambridge University Press, Cambridge.
- Julien, P.Y. and Wargadalam, J. (1995) Alluvial channel geometry: Theory and applications. *Journal of Hydraulic Engineering*, 121(4): 312-325.
- Junk, W.S., Bayley, P.B. and Sparks, R.E. (1989) The flood pulse concept in river floodplain systems. *Canadian Special Publications in Fisheries and Aquatic Sciences*, 103: 110-127.
- Kalliola, R. and Puhakka, M. (1988) River dynamics and vegetation mosaicism: a case study of the River Kamajohnka, northernmost Finland. *Journal of Biogeography*, 15: 703-719.
- Karunaratne, S., Asaeda, T. and Yutani K. (2003) Growth performance of *Phragmites australis* in Japan: influence of geographic gradient. *Environmental and Experimental Botany*, 50: 51-66.
- Kassem, A.A. and Chaudhry, M.H. (2002) Numerical modelling of bed evolution in channel bends. *Journal of Hydraulic Engineering*, 128(5): 507-514.
- Kaufmann, A. and Gupta, M.M. (1985) *Introduction to Fuzzy Arithmetic*. Reinhold, New York.
- Kavvas, M.L. (1999) On the coarse-graining of hydrologic processes with increasing scales. *Journal of Hydrology*, 217: 191-202
- Kikkawa, H., Ikeda, S. and Kitawa, A. (1976) Flow and bed topography in curved open channels. *Journal of the Hydraulics Division, ASCE*, 102(HY9): 1327-1342.

Klir, G.J. and Folger, T. (1987) *Fuzzy Sets, Uncertainty, and Information*. Prentice Hall, Englewood Cliffs, NJ.

Klir, G.J. and Yuan, B. (1995) *Fuzzy Sets and Fuzzy Logic: Theory and Applications*. Prentice Hall P.T .R, Upper Saddle River, New Jersey.

Knighton, D. (1998) *Fluvial Forms and Processes: A New Perspective*. Arnold, London.

Kouwen, N. and Li, R.M. (1980) Biomechanics of vegetative linings. Analysis of flow through vegetation. *Journal of the Hydraulics Division, ASCE*, 106(HY12): 1085-1103.

Lane, S.N. (2005) Roughness – time for a re-evaluation? *Earth Surface and Processes*, 30: 251-253.

Lane, S.N. and Richards, K.S. (1997) Linking channel form and process: Time space and causality revised. *Earth Surface and Processes and Landforms*, 22: 249-260.

Langbein, W.B. (1964) Geometry of river channels. *Journal of the Hydraulics Division, ASCE*, 90(HY2): 301-312.

Langendoen, E.J. (2000) *CONCEPTS – Conservational channel evolution and pollutant transport system: Stream corridor version 1.0*. Research Report No: 16, US Department of agriculture, Agricultural research service, National Sedimentation Laboratory, Oxford, MS.

Leddy, J.O., Ashworth, P.J. and Best, J.L. (1993) Mechanisms of anabranch avulsion within gravel-bed braided rivers: observations from a scaled physical model. In *Braided Rivers*, edited by J.L. Best and C.S. Bristow, Geological Society of London, London, 119-127.

Lee, H. and Hsieh, H. (2003) Numerical simulations of scour and deposition in a channel network. *International Journal of Sediment Research*, 18(1): 32-49.

Lenaerts, T., Gross, D. and Watson, R. (2002). On the modeling of dynamical hierarchies. *Proceedings of the Alife VIII Workshop*, Sydney: University of New South Wales, 37-44.

- Leopold, L.B. and Langbein, W.B. (1962) The concept of entropy in landscape evolution. U.S. Geological Survey, Professional Paper, 500A.
- Leopold, L.B. and Maddock, T. (1953) The hydraulic geometry of stream channels and some physiographic implications. U.S. Geological Survey, Professional Paper, 252 p.
- Leopold, L.B., Wolman, R.G. and Miller, J.G. (1964) Fluvial processes in geomorphology. W.H. Freeman, San Francisco.
- Li, L. and Wang, S.S.Y. (1994) Computational simulation of channel erosion and retreat. Technical Report, CCHE, University of Mississippi, Oxford, Miss.
- Li, R.M. and Shen, H.W. (1973) Effect of tall vegetations on flow and sediment. Journal of the Hydraulics Division, ASCE, 99(HY6): 793-814.
- Lindley, E.S. (1919) Regime Channels. Punjab Engineering Congress, India.
- Lisle, T.E., Ikeda, H. and Iseya, F. (1991) Formation of stationary alternate bars in a steep channel with mixed-size sediment: A flume experiment. Earth Surface Processes and Landforms, 16: 463-469.
- Luo, W., Duffin, K.L., Peronja, E., Stravers, J.A. and Henry, G.M. (2003) A web-based interactive landform simulation model (WILSIM). Computers and Geosciences, 30(3): 215-220.
- Madsen, J.D., Chambers, P.A., James, W.F., Koch, E.W. and Westlake, D.F. (2001) The interaction between water movement, sediment dynamics and submersed macrophytes. Hydrobiologia, Kluwer Academic Publishers, 444: 71-84.
- Magilligan, F.J., Phillips, J.D., James, L.A. and Gomez, B. (1998) Geomorphic and sedimentological controls on the effect of an extreme flood. The Journal of Geology, 106: 87-95.
- Mahoney, J.M. and Rood, S.B. (1998) Streamflow requirements for cottonwood recruitment: an integrative model. Wetlands, 18: 634-645.

- Malanson, G.M. and D.R. Butler, (1990) Woody debris, sediment, and riparian vegetation of a subalpine river, Montana, USA. *Arctic and Alpine Research*, 22(2): 183-194.
- Malanson, G.P. (1999) Considering complexity. *Annals of the Association of American Geographers*, 89: 746-753.
- Martin, Y. and Church, M. (2000) Re-examination of Bagnold's empirical bedload formulae. *Earth Surface Processes and Landforms*, 25: 1011-1024.
- McArdell, B.W. and Faeh, R. (2001) A computational investigation of river braiding. In *Gravel-Bed Rivers*, edited by M.P. Mosley, New Zealand Hydrological Society, Wellington, New Zealand, 73-86.
- Meigh, J.C. (1987) Transport of bed material in a gravel bed river. PhD Thesis, University of East Anglia, Norwich, UK.
- Michaelides, K. and Wainwright, J. (2004) Modelling fluvial processes and interactions. In *Environmental Modelling: Finding Simplicity in Complexity*, edited by J. Wainwright and M. Mulligan, John Wiley and Sons, Ltd, 123-142.
- Micheli, E.R. and Kirchner J.W. (2002) Effects of wet meadow riparian vegetation on streambank erosion. 1. Remote sensing measurements of streambank migration and erodibility. *Earth Surfaces Processes and Landforms*, 27: 627-639.
- Millar, R.G. (2000) Influence of bank vegetation on alluvial channel patterns. *Water Resources Research*, 36: 1109-1118.
- Millar, R.G. and Quick, M.C. (1993) Effect of bank-stability on geometry of gravel rivers. *Journal of Hydraulic Engineering*, 119: 1343-1363.
- Millar, R.G. and Quick, M.C. (1998) Stable width and depth of gravel-bed rivers with cohesive banks. *Journal of Hydraulic Engineering*, 124: 1005-1013.
- Molinas, A. and Yang, C.T. (1986). Computer program user's manual for GSTARS (Generalized Stream Tube model for Alluvial River Simulation), U.S. Bureau of Reclamation, Denver, Colorado.



- Montgomery, D.R. (1999) Process domains and the river continuum. *Journal of the American Water Resources Association*, 35(2): 397-410.
- Murray, A.B. (2003) Contrasting the goals, strategies, and predictions associated with simplified numerical models and detailed simulations. *Geophysical Monograph*, American Geophysical Union, 135(10):1029/135GM11.
- Murray, A.B. and Paola, C. (1994) A cellular model of braided rivers. *Letters to Nature*, 71: 54-57.
- Murray, A.B. and Paola, C. (1997) Properties of a cellular braided stream model. *Earth Surface Processes and Landforms*, 22: 1001-1025.
- Nadaoka, K. and Yagi, H. (1998) Shallow-water turbulence modeling and horizontal large-eddy computation of river flow. *Journal of Hydraulic Engineering*, 124(5): 493-500.
- Nagata, N., Hosoda, T. and Muramoto, Y. (2000) Numerical analysis of river channel processes with bank erosion. *Journal of Hydraulic Engineering*, 126(4): 243-252.
- Nakamura, F. and F.J. Swanson. (1993) Effects of coarse woody debris on morphology and sediment storage of a mountain stream system in western Oregon. *Earth Surface Processes and Landforms*, 18: 43-61.
- Nestler, J.M., Goodwin, R.A. and Loucks, D.P. (2005) Coupling of engineering and biological models for ecosystem analysis. *Journal of Water Resources Planning and Management*. 131(2): 101-109.
- Nicolson, C.R. (1999) Qualitative rule based-modeling of geomorphological change in semi-arid bedrock-influenced rivers. PhD Thesis, University of the Witwatersrand, Johannesburg, South Africa.
- Nield, J.M., Walker, D.J. and Lambert, M.F. (2002) Self-organisation and entropy in the 2-D morphological modelling of an open channel. *Proceedings, Advances in Hydro-Science and -Engineering, Volume VI, May 2004, Brisbane, Australia*, University of Mississippi, 13 p.

- Nilsson, C., Gunnell, G., Johansson, M. and Sperens, U. (1989) Patterns of plant species richness along riverbanks. *Ecology*, 70(1): 77-84.
- O'Neill, R.V., Johnson, A.R. and King, A.W. (1989) A hierarchical framework for analysis of scale. *Landscape Ecology*, 3: 193-205.
- Odgaard, A.J. (1981) Transverse bed slope in alluvial channel bends. *Journal of the Hydraulics Division, ASCE*, 107(HY12): 1677-1694.
- Olsen, N.R. (2003) 3D CFD modeling of self-forming meandering channel. *Journal Hydraulic Engineering, ASCE*, 129(HY5): 366-372.
- Olsen, N.R.B. (1996) Three dimensional numerical modelling of local scour. *Hydroinformatics 96*, Zurich, Switzerland.
- Olsen, N.R.B. and Melaaen, M.C. (1993) 3-D numerical modelling of scour around cylinders. *Journal of Hydraulic Engineering*, 119(9): 1048-1053.
- Osman, A.M. (1985) Channel width response to changes in flow hydraulics and sediment loads. PhD Thesis, Colorado State University, Fort Collins, Colorado.
- Osman, A.M. and Thorne, C.R. (1988) Riverbank-stability analysis. I: Theory. *Journal of Hydraulic Engineering*, 114(2): 134-150.
- Packard, H. and Wolfram, S. (1985) Two-dimensional cellular automata. *Journal of Statistical Physics*, 38(5/6): 901-946.
- Paola, C. (2001) Modelling stream braiding over a range of scales. In *Gravel-Bed Rivers*, edited by M.P. Mosley, New Zealand Hydrological Society, Wellington NZ, 11-46.
- Paola, C. and Foufoula-Georgiou, E. (1991) Statistical geometry and dynamics of braided rivers. In *Gravel-Bed Rivers*, edited by M.P. Mosley, New Zealand Hydrological Society, Wellington NZ, 47-72.
- Paola, C., Heller, P.L. and Angevine, C. L. (1992) The large-scale dynamics of grain-size variation in alluvial basins. I: Theory. *Basin Research*, 4: 73-90.

- Parker, G. (1984) Lateral bed load transport on side slopes. *Journal of Hydraulic Engineering*, 110(2): 197-199.
- Parker, G., Sundararajan, D. and Heinz, S. (1982) Model experiments on mobile, paved gravel bed streams. *Water Resources Research*, 15(5): 1395-1408.
- Parkinson, S., Anderson, K., Conner, J. and Milligan, J. (2003) Sediment transport, supply, and stability in the Hells Canyon reach of the Snake River. Technical Report, Idaho Power Company, FERC No. 1971.
- Parsons, M., McLoughlin, C.A., Roundtree, M.W. and Rogers, K.H. (2003) The biotic and abiotic legacy of a large infrequent flood disturbance in the Sabie River, South Africa. Centre of the Water in the Environment Report, University of the Witwatersrand, Johannesburg, South Africa.
- Partheniades, E. (1965) Erosion and deposition of cohesive soils. *Journal of the Hydraulics Division, ASCE*, 91(HY1): 105-139.
- Passino, K.M. and Yurkovich, S. (1998) *Fuzzy Control*. Addison Wesley Longman, Inc., California, USA.
- Petryk, S. and Bosmajian, G. (1975) Analysis of flow through vegetation. *Journal of the Hydraulics Division, ASCE*, 101(HY): 871-884.
- Peyret, R. and Taylor, T.D. (1983) *Computational Methods for Fluid Flow*. Springer-Verlag, New York.
- Philips, K.R. and Field, R.T. (2005) *Phragmites Australis* expansion in Delaware Bay salt marshes. *Ecological Engineering*, 25: 275-291.
- Phillips, J.D. (1996). Deterministic complexity, explanation, and predictability in geomorphic systems. In *The Scientific Nature of Geomorphology*, edited by B.L. Rhoads and C.F. Thorn, Wiley, New York, 315-335.
- Pickup, G. (1976) Adjustment of stream channel shape to hydrologic regime. *Journal of Hydrology*, 30: 365-373.

- Poff, N.L., Allan, J.D., Bain, M.B., Karr, J.R., Prestegard, K.L., Richter, B.D., Sparks, R.E. and Stromberg, J.C. (1997) The natural flow regime - a paradigm for river conservation and restoration. *Bioscience*, 47: 769-783.
- Pollowy, R.T. (1998) The restoration and management of rivers and streams. By Restoration Ecologist, Article reprint from Land and Water Magazine.
- Proffit, G.T. and Sutherland, A.J. (1983) Transport of nonuniform sediment. *Journal of Hydraulic Research*, 21(1): 33-43.
- Prosser, I.P., Dietrich, W.E. and Stevenson, J. (1995) Flow resistance and sediment transport by concentrated overland flow in a grassland valley. *Geomorphology*, 13: 71-86.
- Qing Huang, H., Nanson, G.C. and Fagan, S.D. (2002) Hydraulic geometry of straight alluvial channels and the principle of least action. *Journal of Hydraulic Research*, 40(2): 153-160.
- Rahuel, J.L. and Holly, F.M., (1989) Modelling of riverbed evolution for bedload sediment mixtures. *Journal of Hydraulic Engineering*, 115(11): 1521-1542.
- Rathburn, S.L. and Wohl, E.E. (2001) One dimensional sediment transport modelling of pool recovery along a mountain channel after a reservoir sediment release. *Regulated Rivers: Research and Management*, 17: 251-273.
- Raudkivi, A.J. (1976) *Loose Boundary Hydraulics*. Pergamon Press Ltd, Oxford.
- Raudkivi, A.J. (1997) Ripples on stream bed. *Journal of Hydraulic Engineering*, 123(1): 58-64.
- Richards, K.S. (2001) Floods, channel dynamics, and riparian ecosystems. In *Gravel-Bed Rivers*, edited by M.P. Mosley, New Zealand Hydrological Society, Wellington NZ, 465-477.
- Richardson, E.V. and Simons, D.B. (1976) River response to development. *River 76*, American Society of Civil Engineers, 1285-1300.

- Richardson, J.E. and Panchang, V.G. (1998) 3-D simulation of scour inducing flow at bridge piers. *Journal of Hydraulic Engineering*, 124(5): 530-540.
- Richter, B.D., Baumgartner, J.V., Wigington, R. and Braun, D.P. (1997) How much water does a river need? *Freshwater Biology*, 37: 231-249.
- Rogers, K.H. (2002) Operationalizing multi-party strategic adaptive management (SAM) of the Sabie River. WRC Report No. 1097/1/02. Water Research Commission, Pretoria.
- Rogers, K.H. and Bestbier, R. (1997) Development of a protocol for the definition of the desired state of riverine systems in South Africa. Department of Environmental Affairs and Tourism, Pretoria.
- Rood, S.B. and Mahoney, J.M. (1990) Collapse of riparian poplar forest downstream from dams in western prairies: probable causes and prospects for mitigation. *Environmental Management*, 14: 451-464.
- Rosgen, D.L. (1994) A Classification of Natural Rivers. *Catena*, Elsevier Science, 22: 169-199.
- Rosgen, D.L. (1996) Applied river morphology. *Wildland Hydrology*, Pagosa Springs, Colorado.
- Rountree, M.W., Heritage, G.L. and Rogers, K.H. (2001) In channel metamorphosis in a semiarid, mixed bedrock alluvial river system: implications for in-stream flow requirements. *Hydro-ecology: Linking Hydrology and Aquatic Ecology*, IAHS, 266: 113-123.
- Rountree, M.W., Rogers, K.H. and Heritage, G.L. (2000) Landscape state change in the semiarid Sabie River, Kruger National Park, in Response to Flood and Drought. *South African Geographical Journal*, 82: 173-181.
- Rowntree, K.M. (1991) An assessment of the potential impact of alien invasive vegetation on the geomorphology of river channels in South Africa. *South African Journal of Aquatic Science*, 17(1): 28-43.

- Rowntree, K.M. and E.S.J. Dollar, (1999) Vegetation controls on channel stability in the Bell River, Eastern Cape, South Africa. *Earth Surface Processes and Landforms*, 24: 127-134.
- Sapozhnikov, V. and Foufoula-Georgiou, E. (1996) Do the current landscape evolution models show self-organized criticality? *Water Resources Research*, 32(4): 1109-1112.
- Sarangi, A. and Bhattacharyaa, K. (2004) Comparison of Artificial Neural Network and regression models for sediment loss prediction from Banha watershed in India. *Agricultural Water Management*. 78(3): 195-208.
- Schumm, S.A. (1977) *The Fluvial System*. New York, John Wiley and Sons, Inc.
- Schneider, M. and Jorde, K. (2003) Fuzzy-rule-based models for the evaluation of fish habitat quality and in-stream flow assessment. International IFIM users' Workshop Fort Collins, Colorado.
- Schweber, S.S. (1993) Physics community and the crisis in physical theory. *Physics Today*, 46: 34-39.
- Scott, M.L., Friedman, J.M. and Auble, G.T. (1996) Fluvial processes and the establishment of bottomland trees. *Geomorphology*, 14: 327-329.
- Sear, D.A., Newson, M.D. and Brookes, A. (1995) Sediment-related river maintenance: the role of fluvial geomorphology. *Earth Surface Processes and Landforms*, 20: 629-647.
- Seminara, G., Colombini, M. and Parker, G. (1996) Nearly pure sorting waves and the formation of bedload sheets. *Journal of Fluid Mechanics*, 312: 253-278.
- Shimizu, Y. and Itakura, T. (1989) Calculation of river bed variation in alluvial channels. *Journal of the Hydraulics Division, ASCE*, 115(3): 367-384.
- Siebel, H.N. and Blom, C.W.P.M. (1998) Effects of irregular flooding on the establishment of tree species. *Acta Botanica Neerlandica*, 47, 231-240.

Simon, A. and Collison, A.J.C. (2002). Quantifying the mechanical and hydrologic effects of riparian vegetation on streambank-stability. *Earth Surface Processes and Landforms*, 27: 527-546.

Simon, A. and Curini, A. (1998) Pore pressure and bank-stability: The influence of matric suction. In *Hydraulic Engineering*, edited by S. Abt, American Society of Civil Engineers, 358-363.

Simon, A., Curini, A., Darby, S.E. and Langendoen, E.J. (1999) Streambank mechanics and the role of bank and near-bank processes in incised channels. In *Incised River Channels: Processes, Forms, Engineering and Management*, edited by S.E. Darby and A. Simon, John Wiley and Sons, London, 123-152.

Simon, A., Curini, A., Darby, S.E. and Langendoen, E.J. (2000) Bank and near-bank processes in an incised channel. *Geomorphology*, 35: 193-217.

Simon, A., Langendoen, E.J., Collison, A. and Layzell, A. (2003) Incorporating bank-toe erosion by hydraulic shear into a bank-stability model: Missouri River, Eastern Montana. *Proceedings, EWRI-ASCE, World Water and Environmental Resources Congress and Related Symposia*, edited by P. Bizier, and P. De Barry, American Society of Civil Engineers, Philadelphia, Pennsylvania.

Simon, A., Wolfe, W.J. and Molinas, A. (1991) Mass wasting algorithms in an alluvial channel model. *Proceedings of the 5th Federal Interagency Sedimentation Conference*, Las Vegas, Nevada, 2: 8-22 to 8-29.

Simons, D.B. and Senturk, F. (1992) *Sediment Transport Technology; Water and Sediment Dynamics*. Water Resources Publications, LLC, Highlands Ranch, Colorado, 897 p.

Smith, D.G. (1976) Effect of vegetation on lateral migration of a glacial meltwater river. *Geological Society of America Bulletin*, 87: 857-860.

Song, C.C.S. and Yang, C.T. (1982) Minimum energy and energy dissipation rate. *Journal of the Hydraulics Division, ASCE*, 108(HY5): 690-706.

- Spedding, N. (1997) On growth and form in geomorphology. *Earth Surface Processes and Landforms*, 22: 261-265.
- Steffler, P. and Blackburn, J. (2002) Two-Dimensional Depth Average Model of River Hydrodynamics and Fish Habitat: Introduction to Depth Averaged Modeling and Users Manual. Edmonton, Alberta, Canada, University of Alberta, 119 p.
- Stølum, H.H. (1996) River meandering as a self-organization process. *Science*, 271(5256): 1710-1713.
- Strobl, R.O. and Forte, F. (2007) Artificial neural network exploration of the influential factors in drainage network derivation. *Hydrological Processes*, 21(22): 2965-2978.
- Stromberg, J.C., Richter, B.D., Patten D.T. and Wolden, L.G. (1993) Response of a Sonoran riparian forest to a 10-year return flood. *Great Basin Naturalist*, 53(2): 118-130.
- Struiksmā, N., Olesen, K.W., Flokstra, C. and de Vriend, H.J. (1985) Bed deformation in curved alluvial channels. *Journal of Hydraulic Research*, 23(1): 57-79.
- Tabacchi, E., Lambs, L., Guillo, H., Planty-Tabacchi A., Muller, E. and Decamps, H. (2000) Impacts of riparian vegetation on hydrological processes. *Hydrological Processes*, 14: 2959-2976.
- Tal, M., Gran K., Murray, B.A., Paola, C. and Hicks, M.D. (2003) Riparian vegetation as a primary control on channel characteristics in multi-thread rivers. In *Riparian Vegetation and Fluvial Geomorphology*, edited by S.J. Bennett and A. Simon, American Geophysical Union, 43-58.
- Teeter, A.M., Johnson, B.H., Berger, C., Stelling, G., Scheffner, N.W., Garcia, M.H. and Parchure, T.M. (2001) Hydrodynamic and sediment transport modelling with emphasis on shallow-water, vegetated areas (lakes, reservoirs, estuaries and lagoons). *Hydrobiologia*, 444: 1-23.
- Thomas, P.W. and Huggett, R.J. (1980) *Modelling in Geography: A Mathematical Approach*. Harper and Row, London.



- Thomas, W.A. and Prashum, A.L., (1977) Mathematical model of scour and deposition. *Journal of the Hydraulics Division, ASCE*, 110(HY11): 1613-1641.
- Thorne, C.E. and Welford, M.R. (1994) The equilibrium concept in geomorphology. *Annals of the Association of American Geographers*, 84(4): 666-696.
- Thorne, C.R. (1990) Effects of vegetation on riverbank erosion and stability. In *Vegetation and Erosion*, edited by J.B. Thornes, Wiley: Chichester, 123-144.
- Thorne, C.R., Amarasinghe, I., Gardiner, J. and Perala-Gardiner Sellin, R. (1997) Bank protection using vegetation with special reference to willows. Engineering and Physical Sciences Research Council and Environmental Agency Report.
- Thorp, J.H., Thoms, M.C. and Delong, M.D. (2006). Ecological regulation in river networks across time and space. *River Research and Applications*, 22: 123-147.
- Tinkler, K. and Wohl, E. (1998) A primer on bedrock channels. In *Rivers Over Rock: Fluvial Processes in Bedrock Channels*. Geophysical Monograph Series, American Geophysical Union, Washington, DC.
- Tsujimoto, T. (1999) Fluvial processes in streams with vegetation. *Journal of Hydraulic Research*, 37(6): 789-803.
- Tsujimoto, T. and Kitamura, T. (1996) Rotational degradation and growth of vegetation along a stream. International conference on new/emerging concepts for rivers, Rivertech 96, Chicago, Illinois, 632-657.
- Turner, A.K. and Schuster, R.L. (Editors) (1996) Special Report 247: Landslides, Investigation and Mitigation, Transportation Research Board, National Research Council, National Academy Press, Washington, DC.
- van Coller, A.L. (1993) Riparian vegetation of the Sabie River: Relating spatial distribution patterns to characteristics of the physical environment. MSc Thesis, University of the Witwatersrand, Johannesburg.
- van Coller, A.L. and Rogers, K.H. (1996) A basis for determining the in-stream flow requirements of the riparian vegetation along the Sabie River within the Kruger National Park. CWE report 2/96. Johannesburg.

van Coller, A.L., Rogers, K.H. and Heritage, G.L. (1997) Linking riparian vegetation types and fluvial geomorphology along the Sabie River within the Kruger National Park, South Africa. *African Journal of Ecology*, 35: 194-212.

van Niekerk, A.W. and Heritage, G.L. (1993) Geomorphology of the Sabie River: Overview and classification. Report No. 2/93. Centre for Water in the Environment, University of the Witwatersrand, Johannesburg.

van Niekerk, A.W., Heritage, G.L., Moon, B.P., Broadhurst, L.J., Rogers, K.H. and James, C.S. (1996) The geomorphological response to changing flow regimes of the Sabie and Letaba river systems. Water Research Commission report. No: K5/376/0/1. Pretoria, South Africa.

van Niekerk, A.W., Heritage, G.L. and Moon, B.P. (1995) River classification for management: the geomorphology of the Sabie River in the Eastern Transvaal. *South African Geographic Journal*, 77: 67-76.

van Rijn, L.C. (1984) Sediment transport, part III: bed forms and alluvial roughness. *Journal of Hydraulic Engineering*, 110(12): 1733-1754.

van Rijn, L.C. (1987) Mathematical modeling of morphological processes in the case of suspended sediment transport. Ph.D. Thesis, Delft University of Technology, Delft, The Netherlands.

van Rijn, L.C. (1993) Principles of sediment transport in rivers, estuaries and coastal seas. Aqua, Amsterdam, The Netherlands.

van Sicle, J. and Beschta, R.L. (1983) Supply based models of suspended sediment transport in streams. *Water Resources Research*, 19(3): 768-778.

Waldron, L.J. (1977) Shear resistance of root permeated homogeneous and stratified soil. *Soil Science Society of America Journal*, 41: 843-849.

Wang, S.S.Y. and Adefo, S.E. (1986) 3-D modelling of river sedimentation processes. Proceedings of the 3rd International Symposium on River Sedimentation, The University of Mississippi, USA.

- Wang, S.S.Y. and Weiming, W.U. (2004) River sedimentation and morphology modeling-state of the art and future development. Proceedings of the Ninth International Symposium on River Sedimentation, October 18 – 21, 2004, Yichang, China.
- Warburton, J. and Davies, T. (1994) Variability of bedload transport and channel morphology in a braided river hydraulic model. *Earth Surface Processes and Landforms*, 19: 403-421.
- Ward, J.V. and Tockner, K. (2000) Linking ecology and hydrology in alluvial flood plains. In European Geophysical Society, 25th General Assembly, Nice, France.
- Whiting, P.J., Dietrich, W.E., Leopold, L.B., Drake, T.G. and Shreve, R.L. (1998) Bedload sheets in heterogeneous sediment. *Geology*, 16: 105-108.
- Wiele, S.M. and Franseen M.A. (2000) Sand transport and bed evolution modelling applications in the Colorado River, Grand Canyon. U.S. Geological Survey, Denver, CO.
- Wiele, S.M. and Franseen, M.A. (1999) Use of reach-averaged properties and characteristic environments in the routing of sand in a river of complex morphology. U.S. Geological Survey, Denver, CO.
- Wiens, J.A. (1998) Spatial scaling in ecology. *Functional Ecology*, 3: 385-397.
- Wilcock, P.R. and Crowe, J.C. (2003) Surface-based transport model for mixed-size sediment. *Journal of Hydraulic Engineering*, 129(2): 120-128.
- Williams, J.J. (1990) Video observations of marine gravel transport. *Geo Marine Letters*, 10: 157-164.
- Wolfram, S. (1984) Cellular automata as models of complexity. *Nature*, 311: 419-424.
- Wu, J. and David, J.L. (2002) A spatially explicit hierarchical approach to modeling complex ecological systems: theory and applications. *Ecological Modelling*, 153: 7-26.

- Wu, W. and Vieira, D.A. (2002) One-dimensional channel network model CCHE1D 3.0 - Technical manual. Technical report No. NCCHE-TR-2002-1, National Centre for Computational Hydroscience and Engineering, The University of Mississippi.
- Wu, W. and Wang, S.S.Y. (2004) Depth-averaged 2-D calculation of tidal flow, salinity and cohesive sediment transport in estuaries. *International Journal of Sediment Research*, 19(3): 172-190.
- Wu, W., Rodi, W. and Wenka, T. (2000a) 3D numerical modeling of flow and sediment transport in open channels. *Journal of Hydraulic Engineering*, 126(1): 4-15.
- Wu, W., Wang, S.S.Y. and Jia, Y. (2000b) Nonuniform sediment transport in alluvial rivers. *Journal of Hydraulic Research*, 38(6): 427-434.
- Yalin, M.S. and Silva, A.M.F. (1999) Regime channels in cohesionless alluvium. *Journal of Hydraulic Research*, 37: 725-742.
- Yalin, M.S. and Silva, A.M.F. (2000) Computation of regime channel characteristics on thermodynamics basis. *Journal of Hydraulic Research*, 38: 57-64.
- Yang, C.T. (1987) Energy dissipation rate approach in river mechanics. In *Sediment Transport in Gravel-Bed Rivers*, edited by C.R. Thorne, J.C. Bathurst and R.D. Hey. John Wiley and Sons, 735-766.
- Yang, C.T. and Song, C.C.S. (1979) Theory of minimum rate of energy dissipation. *Journal of the Hydraulics Division, ASCE*, 105(HY7): 769-784.
- Yang, C.T., Song, C.C.S. and Woldenberg, M.J. (1981) Hydraulic geometry and minimum rate of energy dissipation. *Water Resources Research*, 17: 1014-1018.
- Yang, C.T., Treviño, M.A. and Simões, F.J.M. (1998) Program user's manual for GSTARS 2.0 (Generalized Stream Tube model for Alluvial River Simulation version 2.0), U.S. Bureau of reclamation, Technical Service Centre, Denver, Colorado.
- Yen, B.C. (1991) Hydraulic resistance in open channels; in *Channel Flow: Centennial of Manning's Formula*, edited by B.C. Yen. Water Resources Publications, Littleton, CO. 1-135.

Yulistiyanto, B. (1997) Flow around a cylinder installed in a fixed-bed open channel. PhD Thesis, EPFL, Lausanne.

Zimmerman, R.C., Goodlett, J.C. and Comer, G.H. (1967) The influence of vegetation on channel form of small streams. International Association of Scientific Hydrology, Symposium River Morphology, Publication 75: 255-275.

Zimmermann, C. and Kennedy, J.F. (1978) Transverse bed slope in curved alluvial streams. Journal of the Hydraulics Division, ASCE, 104(HY1): 33-48.

## **Appendix A - One-dimensional water flow model code**

## **Appendix B – Reach scale sediment flow and self-organisation model code**

## **Appendix C - Reach scale reed community model code**



## **Appendix D - Two-dimensional water flow model code**

## **Appendix E – Channel-type scale bar evolution model code**

## **Appendix F – Channel-type scale reed expansion model code**

## **Appendix G – Geomorphological-unit scale water flow code**

**Appendix H – Geomorphological-unit scale bed-form development model  
code**

## **Appendix I – Reed growth at geomorphological-unit scale model code**